Abstract

BLUE, ELIZABETH DODGE. Synthesis and Reactivity of Copper Complexes Possessing Non-dative Ligands (Under the Direction of Dr. T. Brent Gunnoe).

Carbon-nitrogen bonds are prevalent in many areas of chemistry including natural products, pharmaceuticals, conducting polymers, and materials for electronic applications. Late transition metals are often used to catalyze carbon-nitrogen bond-forming reactions with diverse substrates and under relatively mild conditions. Hydroamination and aryl amination catalysis may proceed via Cu(I) amido complexes, and Cu-catalyzed aziridination catalysis may proceed via Cu(III) nitrene intermediates. Detailed investigation of these potential intermediates and reaction mechanisms could further the development of these critical reactions. Besides potential catalytic application, many late transition-metal non-dative complexes possess significant basic and nucleophilic reactivity.

Presented herein are the isolation and characterization of a number of new copper(I) halide complexes and the first two examples of monomeric copper(I) amido complexes, (dtbpe)Cu(NHPh) and (IPr)Cu(NHPh). These Cu(I) anilido complexes have been shown to be more nucleophilic than a related Ru(II) anilido complex in reactivity studies with bromoethane, and reveal increasing nucleophilicity in the order (SIPr)Cu(NHPh) < (IPr)Cu(NHPh) < (IMes)Cu(NHPh) < (dtbpe)Cu(NHPh). (IPr)Cu(NHPh) is thermodynamically favored over (IPr)Cu(Ph)/NH_2Ph or $[(IPr)Cu(\mu\text{-}H)]_2/NH_2Ph$, respectively. Computational studies are consistent with the observed reactivity and indicate strong Cu-N bonds with nucleophilic amido nitrogen.

The two amido complexes (dtbpe)Cu(NHPh) and (IPr)Cu(NHPh) are active for hydroamination catalysis of electron-withdrawing olefins, and (IPr)Cu(NHPh) is observed to undergo stoichiometric and catalytic aryl amination with PhI and PhOTf. The mechanism and analysis of the scope of these reactions will continue to be investigated. Reactions towards synthesis of a Cu(III) nitrene complex with LCu(I) (L = dtbpe, NN, or IPr) complexes have largely resulted in decomposition to amine products and Cu(II) species. However, reactions with (NN)Cu(NCMe) complexes and phenyl azide did result in formation of a non-isolable transient species which may be either a Cu(III) nitrene or a Cu(II) species. Reaction of (IPr)Cu(OTf) with strong acid yields a protonated carbene ligand indicated by a downfield peak which binds η^2 through the imidazolium phenyl ring of the amido complex. The synthesis and reactivity studies described herein have provided a foundation for continued fundamental studies of copper(I) non-dative species and mechanistic and applied C-X (X = N, O, or S) bond-forming catalytic investigations.

Synthesis and Reactivity of Copper Complexes Possessing Non-dative Ligands

by

Elizabeth D. Blue

A dissertation submitted to the Graduate Faculty of

North Carolina State University

In partial fulfillment of the

Requirements for the degree of

Doctor of Philosophy

CHEMISTRY

Raleigh, NC

2006

Approved by:

_____	_____
T. Brent Gunnoe Chair of Advisory Committee	James D. Martin
_____	_____
Christian Melander	David A. Shultz

Dedication

This work is dedicated to Andrew. This would never have been completed without your love, sense of humor and support.

Biography

Elizabeth Dodge Blue was born in 1975 in Milledgeville, GA to Frederick and Mary Dodge. Years through age 11 were spent in the Baldwin County public schools and trying to do everything her brother Bryan, four years senior, could do including soccer, reading maps, bicycle stunts and climbing fences. In 1987, the Dodge family relocated to Marion, NC, where she completed secondary school at East McDowell Junior High and McDowell High in 1994. She continued her education by pursuing a Chemical Engineering degree at NC State University. At NC State, she enjoyed participating in the NCSU chapter of Habitat for Humanity, as well as cheering on the Wolfpack. She worked for three semesters as a co-op engineer at the National Starch and Chemical pilot plant in Salisbury, NC, and spent one semester taking no technical classes at all in Santander, Spain. One fateful night during exam week sophomore year, she met Andrew Blue, who married her upon her graduation, even though she took some of his pizza. After graduating in Chemical Engineering with a Spanish minor in 1999, Elizabeth went to work as a process engineer for Allied Signal/Honeywell in Moncure, NC. After deciding that teaching was her calling, Elizabeth returned to NC State in 2001 to pursue studies in Chemistry under the direction of Brent Gunnoe. After numerous years pursuing copper amido and nitrene chemistry in the Gunnoe group, she graduated in June 2006.

Acknowledgements

I would like to thank my advisor, Brent Gunnoe, for *lots* of patience and for being an excellent mentor, and for always keeping me on my toes with his dry wit! I couldn't imagine working under the direction of anyone else. Many, many, innumerable thanks for everything to the entire Gunnoe group, past and present: Dave, Prakash, Ben, Marty, Yuee, Karl, Colleen, John, Laurel, Sam, Nick, Tai and Hong Yan. Y'all are the greatest and I've really enjoyed working with you. Best of luck in all you do in the future – I know you will all be great successes. Thanks especially to Team Copper and the glovebox 3 peeps!

Thanks to my committee members: Jim Martin, Dave Shultz, Christian Melander, Mike Whangbo, Paul Maggard, and Fred Lado for your advice and help. Thanks to Paul Boyle for all your assistance in collecting X-ray data and for the help finding, interpreting, and managing structures. Thanks to Dr. Petersen at WVU for solving lots of my crystal structures – even the ones that weren't exactly what we thought they were going to be! Thanks to Brent, Greg Neyhart, and Jim Martin for taking a chance and letting me teach in their courses.

And before I get in trouble, I would like to thank my husband, Andrew Blue, and my parents, Fred and Mary Dodge, and for all their love and support. Andrew, I can't thank you enough for all of your patience and encouragement. You've seen me at my worst, and for some reason, stuck around! Mom and Dad, you have taught me so much, above all to try my best and to believe in myself. Many thanks for all that you have taught me and done, and for all the great meals you brought for the freezer. Also, thanks to the rest of my family and to the Blue clan for all their love and support through the years. Last, but not least, thanks to

the Natureboys for being my main source of entertainment and stress-relief! To Mrs. Harwood for all the funny postcards, and to all my other friends and family members who have encouraged me and made me laugh over the years.

Table of Contents

List of Figures

List of Tables

List of Schemes

List of Symbols and Abbreviations

dmpe	1,2-bis(dimethylphosphino)ethane
dppp	1,3-bis-(diphenylphosphino)propane
dtbpe	1,2-bis(di-*t*-butylphosphino)ethane, Ar = 2,6-di-isopropylphenyl
HOMO	highest occupied molecular orbital
IPr	1,3-bis(2,6-diisopropylphenyl)imidazol-2-ylidene
LUMO	lowest unoccupied molecular orbital
M	any metal
Me	methyl (CH_3)
NHC	*N*-Heterocyclic Carbene (a ligand)
NMR	nuclear magnetic resonance
NN	β-diketiminate ligand
PCHP	1,3-$(CH_2P^tBu_2)_2C_6H_4$
PCP	2,6-$(CH_2P(R)_2)_2C_6H_3$
Ph	phenyl
PhINTs	N-*p*-(tosylsulfonyl)imino phenyliodinane
PPh_3	triphenylphosphine
^{t}Bu	*tert*-butyl
Tp	hydridotris(pyrazolyl)borate
Z_{eff}	effective nuclear charge

Chapter 1: Introduction

1.1 Introduction to Homogeneous Catalysis and Transition-Metal Non-Dative Complexes

Organometallic chemistry is at the interface of organic and inorganic chemistry and is uniquely poised to contribute to the development of new synthetic technologies for the preparation of organic compounds. Catalysts can allow chemists to make reactions more atom, energy, and financially economical. Although there are disadvantages to homogenous catalysis when compared with heterogeneous catalysis in terms of industrial scale processes and catalyst recycling, homogenous catalysts offer potential advantages including more active catalysts allowing milder reaction conditions, increased selectivity, and catalyst tunability. In addition, understanding of catalytic reaction mechanisms can lead to rational catalyst development.

A prime example of organometallic catalysis that has had significant industrial and synthetic impact is the mechanistic understanding and development of olefin metathesis catalysts, which resulted in the award of the 2005 Nobel Prize in Chemistry to Chauvin, Grubbs, and Schrock.[1] Recently, new generation catalysts based on Grubb's catalysts have been approved for use in pharmaceutical processes.[2] In another notable application, the 2001 Nobel prize in Chemistry was awarded to another trio of organometallic chemists, Noyori and Knowles for enantioselective hydrogenation catalysis and Sharpless for enantioselective epoxidation catalysis.[3] Another area that is in active development and holds promise for industrial development is catalytic C-H activation.[4-7]

In the field of carbon-heteroatom bond formation, Hartwig and Buchwald have made significant progress in aryl amination catalysis with palladium catalysts, and more recently Buchwald has shown that copper can catalyze these reactions as well.[8-12] The mechanism of metal-catalyzed aryl amination will be discussed in detail below; however, one important result of these studies is that for the palladium-catalyzed reaction, palladium amido complexes are likely catalytic intermediates.[13, 14] Another area of note in carbon-heteroatom bond formation is the synthesis of aziridines from olefins catalyzed by late transition-metal complexes.[15-19] These reactions are also proposed to proceed via late-metal non-dative complexes, in this case nitrene complexes. These amido and nitrene complexes are the type of non-dative complexes that will be the focus of this work. Dative bonds are traditional coordinate bonds, and covalent bonds in metal complexes such as methyl ligands are considered non-dative; however, for our purposes non-dative will refer to covalent and polar covalent metal-heteroatom bonds.

1.1.1 Bonding in Late Transition-metal Non-dative Complexes

In addition to the practical interest in late transition-metal non-dative compounds for understanding and improvement of C-N bond-forming catalysis, metal amido and nitrene complexes are of interest from a fundamental perspective. Amido species possess a σ-bond and the potential for ligand to metal π-donation to create a π-bond (Figure 1.1). Metal nitrenes also involve interactions of σ and π symmetry, with potential for a second π interaction if the nitrogen lone pair donates into the metal center to form a bond order

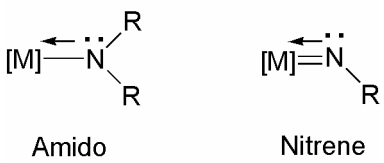

Figure 1.1. Amido and nitrene complexes.

between two and three. Transition-metal amido complexes demonstrate widely varying reactivity:[20] whereas some late transition-metal amido complexes deprotonate relatively weak acids easily,[21-23] other late transition-metal amides such as $TpOs(NHPh)Cl_2$ (Tp = hydridotris(pyrazolyl)borate) do not react as nucleophiles or bases, even with very strong acids such as HCl.[24] In general, the chemistry of late metal complexes with M-N and other heteroatom bonds is less developed than that of M-C and M-H bonds. Nitrogen heteroatoms are more electronegative than H and C, and thus it is not surprising that these bonds tend to be more ionic in nature. Hard-Soft acid base theory[25] would predict M-N or M-O bonds for late transition-metals to be weak based upon the energetic disparity between a hard base ligand and a soft metal acid. In contrast to this prediction, it has been found that late transition-metal M-N and M-O bonds can be relatively strong.[26, 27]

The nucleophilicity and basicity observed for many late transition-metal amido complexes is striking and two principle complementary theories have been have been advanced to explain this reactivity.[21, 28, 29] Mayer[30] and Caulton[31] have proposed that for late transition-metals with filled d orbitals of π-symmetry, the lone pair on the heteroatom (e.g. nitrogen of amido ligand) and the HOMO of the metal center are destabilized due to filled/filled interactions (Figure 1.2). Relative to systems in which the metal dπ orbital is vacant, this causes negative charge to be localized on the nitrogen and thus gives a

nucleophilic and basic amido ligand. This so-called "π conflict" may be an active or inactive contribution to the reactivity of the amido complexes. Qualitatively, for metal centers with

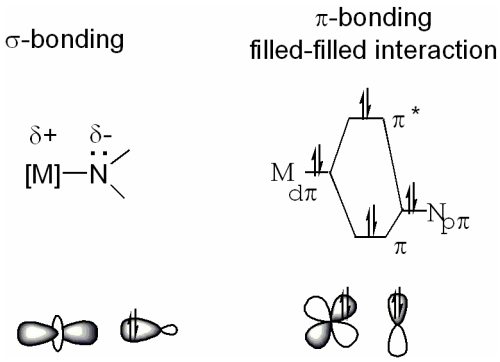

Figure 1.2. σ- and π-bonding in amido complexes.

unfilled orbitals of π-symmetry, the nitrogen lone pair donates into the metal orbitals if they are of appropriate symmetry and energy to create a more charge neutral amido ligand. Bergman and Holland have invoked the ionic character of M-N or M-O bonds to explain the strong nucleophilicity and basicity of these amido ligands.[32] They find from experimental evidence a strong electrostatic σ-bonding component to the M-N bond, which would account for the strength of the bond and give it significant polar character.

Nitrene ligands can donate four or up to six electrons to a metal center, and most nitrene ligands are coordinated to high oxidation state metal centers. Substantial bending of the M=N-R angle can indicate donation of four electrons and sp^2 hybridization and localization of a lone pair on the nitrogen. An angle of 180° implies that the nitrogen is sp hybridized and likely donates a lone pair to the metal center for a total of six electrons and a bond order of three. This is not always the case; however, as sterics and other multiply bonded donor ligands affect the bonding picture and can significantly shift the bond angle

from the expected orientation.[33,34] Early, high valent transition-metals primarily form nucleophilic species where the lone pair donation to the metal LUMO is not significant. The early transition-metal M-N bond is polarized with negative charge density on the nitrogen and is susceptible to attack by electrophiles or protonation, whereas the metal-centered LUMO can be attacked by nucleophiles. In general and qualitatively, as the metal identity is varied from left to right in the periodic table, less of the negative charge is predicted to be localized on the nitrogen (Figure 1.3).[34] From left to right, the energy of the metal d-orbitals are lowered as the Z_{eff} increases and the LUMO may transition from nitrogen-based to metal-based, allowing increased delocalization of the nitrogen lone pair to the metal. This potentially shifts the reactivity of late transition-metal nitrene complexes toward an electrophilic nitrogen ligand and renders them more likely to be attacked by nucleophiles. Although such an effect has been implicated in catalytic and stoichiometric reactions (e.g., olefin aziridination and nitrene transfer to phosphines), the paucity of late transition-metal nitrene complexes causes uncertainty as to whether these complexes are indeed electrophilic

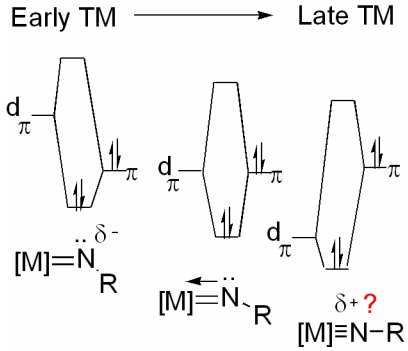

Figure 1.3. Trend in nitrene bonding for early vs. late transition-metals.

at nitrogen. Importantly, the qualitative description of metal-nitrene bonding depicted in Figure 1.3 does not take into account the effect of varying the oxidation state of the metal

center. For example, late transition-metal complexes with filled orbitals of dπ symmetry may result in nucleophilic nitrene ligands because the metal cannot accept lone pair donation.

1.1.2 Paucity of Monomeric Cu(I) Amido Complexes and Cu(I)OR Complexes

As noted, the bonding of monomeric non-dative complexes often leads to late transition-metal amido complexes that are nucleophilic, and the reactivity of late transition-metal nitrene complexes is also of interest. An additional incentive to study these complexes is their scarcity. Until our work, there were no examples of isolable monomeric copper(I) amido complexes, although there are numerous examples of copper(I) amido complexes with bridging amido ligands and chelating ligands containing amido moieties.[35-46] One example of a dimeric chloride-bridged Cu(II) amide has also been reported in the literature.[47] In addition, there are very few non-dative copper(I) complexes reported in general. Copper(I) alkoxide and aryloxide complexes are related heteroatom non-dative complexes, and there are relatively few monomeric Cu(I) aryloxide and alkoxide complexes.[48-50] For example, Floriani et al. isolated a (*p*-tolyl isonitrile)Cu(OPh) complex, and Yamamoto et al. have isolated complexes of the type $(PPh_3)_3Cu(OR)$. More recently, Sadighi et al. have reported (IPr)Cu(O^tBu) (IPr = 1,3-bis(2,6-diisopropylphenyl)imidazol-2-ylidene), a precursor for the synthesis of a Cu(I) methyl complex. In the quest for isolation of biologically relevant Cu(III) oxo complexes, a number of dimeric Cu(II) μ–alkoxide complexes have been isolated.[51-53]

1.2 Late Transition-Metal Amido Complexes

1.2.1 Synthesis of Late Transition-metal Amido Complexes

Although there are relatively few isolable *monomeric* late transition-metal amido complexes, the numbers have been increasing in recent years. According to a literature search, monomeric amido complexes have been isolated for all of the late transition-metals (defined in this case as groups 8-11) except for silver, and until our work, copper. Indeed, even the typically most reactive of the amido complexes, the "parent amido" where the amido group is NH_2, have been isolated for several late transition-metals including rhenium, iron, ruthenium, platinum, nickel and iridium.[21, 54-62]

A number of methods have been developed over the years for the synthesis of late transition-metal amido complexes (Scheme 1.1). The most common and versatile synthetic method for isolation of amido complexes is metathesis of a [M]X (X = F, Cl, Br) metal halide complex with a lithium or sodium amide.[20, 60, 63] Several of the reactive parent amido complexes have been synthesized by this method with $NaNH_2$ in the presence of excess NH_3.[56, 58] A second common method, deprotonation of amine complexes has been used, for example, by Gunnoe and coworkers in the synthesis of the Tp ruthenium(II) amido complexes [TpRu(L)(L')(NH_2R)][OTf] (L = L' = PMe_3, $P(OMe)_3$ or L = CO and L' = PPh_3; R = H or ^{t}Bu) and the PCP pincer-ligated (PCP)Ru(CO)(NH_2) (PCP = 2,6-($CH_2P(^iPr)_2)_2C_6H_3$).[59, 64] N-H activation of amines by an alkoxide complex has allowed isolation of palladium amido complexes.[65] This method has also been used to allow isolation of the only, until our work, group 11 amido complex via N-H activation of an amine by the corresponding gold(III) alkoxide complex.[66, 67] More novel synthetic methods include

synthesis of an Os(IV) amido complex from a nitrido complex[24] and imine insertion into a M-C bond.[68]

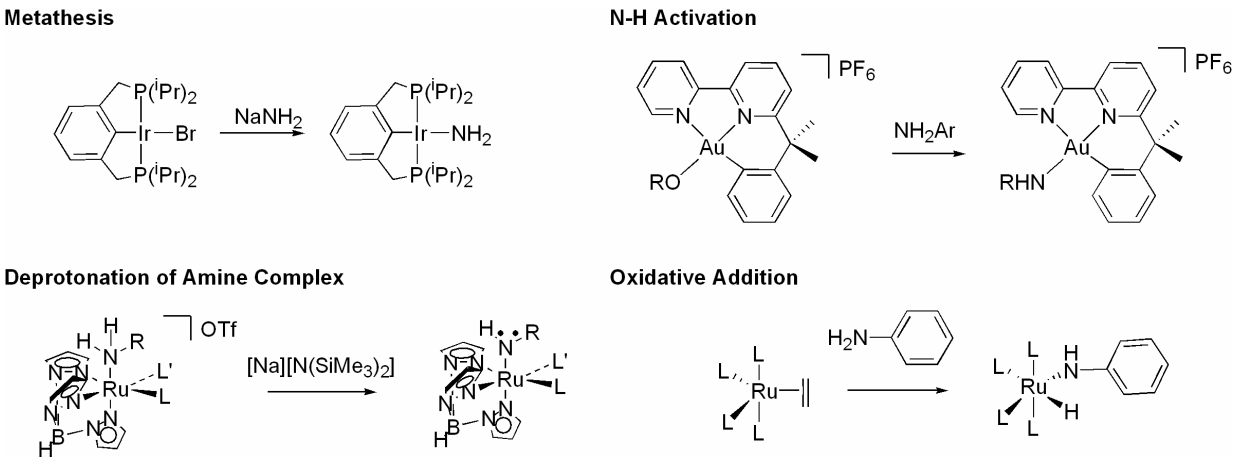

Scheme 1.1. Common synthetic methods for late transition-metal amido complexes.

Oxidative addition of amines is a particularly promising method of amido complex synthesis in terms of incorporation into catalytic cycles and was first observed by Milstein et al. in the synthesis of an Ir(III) amido complex, which was stabilized by an amido norbornene substituent. Later Bergman et al. observed this reaction in the synthesis of a terminal Ru(II) anilido complex.[69, 70] Recently, a reaction with great potential, the oxidative addition of ammonia to form an iridium parent amido hydride was reported by Hartwig, Goldman, et al. (Scheme 1.2).[62] This type of reaction could be utilized to transform some of the simplest building blocks of chemistry, ammonia and olefins, into useful organic compounds in an atom economical manner.

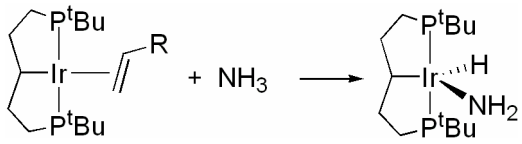

Scheme 1.2. Oxidative addition of ammonia to form an Ir(III) parent amido hydride complex.

1.2.2 Reactivity of Relevant Late Transition-metal Amido Complexes

As described above, the character of amido ligands depends largely upon the identity and electron count of the metal center. That is, for early transition-metal and high valent late transition-metal centers the nucleophilicity of the amido ligand may be reduced, and for low valent late transition-metals with filled dπ orbitals, the M-N bonding possesses significant polarity and the amido ligand is more likely to be nucleophilic/basic. The polar character of the late transition-metal amido bond leads to interesting reactivity, including addition to aldehydes and oxidation/deprotonation to form nitrene complexes.[60, 71] Related to the Buchwald-Hartwig Pd-catalyzed aryl amination reactions, Pd(II) phenyl amido complexes have been shown to reductively eliminate to form new C-N bonds, which is discussed in more detail below.[14] Most germane to our interests is the nucleophilicity and basicity of late transition-metal amido complexes which is demonstrated by their ability to deprotonate very weak acids and react as nucleophiles in substitution reactions.[28]

1.2.3 Basicity and Nucleophilicity Studies

Bergman and coworkers have isolated a Ru(II) parent amido complex, $(dmpe)_2Ru(H)(NH_2)$ (dmpe = 1,2-bis(dimethylphosphino)ethane), and studied its

reactivity.[22, 23, 58] This complex was shown to react with 1,4-cyclohexadiene to form $(dmpe)_2Ru(H)_2$ in > 95% yield along with benzene and free ammonia, and to catalyze the conversion of 1,4-cyclohexadiene to 1,3-cyclohexadiene (Scheme 1.3). In a related reaction, 9,10-dihydroanthracene was dehydrogenated by $(dmpe)_2Ru(H)(NH_2)$ to form anthracene in > 95% yield along with ammonia and $(dmpe)_2Ru(H)_2$. Reactions with substrates of varying acidity reveal that the parent amido ligand is highly basic. Reaction with fluorene yields $[(dmpe)_2Ru(H)(NH_3)]$[fluorenide] in approximately 90% yield, and the ammine ligand was not displaced to form a fluorenide complex. When the parent amido complex is reacted with the weak acids phenylacetylene, 1,2-propadiene, phenylacetonitrile and cyclobutanone these substrates are deprotonated and ammonia is displaced, forming new Ru(II) complexes. These reactions all proceed in relatively good yields (60-90%) at room temperature. Reaction with triphenylmethane allows observation of equilibrium between $(dmpe)_2Ru(H)(NH_2)/Ph_3CH$ and $[(dmpe)_2Ru(H)(NH_3)][Ph_3C]$ by low temperature NMR, and gives a calculated value at 25 °C $K_{eq} = 3.6 \times 10^{-1}$, and further demonstrates the significant basicity of $(dmpe)_2Ru(H)(NH_2)$.

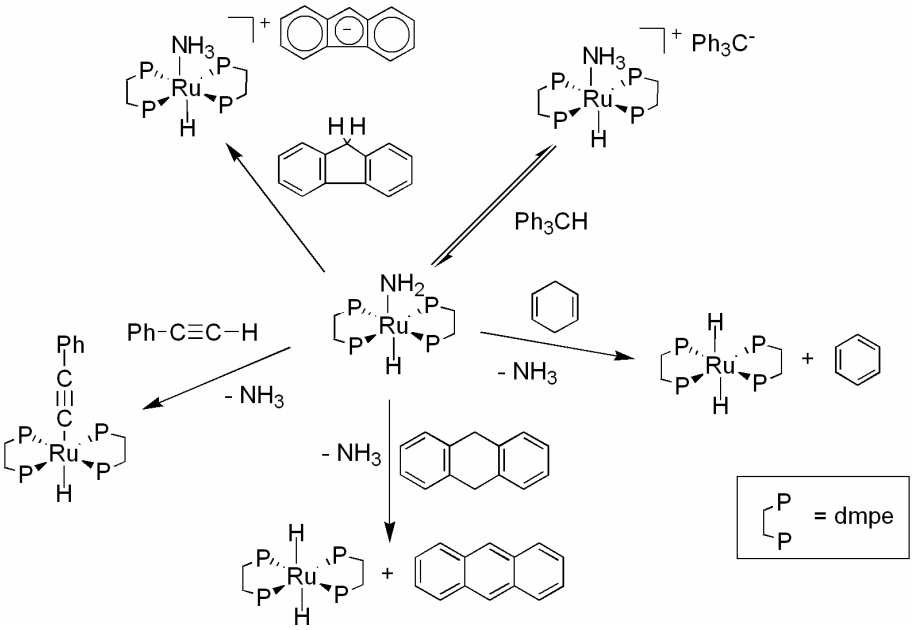

Scheme 1.3. Basic reactivity of $(dmpe)_2Ru(H)(NH_2)$ with acidic C-H bonds.

Although not directly observed, evidence suggests that $(dmpe)_2Ru(H)(NH_2)$ also reacts with toluene-d_8 and results in H/D exchange at room temperature. Deuterium is incorporated into the methylene and methyl protons of dmpe and the amido ligand and H is incorporated regioselectively into the methyl of toluene-d_8. Reactions of $(dmpe)_2Ru(H)(NH_2)$ with $^{15}NH_3$ reveal that H/D exchange does not proceed by ammonia dissociation (Scheme 1.4).

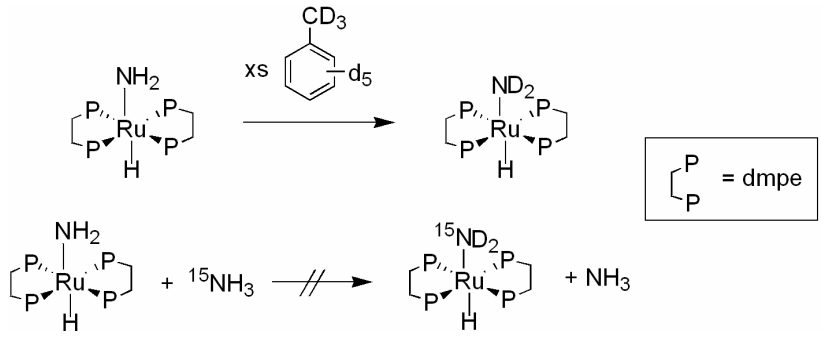

Scheme 1.4. Isotope exchange between $(dmpe)_2Ru(H)(NH_2)$ and toluene-d_8.

In addition to the work with the ruthenium parent amido complex, Bergman and coworkers have recently reported an analogous iron(II) parent amido complex, $(dmpe)_2Fe(H)(NH_2)$.[72] This complex is similar in reactivity to the ruthenium complex in that it deprotonates several weak acids, such as fluorene, and participates in H/D exchange with toluene-d_8. However, when compared directly with $(dmpe)_2Ru(H)(NH_2)$, the iron parent amido complex proves to be less basic. When the iron ammine complex $[(dmpe)_2Fe(H)(NH_3)][fluorenide]$ is reacted with $(dmpe)_2Ru(H)(NH_2)$, the resulting equilibrium favors formation of $(dmpe)_2Fe(H)(NH_2)$ and $[(dmpe)_2Ru(H)(NH_3)][fluorenide]$ (Scheme 1.5). Conversely, addition of $(dmpe)_2Fe(H)(NH_2)$ to independently synthesized $[(dmpe)_2Ru(H)(NH_3)][fluorenide]$ does not result in deprotonation of the ruthenium ammine complex. While $(dmpe)_2Fe(H)(NH_2)$ catalyzes isomerization of 1,4-cyclohexadiene to 1,3-cyclohexadiene it does not produce benzene. The lower relative basicity of $(dmpe)_2Fe(H)(NH_2)$ is proposed to be due to the increased electron richness of ruthenium as compared to iron, presuming that this results in greater electron density on the amido nitrogen.

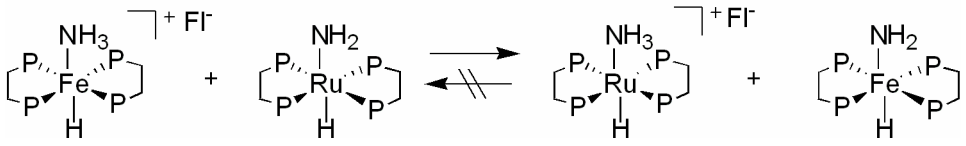

Scheme 1.5. Comparison of Fe(II) and Ru(II) parent amido basicity (Fl = fluorenide).

Dr. K.N. Jayaprakash and Dr. David Conner of the Gunnoe Group have synthesized a series of TpRu(II) parent amido complexes, $(Tp)Ru(L)(L')(NH_2)$ (L = L' = PMe_3 or $P(OMe)_3$, or L = CO and L' = PPh_3), a TpRu(II) alkyl amido complex,

$TpRu(PMe_3)_2(NH^tBu)$, and the PCP (PCP = 2,6-$(CH_2P(^tBu)_2)_2C_6H_3$) pincer-ligated Ru(II) amido complex $(PCP)Ru(CO)(NH_2)$.[21, 59, 64] These complexes are reactive and have been characterized by multinuclear NMR and mass spectrometry. Reaction of $TpRu(PMe_3)_2(NHR)$ (R = ^{t}Bu or H) with 1,4-cyclohexadiene at 75 °C yields the corresponding hydride complex $TpRu(PMe_3)_2(H)$ and benzene. For the reaction with $TpRu(PMe_3)_2(NH_2)$, isomerization of 1,4-cyclohexadiene of 1,3-cyclohexadiene is also observed and is more rapid than conversion to benzene. This reaction is proposed to proceed by deprotonation of 1,4-cyclohexadiene to form an amine complex anion and a cyclohexadienyl anion. Reprotonation of the cyclohexadienyl anion can produce 1,4-cyclohexadiene or 1,3-cyclohexadiene and reform the parent amido complex. Alternatively, ammonia dissociation from $[TpRu(PMe_3)_2(NH_3)]$[cyclohexadienyl] can lead to hydride abstraction to produce the hydride complex $TpRu(PMe_3)_2(H)$ and benzene (Scheme 1.6).

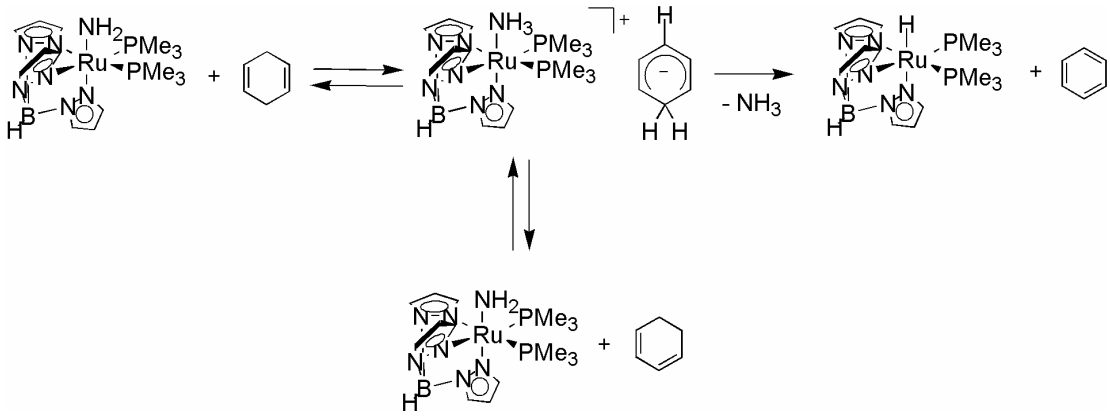

Scheme 1.6. Production of benzene and isomerization of 1,4-cyclohexadiene mediated by $TpRu(PMe_3)_2(NH_2)$.

Reaction of the $TpRu(L)(L')(NH_2)$ complexes with phenylacetylene at room temperature results in deprotonation of phenyl acetylene to form the ion pair

[TpRu(L)(L')(NH_3)][PhC≡C], which is observed by ^{1}H NMR spectroscopy (Scheme 1.7). Further heating of these ion pairs does not yield the corresponding phenylacetylide complexes, but provides multiple uncharacterized TpRu products. However, when phenylacetylene is reacted with TpRu(PMe_3)$_2$(NH^tBu), the amine ion pair [TpRu(PMe_3)$_2$($NH_2{}^tBu$)][PhC≡C], is formed at room temperature, and upon heating to 80 °C the t-butyl amine dissociates and the phenylacetylide TpRu(PMe_3)$_2$(C≡CPh) is formed. This ammonia complex appears to coordinate more strongly than the amine.

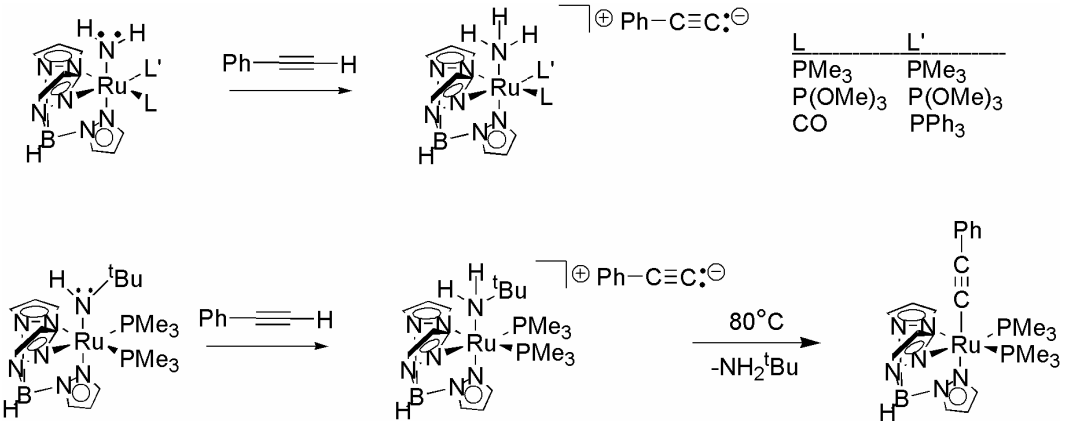

Scheme 1.7. Reactions of TpRu(L)(L')(NHR) with phenylacetylene.

(PCP)Ru(CO)(NH_2) has been synthesized by Gunnoe et al. to probe the effect of coordination number on the reactivity of Ru(II) parent amido complexes.[59] This five-coordinate unsaturated parent amido complex could have an advantage in targeting reactions with non-polar substrates such as C-H and H-H bonds in contrast to the octahedral TpRu complexes due to the open coordination site which can potentially bind and activate C-H and H-H bonds. (PCP)Ru(CO)(NH_2) was synthesized by deprotonation of the ammonia complex (PCP)Ru(CO)(NH_3)Cl with [Na][N($SiMe_3$)$_2$]. Similar to TpRu systems described above, the

(PCP)Ru parent amido complex also deprotonates phenylacetylene and dissociates ammonia to form the phenylacetylide complex (PCP)Ru(CO)(C≡CPh). In addition, the open coordination site allows rapid reaction with the non-polar bond of H_2 to release ammonia and form (PCP)Ru(CO)(H). This reaction is proposed to proceed via coordination of H_2, heterolytic cleavage of H_2 by the amide ligand to form the ammine hydride complex (PCP)Ru(CO)(NH_3)(H), observed at low temperature, followed by dissociation of the ammonia (Scheme 1.8). (PCP)Ru(CO)(NH_2) does not; however, activate the C-H bonds of methane, and computational studies reveal that this reaction is endoergic by 14 kcal/mol.

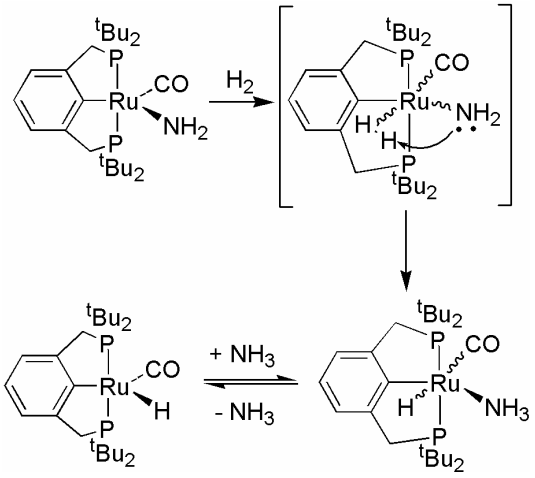

Scheme 1.8. Reaction of the parent amido complex (PCP)Ru(CO)(NH_2) with H_2.

In addition to the work with ruthenium parent amido complexes, Gunnoe and coworkers have examined the reactivity of the series of TpRu anilido complexes TpRu(L)(L')(NHPh) (L = L' = PMe_3 or $P(OMe)_3$, or L = CO and L' = PPh_3).[29, 73] When reacted with phenylacetylene at room temperature, the anilido complexes do not deprotonate the weak acid, but upon heating to 80 °C, the phenylacetylide complex and free aniline are formed.[64] However, this reaction was found to be catalyzed by the Ru(II) triflate species

$TpRu(PMe_3)_2OTf$ (Scheme 1.9). The proposed mechanism is reaction of the triflate complex with phenylacetylene to produce a vinylidene complex, which can be deprotonated by an equivalent of $TpRu(PMe_3)_2(NHPh)$ to produce the phenylacetylide complex and $[TpRu(PMe_3)_2(NH_2Ph)][OTf]$. The amine complex can then dissociate aniline to reform the triflate complex. When the anilido complexes are reacted with malononitrile, they demonstrate acid-base equilibria and the pKa of these complexes is similar to malononitrile in methylene chloride.[29] None of the TpRu anilido complexes react with 1,4-cyclohexadiene to yield benzene. These results show that these anilido complexes are basic, but less so than the parent and alkyl amido complexes studied. The anilido complexes also showed greater stability in that solid-state structures were obtained for $TpRu(CO)(PPh_3)(NHPh)$ and $TpRu\{P(OMe)_3\}_2(NHPh)$.[29, 73]

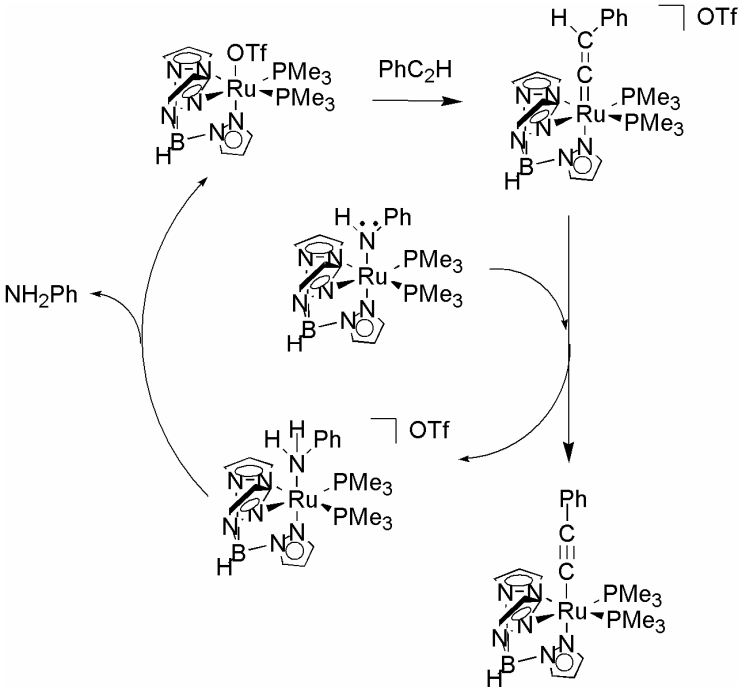

Scheme 1.9. Production of phenylacetylide complex $TpRu(PMe_3)_2(C_2Ph)$ catalyzed by the triflate complex $TpRu(PMe_3)_2OTf$.

As mentioned above, in contrast to the strong basicity of the Ru(II) and Fe(II) amido complexes, an Os(IV) phenyl amido complex has been synthesized by Mayer et al. and has been shown to be quite inert, even to strong acids.[24] When $TpOs(Cl)_2(NHPh)$ is combined with HCl, no reaction is observed (Scheme 1.10). Only extreme reaction conditions, reaction with HCl/Et_2O in $CDCl_3$ at 80 °C for 7 days result in a small conversion (~ 12%) of the amido complex to $TpOsCl_3$ and aniline. Reaction with 2 equivalents of HOTf does give quantitative conversion to $[TpOsCl_2(NH_2Ph)][OTf]$, but the amine complex is easily deprotonated by water or chloride ion. This remarkable inertness towards protonation is likely due to both the Os-N π-bonding and the inductive effect of the electron deficient Os(IV).

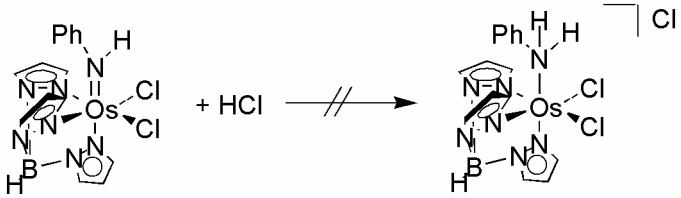

Scheme 1.10. Os(IV) anilido complex is not protonated by strong acids.

1.2.4 Stability of Anilido Complexes

Unlike the Os(IV) anilido complex, TpRu(II) anilido complexes cannot formally engage in amido-to-metal π-donation of the amido lone pair which would attenuate nucleophilicity and basicity. Those Ru(II) systems are d^6 and possess filled dπ orbitals. Nonetheless, the reactivity difference between the alkyl and parent amido complexes and the anilido complexes are notable. Although the anilido nitrogen cannot π-donate to the metal center, stabilization by donation of electron density to the π* orbitals of the phenyl ring is

possible. This donation can be observed in two physical manifestations: 1) the shortening of the N_{amido}-C_{phenyl} bond distances along with shifts in the phenyl ring bond distances and 2) in hindered bond rotation about the N_{amido}-C_{phenyl} bond, which can be observed by variable temperature NMR. These effects have been reported for a Pt(II) anilido complex and the Ru(II) anilido complexes discussed above.[29, 73, 74]

For example, resonance structures can be drawn for delocalization of the amido lone pair into the phenyl π* system, as shown below for TpRu(L)(L')(NHPh) (L = L' = PMe_3 or $P(OMe)_3$, or L = CO and L' = PPh_3) (Scheme 1.11) Variable temperature NMR studies revealed varying levels of hindered bond rotation for the Ru-N and N_{amido}-C_{phenyl} bonds depending upon the ancillary ligands in the complex (Figure 1.4). For the least electron rich

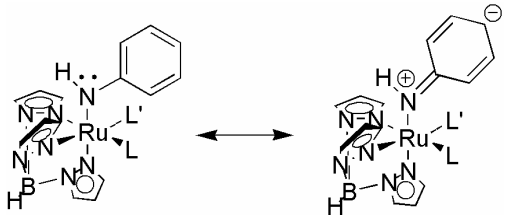

Scheme 1.11. Resonance structures for the Ru(II) anilido complexes TpRu(L)(L')(NHPh).

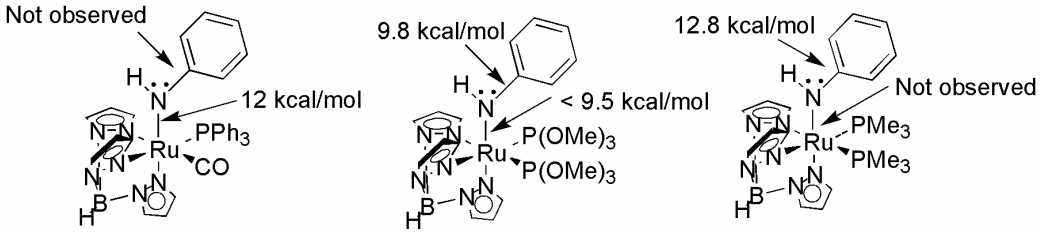

Figure 1.4. Relative barriers to bond rotation for a series of Ru(II) anilido complexes.

complex of the series, $TpRu(CO)(PPh_3)(NHPh)$, a small Ru-N rotational barrier of 12 kcal/mol is observed, which is likely attributable to steric effects. No barrier to N_{amido}-C_{phenyl} bond rotation was observed on the NMR timescale at the accessible temperatures (to -100 °C). For $TpRu\{P(OMe)_3\}_2(NHPh)$, both the Ru-N and the N_{amido}-C_{phenyl} rotational barriers can be observed with values of < 9.5 kcal/mol (estimated) and 9.8 kcal/mol, respectively. The most hindered N_{amido}-C_{phenyl} bond rotation was observed for $TpRu(PMe_3)_2(NHPh)$ with a value of 12.8 kcal/mol, but no notable Ru-N bond rotation energy barrier. This demonstrates that for the most electron-rich amido systems, the electron density of the amido ligand is likely stabilized by delocalization of electron density into the phenyl π* system, which is manifested in an increase in N_{amido}-C_{phenyl} rotational barrier. The effects of this stabilization can also be observed in Hammett studies of phenyl amido complexes.

1.2.5 Amination Catalysis

Species that contain carbon-nitrogen bonds include amines, amides, ammonium and alkylammonium salts, ureas, carbamates, isocyanates, amino acids, polyanilines and nitrogen heterocycles.[8, 75] These compounds are important in many areas of chemistry, but are of particular interest in biologically-active molecules. Many of the top pharmaceuticals contain C-N bonds and amine or amide groups. For example, salbutamol is one of the leading asthma drugs (Figure 1.5).[76, 77]

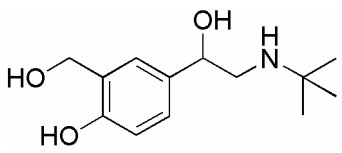

Figure 1.5. Salbutamol – a leading asthma drug.

Traditionally, the synthesis of amines is attained by reductive amination or arene nitration.[78] These reactions can be catalyzed by various metals and metal compounds in either solution or on solid supports, or as part of an enzymatic process with ammonia. Amination reactions can be accomplished through a number of different methods including the use of olefins, alcohols, allyls, arynes, and alkyl or aryl halides as substrates to form a C-N bond.[75, 79] Catalysis of the conversion of alcohol and amines to higher order amines typically requires high temperatures, 100 °C to 500 °C. Metal compounds that have been used for this process include heterogeneous catalysts such as Ni, Rh, or Pd on alumina.[75] In addition, photolytic processes that utilize homogenous catalysts such as Mo_6Cl_{12}, $Fe(CO)_5$ and $P(OEt)_3$, or Hg have been reported. Another route is olefin or alkyne hydroamination, or the net addition of N-H bonds across alkene or alkyne multiple bonds. These reactions can occur with activated alkenes in the absence of catalyst, although the yields are low in the slow reaction and a mixture of products typically results (see below).

1.2.6 Aryl Amination

Recent efforts in the area of aryl amination by Hartwig, Buchwald, and others have resulted in catalysts that aminate aryl halides and sulfonates with a variety of substrates (Scheme 1.12).[8, 9] These groups have developed palladium-catalyzed amination reactions through many iterations of altering the ligands and metal precursor to develop a diverse arsenal of reactions. This approach has already been used in synthesis of organic targets including functionalized pyrido[2,3-b] indoles and more recently in the synthesis of a

potential Alzheimer's disease treatment.[80, 81] The inspiration for these reactions came from Kosugi, who in 1983 used catalytic amounts of Pd complexes with stoichiometric amounts

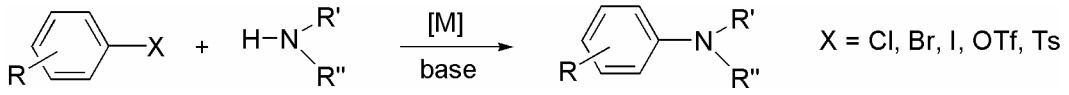

Scheme 1.12. Pd-catalyzed aryl amination catalysis (Buchwald-Hartwig).

of tin amides to react with aryl halides to form aryl amines.[82] Hartwig and Buchwald concurrently accomplished the first tin-free amination of this type in 1995.[83, 84] L_2Pd complexes were used where L = $P(OR)_3$ with a base to affect the amination of aryl halides with amine at 100 °C in substantial yields (> 80%). They also found that it was possible to aminate intramolecularly to form nitrogen heterocycles in high yield, and that chelating ligands improved the reactivity and reduced substrate sensitivity to allow amination with electron-rich, electron-poor, hindered or unhindered aryl bromides or iodides.[8, 9, 85] Most remarkably, Buchwald et al. have accomplished room temperature Pd-catalyzed aryl amination of aryl chlorides, which are both less expensive and more readily available than aryl bromides and iodides, but less activated.[86] More recently Nolan and coworkers have developed "Buchwald-Hartwig" amination catalysis with (NHC)Pd (NHC = *N*-heterocyclic carbene ligand) complexes that are also active for amination of aryl halides (bromide and chloride) at room temperature or relatively low temperatures (50-60 °C), and for aryl bromides with remarkably low catalyst loadings (0.05 – 0.001 mol%).[87-89] In addition to high activity and mild reaction conditions, a number of these (NHC)Pd catalysts are moisture- and air-stable. Other metals that have been utilized for this catalysis include Ni

and Cu, the latter of which will be discussed below. Ni catalysts have been used to aminate aryl chlorides and to aminate using diarylamines.[90, 91]

1.2.7 Pd Mechanism (Hartwig/Buchwald)

In conjunction with and assisting in the development in the aryl amination catalysis were the mechanistic studies performed to elucidate the reactivity of the palladium catalyzed amidation. Palladium(II) amido intermediates have been identified in the catalytic cycle, and model systems have been isolated to assist in the understanding of the oxidative addition and reductive elimination steps that are involved.[13, 14] Experimental evidence shows that $L_2Pd(0)$ is the resting state of the catalyst, and oxidative addition of the aryl halide species is the rate-limiting step for monophosphine-ligated systems. Recently, a revised mechanistic study of (BINAP)Pd(0) catalyzed aryl amination was published jointly by the research groups of Hartwig, Blackmond and Buchwald.[92] The precatalyst is a $(BINAP)_2Pd$ complex, and the dissociation and re-association of the second BINAP ligand had previously been thought to be part of the catalytic cycle.[93] However, new catalytic data reveal that the dissociation of one of the BINAP ligands lies off the catalytic cycle and in fact leads to an induction period for the reaction while the active catalyst (BINAP)Pd is produced (Scheme 1.13). The reaction then proceeds via oxidative addition of the aryl halide, followed by coordination of the amine. The amine is deprotonated by the base, and a Pd(II) aryl amido complex is formed. Reductive elimination forms the new aryl amine and reforms the (BINAP)Pd active catalyst. In general, the reductive elimination of product can be favored by increasing the

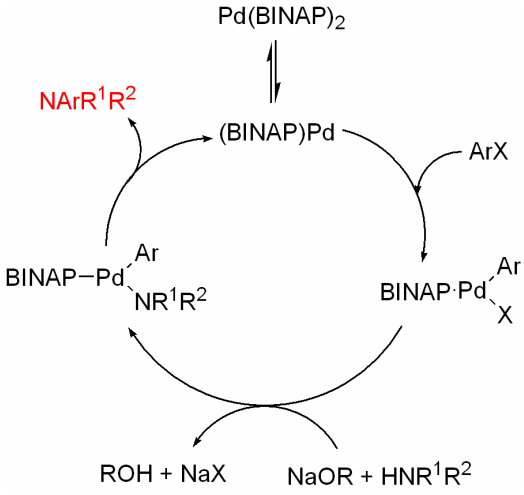

Scheme 1.13. Mechanism of aryl amination catalyzed by (BINAP)Pd(0).

nucleophilicity of the amine, increasing the electrophilicity of the aryl substrate, and the use of bulky ligands. Future challenges for Buchwald-Hartwig amination catalysis include increasing the scope of the reaction and continuing towards milder reaction conditions, and perhaps someday incorporation with C-H activation to aminate unactivated substrates.

1.2.8 Cu Aryl Amination Catalysis

An alternative to the palladium systems is the less expensive and air-stable copper catalysts that are currently being developed by Buchwald and others. Copper has a bulk market price of approximately \$0.21 per ounce[94] whereas Pd is priced greater than 1500 times that at \$362 per ounce.[95] Even if low turnover numbers are achieved with copper, the low cost of copper may allow industrially viable processes.

Building upon the reactivity seen with the Ullmann coupling reaction where substitution of an aryl halide by copper compounds can form C-C bonds, a number of relatively mild C(aryl)-X (X = O, N, S) coupling methods have been developed in the past

several years.[96, 97] Early copper-catalyzed C-N coupling reactions required high temperatures, strong bases, were limited in substrates or required stoichiometric amounts of copper.[98] More recently, Buchwald, Venkataraman and others have shown that milder and catalytic amination reactions can be accomplished using copper. Venkataraman sought to synthesize a triphenylamine with ortho ester groups, and found that Pd(0) catalysts were not successful, but that $Cu(PPh_3)_3Br$ is air-stable and forms the desired product in good yield.[99]

In 2001, Buchwald reported the use of air-stable copper iodide for catalysis of amidation of aryl halides and sulfonates with nitrogen heterocycles, amides, and secondary amines with a diamine ligand and typically 1-10 mol% catalyst.[10] This same copper salt can be used to run reactions in air with ethylene glycol as the ligand.[100] The reactions with diamine ligand are slightly air sensitive and must be run under an inert atmosphere, but the reagents can be handled in air and no special purification steps must be taken for the reagents or solvents. Relatively low temperatures of 60-100°C are used, the amines can contain electron donating or withdrawing groups, and reactivity can be accomplished with various bases. Intramolecular amination can occur and indoles may be arylated with this system with functional groups tolerated including alkyl- or aryl amines, amides, cyano, nitro, ester, allyl, and hydroxyl groups.[101, 102] A summary of the remarkable array of chemistry that can be accomplished using this system can be found in a recent patent.[11] Of note is the complement of the Pd and Cu amination systems to each other. Buchwald has reported that in amidation reactions of primary aminobenzamides that Pd catalyst arylates selectively at the aniline NH_2 group, whereas Cu catalysis is exclusive for the coupling at the amide NH_2.[103]

1.2.9 Cu Mechanism

Very few mechanistic studies had been performed on the copper-catalyzed aryl amination catalysis. By analogy to the palladium-catalyzed systems, a copper amido intermediate has been postulated to be active in these reactions. However, a catalytic cycle directly analogous to the Pd system would involve a Cu(III) complex, which is a rarely observed oxidation state for copper, and oxidative addition of an aryl halide to Cu(I) is unlikely (Scheme 1.14). Recently, the mechanism of amidation of aryl iodides with diamine

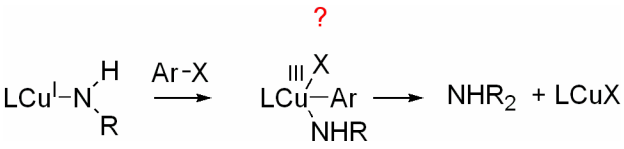

Scheme 1.14. Potential mechanism of Cu-catalyzed arylamination that proceeds via a Cu(III) intermediate.

ligands and CuI was investigated by Buchwald et al.[104] Their studies suggest that a copper amido complex is indeed an intermediate. They produced, in situ, a copper amide species which performed stoichiometric amidation of aryl iodide in the presence of diamine ligand (Scheme 1.15). This reaction occurred at 0 °C with complete conversion to the amine product; however the diamine copper amide complex was not isolated, only observed by ^{1}H

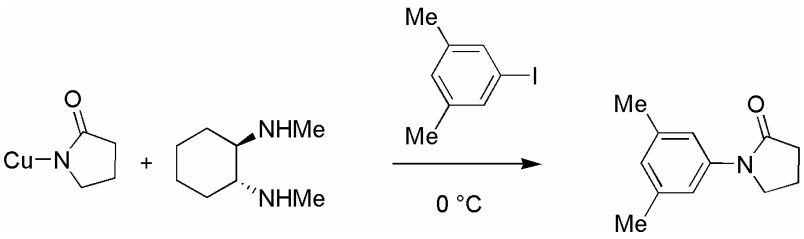

Scheme 1.15. Stoichiometric aryl amination by transiently observed Cu(I) amide complex.

NMR spectroscopy. These results, along with the rarity of Cu(III) species, suggest an alternate mechanism from that observed in the Pd-catalyzed reactions. Deprotonation of the amine substrate by the base allows formation of the amide complex followed by reaction with the aryl halide to form the amine product (Scheme 1.16). The nature of the interaction with the proposed amido intermediate is unclear. In his mechanistic studies on the Ullmann condensation using aryl halides to synthesize aryl amines, Paine proposed an aryl complex-assisted substitution reaction.[105] Further studies to definitively understand the nature of the catalytic pathway, and in particular, the interaction of the putative amido intermediate with the aryl halide would be of use in the development of this catalysis.

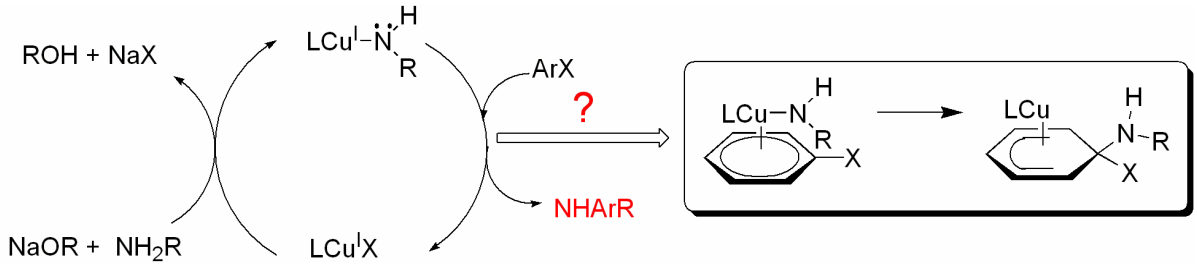

Scheme 1.16. Proposed catalytic cycle for copper catalyzed aryl amination.

1.2.10 Hydroamination

Another useful C-N bond-forming reaction that can be catalyzed by late transition-metal complexes with amido complexes as possible intermediates is olefin or aklyne hydroamination.[106] This reaction of olefins with amines to form new higher order amines can proceed with "Markovnikov" or "anti-Markovnikov" selectivity, producing either the more highly substituted branched amine or the linear (or less substituted) amine, respectively (Scheme 1.17). Both products are useful, with the branched Markovnikov products used for

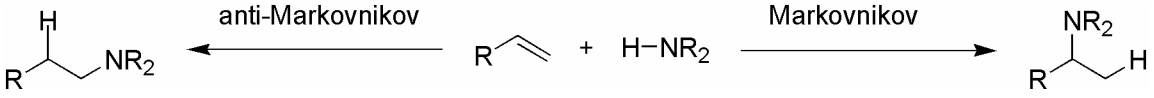

Scheme 1.17. Regioselectivity of hydroamination reaction.

natural products and fine chemical syntheses and the linear anti-Markovnikov products manufactured on large scale as bulk chemicals. In most cases, these reactions are thermally favored at reasonable temperatures. With electron-deficient activated olefins (those possessing keto, ester, nitrile, sulfoxide, or nitro groups), the reaction can proceed in the absence of a catalyst (depending on the substrates) to give anti-Markovnikov products, although the reaction can be aided by catalysts. However, for unactivated (or less activated) olefins, a catalyst is necessary to overcome activation barriers: electronic repulsion between the electron-rich multiple bond and the amine lone pair, negative reaction entropy and low thermodynamic driving forces. Even in cases where the reaction does not require catalyst, the need for forcing conditions can decrease selectivity and yield.

The hydroamination of olefins can be catalyzed by acids, although these reactions typically require relatively elevated temperatures. These conditions are often incompatible with functionality of the substrates. Intramolecular hydroamination to form pyrrolidenes and piperidines catalyzed by triflic or sulfuric acid at 100 °C with tosyl-protected amines was reported by Hartwig et al.[107] For the terminal olefins studied with the reaction, the regioselectivity was Markovnikov, and a mechanism involving amine protonation (due to the leveling effect of a solution containing basic amine and strong Brønsted acid), followed by transfer of the proton to the double bond and formation of the new C-N bond was proposed. More recently, Bergman et al. have shown that anilinium salts, formed in situ by trityl cation

and amine, catalyze Markovnikov hydroamination of olefins such as norbornene, electron-withdrawing *para*-substituted styrene, and cycloalkenes at moderate to high temperatures (40 °C – 135 °C).[108] In addition, the related hydroalkoxylation of activated olefins has been shown to be catalyzed by alkyl phosphines.[109]

Lanthanide systems have been developed by Marks and coworkers for inter- and intra-molecular hydroamination of unactivated olefins.[110] These metallocene and non-metallocene systems generally yield Markovnikov regioselectivity and have been shown to be enantioselective when chiral and enantiopure ligands are used on the metal center.[111] The hydroamination of a few substituted styrene compounds has been catalyzed by the lanthanide complexes, and for the electron-withdrawing vinylarenes, the selectivity is anti-Markovnikov.[112] But, in general, these catalysts are limited by their lack of functional group tolerance. In addition, the rates for intermolecular hydroamination are substantially slower than for intramolecular hydroamination with these systems.

Late transition-metal complexes for hydroamination catalysis have also been developed in recent years. Hartwig and coworkers have developed Pd catalysts for Markovnikov hydroamination of vinyl arene and Rh catalysts for anti-Markovnikov hydroamination of vinyl arenes.[113-117] The reaction mechanism for the Pd complexes has been shown to proceed via an η^3-phenethyl complex that is activated towards intermolecular attack by the amine. The Rh catalysts have been shown to selectively produce anti-Markovnikov hydroamination products, but β-hydride elimination to form enamines complicates the transformation. Most recently, Hartwig et al. reported an intramolecular hydroamination with bisphosphine Rh(I) catalysts to synthesize 3-arylpiperidines, and with

some of the ligands, for example dppp (dppp = 1,3-bis-(diphenylphosphino)propane), no enamine was detected.[117] Anti-Markovnikov hydroamination of activated olefins by Ni(II) has been reported, and this reaction likely proceeds by coordination of the olefin, followed by amine nucleophilic addition.[118] Further development of this catalysis seeks to generate general procedures that are functional group tolerant, able to hydroaminate unactivated alkyl olefins, and to access high enantioselectivities.

1.3 Late Transition-Metal Nitrene Complexes

The first organoimido transition-metal complex prepared was *tert*-butylimidotrioxo osmium (VIII) by Clifford and Kobayashi in 1956.[33] Since then a variety of early and late transition-metal imido complexes have been synthesized, with the majority of the complexes being composed of early and middle transition-metals in high oxidation states.[33, 34] Relatively few group 9 and 10, and no monomeric group 11 nitrene complexes have been isolated. The reactivity of nitrene ligands can vary widely depending upon the identity of the metal center, metal oxidation state, and the ancillary ligands including steric factors. In general, early transition-metal complexes are unreactive and the nitrene often serves primarily as an ancillary ligand.

1.3.1 Synthesis of Late Transition-metal Nitrene Complexes

Nitrene complexes can be synthesized by a number of methods, including cleavage of an α-bond precursor (for example, removal of H^+, $H\cdot$ or H^- from an amido complex), reaction with azides, reaction with substrates possessing electropositive leaving groups such

as silylamines, protonation or hydride addition to nitride complexes and exchange with other multiply-bonded complexes such as oxo ligands, among others.[33, 34] Recent examples of pertinent late transition-metal nitrene complexes include Co(III) nitrene and oxo complexes synthesized by Warren et al., which posses bridging nitrene ligands, with the exception of a terminal adamantyl nitrene.[119] A related Ni(III) adamantyl nitrene was also isolated.[120] These were all synthesized by reaction of a complex with a labile ligand with azides. Peters et al. have isolated a terminal Fe(III) imido complex by addition of *p*-tolyl azide to a Fe(I) phosphine complex.[121] Hillhouse et al. utilized oxidation and deprotonation of a terminal Ni(II) amido complex to synthesize a nitrene complex.[71] Bergman et al. have isolated a terminal Ir(III) imido by reaction of $[(Cp^*)Ir(Cl)_2]_2$ with $LiNH^tBu$[122] A terminal Ru imido was synthesized by Wilkinson et al. via oxidation of an amido complex by controlled addition of O_2.[123]

1.3.2 Aziridination Catalysis

Aziridines are versatile synthetic precursors as well as functional groups for biologically active materials. They are of interest for synthetic chemists as pharmaceutical targets and natural products, as well as their subsequent use in transformations such as ring-opening reactions,[124, 125] The synthesis of these strong electrophiles by nitrene transfer to an olefin is a very promising homogenous catalysis route.[15, 19] Groves et al. accomplished the first example of a nitrene transfer to an olefin in 1983.[126] They demonstrated the stoichiometric aziridination of olefins by a Mn nitrido complex that proceeds through a proposed nitrene intermediate. The next year Mansuy reported the catalytic aziridination of

alkenes with Mn and Fe porphyrin complexes utilizing PhINTs (N-*p*-(tosylsulfonyl)imino phenyliodinane) as the nitrogen source.[18] Evans and his group achieved a breakthrough with enantioselective catalytic nitrene transfer to olefins using PhINTs as the nitrene source.[127] This reaction utilizes bis(oxazoline) ligands and inexpensive copper (I) and copper(II) salts as catalysts. Yields of 23% to 95% with excess olefin and 5-10 mol % catalyst were reported, and cinnamate esters gave the highest enantioselectivities for these reactions. Simple olefins gave lower % ee, and ligand tuning improved selectivity with styrene.[127] Polar solvents were found to be most effective for high enantioselectivity. Jacobsen developed chiral 1,2-diimine derivatives as ligands for Cu(II) salts that were highly enantioselective (up to 98% for some substrates) catalysts for aziridination of olefins with at least one aromatic group with 5-10 % catalyst loading.[128] The systems of Evans and Jacobsen are complimentary, as Evans observed high % ee with trans olefins, whereas Jacobsen noted high % ee with cis olefins.

Another interesting development in aziridination catalysis was the discovery that the enantioselectivity of the catalyst can be imposed solely by use of a chiral counterion because it pairs closely with the cationic metal complex to create a "chiral pocket."[129] Relatively low % ee are detected with these systems (0-30%), and the enantioselectivity is dependent on the use of a non-polar solvent. Other catalysts for aziridination include copper exchanged zeolite (CuHY) with bis(oxazoline) ligands and PhINNs (*p*-nitrophenylsulfonyl iminoiodinane), which was found to yield higher enantioselectivities than the homogeneous reaction.[130, 131] Nishikori and Katsuki have developed asymmetric catalysis with an optimized salen Mn catalyst that has achieved the highest selectivity for styrene aziridination

with 94% ee.[132] Rhodium(II) systems were not effective with PhINTs as the nitrene precursor, but worked well with PhINNs with respectable % ee.[133] Ruthenium porphyrin complexes are also active for aziridination; however, Mn, Ru, and Rh also undergo a competing reaction that is desirable in other contexts: nitrogen insertion into a C-H bond.[19] More recent improvements include use of monomeric biaryl Schiff base Cu complexes with PhINTs which react in minutes to accomplish high selectivity; 99% ee for 6-acyl-2,2-dimethylchromene, and 88-98% ee with cinnamate esters.[134]

In these reactions PhINTs is used almost exclusively as the nitrene source, but is less than ideal since it is highly insoluble, somewhat expensive and tedious to make, and it gives the stoichiometric byproduct iodobenzene.[15] Other nitrene sources that have been used are Chloramine T, Bromamine T, TsN_3, PhINTs analogues with different substitution patterns on the aryl group, and generation of the PhINTs *in situ* by addition of precursors.[19] PhINNs gives improved yields as compared to PhINTs in the cases of rhodium(II) systems and the Evans bis(oxazoline) Cu systems.[135, 136] The removal of the *N*-sulfonyl group from the aziridines produced using these nitrene precursors can be difficult. Methods of removal have been investigated for certain substrates; however, ring opening is a competing and often undesirable side reaction.[137, 138] The SES group (trimethylsilylethanesufonyl) from PhINSES can be removed with CsF_2 in 89% yield.[139] *Ultimately, the development of catalytic reactions using non-tosyl nitrene sources would expand the utility of this chemistry.*

1.3.3 Mechanistic Studies

The mechanism of olefin aziridination reactions has been proposed to involve the formation of metal nitrene intermediates. Groves first postulated this in the 1983 report of stoichiometric aziridination when he observed NMR and IR evidence of an acylimido intermediate.[126] Significant efforts have been made to investigate the nature of the catalytic intermediate. Late transition-metal nitrene complexes are rare, and no copper nitrene complexes have been isolated, thus limiting the studies performed and the depth of the understanding of the mechanism. The exact oxidation state of the metal catalyst and the nature of the nitrene have been a point of unresolved debate. Pérez et al., based on Hammett studies, propose an electrophilic, paramagnetic Cu(II), radical nitrene intermediate.[140] Other Hammett studies concur on the point of an electrophilic nitrene, and postulate an early transition state with minimal charge build up.[141] Evans found that starting from either Cu(I) or Cu(II) salts had no effect upon the enantiomeric excess in the asymmetric catalysis with bis(oxazoline) ligands, therefore a common metal species and oxidation state is most likely reached in either case.[127] They proposed that the oxidation state is Cu(II) based upon UV-Vis spectra, comparing LCu(I) treated with PhINTs and the LCu(II) complex alone.[16]

Jacobsen's results also support a nitrene intermediate, analogous to the oxo intermediate observed in epoxidation catalysis, but with a Cu(I) salt as the resting state and a Cu(III) nitrene as the nitrene transfer species. An alternative proposal to the formation of a metal nitrene is the metal serving as a simple Lewis acid where the nitrogen-iodobenzene bond of PhINTs does not cleave upon nitrogen addition to the catalyst and the intermediate is a copper amido (Scheme 1.18). If the Lewis acid mechanism were active, then a change in

substituents on the phenyl ring of the iodobenzene should alter the reactivity of the catalyst. However, no change in yields or enantioselectivities was observed upon alteration of the aryl

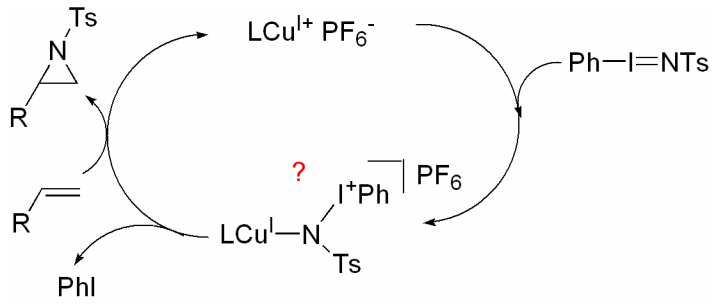

Scheme 1.18. Proposed catalytic cycle in which Cu(I) acts as a Lewis acid.

group.[142] These investigations also used tosyl azide, TsN_3, as the nitrogen source because it is known to rapidly release N_2 upon photochemical excitation. This reaction resulted in the same % ee as observed with PhINTs. These results support a discrete nitrene intermediate, and thus a Cu(I) resting state is proposed that oxidatively adds PhINTs to form a Cu(III) intermediate, which then reacts with olefin to form the aziridine and return the catalyst to the Cu(I) resting state (Scheme 1.19).

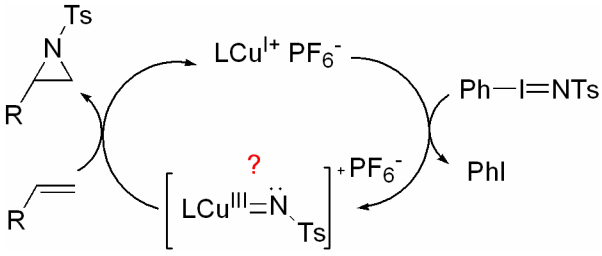

Scheme 1.19. Proposed catalytic cycle of Cu-catalyzed aziridination.

DFT calculations conclude stabilization of the M=NTs species occurs by formation of a three-membered N-S-O ring.[141] Norrby et al. predicted a different, four-membered ring transition state where Cu, N, S, and O form a ring to stabilize the nitrene intermediate,

thereby implying that the sulfonyl group is essential for catalysis.[143] Kinetic studies showed that formation of the metallanitrene was the rate-determining step. Their computational studies determined the intermediate species in the reaction to be a square planar singlet nitrene, but there was also a triplet intermediate with an elongated Cu-N bond which resembled a Cu(II) d^9 species where there was radical character (Figure 1.6). Olefin binding to nitrogen is possible because the triplet and singlet states were calculated to be of similar energy, which could account for the different concerted and radical pathways giving different selectivities with small changes in the catalyst system. Another pathway that is available is a concerted, stereospecific - in the case of highly enantioselective aziridination – or radical pathway – in the case of reactions where a cis-olefin is transformed into both the cis and the trans aziridine.[144]

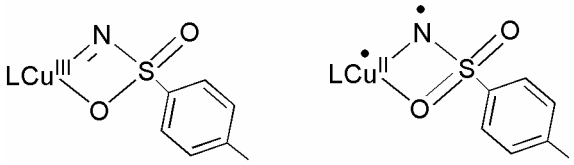

Figure 1.6. Potential tosyl-stabilized nitrene intermediate.

The Hillhouse group recently reported more direct evidence for a nitrene intermediate. They synthesized (dtbpe)Ni=NAr (dtbpe = 1,2-bis(di-*t*-butylphosphino)ethane, Ar = 2,6-di-isopropylphenyl),[71] and this species undergoes transfer of the 2,6-di-isopropylphenyl imido group to ethylene by way of a proposed nickel (II) azametallacyclobutane intermediate followed by reductive elimination to give the diisopropylphenylaziridine. This reaction occurs at 70 °C over the course of about 8 days to give 58% yield, and tests with trans-ethylene-d_2 show retention of stereochemistry, which

supports a concerted reaction mechanism.[145] The results of this study may be closely related to the chemistry observed with copper-catalyzed aziridination reactions. The isolation and reactivity studies of a copper nitrene that is active for aziridination could allow for isolation of an intermediate and kinetic studies to clarify the understanding of this mechanism and design specific catalysts for these reactions.

1.4 Summary

Late transition metals are often used to catalyze C-N bond-forming reactions with diverse substrates and under relatively mild conditions. Hydroamination and aryl amination catalysis may proceed via Cu(I) amido complexes, and Cu-catalyzed aziridination catalysis may proceed via Cu(III) nitrene intermediates. Detailed investigation of the potential intermediates and reaction mechanisms could further the development of these critical reactions. Besides potential catalytic application, many late transition-metal non-dative complexes possess significant basic and nucleophilic reactivity. The work presented herein pursues the synthesis, characterization and reactivity of Cu(I) amido complexes and Cu(III) nitrene complexes. In addition, the potential application of these complexes to catalytic C-N bond formation and mechanistic studies is investigated.

References

1. Ahlberg, P. Development of the metathesis method in organic synthesis. http://nobelprize.org/chemistry/laureates/2005/chemadv05.pdf (April 5, 2006),
2. Thayer, A., Companies Tout New Chemo- And Biocatalyst Developments. *Chem. Eng. News* March 13, **2006**, p 26.
3. Ahlberg, P. Catalytic asymmetric synthesis. http://nobelprize.org/chemistry/laureates/2001/chemadv.pdf (April 5, 2006),
4. Jia, C.; Kitamura, T.; Fujiwara, Y. *Acc. Chem. Res.* **2001,** 34, 633-639.
5. Labinger, J. A.; Bercaw, J. E. *Nature* **2002,** 417, 507-514.
6. Lail, M.; Arrowood, B. N.; Gunnoe, T. B. *J. Am. Chem. Soc.* **2003,** 125, 7506-7507.
7. Ritleng, V.; Sirlin, C.; Pfeffer, M. *Chem. Rev.* **2002,** 102, 1731-1770.
8. Hartwig, J. F., Palladium-Catalyzed Amination of Aryl Halides and Sulfonates. In *Modern amination methods*, Ricci, A., Ed. Wiley-VCH: Weinheim ; Cambridge, 2000; pp 195-262.
9. Buchwald, S. L., Practical Palladium Catalysts for C-N and C-O bond Formation. In *Top. Curr. Chem.*, Miyaura, N., Ed. Springer: Berlin, 2002; Vol. 219, pp 131-209.
10. Klapars, A.; Antilla, J. C.; Huang, X. H.; Buchwald, S. L. *J. Am. Chem. Soc.* **2001,** 123, 7727-7729.
11. Buchwald, S. L.; Klapars, A.; Antilla, J. C.; Job, G. E.; Wolter, M.; Kwong, F. Y.; Nordmann, G.; Hennessy, E. J. Copper-Catalyzed Formation of Carbon-Heteroatom and Carbon-Carbon Bonds. U.S. Patent 6,759,554, July 6, 2004.
12. Hartwig, J. F. *Acc. Chem. Res.* **1998,** 31, 852-860.
13. Louie, J.; Paul, F.; Hartwig, J. F. *Organometallics* **1996,** 15, 2794-2805.
14. Driver, M. S.; Hartwig, J. F. *J. Am. Chem. Soc.* **1997,** 119, 8232-8245.
15. Jacobsen, E. N., Aziridination. In *Comprehensive Asymmetric Catalysis II*, Jacobsen, E. N.; Pfaltz, A.; Yamamoto, H., Eds. Springer: New York, 1999; pp 607-618.
16. Evans, D. A.; Bilodeau, M. T.; Faul, M. M. *J. Am. Chem. Soc.* **1994,** 116, 2742-2753.
17. Lebel, H.; Huard, K.; Lectard, S. *J. Am. Chem. Soc.* **2005,** 127, 14198-14199.
18. Mansuy, D.; Mahy, J. P.; Dureault, A.; Bedi, G.; Battioni, P. *Chem. Commun.* **1984**, 1161-1163.
19. Muller, P.; Fruit, C. *Chem. Rev.* **2003,** 103, 2905-2919.
20. Bryndza, H. E.; Tam, W. *Chem. Rev.* **1988,** 88, 1163-1188.
21. Jayaprakash, K. N.; Conner, D.; Gunnoe, T. B. *Organometallics* **2001,** 20, 5254-5256.
22. Fulton, J. R.; Bouwkamp, M. W.; Bergman, R. G. *J. Am. Chem. Soc.* **2000,** 122, 8799-8800.
23. Fulton, J. R.; Sklenak, S.; Bouwkamp, M. W.; Bergman, R. G. *J. Am. Chem. Soc.* **2002,** 124, 4722-4737.
24. Soper, J. D.; Bennett, B. K.; Lovell, S.; Mayer, J. M. *Inorg. Chem.* **2001,** 40, 1888-1893.
25. Pearson, R. G. *J. Am. Chem. Soc.* **1963,** 85, 3533-3539.
26. Bryndza, H. E.; Fong, L. K.; Paciello, R. A.; Tam, W.; Bercaw, J. E. *J. Am. Chem. Soc.* **1987,** 109, 1444-1456.

27. Holland, P. L.; Andersen, R. A.; Bergman, R. G.; Huang, J. K.; Nolan, S. P. *J. Am. Chem. Soc.* **1997,** 119, 12800-12814.
28. Fulton, J. R.; Holland, A. W.; Fox, D. J.; Bergman, R. G. *Acc. Chem. Res.* **2002,** 35, 44-56.
29. Conner, D.; Jayaprakash, K. N.; Gunnoe, T. B.; Boyle, P. D. *Inorg. Chem.* **2002,** 41, 3042-3049.
30. Mayer, J. M. *Comments Inorg. Chem.* **1988,** 8, 125-135.
31. Caulton, K. G. *New J. Chem.* **1994,** 18, 25-41.
32. Holland, P. L.; Andersen, R. A.; Bergman, R. G. *Comments Inorg. Chem.* **1999,** 21, 115-129.
33. Wigley, D. E., Organoimido Complexes of the Transition-Metals. In *Prog. Inorg. Chem.*, 1994; Vol. 42, pp 239-482.
34. Nugent, W. A.; Mayer, J. M., *Metal-ligand multiple bonds : the chemistry of transition metal complexes containing oxo, nitrido, imido, alkylidene, or alkylidyne ligands*. Wiley: New York, 1988.
35. Chen, H.; Olmstead, M. M.; Shoner, S. C.; Power, P. P. *J. Chem. Soc., Dalton Trans.* **1992**, 451-457.
36. Hope, H.; Power, P. P. *Inorg. Chem.* **1984,** 23, 936-937.
37. Power, P. P. *Prog. Inorg. Chem.* **1991,** 39, 75-112.
38. Gambarotta, S.; Bracci, M.; Floriani, C.; Chiesivilla, A.; Guastini, C. *J. Chem. Soc., Dalton Trans.* **1987**, 1883-1888.
39. Tsuda, T.; Miwa, M.; Saegusa, T. *J. Org. Chem.* **1979,** 44, 3734-3736.
40. Tsuda, T.; Watanabe, K.; Miyata, K.; Yamamoto, H.; Saegusa, T. *Inorg. Chem.* **1981,** 20, 2728-2730.
41. Kitagawa, Y.; Oshima, K.; Yamamoto, H.; Nozaki, H. *Tetrahedron Lett.* **1975**, 1859-1862.
42. Harkins, S. B.; Peters, J. C. *J. Am. Chem. Soc.* **2004,** 126, 2885-2893.
43. James, A. M.; Laxman, R. K.; Fronczek, F. R.; Maverick, A. W. *Inorg. Chem.* **1998,** 37, 3785-3791.
44. Link, H.; Reiss, P.; Chitsaz, S.; Pfistner, H.; Fenske, D. *Z. Anorg. Allg. Chem.* **2003,** 629, 755-768.
45. Reiß, P.; Fenske, D. *Z. Anorg. Allg. Chem.* **2000,** 626, 1317-1331.
46. Keen, A. L.; Doster, M.; Han, H.; Johnson, S. A. *Chem. Commun.* **2006**, 1221-1223
47. Nyburg, S. C.; Parkins, A. W.; Sidi-Boumedine, M. *Polyhedron* **1993,** 12, 1119-1122.
48. Fiaschi, P.; Floriani, C.; Pasquali, M.; Chiesi-Villa, A.; Guastini, C. *Chem. Commun.* **1984**, 888-890.
49. Mankad, N. P.; Laitar, D. S.; Sadighi, J. P. *Organometallics* **2004,** 23, 3369-3371.
50. Osakada, K.; Takizawa, T.; Tanaka, M.; Yamamoto, T. *J. Organomet. Chem.* **1994,** 473, 359-369.
51. Dai, X. L.; Warren, T. H. *Chem. Commun.* **2001**, 1998-1999.
52. Gultneh, Y.; Karlin, K. D., Binding and Activation of Molecular Oxygen by Copper Complexes. In *Prog. Inorg. Chem.*, Lippard, S. J., Ed. John Wiley and Sons: New York, 1987; Vol. 35, pp 219-327.

53. Mahapatra, S.; Halfen, J. A.; Wilkinson, E. C.; Pan, G. F.; Wang, X. D.; Young, V. G.; Cramer, C. J.; Que, L.; Tolman, W. B. *J. Am. Chem. Soc.* **1996,** 118, 11555-11574.
54. Dewey, M. A.; Knight, D. A.; Arif, A.; Gladysz, J. A. *Chem. Ber.* **1992,** 125, 815-824.
55. Tahmassebi, S. K.; McNeil, W. S.; Mayer, J. M. *Organometallics* **1997,** 16, 5342-5353.
56. Fox, D. J.; Bergman, R. G. *J. Am. Chem. Soc.* **2003,** 125, 8984-8985.
57. Joslin, F. L.; Johnson, M. P.; Mague, J. T.; Roundhill, D. M. *Organometallics* **1991,** 10, 41-43.
58. Kaplan, A. W.; Ritter, J. C. M.; Bergman, R. G. *J. Am. Chem. Soc.* **1998,** 120, 6828-6829.
59. Conner, D.; Jayaprakash, K. N.; Cundari, T. R.; Gunnoe, T. B. *Organometallics* **2004,** 23, 2724-2733.
60. Campora, J.; Palma, P.; delRio, D.; Conejo, M. M.; Alvarez, E. *Organometallics* **2004,** 23, 5653-5655.
61. Rais, D.; Bergman, R. G. *Chem. -Eur. J.* **2004,** 10, 3970-3978.
62. Zhao, J.; Goldman, A. S.; Hartwig, J. F. *Science* **2005,** 307, 1080 -1082.
63. Campora, J.; Matas, I.; Palma, P.; Graiff, C.; Tiripicchio, A. *Organometallics* **2005,** 24, 2827-2830.
64. Conner, D.; Jayaprakash, K. N.; Wells, M. B.; Manzer, S.; Gunnoe, T. B.; Boyle, P. D. *Inorg. Chem.* **2003,** 42, 4759-4772.
65. Driver, M. S.; Hartwig, J. F. *Organometallics* **1997,** 16, 5706-5715.
66. Cinellu, M. A.; Minghetti, G.; Pinna, M. V.; Stoccoro, S.; Zucca, A.; Manassero, M. *Eur. J. Inorg. Chem.* **2003**, 2304-2310.
67. Cinellu, M. A.; Minghetti, G.; Pinna, M. V.; Stoccoro, S.; Zucca, A.; Manassero, M. *J. Chem. Soc., Dalton Trans.* **1999**, 2823-2831.
68. Krug, C.; Hartwig, J. F. *J. Am. Chem. Soc.* **2004,** 126, 2694-2695.
69. Casalnuovo, A. L.; Calabrese, J. C.; Milstein, D. *J. Am. Chem. Soc.* **1988,** 110, 6738-6744.
70. Hartwig, J. F.; Andersen, R. A.; Bergman, R. G. *Organometallics* **1991,** 10, 1875-1887.
71. Mindiola, D. J.; Hillhouse, G. L. *J. Am. Chem. Soc.* **2001,** 123, 4623-4624.
72. Fox, D. J.; Bergman, R. G. *Organometallics* **2004,** 23, 1656-1670.
73. Jayaprakash, K. N.; Gunnoe, T. B.; Boyle, P. D. *Inorg. Chem.* **2001,** 40, 6481-6486.
74. Albeniz, A. C.; Calle, V.; Espinet, P.; Gomez, S. *Inorg. Chem.* **2001,** 40, 4211-4216.
75. Roundhill, D. M. *Chem. Rev.* **1992,** 92, 1-27.
76. Daemmrich, A.; Bowden, M. E., A Rising Drug Industry. *Chem. Eng. News.* June 20, **2005**, pp 28-42.
77. Marasco, C., Salbutamol. *Chem. Eng. News* June 20, **2005**, p 114.
78. Carey, F. A., *Organic Chemistry*. 3rd ed.; McGraw-Hill: New York, 1996.
79. Muller, T. E.; Beller, M. *Chem. Rev.* **1998,** 98, 675-703.
80. Abouabdellah, A.; Dodd, R. H. *Tetrahedron Lett.* **1998,** 39, 2119-2122.
81. Hennessy, E. J.; Buchwald, S. L. *J. Org. Chem.* **2005,** 70, 7371-7375.
82. Kosugi, M.; Kameyama, M.; Migita, T. *Chem. Lett.* **1983**, 927-928.

83. Louie, J.; Hartwig, J. F. *Tetrahedron Lett.* **1995,** 36, 3609-3612.
84. Guram, A. S.; Rennels, R. A.; Buchwald, S. L. *Angew. Chem., Int. Ed. Eng.* **1995,** 34, 1348-1350.
85. Wolfe, J. P.; Wagaw, S.; Marcoux, J. F.; Buchwald, S. L. *Acc. Chem. Res.* **1998,** 31, 805-818.
86. Old, D. W.; Wolfe, J. P.; Buchwald, S. L. *J. Am. Chem. Soc.* **1998,** 120, 9722-9723.
87. Grasa, G. A.; Viciu, M. S.; Huang, J.; Nolan, S. P. *J. Org. Chem.* **2001,** 66, 7729-7737.
88. Marion, N.; Ecarnot, E. C.; Navarro, O.; Amoroso, D.; Bell, A.; Nolan, S. P. *J. Org. Chem.* **2006,** 71, 3816-3821.
89. Marion, N.; Navarro, O.; Mei, J.; Stevens, E. D.; Scott, N. M.; Nolan, S. P. *J. Am. Chem. Soc.* **2006,** 128, 4101 - 4111.
90. Desmarets, C.; Schneider, R.; Fort, Y. *J. Org. Chem.* **2002,** 67, 3029-3036.
91. Chen, C.; Yang, L. M. *Org. Lett.* **2005,** 7, 2209-2211.
92. Shekhar, S.; Ryberg, P.; Hartwig, J. F.; Mathew, J. S.; Blackmond, D. G.; Strieter, E. R.; Buchwald, S. L. *J. Am. Chem. Soc.* **2006,** 128, 3584-3591.
93. Alcazar-Roman, L. M.; Hartwig, J. F.; Rheingold, A. L.; Liable-Sands, L. M.; Guzei, I. A. *J. Am. Chem. Soc.* **2000,** 122, 4618-4630.
94. Monthly average prices. http://www.lme.co.uk/dataprices_monthlyaverages.asp (4/30/06),
95. Past Historical London Fix. http://www.kitco.com/gold.londonfix.html (4/30/06),
96. Ullmann, F. *Ber. Dtsch. Chem. Ges.* **1903,** 36, 2382-2384.
97. Ley, S. V.; Thomas, A. W. *Angew. Chem., Int. Ed. Eng.* **2003,** 42, 5400-5449.
98. Lindley, J. *Tetrahedron* **1984,** 40, 1433-1456.
99. Gujadhur, R. K.; Bates, C. G.; Venkataraman, D. *Org. Lett.* **2001,** 3, 4315-4317.
100. Kwong, F. Y.; Klapars, A.; Buchwald, S. L. *Org. Lett.* **2002,** 4, 581-584.
101. Klapars, A.; Huang, X. H.; Buchwald, S. L. *J. Am. Chem. Soc.* **2002,** 124, 7421-7428.
102. Antilla, J. C.; Klapars, A.; Buchwald, S. L. *J. Am. Chem. Soc.* **2002,** 124, 11684-11688.
103. Huang, X. H.; Anderson, K. W.; Zim, D.; Jiang, L.; Klapars, A.; Buchwald, S. L. *J. Am. Chem. Soc.* **2003,** 125, 6653-6655.
104. Strieter, E. R.; Blackmond, D. G.; Buchwald, S. L. *J. Am. Chem. Soc.* **2005,** 127, 4120 -4121.
105. Paine, A. J. *J. Am. Chem. Soc.* **1987,** 109, 1496-1502.
106. Beller, M.; Seayad, J.; Tillack, A.; Jiao, H. *Angew. Chem., Int. Ed. Eng.* **2004,** 43, 3368-3398.
107. Schlummer, B.; Hartwig, J. F. *Org. Lett.* **2002,** 4, 1471-1474.
108. Anderson, L. L.; Arnold, J.; Bergman, R. G. *J. Am. Chem. Soc.* **2005,** 127.
109. Stewart, I. C.; Bergman, R. G.; Toste, F. D. *J. Am. Chem. Soc.* **2003,** 125, 8696-8697.
110. Hong, S.; Marks, T. J. *Acc. Chem. Res.* **2004,** 37, 673-686.
111. Hong, S.; Marks, T. J. *J. Am. Chem. Soc.* **2002,** 124, 7886-7887.
112. Ryu, J. S.; Li, G. Y.; Marks, T. J. *J. Am. Chem. Soc.* **2003,** 125, 12584-12605.
113. Kawatsura, M.; Hartwig, J. F. *J. Am. Chem. Soc.* **2000,** 122, 9546-9547.

114. Utsunomiya, M.; Kuwano, R.; Kawatsura, M.; Hartwig, J. F. *J. Am. Chem. Soc.* **2003,** 125, 5608-5609.
115. Hartwig, J. F. *Pure Appl. Chem.* **2004,** 76, 507-516.
116. Johns, A. M.; Utsunomiya, M.; Incarvito, C. D.; Hartwig, J. F. *J. Am. Chem. Soc.* **2006,** 128, 1828-1839.
117. Takemiya, A.; Hartwig, J. F. *J. Am. Chem. Soc.* **2006,** 128, 6042-6043.
118. Fadini, L.; Togni, A. *Chem. Commun.* **2003**, 30-31.
119. Dai, X.; Kapoor, P.; Warren, T. H. *J. Am. Chem. Soc.* **2004,** 126, 4798-4799.
120. Kogut, E.; Wiencko, H. L.; Zhang, L.; Cordeau, D. E.; Warren, T. H. *J. Am. Chem. Soc.* **2005,** 127, 11248-11249.
121. Brown, S. D.; Betley, T. A.; Peters, J. C. *J. Am. Chem. Soc.* **2003,** 125, 322-323.
122. Walsh, P. J.; Hollander, F. J.; Bergman, R. G. *J. Am. Chem. Soc.* **1988,** 110, 8729-8731.
123. Danopoulos, A. A.; Wilkinson, G.; Hussain-Bates, B.; Hursthouse, M. B. *Polyhedron* **1992,** 11, 2961-2964.
124. Tanner, D. *Angew. Chem., Int. Ed. Eng.* **1994,** 33, 599-619.
125. Kolb, H. C.; Finn, M. G.; Sharpless, K. B. *Angew. Chem., Int. Ed. Eng.* **2001,** 40, 2004-2021.
126. Groves, J. T.; Takahashi, T. *J. Am. Chem. Soc.* **1983,** 105, 2073-2074.
127. Evans, D. A.; Faul, M. M.; Bilodeau, M. T.; Anderson, B. A.; Barnes, D. M. *J. Am. Chem. Soc.* **1993,** 115, 5328-5329.
128. Li, Z.; Conser, K. R.; Jacobsen, E. N. *J. Am. Chem. Soc.* **1993,** 115, 5326-5327.
129. Llewellyn, D. B.; Adamson, D.; Arndtsen, B. A. *Org. Lett.* **2000,** 2, 4165-4168.
130. Taylor, S.; Gullick, J.; McMorn, P.; Bethell, D.; Page, P. C. B.; Hancock, F. E.; King, F.; Hutchings, G. J. *J. Chem. Soc., Perkin Trans. 2* **2001**, 1714-1723.
131. Gullick, J.; Taylor, S.; McMorn, P.; Bethell, D.; Page, P. C. B.; Hancock, F. E.; King, F.; Hutchings, G. *J. Mol. Catal. A: Chem.* **2002,** 180, 85-89.
132. Nishikori, H.; Katsuki, T. *Tetrahedron Lett.* **1996,** 37, 9245-9248.
133. Müller, P.; Baud, C.; Jacquier, Y.; Moran, M.; Nägeli, I. *Journal of Physical Organic Chemistry* **1996,** 9, 341-347.
134. Gillespie, K. M.; Sanders, C. J.; O'Shaughnessy, P.; Westmoreland, I.; Thickitt, C. P.; Scott, P. *J. Org. Chem.* **2002,** 67, 3450-3458.
135. Sodergren, M. J.; Alonso, D. A.; Andersson, P. G. *Tetrahedron: Asymmetry* **1997,** 8, 3563-3565.
136. Sodergren, M. J.; Alonso, D. A.; Bedekar, A. V.; Andersson, P. G. *Tetrahedron Lett.* **1997,** 38, 6897-6900.
137. Bergmeier, S. C.; Seth, P. P. *Tetrahedron Lett.* **1999,** 40, 6181-6184.
138. Alonso, D. A.; Andersson, P. G. *J. Org. Chem.* **1998,** 63, 9455-9461.
139. Aggarwal, V. K.; Thompson, A.; Jones, R. V. H.; Standen, M. C. H. *J. Org. Chem.* **1996,** 61, 8368-8369.
140. Diaz-Requejo, M. M.; Peréz, P. J.; Brookhart, M.; Templeton, J. L. *Organometallics* **1997,** 16, 4399-4402.
141. Gillespie, K. M.; Crust, E. J.; Deeth, R. J.; Scott, P. *Chem. Commun.* **2001**, 785-786.
142. Li, Z.; Quan, R. W.; Jacobsen, E. N. *J. Am. Chem. Soc.* **1995,** 117, 5889-5890.

143. Brandt, P.; Sodergren, M. J.; Andersson, P. G.; Norrby, P. O. *J. Am. Chem. Soc.* **2000,** 122, 8013-8020.
144. Zhang, W.; Lee, N. H.; Jacobsen, E. N. *J. Am. Chem. Soc.* **1994,** 116, 425-426.
145. Waterman, R.; Hillhouse, G. L. *J. Am. Chem. Soc.* **2003,** 125, 13350-13351.

Chapter 2: Synthesis and Reactivity of Phosphine-Ligated Copper(I) Halide, Anilido, and Methyl Complexes

Late transition-metal M-X (X = N, O) bonds can be highly reactive, but there are very few monomeric, well defined Cu-X complexes. Copper amido and nitrene complexes are anticipated to be highly reactive and useful towards C-X bond-forming reactions, and Cu-R (R = C, H) complexes may form in these catalytic cycles. The goal of this chemistry is to isolate well-defined, tunable monomeric Cu-X and Cu-R systems. The chemistry presented herein focuses initially on the synthesis and characterization of new copper(I) halide complexes with bulky, donating phosphine ligands. These complexes were utilized as substrates for the synthesis of novel monomeric non-dative copper(I) complexes, and the fundamental and catalytic reactivity of these complexes is described, including hydroamination catalysis and attempts to synthesize a copper(III) nitrene. In addition to the non-dative complexes synthesized, the synthesis and reactivity of a copper(I) methyl complex were investigated for potential C-H activation.

2.1 Ligand Rationale

An important aspect of the successful isolation of the proposed Cu systems was ancillary ligand identity. Of particular interest is the ability of the ligand to enforce a predilection toward monomeric species without inhibiting reactivity. In addition, the ligand donating ability and symmetry can possibly help maximize metal-amido/nitrene bonding interactions.

Chelating bisphosphine ligands establish the appropriate $[L_2Cu\text{-}X]^n$ (X = NR_2, NR) structure that will leave the necessary orbitals vacant for Cu(I) to π-interact with an amido ligand and for Cu(III) to form π-bonding with a nitrene (Figure 2.1). The $3a_1$ orbital can bond with the amido σ-donor pair, and the $2b_1$ orbital, which is a relatively low-lying p-orbital, can potentially accept lone pair donation. Phosphine ligands were chosen because of their flexible donating ability and the variety of bite angles and geometries available. For example, systematic variation of the P-Cu-P bond angle impacts the energy of 3a, and presumably would influence the $Cu\text{-}N_{amido}$ σ-bonding and, hence, amido reactivity. Monophosphines have been categorized by Tolman in terms of their electronic effects (χ) and in terms of their steric effects by the ligand cone angle (θ).[1] Tolman's studies recognized the importance of sterics in these phosphine ligands in that they can affect orbital overlap as well as alter reactivity due to steric crowding. Piet van Leeuwen and coworkers have extended this concept to the popular bisphosphine ligands,[2] which is where our interests lie due to the $L_2Cu\text{-}X$ structure sought.

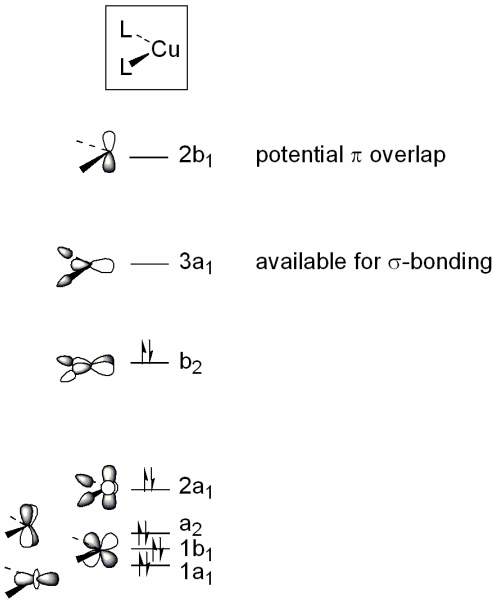

Figure 2.1. Partial molecular orbitals of C_{2v} d^{10} Cu (I): set up to σ- and possibly π- bond with NR_2 group.

2.2 Synthesis of Cu(I) Halide Complexes and Macrocycle

One useful class of chelating phosphine ligands are the PCP (PCP = 2,6-$(CH_2PR_2)_2C_6H_3$ {R = ^{t}Bu or ^{i}Pr}) "pincer" ligands that coordinate in a meridional fashion to metal centers.[3] Complexes possessing these ligands have been found to have high catalytic activity for dehydrogenation and are thermally stable.[4-7] In our group, they have allowed the isolation of a five-coordinate unsaturated Ru(II) amido complex and amidinate complexes.[8, 9] These ligands are typically used in the monoanionic, meridionally coordinating form; however, we sought a neutral two-coordinate donating phosphine ligand and thus utilized the PCHP (PCHP = 1,3-$(CH_2P^tBu_2)_2C_6H_4$) form of the ligand.

PCHP was reacted with CuCl to make a precursor for the preparation of amido complexes via amide-chloride metathesis. When CuCl is added slowly to an excess of PCHP ligand, a multinuclear complex with six CuCl units and six bridging, bis-chelating

phosphine ligands is formed (Scheme 2.1).[10] Multinuclear Cu and Au complexes often exhibit novel photophysical, electrochemical, and magnetic properties.[11-17] This complex crystallizes in a unique structure and in the solid state as a macrocycle that incorporates 48 atoms into the large ring structure (if the aryl moieties are each counted as contributing 3 atoms to the macrocycle) and in which each copper atom is bound by phosphorus atoms from two different PCHP ligands. The macrocycles stack such that a channel with an inner diameter of 4.5 Å and an outer diameter approximately 24 Å is formed and runs throughout the crystal (Figure 2.2, Figure 2.3). At the center of the cylinder are chains of disordered acetonitrile molecules, one per copper macrocycle, which coincide with the threefold symmetry axis. Nine disordered CH_2Cl_2 molecules per copper macrocycle occupy sites within the channel and surrounding the clusters. The Cu-P1 and Cu-P2 bond lengths are 2.2598(4) and 2.639(5) Å respectively, and 2.2591(5) and 2.2627(5) Å for a second unique molecule (Figure 2.4, Table 2.1). The Cu-Cl bond lengths for the two molecules are 2.3235(5) Å and 2.3293(5). The coordination geometry is distorted trigonal planar with P2-Cu-P1, P2-Cu-Cl, and P1-Cu-Cl bond angles of 147.10(2), 107.39(2), and 105.5(2) (146.28(2), 106.747(17), and 106.97(2) for the second unique molecule), respectively. The novel structure of this complex is a result of the large bite angle of the PCHP ligand.

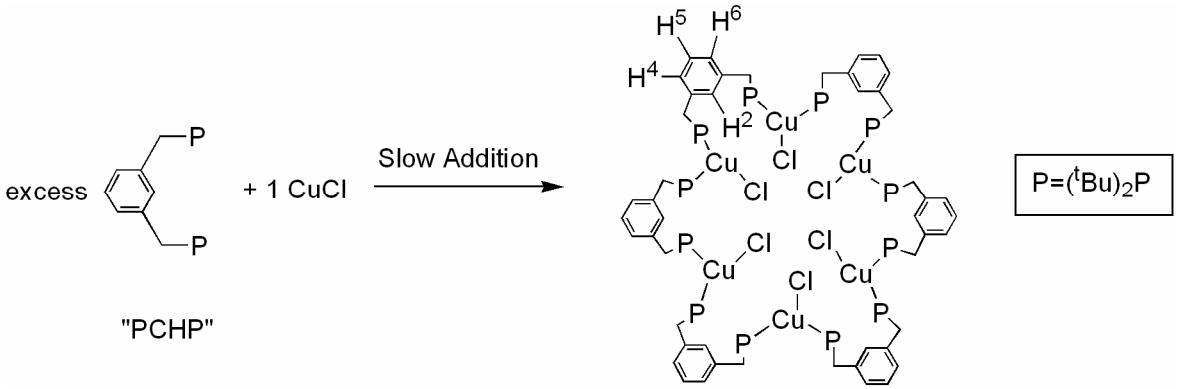

Scheme 2.1. Synthesis of hexanuclear complex of $[Cu_6Cl_6(\mu\text{-PCHP})_6]$.

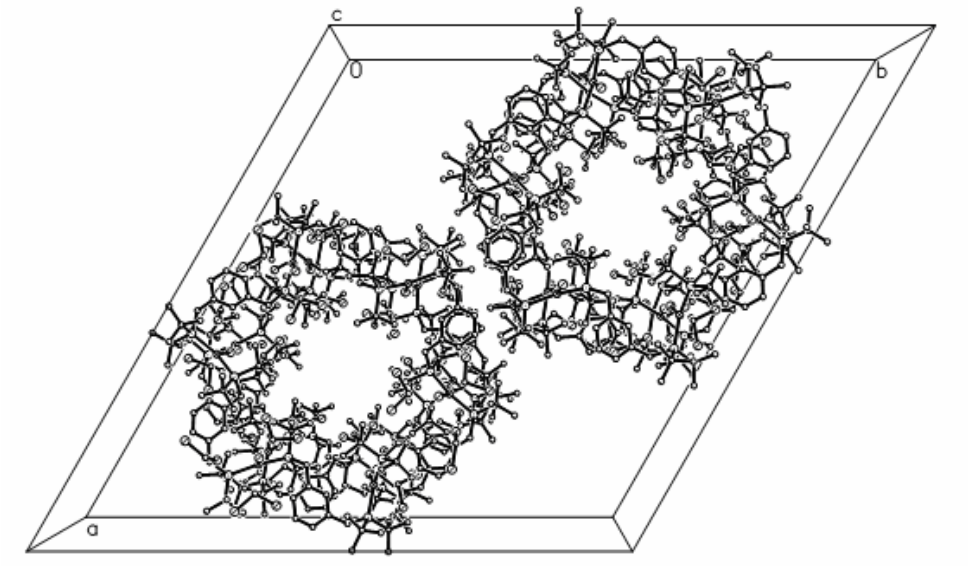

Figure 2.2. View of stacked molecules of hexanuclear complex $[Cu_6Cl_6(\mu\text{-PCHP})_6]$.

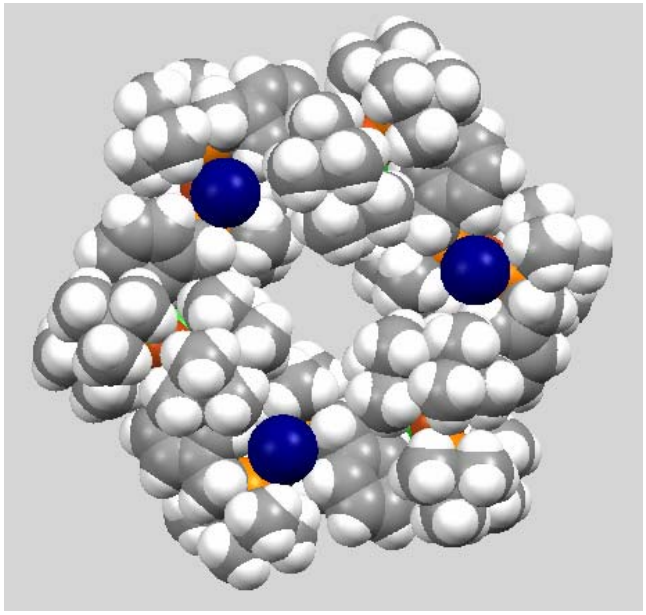

Figure 2.3. Space-filling model of hexanuclear complex $[Cu_6Cl_6(\mu\text{-PCHP})_6]$.

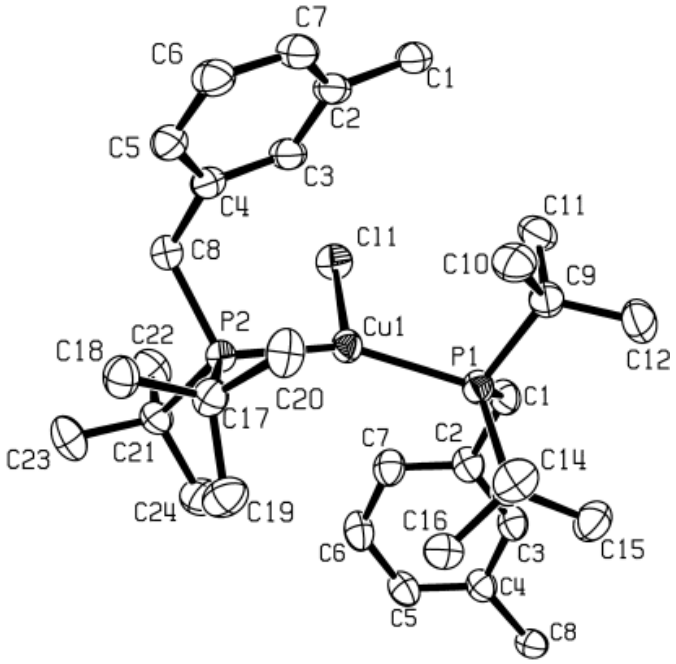

Figure 2.4. ORTEP of one asymmetric unit of $[Cu_6Cl_6(\mu\text{-PCHP})_6]$ (30% probability). Selected Bond Distances (Å): Cu(1)-P(1), 2.2639(5); Cu(1)-Cl(1), 2.3235(5); Cu(1)-P(2), 2.2598(4). Selected Bond Angles (º): C(1)-P(1)-Cu(1), 108.94(6); P(1)-Cu(1)-Cl(1), 105.50(2); P(2)-Cu(1)-P(1), 147.10(2); P(2)-Cu(1)-Cl(1), 107.38(2).

Table 2.1. Selected crystallographic data and collection parameters for $[Cu_6Cl_6(\mu\text{-PCHP})_6]$.

	$[Cu_6Cl_6(\mu\text{-PCHP})_6]\cdot CH_3CN$
empirical formula	$C_{155}H_{285}C_{l24}Cu_6N_1P_{12}$
formula wt	3766.52
crystal system	rhombohedral
space group	*R*-3
a, Å	41.098(2)
b, Å	41.098(2)
c, Å	20.512(1)
β, °	90.0
V (Å^3)	30005(3)
Z	6
D_{calcd}, g cm^{-3}	1.251
crystal size (mm)	0.30 × 0.26 × 0.22
*R*1, w*R*2 {I>2σ(I)}	0.0325, 0.0811
GOF	1.025

Variable temperature ^{1}H NMR analyses of $[Cu_6Cl_6(\mu\text{-PCHP})_6]$ revealed a fluxional process. At ambient temperature (10-25 °C) spectra consistent overall D_{6h} symmetry are observed. For example, the methylene and ^{t}Bu protons of the PCHP ligand are equivalent, indicating mirror symmetry (Figure 2.5). At –10°C, sharp resonances were observed with a singlet at δ = 8.68 ppm (aromatic H2), doublets at δ = 8.25 and 7.04 ppm (aromatic H4 and H6), a triplet at δ = 7.13 ppm (aromatic H5), multiplets at approximately δ = 3.0 ppm corresponding to the methylene protons, and four phosphine ^{t}Bu resonances between δ = 1.0 and 1.8 ppm (Figure 2.6). The aromatic C2-H2 (See Scheme 2.1 for labeling) bonds remain intact as indicated by the downfield resonance at δ = 8.68 ppm. Therefore, the ^{1}H NMR spectrum obtained at -10 °C is consistent with C_6 molecular symmetry, with all six PCHP ligands equivalent and a lack of mirror symmetry (all methylene protons and ^{t}Bu groups are

inequivalent). The $\Delta G_{298}^{\ddagger}$ = 12.2 kcal/mol for this exchange was calculated using line broadening.

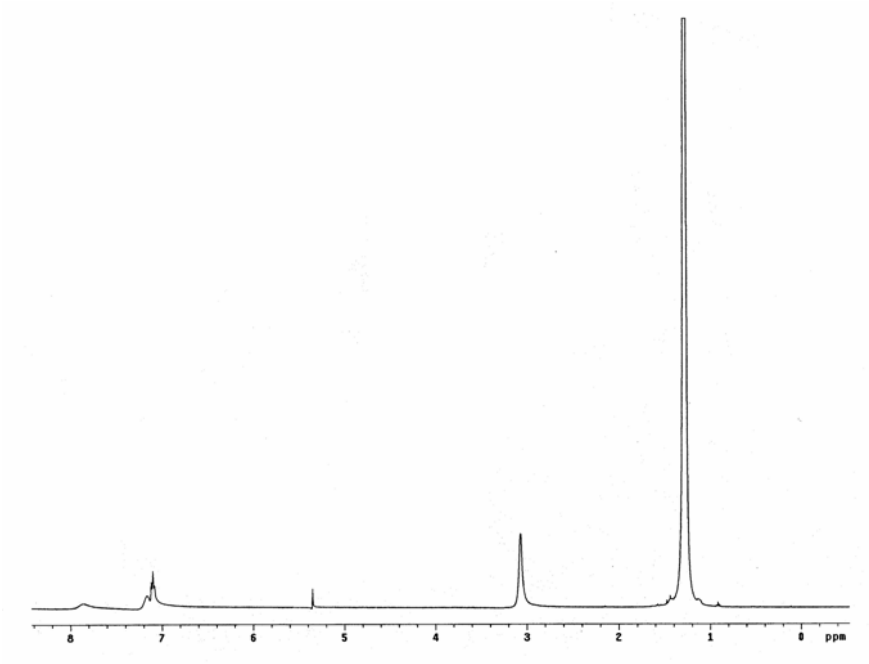

Figure 2.5. ^{1}H NMR of macrocycle $[Cu_6Cl_6(\mu\text{-PCHP})_6]$ at room temperature suggesting D_{6h} molecular symmetry.

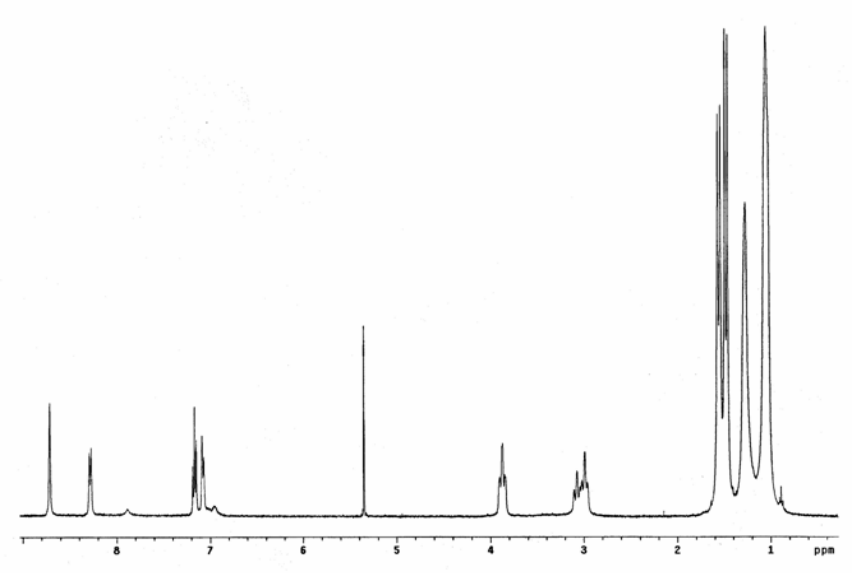

Figure 2.6. ^{1}H NMR spectrum of macrocycle $[Cu_6Cl_6(\mu\text{-PCHP})_6]$ at -10 °C suggesting C_6 molecular symmetry.

At temperatures less than -10 °C the ^{1}H NMR spectra broaden, presumably as a result of the conversion from C_6 to lower molecular symmetry; however, the slow exchange regime was not accessed at -70 °C. The ^{31}P NMR spectra (CD_2Cl_2) obtained between -10 °C and room temperature are consistent with the suggested fluxionality of $[Cu_6Cl_6(\mu\text{-PCHP})_6]$. At -10 °C, the ^{31}P NMR spectrum reveals an AB pattern (J = 126 Hz) with resonances at δ = 38.6 and 36.4 ppm, which is consistent with C_6 molecular symmetry (that is, the two phosphorus atoms on each copper atom are inequivalent). When a solution of the macrocyclic complex in C_6D_6 was warmed to 70 °C, the signals coalesced into a single broad phosphine resonance.

The emission spectra of $[Cu_6Cl_6(\mu\text{-PCHP})_6]$ showed a maximum fluorescence at 354 nm and the λ_{max} of the electronic spectra was at 232 nm ($\varepsilon = 1.07\text{x}10^5$ L mol^{-1} cm^{-1}). This electronic transition corresponds well with the $[Cu_2(dcpm)_2]X_2$ (dcpm = bis(dicyclohexyl-

phosphino)methane, X = ClO_4^-, PF_6^- or I^-) complexes prepared by Che et al. and is thought to be a 3d $\rightarrow$ 4s metal-metal transition.[18] When reacted with lithium amides; however, metathesis was not successful, most likely due to the stable structure of the hexamer and the steric bulk around the metal centers. In addition, the large bite angle of PCHP does not result in monomeric copper complexes.

2.3 Synthesis of a Copper(I) Anilido Complex

Due to the bridging complexes observed with the PCHP ligand, attention was shifted to bis-chelating phosphine ligands with smaller bite angles (average P-M-P bond angle). The ligand BINAP (BINAP = 2,2'-bis(diphenylphosphino)-1,1'-binaphthyl), with a bite angle of 92.77°,[2] was used to synthesize and fully characterize (BINAP)CuOTf and [(BINAP)Cu(NCMe)][PF_6]. Attempts to convert these complexes to copper amido complexes by reacting them with lithium amides, sodium amides and with combinations of amines and bases resulted in all cases in liberation of free BINAP and reduction of the metal center to Cu(0), as observed by a copper mirror on the glassware (Scheme 2.2). These results are likely due to the reduced electron donating ability of aryl phosphine ligands compared to alkyl phosphine ligands. Thus, it was necessary to introduce more donating ligands in an effort to inhibit reduction of Cu(I).

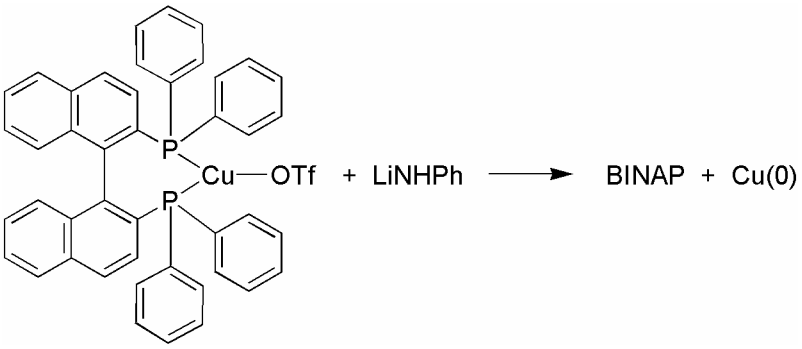

Scheme 2.2. Reaction of (BINAP)CuCl with LiNHPh.

The ligand dtbpe (dtbpe = 1,2-bis(di-*tert*-butylphosphino)ethane) was identified as a suitable candidate given its relatively small bite angle (89.74°) and strongly donating nature.[2] The *t*-butyl groups also have the added advantage of being bulky so as to provide protection of the metal center from dimerization. The complexes $[(dtbpe)Cu(\mu\text{-}Cl)]_2$ and $[(dtbpe)Cu(NCMe)][PF_6]$ were synthesized as possible precursors for amido systems. These complexes were characterized by ^{1}H, ^{13}C and ^{31}P NMR, cyclic voltammetry and elemental analysis (^{1}H NMRs: $[(dtbpe)Cu(\mu\text{-}Cl)]_2$, Figure 2.7; $[(dtbpe)Cu(NCMe)][PF_6]$, Figure 2.8). The ^{1}H NMR spectrum of these complexes reveal coupling of the *tert*-butyl methyl protons to the phosphorus as virtual triplets. The oxidations for the Cu(II/I) couple for $[(dtbpe)Cu(\mu\text{-}Cl)]_2$ and $[(dtbpe)Cu(NCMe)][PF_6]$ were both reversible ($E_{1/2}$ = 0.88 V and $E_{1/2}$ = 1.29 V respectively). The IR active C≡N stretch was present at 2276 cm^{-1}. The solid-state structure of the copper chloride complex was shown to be a dimer with approximately tetrahedral metal centers using X-ray crystallography of a single crystal (Figure 2.9, Table 2.2). The distorted tetrahedron reveals bond angles about the Cu metal center of 95.73(3)° and 94.40(3)° for the Cl-Cu-Cl bond angle and P-Cu-P bond angle, respectively. The Cl1-Cu-P1 and Cl1-Cu-P2 bond angles are 118.71(3)° and 115.23(3)°, respectively. The Cu-Cl bond

distance is 2.3844(9) Å, and the two Cu-P bond distances are very similar, Cu1-P1, 2.2863(8) Å and Cu1-P2, 2.2832(9) Å.

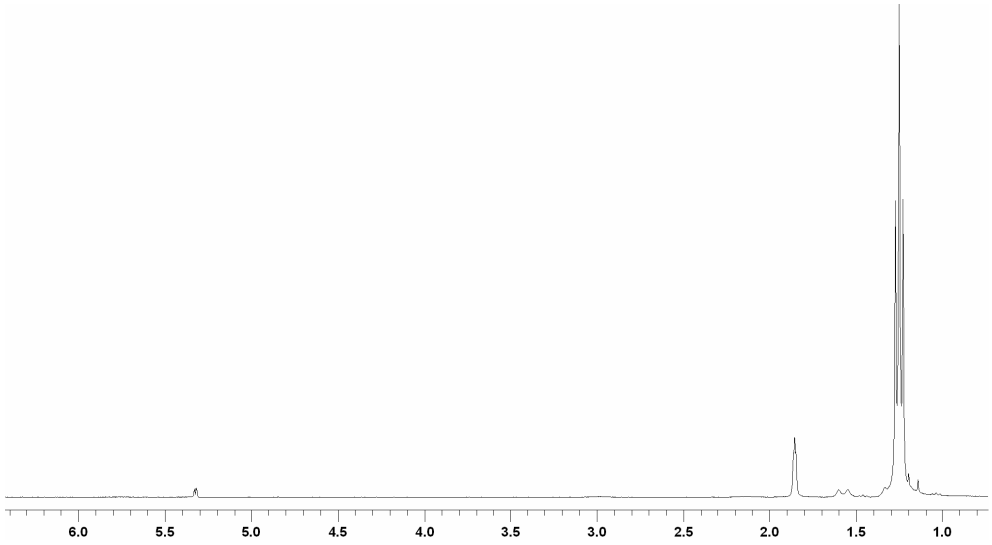

Figure 2.7. ^{1}H NMR spectrum of $[(dtbpe)Cu(\mu\text{-}Cl)]_2$ in CD_2Cl_2.

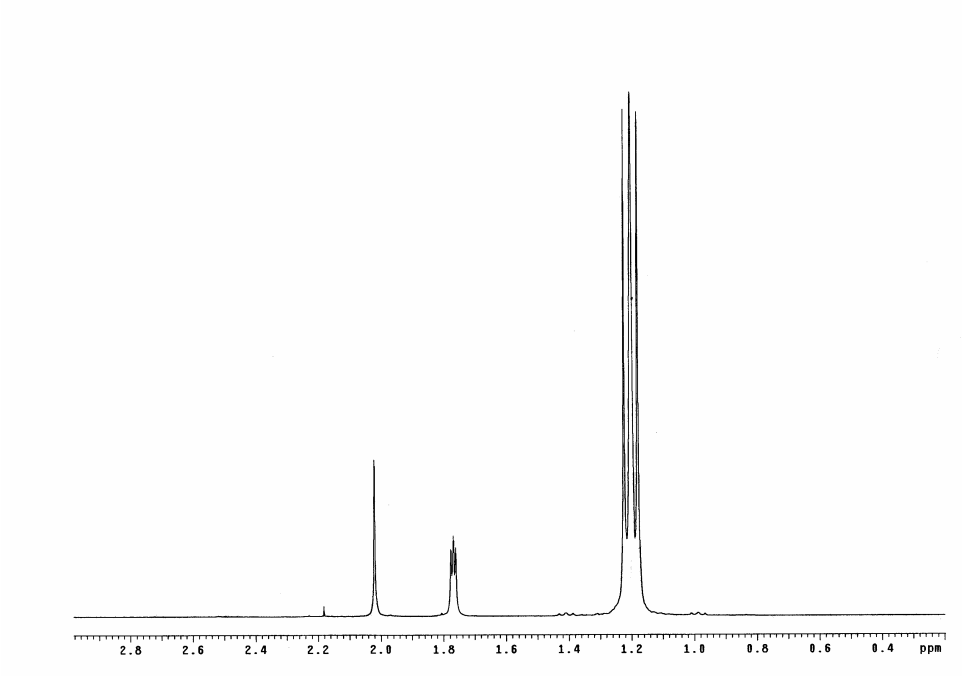

Figure 2.8. ^{1}H NMR spectrum of $[(dtbpe)Cu(NCMe)][PF_6]$ in $CDCl_3$.

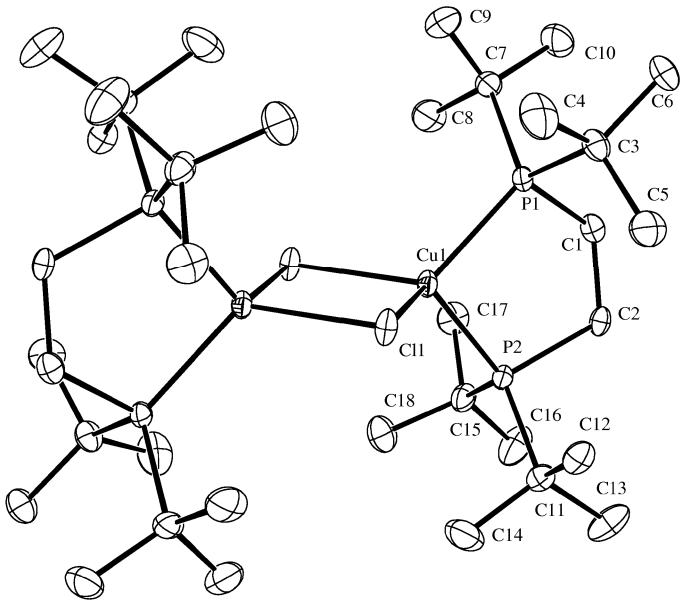

Figure 2.9. ORTEP (30% probability) of $[(dtbpe)Cu(\mu\text{-}Cl)_2]_2$ (hydrogen atoms omitted for clarity); Selected bond lengths (Å): Cu1-Cl1, 2.3844(9); Cu1-P1, 2.2863(8); Cu1-P2, 2.2832(9). Selected bond angles (°): Cl1-Cu-Cl1a, 95.73(3); Cl1-Cu-P1, 118.71(3); Cl1-Cu-P2, 115.23(3); P1-Cu-P2, 94.40(3); Cu1-Cl1a-Cu1a, 84.27(3).

Table 2.2. Selected crystallographic data and collection parameters for $[(dtbpe)Cu(\mu\text{-}Cl)_2]_2$.

	$[(dtbpe)Cu(\mu\text{-}Cl)_2]_2$
empirical formula	$C_{18}H_{40}ClCuP_2$
formula wt	417.46
crystal system	monoclinic
space group	$P2_1/c$
a, Å	11.3260(7)
b, Å	15.3216(9)
c, Å	13.7667(9)
β, ^{o}	112.7524(18)
V (Å^3)	2203.1(2)
Z	4
D_{calcd}, g cm^{-3}	1.259
crystal size (mm)	0.30× 0.07 × 0.07
*R*1, w*R*2 {I>2σ(I)}	0.051, 0.060
GOF	2.32

The [(dtbpe)Cu(NCMe)][PF_6] complex was reacted with [Li][NHPh] using methylene chloride as the solvent. The isolated product was consistent with (dtbpe)Cu(NHPh) by ^{1}H NMR spectroscopy, but was not clean. Column chromatography on silica in acetonitrile was performed, and this resulted in the formation and isolation of [(dtbpe)Cu(NH_2Ph)][PF_6]. This amine complex can be directly synthesized by reacting [(dtbpe)Cu(NCMe)][PF_6] with aniline in 91% yield (Scheme 2.3), and was characterized by multinuclear NMR, X-ray crystallography, IR and elemental analysis (^{1}H NMR Figure 2.10). The ^{1}H NMR spectrum reveals an N-H resonance of 5.46 ppm (δ, $CDCl_3$), and the symmetric and asymmetric N-H stretches in the IR are 3345, 3295 cm^{-1}, respectively. Attempts to deprotonate the amine ligand with [Na][$N(SiMe_3)_2$] resulted in production of aniline, although the ^{1}H NMR spectrum were collected in $CDCl_3$, which in retrospect likely decomposed the amido complex,.

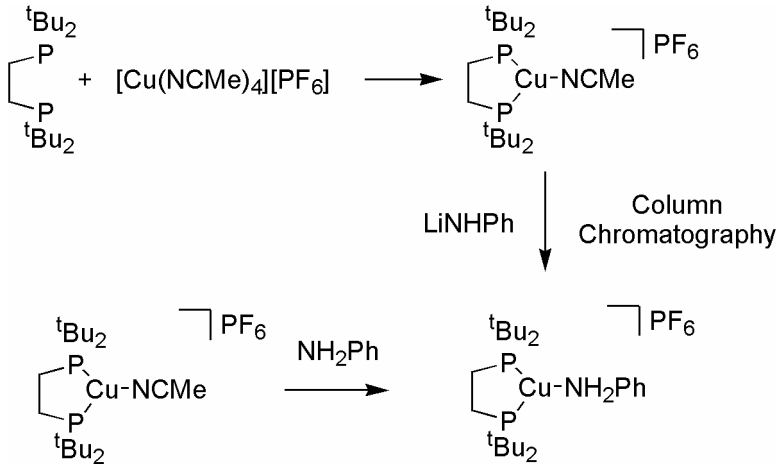

Scheme 2.3. Synthesis of the copper(I) amine complex [(dtbpe)Cu(NH_2Ph)][PF_6].

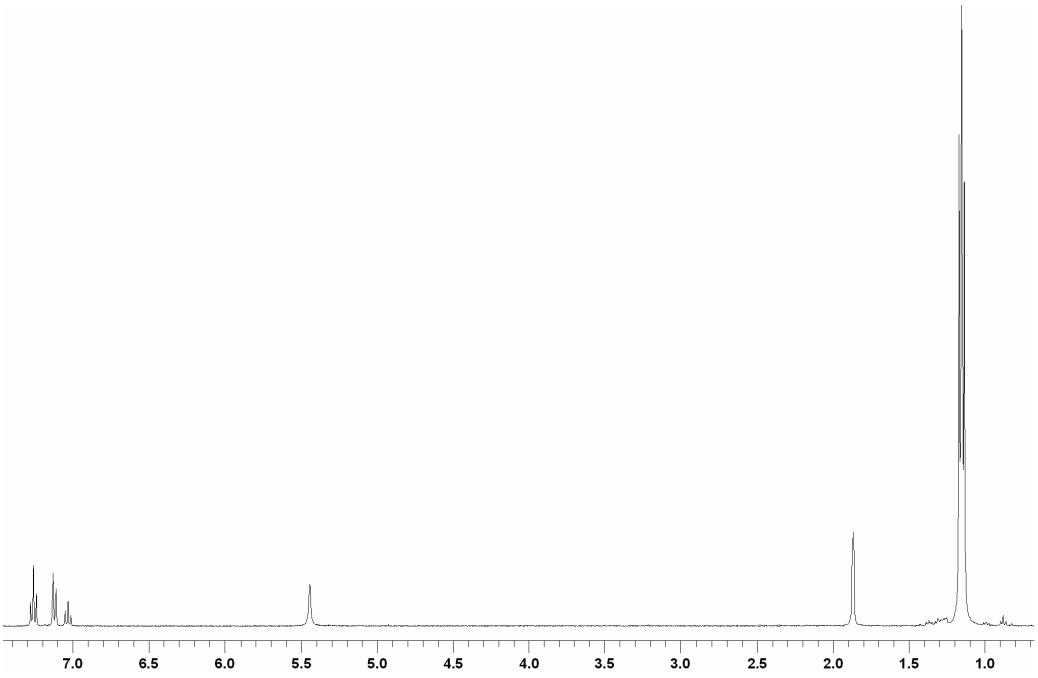

Figure 2.10. ^{1}H NMR spectrum of [(dtbpe)Cu(NH_2Ph)][PF_6] in $CDCl_3$.

A single crystal of [(dtbpe)Cu(NH_2Ph)][PF_6] was grown from a saturated solution of the amine complex in THF layered with cyclopentane, and the solid-state structure was solved (Figure 2.11, Table 2.3). The three coordinate copper center reveals distorted trigonal planar geometry with a small bond angle of 95.95(3)° for P1-Cu-P2 and larger bond angles for N1-Cu-P1 and N1-Cu-P2 of 131.33(8)° and 132.36(8)°, respectively. The Cu-N and N-C_{ipso} bond distances are 2.010(2) Å and 1.444(4) Å, respectively. The P-Cu-N-C_{ipso} torsion angle is 36.92° and the face of the aryl ring is approximately perpendicular to the P-C-P plane.

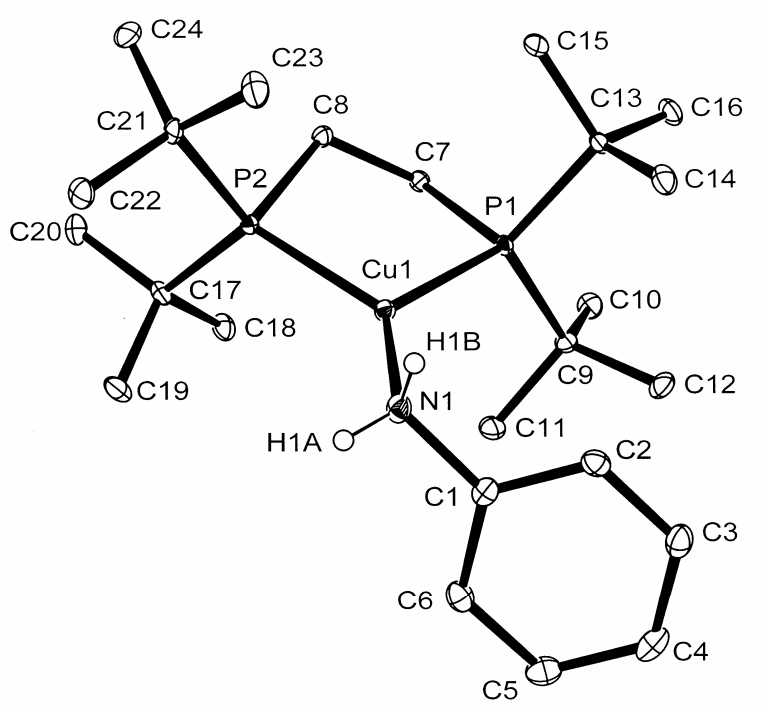

Figure 2.11. ORTEP (30% probability) of [(dtbpe)Cu(NH_2Ph)][PF_6] (counterion and most hydrogen atoms omitted for clarity); Selected bond lengths (Å): Cu1-P1, 2.2719(10); Cu1-P2, 2.2637(9); Cu1-N1, 2.010(2); N1-C1, 1.444(4); C1-C2, 1.390(4); C2-C3, 1.385(4); C3-C4, 1.378(5); C4-C5, 1.383(5); C5-C6, 1.386(4); C1-C6, 1.385(4). Selected bond angles (°): P1-Cu-P2, 95.95(3); N1-Cu-P1, 131.33(8); N1-Cu-P2, 132.36(8); Cu-N1-C1, 114.28(18).

Table 2.3. Selected crystallographic data and collection parameters for [(dtbpe)Cu(NH_2Ph)][PF_6].

	[(dtbpe)Cu(NH_2Ph)][PF_6]
empirical formula	$C_{24}H_{47}BCuF_4NP_2$
formula wt	561.93
crystal system	monoclinic
space group	$P2_1/c$
a, Å	11.199(3)
b, Å	16.080(3)
c, Å	15.882(3)
β, ^{o}	97.36(3)
V (Å^3)	2836.5(11)
Z	4
D_{calcd}, g cm^{-3}	1.316
crystal size (mm)	0.36 × 0.28 × 0.24
*R*1, w*R*2 {I>2σ(I)}	0.041, 0.041
GOF	1.27

The $[(dtbpe)Cu(\mu\text{-}Cl)]_2$ complex formed two equivalents of (dtbpe)Cu(NHPh) and LiCl upon reaction with LiNHPh in benzene (Scheme 2.4). After filtration and removal of solvent, the Cu(I) amido complex was isolated.[19] An alternative route was also found to the Cu anilido complex, where $[CuNHPh]_4$ could be synthesized by the published procedure and was then reacted with dtbpe ligand to form the amido cleanly.[20, 21] The ^1H and ^{13}C NMR spectra of (dtbpe)Cu(NHPh) are shown in Figure 2.12 and Figure 2.13. The N-H bond in the IR stretches at 3332 cm^{-1}, and the N-H in the ^1H NMR has a resonance of 4.70 ppm (δ, C_6D_6). Although a number of bridging copper (I) amido complexes have been reported,[20, 22-27] this was the first example of a fully characterized monomeric copper(I) amido complex.

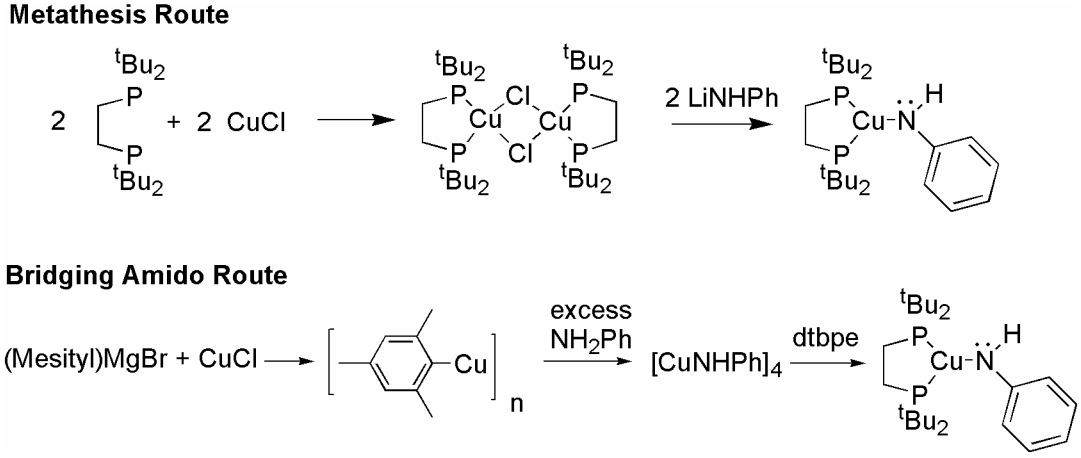

Scheme 2.4. Synthesis of the copper(I) anilido complex (dtbpe)Cu(NHPh).

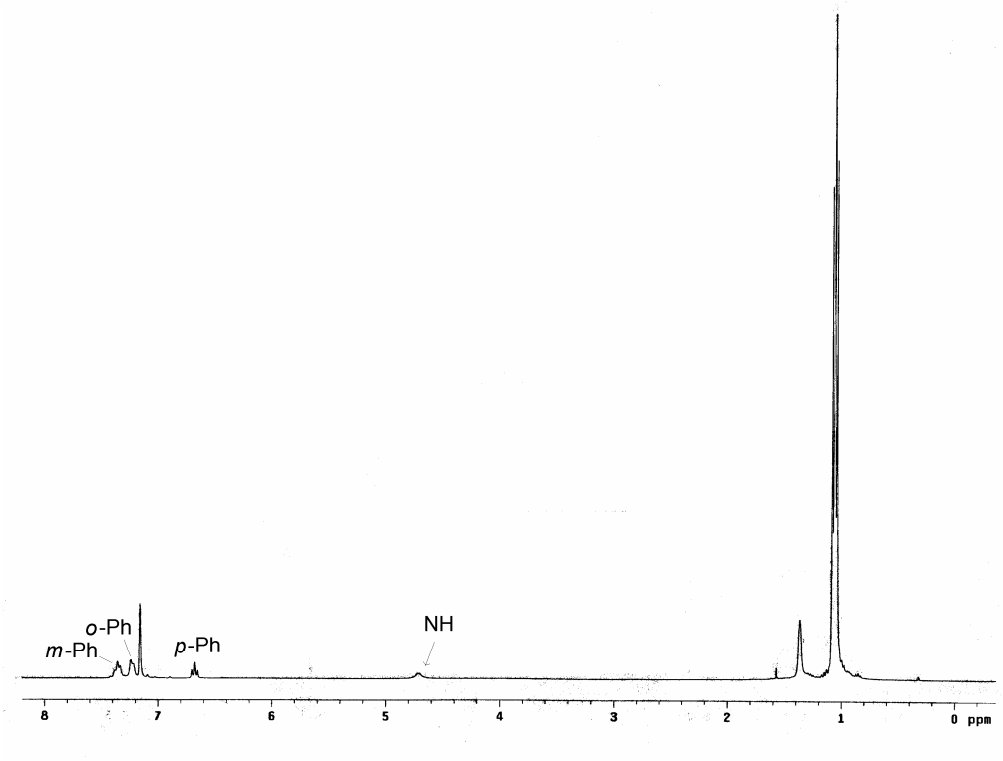

Figure 2.12. ^{1}H NMR spectrum of (dtbpe)Cu(NHPh) in C_6D_6.

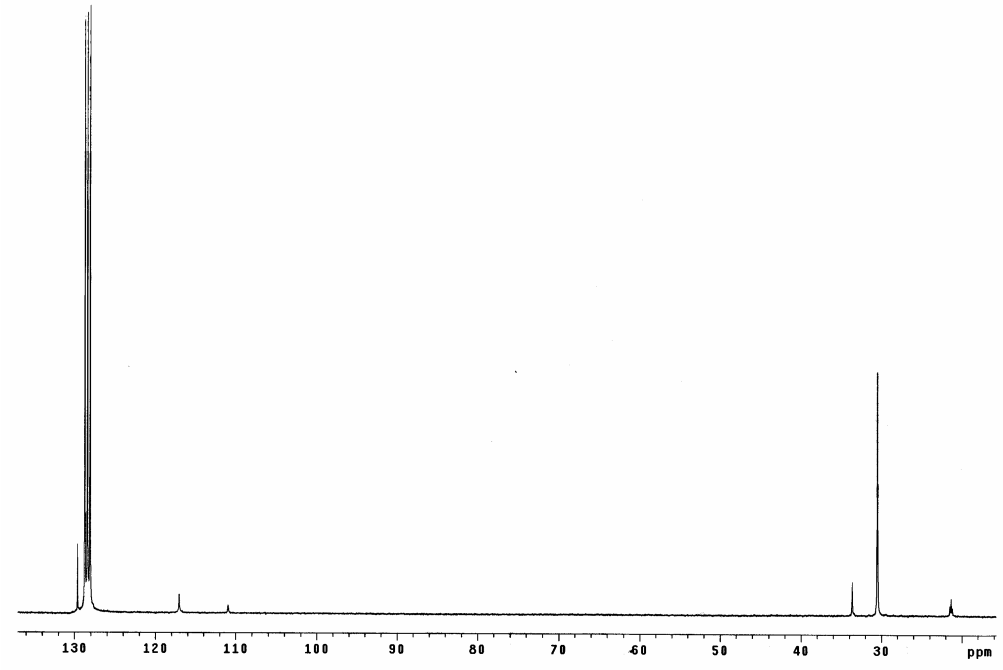

Figure 2.13. ^{13}C NMR spectrum of (dtbpe)Cu(NHPh) in C_6D_6.

2.3.1 Structure and Properties

A cyclic voltammogram of the cationic amine complex [(dtbpe)Cu(NH_2Ph)][PF_6] gave an irreversible oxidation at 1.3 V (vs NHE) whereas the amido irreversible oxidation is at 0.1 V, giving a change in oxidation potential of 1.2 V. These oxidation potentials may be ligand-based or the shift may be due to decreased electron density at the metal center upon deprotonation of the amine ligand. This is significantly less than the 2.0 V difference between the amine and amide complexes in octahedral Ru(II) systems synthesized in our group, and may indicate increased electron density at the anilido nitrogen for (dtbpe)Cu(NHPh) as compared to the Ru(II) systems.[28]

X-Ray quality crystals of the copper anilido system were grown by layering a solution of the complex in THF with hexanes (Figure 2.14). The solid-state structure is depicted in Figure 2.4. In the solid-state the phenyl-N-H plane is aligned approximately coplanar with the P-Cu-P plane with torsion angles for P-Cu-C_{ipso}-C of 11.23° and 4.63° for the two independent molecules, which leads to symmetry inequivalent phosphorus atoms. If this geometry were the same as the solution structure, the phosphorus and t-butyl groups on the ligand should give different resonances. However, a single broad resonance is observed by ^{31}P VT NMR experiments (to -80°C) in toluene-d_8 which does not decoalesce, leading to the most likely conclusion that Cu-N bond rotation is rapid in solution, or perhaps that the perpendicular alignment of the amido group is preferred in solution.

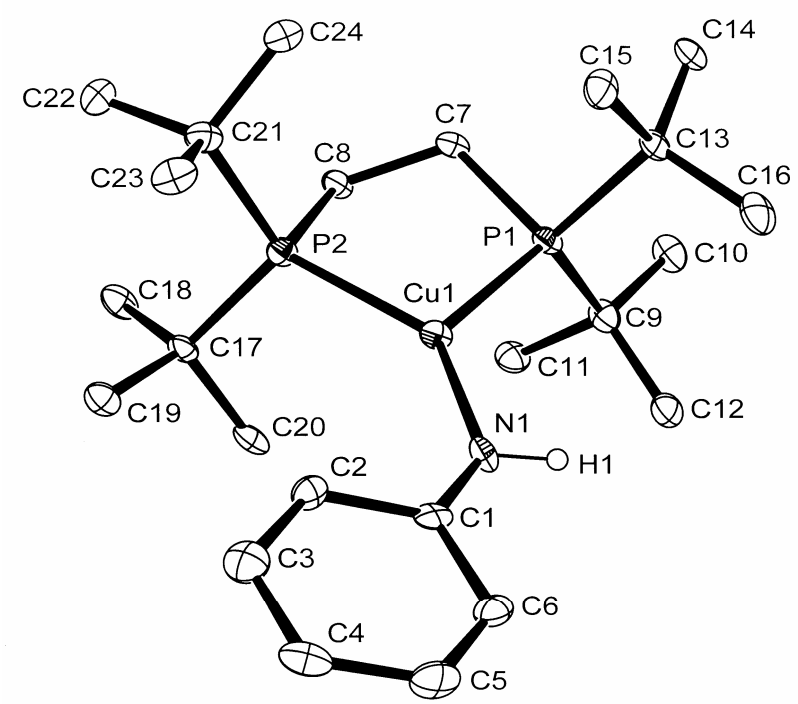

Figure 2.14. ORTEP (30% probability) of (dtbpe)Cu(NHPh) (most hydrogen atoms omitted for clarity); Selected bond lengths (Å): Cu1-P1, 2.298(2); Cu1-P2, 2.261(2); Cu1-N1, 1.890(6); N1-C1, 1.354(9); C1-C2, 1.421(10); C2-C3, 1.382(11); C3-C4, 1.380(12); C4-C5, 1.381(12); C5-C6, 1.370(11); C1-C6, 1.415(11). Selected bond angles (°): P1-Cu-P2, 93.19(8); N1-Cu-P1, 125.63(16); N1-Cu-P2, 141.00(16); Cu-N1-C1, 134.5(5).

Table 2.4. Selected crystallographic data and collection parameters for (dtbpe)Cu(NHPh).

	(dtbpe)Cu(NHPh)
empirical formula	$C_{29}H_{56}CuNP_2O_{0.5}$
formula wt	552.26
crystal system	monoclinic
space group	$P2_1/c$
a, Å	19.486(4)
b, Å	14.682(3)
c, Å	21.649(8)
β, °	99.58(3)
V (Å^3)	6107(3)
Z	8
D_{calcd}, g cm^{-3}	1.201
crystal size (mm)	0.50 × 0.30 × 0.10
*R*1, w*R*2 {I>2σ(I)}	0.067, 0.068
GOF	1.59

There are some points of interest in the cystalline structures of the amido and the amine complexes (dtbpe)Cu(NHPh) and [(dtbpe)Cu(NH_2Ph)][PF_6]. As mentioned above, the phenyl ring in the amine system is approximately perpendicular to the P-Cu-P plane (Figure 2.15). This planarity is presumably to avoid steric crowding due to the *tert*-butyl groups on the ligand. In comparison, the phenyl ring of the amido is rotated relative to the orientation of the amine into the P-Cu-P plane, and is coplanar with the P-Cu-P plane. The difference between the orientation of the phenyl ring of (dtbpe)Cu(NHPh) and [(dtbpe)Cu(NH_2Ph)][PF_6] could be due to sterics or electronics. The amine is has no lone pair available for π-bonding to the metal center, and thus the orientation is likely optimized to minimize steric interaction. However, the amido has a lone pair available for π-interaction with the metal center, and the geometry of the amido is such that the LUMO of the metal center, which is mostly p in character, is available to accept π-donation from the lone pair on the nitrogen potentially giving the Cu-N bond some multiple character (Figure 2.16). Also, the amide lone pair could be delocalized into the anti-bonding π∗ orbital on the ipso carbon of the phenyl ring. The Cu-N_{amido} and N_{amido}-C_{ipso} bond distances are 1.890(6) Å and 1.354(9) Å, respectively.

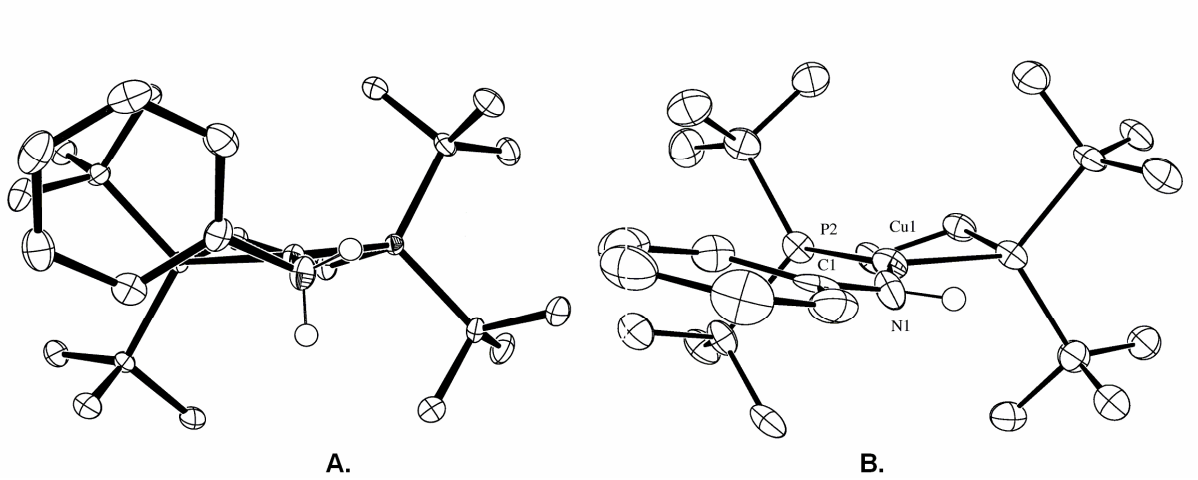

Figure 2.15. Comparison of ligand orientation around copper for A) Cu(I) amine complex and B) Cu(I) amido complex.

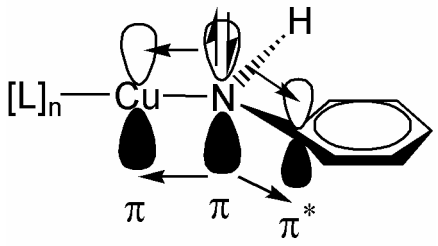

Figure 2.16. Potential delocalization of anilido nitrogen lone pair.

In addition to the change in orientation of the phenyl ring in going from the amine to the amido, the Cu-N bond shortens by ~0.1 Å while the N_{amido}-C_{ispo} phenyl bond shortens by 0.09 Å (Figure 2.17). The N_{amido}-C_{ispo} bond shortening is most likely due to the donation of the lone pair into the π* orbital on the ipso carbon. The Cu-N bond shortening could be a result of donation of the lone pair to the metal center (Cu=N multiple bonding) or increased electrostatic attraction between the positively charged metal center and the increased electron density on the amido nitrogen. The Cu-N bond distance of 1.890(6) is consistent with a Cu-N single bond. The Cu-N single and double bond lengths were predicted using the Pauling and Shomaker-Stevenson covalent radii, with corrections for electronegativity (eq 1 and 2).[29]

The Cu-N bond distance observed for (dtbpe)Cu(NHPh) is 0.02 Å longer than the predicted Cu-N single bond; therefore, there is likely little, if any, multiple bonding present in the amido complex.

$$0.74 + 1.176 - [0.04 * (3.04 - 1.90)] = 1.87 \text{ Å} \quad \text{(single bond)} \quad (1)$$

$$0.62 + 1.176 - [0.04 * (3.04 - 1.90)] = 1.75 \text{ Å} \quad \text{(double bond)} \quad (2)$$

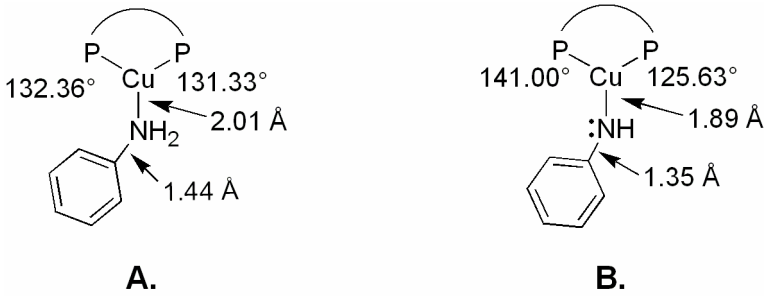

Figure 2.17. Comparison of C-N and N_{amido}-C_{ipso} bond distances around copper for A) Cu(I) amine complex and B) Cu(I) amido complex.

2.3.2 Reactivity of (dtbpe)Cu(NHPh)

The copper anilido species (dtbpe)Cu(NHPh) is unstable to moisture and oxygen; however, it is persistent for several days in an inert atmosphere and in the freezer for approximately one month. In solutions of methylene chloride, (dtbpe)Cu(NHPh) reacts to produce the $[(dtbpe)Cu(\mu\text{-}Cl)]_2$ dimer over a period of about an hour at room temperature (eq 3). It was found that combination with *p*-toluidine resulted in no reaction and did not form the new *p*-tolyl amido complex (dtbpe)Cu(NH*p*-tolyl) at room temperature. Heating the reaction mixture resulted in decomposition of (dtbpe)Cu(NHPh). Attempts to protonate the anilido ligand with HBF_4 to form the amine complex resulted in rapid decomposition to intractable products.

$$(dtbpe)Cu(NHPh) + CH_2Cl_2 \longrightarrow [(dtbpe)Cu(\mu\text{-}Cl)]_2 \quad (3)$$

Trityl (triphenylcarbenium) cation is often used to abstract a hydride, and could potentially be used to isolate a Cu(III) nitrene from a Cu(I) amido complex. Hydride abstraction by trityl cation occurs by oxidation of the metal complex to form trityl radical, which can then abstract a hydrogen atom to form triphenylmethane (A. in Scheme 2.5). For example, for (dtbpe)Cu(NHPh), first a Cu(II) amido complex could form followed by hydrogen atom abstraction to form a Cu(III) nitrene and triphenyl methane (B. in Scheme 2.5). However, when (dtbpe)Cu(NHPh) is reacted with $[Ph_3C][PF_6]$ (triphenylcarbenium

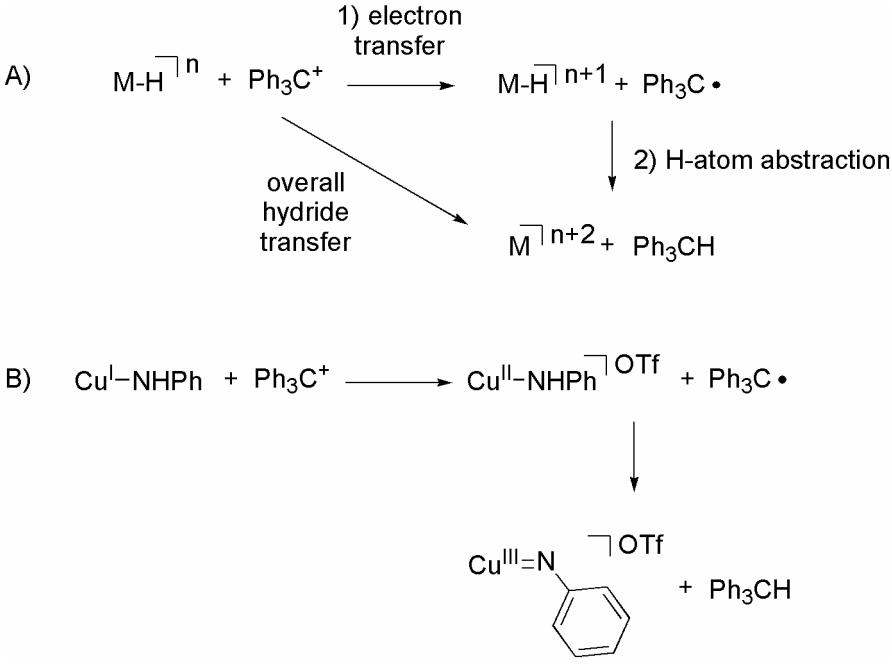

Scheme 2.5. A) Mechanism of hydride abstraction by trityl cation. B) Proposed formation of Cu(III) nitrene by hydride abstraction from a Cu(I) amido complex.

hexafluorophosphate) the organic product *N*-trityl amine is isolated. Presumably, the nucleophilic amido ligand of (dtbpe)Cu(NHPh) attacks the electron-poor trityl cation to form the amine (Scheme 2.6). The oxidation potential of the copper metal center (Cu amide (II/I)

= 0.1 V) favors oxidation by trityl cation (0.4 V) with a negative ΔG°, thus it is surprising that the oxidation does not occur. This result is in contrast to that observed with TpRu(CO)(NHPh)(PPh_3) by members of our group. When this Ru complex is reacted with trityl cation, oxidation and hydrogen atom abstraction from the phenyl ring occur to form a highly colored biphenyl complex.[30] TpRu(CO)(NHPh)(PPh_3) (0.11 V) has a very similar oxidation potential to (dtbpe)Cu(NHPh), and the electron transfer pathway may be made more competitive by the steric bulk of the Tp complex, and perhaps the reduced nucleophilicity when compared to the Cu amido complex. Therefore, the oxidation pathway does not appear to be kinetically competitive with the nucleophilic pathway for the copper amido, and the reaction to form the organic amine is observed.

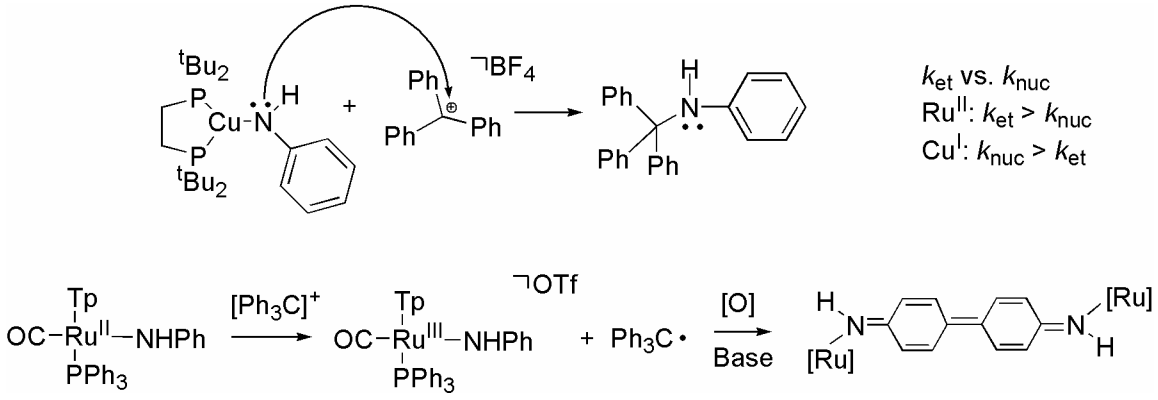

Scheme 2.6. Competition between nucleophilic attack and single electron oxidation for Cu(I) and Ru(II) anilido complexes.

It is known that Ru^{II}, d^6 amido complexes are nucleophilic, and we were interested to further explore the nucleophilicity of (dtbpe)Cu(NHPh) observed in the reaction with trityl cation. The nucleophilicity of the copper amido complex was compared directly with a Ru^{II} system through reactions with alkyl halides. Upon combination of (dtbpe)Cu(NHPh) and phenethylchloride, a base-initiated elimination occurs to form styrene; however, this

occurred with very low yield of styrene (~ 5%) after 6 hours (Scheme 2.7). This reaction was carried out at elevated temperatures (80-90 °C), and the copper amido complex rapidly decomposed with aniline production in approximately 50%.

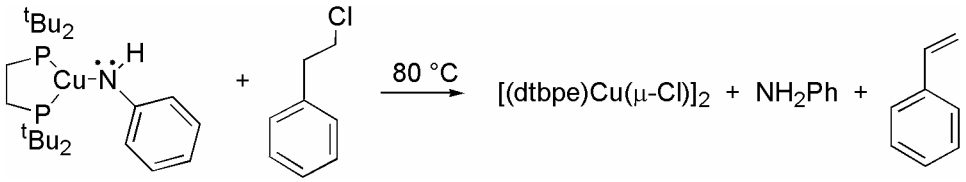

Scheme 2.7. Reaction of (dtbpe)Cu(NHPh) with phenethylchloride to produce styrene.

The kinetics of nucleophilic substitution of alkyl halides with the copper amido complex to form secondary amines was tested using ethylbromide and ethyliodide (Scheme 2.8). It was found that for ethylbromide the reaction to form ethylaniline at 25 °C occurred with a half life of 21.0(6) min (k_{obs} = 5.5(2) × 10^{-4} s^{-1}) under pseudo-first order reaction conditions (Figure 2.18). For ethyliodide the reaction was complete within 10 minutes at room temperature, consistent with the faster reactivity expected for iodide leaving groups in S_N2 type reactions. This was compared with the reaction of ethylbromide with $TpRu(PMe_3)_2(NHPh)$ by Dave Conner. It was found that heating the Ru(II) amido and ethylbromide to 80 °C produced ethylaniline with a $t_{1/2}$ = 22 hours, much longer than that required for the Cu amido. The rates of these reactions at the corresponding temperatures corresponds to $\Delta G^{\ddagger}$ values of 21.7 kcal/mol for (dtbpe)Cu(NHPh) and 29.0 kcal/mol for $TpRu(PMe_3)_2(NHPh)$. Thus, the copper anilido complex reacts more rapidly with alkyl halides than the ruthenium anilido complex and the reaction has significantly lower activation energy, indicating overall enhanced nucleophilic reactivity of the amido nitrogen for the copper complex compared to $TpRu(PMe_3)_2(NHPh)$.

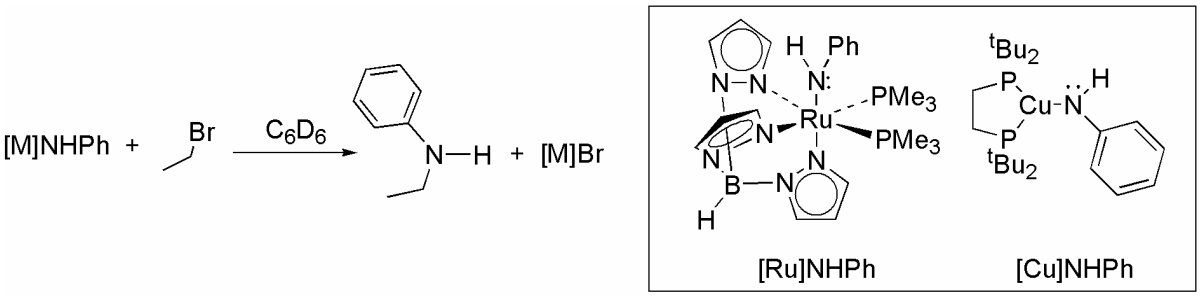

Scheme 2.8. Nucleophilic reaction of amido complexes.

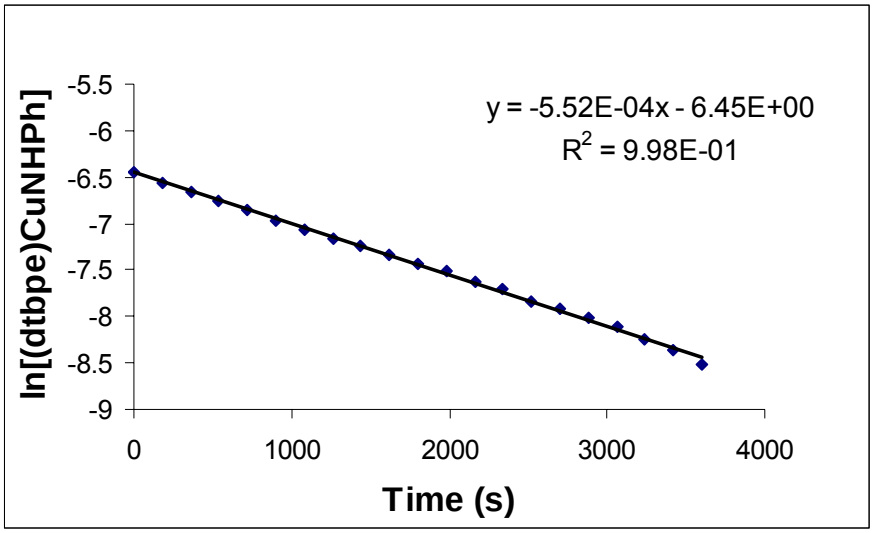

Figure 2.18. Representative plot of ln[(dtbpe)Cu(NHPh)] versus time for the formation of ethyl aniline with 12 equivalents of bromoethane in C_6D_6.

We had anticipated due to the potential for amido lone pair donation into Cu pπ orbitals that the nucleophilicity of the copper(I) amido complex might be attenuated compared to complexes that lack empty orbitals of π symmetry (e.g., $TpRu(PMe_3)_2(NHPh)$). However, it has been shown by the nucleophilic reactivity that this characteristic of low valent late transition-metal amides has not been reduced, and at least in these reactions, is enhanced. Inability of the lone pair to donate due to energy mismatch between the amido

lone pair and the Cu 4p orbital may contribute to weak amido lone pair pπ interactions. This lack of lone pair donation, along with a low coordination number and the fact that Cu(I) is less electronegative than Ru(II) (1.9 vs. 2.2),[31] result in a more nucleophilic and reactive nitrogen for the copper species. Furthermore, the nucleophilic reactivity observed for (dtbpe)Cu(NHPh) indicates weak Cu-N π-bonding, which is consistent with the Cu-N bond distance observed and the lack of observation of a Cu-N rotational barrier.

2.4 Catalytic Hydroamination of Olefins

Because the amido complex (dtbpe)Cu(NHPh) was observed to be quite nucleophilic, reactions with olefins possessing electron-withdrawing groups and primary and secondary amines were carried out. There are two possible pathways for C-N bond-formation utilizing the nucleophilic amido complex (dtbpe)Cu(NHPh) (Scheme 2.9). In pathway 1, the nucleophilic amido ligand may attack the electropositive end of the olefin. However, it is possible that the reaction could proceed via pathway 2 in which the olefin coordinates to the metal center and inserts into the Cu-N bond. There are very few examples of the second type of reactivity for M-X (X = OR, NHR) complexes.[32-34] Reaction of acrylonitrile and aniline in the presence of 5 mol% (dtbpe)Cu(NHPh) yields the anti-Markovnikov amine 3-(phenylamino)propionitrile in approximately 95% conversion after 3 hours at room temperature, as monitored by ^{1}H NMR. The product is consistent with anti-Markovnikov selectivity, that is, formation of the linear product (Section 1.2.10). Control reactions with both the amido complex precursors: (dtbpe)CuCl and free dtbpe ligand resulted in no observed amine product. (dtbpe)Cu(NHPh) has proved to catalyze hydroamination of a

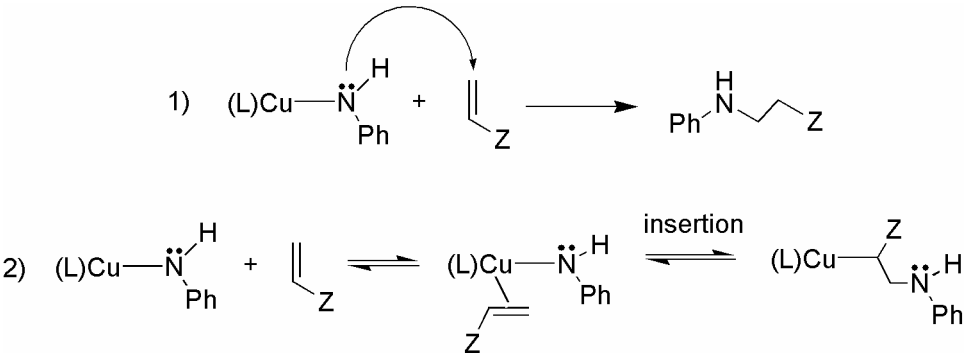

Scheme 2.9. Possible pathways of C-N bond formation by (dtbpe)Cu(NHPh).

number of substrates, all with anti-Markovnikov selectivity, consistent with electron-withdrawing olefins. Reactions with a range of electron-withdrawing olefins also produced anti-Markovnikov hydroamination (Table 2.5). Reaction with methyl vinyl ketone yielded 92% of 4-(phenylamino)-2-butanone within 5 minutes at room temperature. Reactions with methylacrylate yielded 99% of 4-(phenylamino)-butan-2-one in 4 hours. The hydroamination of the internal olefin 2-cyclohexenone with aniline gave 66% conversion after 3 days. For the reaction of the secondary amine diethylamine with acrylonitrite, 95% conversion in 12 hours was achieved. When sterically hindered amines were reacted with acrylonitrile, the rate was slowed considerably. For example, 86% conversion of dibenzylamine was observed after 7 days and only 58% conversion after 11 days with di-*t*-butylamine.

There are very few examples of hydroamination catalysis with substituted styrenes.[35, 36] Reactions with the substituted styrenes *p*-nitrostyrene and *p*-cyanostyrene produced 29% conversion after 8 hours and 6% conversion after 18 hours respectively, but only upon heating to 50 °C. It is likely that both the functional groups and the elevated temperature decompose the catalyst and inhibit reactivity. With the less activated substrates *p*-

trifluoromethylstyrene, *p*-bromostyrene, *p*-chlorostyrene and styrene, no production of the amine product was observed even after heating to 50 °C and 80 °C. Due to the thermal instability of the amido complex, which decomposes in the absence of other substrates upon heating to 60 °C, development of more reactive or more robust amido complexes may improve catalyst substrate scope.

Table 2.5. Catalytic hydroamination of olefins by (dtbpe)Cu(NHPh).

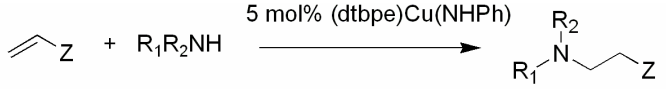

Olefin	Nucleophile	Product	Temp (°C)	Time (hr)	% conv.
	$PhNH_2$	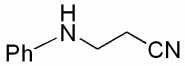	RT	3	> 95
	$PhNH_2$	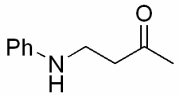	RT	5 mins	92
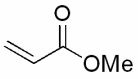	$PhNH_2$	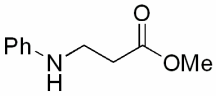	RT	4	99
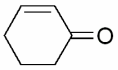	$PhNH_2$	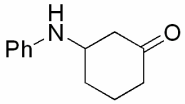	RT	3	66
	$^tBuNH2$	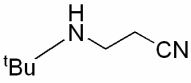	RT	11 days	58
	Et_2NH	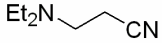	RT	12	95
	$(PhCH_2)_2NH$	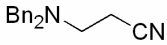	RT	7 days	86
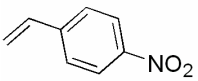	$PhNH_2$	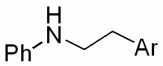	50	8	29
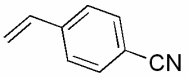	$PhNH_2$	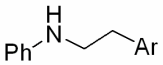	50	18	6
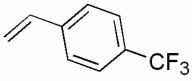	$PhNH_2$	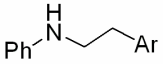	50	18	0
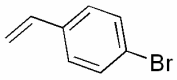	$PhNH_2$	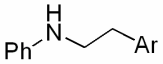	50	18	0
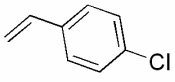	$PhNH_2$	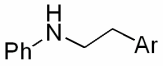	80	24	0
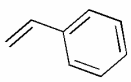	$PhNH_2$	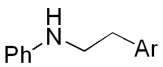	80	48	0

2.5 Attempted Synthesis of Copper Nitrene Complex

The (dtbpe)Cu^{I} complexes synthesized are potential substrates for the isolation of Cu(III) nitrene complexes due to the bulk, geometry and donating ability of the dtbpe ligand. Numerous reactions directed toward the preparation of monomeric nitrene complexes from (dtbpe)Cu(NHPh) were attempted. The conversion of Cu^{I}-NHPh amido complex to formally $[Cu^{III}\text{-NHPh}]^{+}$ requires net removal of a hydride from the anilido ligand. This can be accomplished by hydride removal, single electron oxidation and hydrogen atom abstraction, or net two electron oxidation and deprotonation (Scheme 2.10). Attempts to oxidize and

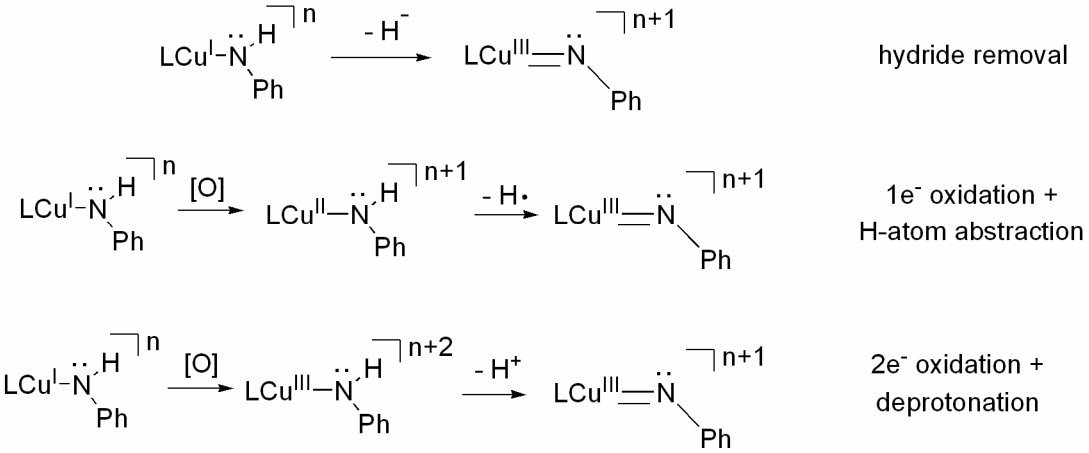

Scheme 2.10. Pathways for overall hydride removal from Cu^{I}-NHPh to produce $[Cu^{III}\text{-NHPh}]^{+}$.

deprotonate the copper(I) amido included using AgOTf with various bases, Sm(III)OTf as a two-electron oxidant with base, or TEMPO with ferrocenium (Scheme 2.11). All of these reactions resulted in decomposition of the copper complex to unidentified products. In addition, as mentioned above (2.3.2), trityl cation was reacted with (dtbpe)Cu(NHPh) in an attempt to abstract net hydride; however, the production of trityl amine was observed.

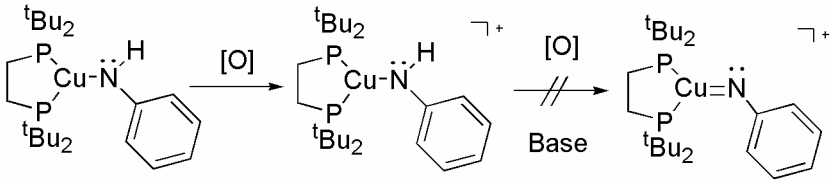

Scheme 2.11. Aryl nitrene synthesis attempts by oxidation and deprotonation.

Another potential pathway to produce a Cu(III) nitrene species is reaction of a nitrene source with a Cu(I) complex that possesses a labile ligand. When [(dtbpe)Cu(NCMe)][PF_6] is reacted with PhINTs as the nitrene source, [(κ^1- dtbpe=NTs)Cu(μ-PF_2O_2)]$_2$ is produced. This reaction reveals that the phosphorus ligand is prone to attack by the nitrene. A crystal structure of the product of this reaction revealed that one "arm" of the chelating ligand had released from the metal center, forming a P=NTs moiety (Figure 2.19). The overall structure is a dimer bridged by a $[PF_2O_2]^{-1}$ moiety, which is most likely formed upon hydrolysis of

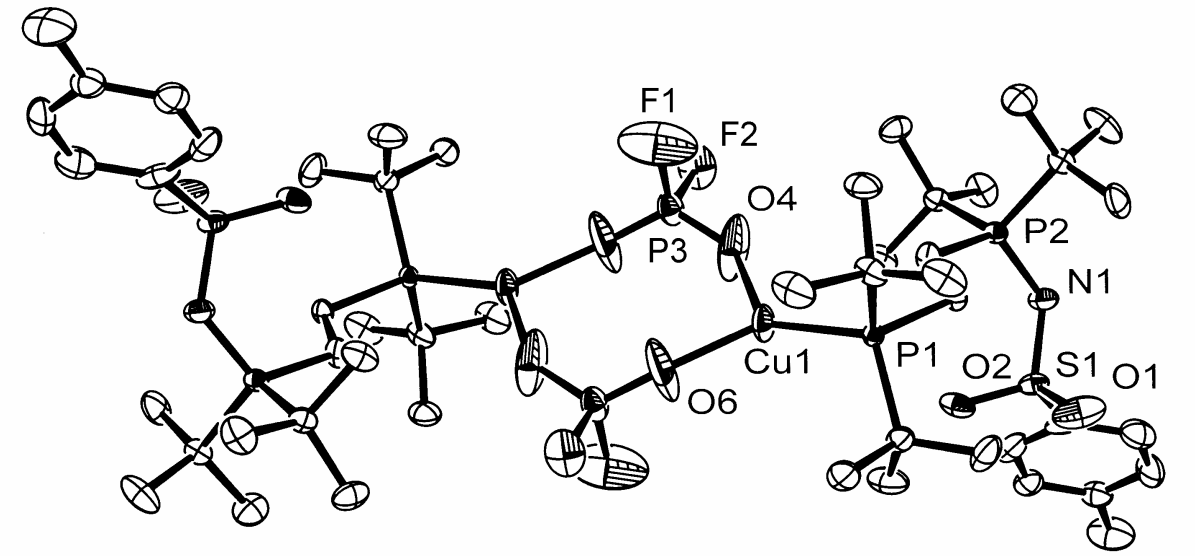

Figure 2.19 ORTEP (30% probability) of [(κ^1- dtbpe=NTs)Cu(μ-PF_2O_2)]$_2$ (most hydrogen atoms omitted for clarity); Selected bond lengths (Å): Cu1-O4, 2.007; Cu1-O6, 1.976; Cu1-P1, 2.148; P2-N1, 1.599. Selected bond angles (°): O6-Cu1-O4, 129.71; P1-Cu1-O4, 128.52; P1-Cu1-O6, 100.75.

PF_6^- by trace amounts of water in the PhINTs reagent (Scheme 2.12).[37-39] Reaction of PhINTs with phosphines can produce a phosphinimine directly and spontaneously. Reaction of free dtbpe with one equivalent of PhINTs results in appearance of a new resonance in the ^{31}P NMR significantly downfield from that of the free ligand and consistent with the species observed in the reaction of [(dtbpe)Cu(NCMe)][PF_6] with PhINTs (δ = 62.0 ppm versus δ = 38.5 ppm for free ligand). It is unclear whether this reaction occurs via a Cu(III) nitrene complex, or by direct reaction of the nitrene source and the phosphorous to form a phosphinimine (P=N) (Scheme 2.13). Thus, phosphine ligands are poor candidates for isolation of nitrene complexes.

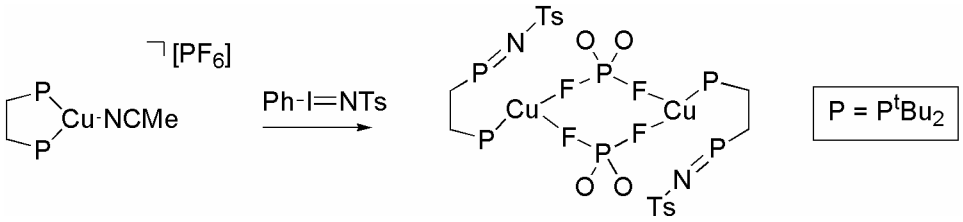

Scheme 2.12. Reaction of [(dtbpe)Cu(NCMe)][PF_6] with PhINTs to form bridging phosphinimine complex.

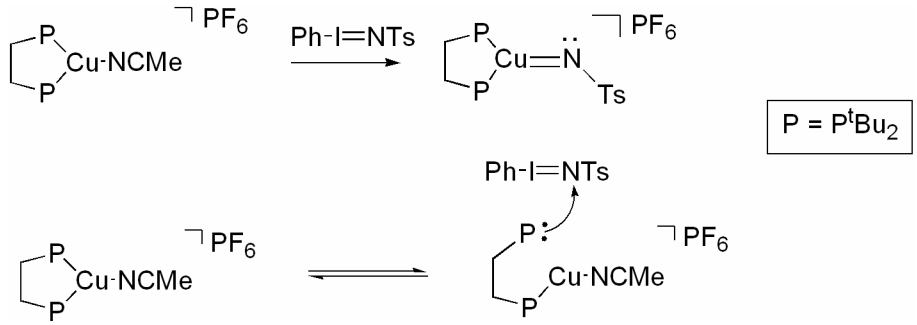

Scheme 2.13. Potential mechanisms for formation of phosphinimine from reaction of [(dtbpe)Cu(NCMe)][PF_6] and PhINTs.

2.6 Synthesis and Reactivity of a Bisphosphine Methyl Complex

Our group has investigated C-H activation and hydroarylation catalysis by Ru(II) methyl and phenyl complexes and continues to explore the potential for these complexes in second-generation catalysts.[40-44] Recent work has revealed the potential for non-dative Ru(II) hydroxide and amido complexes to activate C-H bonds.[45, 46] In addition, catalytic C-X (X = N, O, or S) bond-forming reactions could involve formation of Cu-R species, for example, the hydroamination mechanism could occur via insertion of the olefin in to the Cu-N bond to form a copper alkyl species. Therefore, reactions were undertaken to investigate synthesis of copper(I) alkyl complexes and application towards C-H and X-H (X = O, N, S) activation reactions and catalysis. In addition, there are very few well-defined, monomeric copper hydride, alkyl and aryl complexes, all of which are quite reactive.[47-50]

Reaction of dtbpe with Cu(OAc) results in formation of (dtbpe)Cu(OAc) in 80% isolated yield. This complex was characterized by ^{1}H, ^{13}C and ^{31}P NMR and elemental analysis. The resonance due to the methyl in the ^{1}H NMR appears as a singlet at $\delta = 2.02$, and the carbonyl resonance appears at $\delta = 178.6$ in the ^{13}C NMR (Figure 2.20). A single crystal of this complex was grown, and this crystal structure revealed three independent molecules in an asymmetric unit cell, with a κ^2 coordination mode for the acetate ligand (Figure 2.21). The κ^2 coordination mode is distinct from the κ^1 coordination mode observed for (NHC)Cu(OAc) (NHC = *N*-heterocyclic carbene).[50]

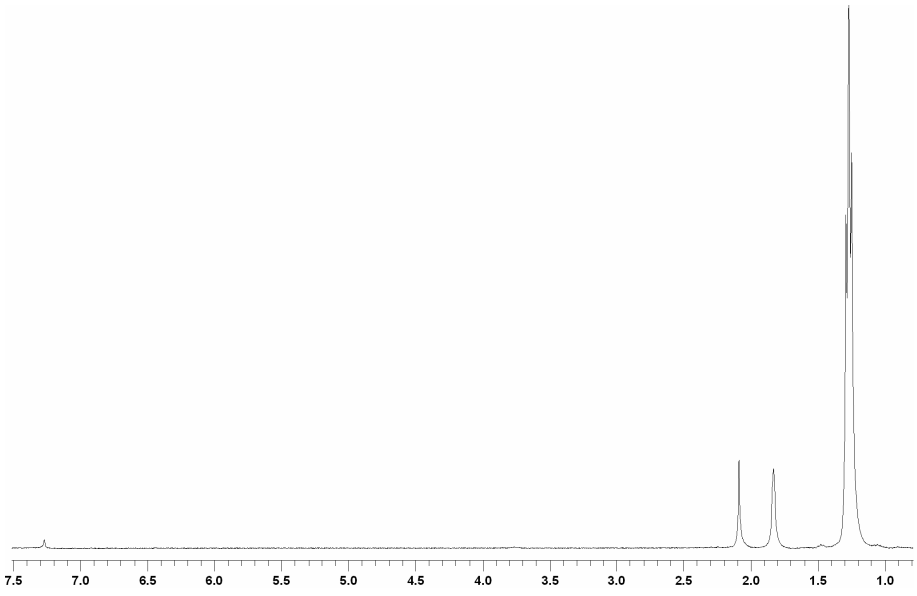

Figure 2.20. ^{1}H NMR spectrum of (dtbpe)Cu(OAc) in $CDCl_3$.

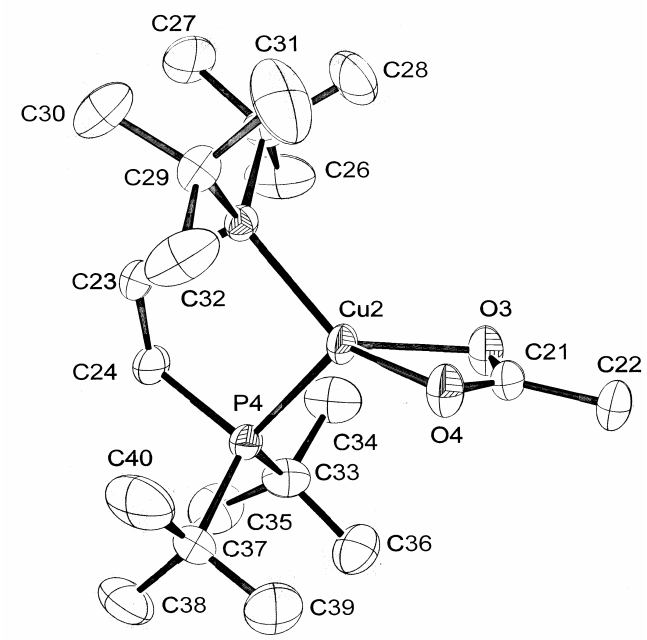

Figure 2.21. ORTEP (30% probability) of (dtbpe)Cu(OAc) (hydrogen atoms omitted for clarity); Selected bond lengths (Å): Cu2-O3, 2.121(2); Cu2-O4, 2.172(2); Cu2-P3, 2.2358(7); Cu2-P4, 2.2529(8); C21-O3, 1.254(4); C21-O4, 1.240(3); C21-C22, 1.515(4). Selected bond angles (º): Cu2-O4-C21, 88.0(2); Cu2-O3-C21, 90.0(2); O3-C21-O4, 121.2(2); O3-C21-C22, 119.5(3); O4-C21-C22, 119.4(3); P3-Cu2-P4, 95.87(3); O3-Cu2-O4, 60.78(8); P3-Cu2-O3, 131.26(7); P4-Cu2-O3, 119.32(7); P4-Cu2-O4, 122.49(7).

Table 2.6. Selected crystallographic data and collection parameters for (dtbpe)Cu(OAc).

	(dtbpe)Cu(OAc)
empirical formula	$C_{20}H_{43}CuO_2P_2$
formula wt	441.02
crystal system	triclinic
space group	$P\bar{1}$
a, Å	15.1868(9)
b, Å	15.6168(9)
c, Å	16.028(1)
β, °	98.581(1)
V (Å^3)	3652.4(4)
Z	6
D_{calcd}, g cm^{-3}	1.203
crystal size (mm)	0.36 × 0.38 × 0.40
*R*1, w*R*2 {I>2σ(I)}	0.067, 0.068
GOF	1.044

Reaction of (dtbpe)Cu(OAc) in diethyl ether at -60 °C with Me_3Al results in the formation of (dtbpe)Cu(Me) in 25% isolated yield (Scheme 2.14). Due to the alkyl groups on the phosphine ligand and the methyl group, the complex is quite soluble, and isolation was achieved by overnight precipitation at -20 °C from a minimal amount of hexanes. This

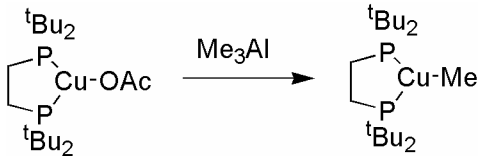

Scheme 2.14. Synthesis of (dtbpe)Cu(Me).

complex is very unstable and decomposes after a day at room temperature under a nitrogen atmosphere, but it can be kept at -20 °C in an inert atmosphere for up to a week. Thus, a crystal structure of this complex was not obtained, but the ^{1}H and ^{13}C NMR are consistent with the formation of (dtbpe)Cu(Me) (Figure 2.22 and Figure 2.23). The methyl peak is a broad singlet observed at δ = 0.35 ppm in the ^{1}H NMR and a broad singlet at -7.1 ppm in the ^{13}C NMR.

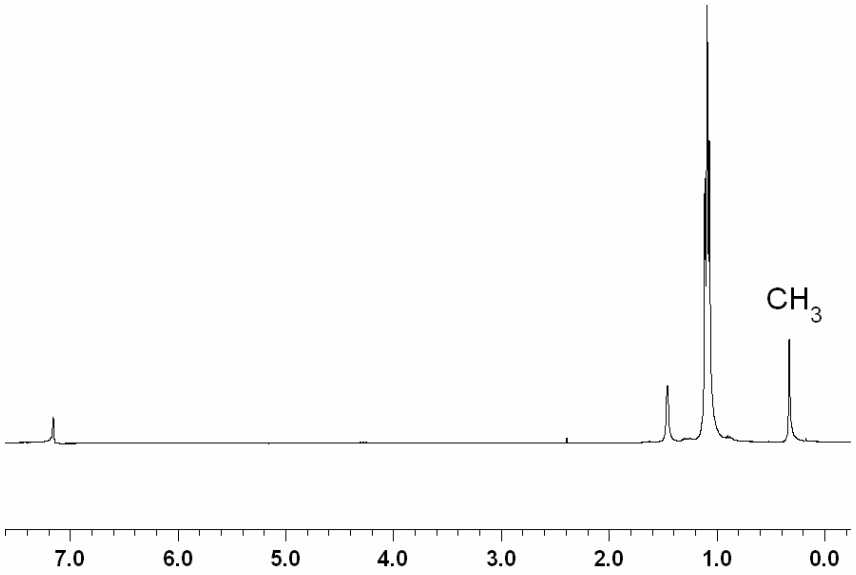

Figure 2.22. ^{1}H NMR spectrum of (dtbpe)Cu(Me) in C_6D_6.

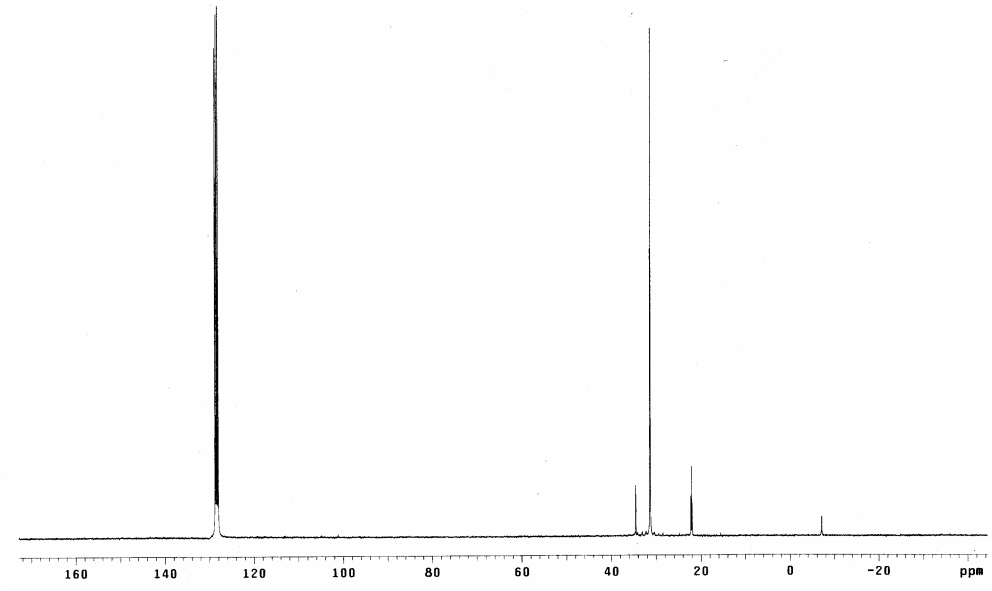

Figure 2.23. ^{13}C NMR spectrum of (dtbpe)Cu(Me) in C_6D_6.

Heating a solution of (dtbpe)Cu(Me) in C_6D_6 to 80 °C for 18 hours results in the formation of ethane and free dtbpe ligand, as confirmed by addition of free ligand (Scheme 2.15). In addition, heating (dtbpe)CuMe in C_6D_6 with 5 equivalents furan to 80 °C for 18 hours gives identical results. Thus, aromatic C-H(D) activation is not observed by (dtbpe)Cu(Me) for benzene-d_6 or furan. Similar reactivity was observed with (NHC)Cu(Me) (NHC = *N*-heterocyclic carbene) complexes in our group.[51, 52]

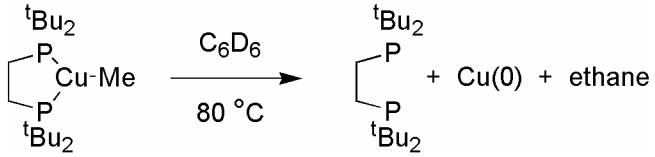

Scheme 2.15. Heating (dtbpe)Cu(Me) in C_6D_6.

2.7 Summary

We have synthesized a series of phosphine-ligated copper(I) halide, amine, amido, and methyl complexes. Most significantly, the first example of a monomeric copper(I) amido complex is reported and fully characterized. Reactivity studies reveal that this complex is not thermally stable and is very sensitive to moisture and air. The complex is quite nucleophilic and significantly more reactive than an analogous TpRu anilido complex. In addition, it is active for room temperature anti-Markovnikov hydroamination catalysis of electron-withdrawing olefins. However, reactions with minimally activated styrenes were not successful. Attempts to synthesize nitrene complexes from the amido complex and other phosphine-ligated complexes were not successful and resulted in formation of a phosphinimine, indicating that phosphine ligands are not good candidates for the isolation of

a copper(III) nitrene complex. The synthesis of a copper(I) methyl complex is reported; however, this complex does not activate the C-H bond of benzene or furan, but results in the release of ethane and decomposition of the metal complex upon heating.

2.8 General Experimental Methods.

All reactions and procedures were performed under anaerobic conditions in a nitrogen-filled glovebox or using standard Schlenk techniques. Glovebox purity was maintained by periodic nitrogen purges and monitored by an oxygen analyzer. ^{1}H and ^{13}C NMR spectra were obtained on a Varian Mercury 300 or 400 MHz. All ^{1}H and ^{13}C NMR spectra were referenced against tetramethylsilane using residual proton signals (^{1}H NMR) or the ^{13}C resonances of the deuterated solvent (^{13}C NMR). ^{31}P NMR spectra were obtained on a Varian 300 or 400 MHz spectrometer and referenced against external 85% H_3PO_4. Variable-temperature NMR experiments were performed on a Varian Mercury 300 or 400 MHz spectrometer. IR spectra were obtained on a Mattson Genesis II spectrometer either as thin films on a KBr plate or in solution using a KBr solution cell. Electrochemical experiments were performed under a nitrogen atmosphere using a BAS Epsilon Potentiostat. Cyclic voltammograms were recorded in a standard three-electrode cell from -2.00 V to +2.00 V with a glassy carbon working electrode and tetrabutylammonium hexafluorophosphate as electrolyte. Tetrabutylammonium hexafluorophosphate was dried under dynamic vacuum at 140 °C for 48 h prior to use. All potentials are reported versus NHE (normal hydrogen electrode) using cobaltocenium hexafluorophosphate as an internal standard. Elemental analyses were performed by Atlantic Microlabs, Inc.

Hexanes and CH_2Cl_2 were purified by passage through a column of activated alumina. THF and benzene were dried by distillation over sodium/benzophenone. Pentane and cyclopentane were distilled over sodium. Diethyl ether was degassed and stored over 4 Å sieves. Acetonitrile was distilled over calcium hydride. C_6D_6, $CDCl_3$, toluene-d_8 and CD_2Cl_2 were degassed via three freeze-pump-thaw cycles and stored over 4 Å sieves. Styrene was passed through a silica column and vacuum distilled. Aniline was dried over CaH_2 followed by vacuum distillation. Bromoethane and iodoethane were degassed and stored over 4Å molecular sieves. Methyl acrylate was washed with aqueous NaOH and subsequently dried over $CaCl_2$ followed by vacuum distillation. Acrylonitrile was washed with dilute H_2SO_4, followed by aqueous Na_2CO_3, then shaken over 4Å molecular sieves and distilled. Benzylamine was washed with aqueous NaOH prior to distillation from zinc dust. Anhydrous ethanol was used as purchased from Aldrich. CuCl was used as purchased from Strem (puratrem).

LiNHPh was generated by reaction of aniline with 1 equivalent of *n*-BuLi in benzene followed by addition of hexanes and vacuum filtration to collect the resulting white precipitate. $[Ph_3C][OTf]$ was prepared by reaction of $[Ph_3C][Cl]$ with [TMS][OTf] in CH_2Cl_2, followed by precipitation with hexanes. The bisphosphine ligand, dtbpe, was synthesized by a reported procedure; however, a detailed procedure is given below to aid in synthesis.[53] PCHP,[3] $[Cu(NCMe)_4][PF_6]$[54] and $TpRu(PMe_3)_2(NHPh)$[28] were prepared according to previously reported procedures. $[Cu(NHPh)]_4$ was prepared according to a previously reported procedure,[20] and the precursor mesitylcopper, was prepared according to a separate procedure.[21] PhINTs was prepared according to the published procedure, using

the water-free preparation reported by Andersson et al.[55, 56] All other reagents were used as purchased from commercial sources.

Synthesis of $[Cu_6Cl_6(\mu\text{-PCHP})_6]$. The white powder PCP was weighed out (0.414 g, 1.05 mmol) and dissolved in approximately 30 mL of CH_2Cl_2. A CuCl solution was added dropwise (0.0523 g , 0.528 mmol in approximately 20 mL of CH_2Cl_2). The solution was allowed to stir overnight and the volume was then reduced under vacuum to approximately 10 mL. The product was precipitated with hexanes and isolated in a medium porosity frit, washed with hexanes and ether, and dried under vacuum to yield a white solid (0.160 g, 0.054 mmol, 61% yield). X-ray quality crystals were grown from a saturated CH_2Cl_2 solution layered with hexanes. UV-vis (CH_2Cl_2): λ_{max} = 230 nm ($\varepsilon = 1.08 \times 10^5$ M^{-1} cm^{-1}). Fluorimetry Emission (CH_2Cl_2): λ_{max} = 354 nm. ^{1}H NMR (CD_2Cl_2, -10 °C, δ) (Integration for one PCP): 8.684 (1H, s, Ph-H2), 8.252 (1H, d, *J* = 8 Hz, Ph-H4 or H6), 7.134 (1H, t, *J* = 7 Hz, Ph-H5), 7.045 (1H, d, *J* = 7.2, Ph-H4 or H6), 3.84 (2H, t, *J* = 10Hz), 3.0 (2H, m, methylene), 1.52 (9H, d, $^2J_{PH}$ = 12, t-butyl), 1.45 (9H, d, $^2J_{PH}$ = 12, t-butyl), 1.24 (9H, bs, t-butyl), 1.02 (9H, bs, t-butyl). ^{13}C NMR (CD_2Cl_2, δ): 139.2 (s, Ph-2H), 128.2 (s, Ph-H4 or H6?), 127.6 (bs, Ph-H5), 34.2 (s, methylene), 30.2 (s, t-bu), 28.3 (s, methylene?) ^{31}P NMR (CD_2Cl_2, -10 °C, δ): 38.6, 36.4 ($^2J_{PP}$ = 126 Hz). CV (THF, TBAH, 100 mV/s): $E_{p,a}$ = 1.04 V (Cu(II/I)). Anal Calc for $C_{144}H_{264}Cu_6Cl_6P_{12}$: C, 58.40; H, 8.99; Found: C, 58.47; H, 9.04.

Synthesis of (BINAP)CuOTf. BINAP (0.775 g, 1.25 mmol) was dissolved in 5 mL of CH_3CN and was slowly added to a solution of CuOTf-benzene (0.402 g, 1.24 mmol) in 30 mL of CH_2Cl_2. The resulting solution was stirred for 3 h at room temperature, and the

solvent was removed in vacuo. A yellow solid was recrystallized from CH_2Cl_2 and hexanes (0.863 g, 83% yield). ^{1}H NMR (CD_2Cl_2, δ): 7.84 (4H, m), 7.61 (4H, m), 7.50 (6H, m), 7.34 (2H, t, *J* = 7 Hz), 7.27 (2H, m), 7.10 (6H, m), 6.79 (2H, t, *J* = 7 Hz), 6.74 (2H, d, *J* = 9 Hz), 6.64 (4H, t, *J* = 7 Hz). ^{13}C NMR (CD_2Cl_2, δ): 135.3 (t, *J* = 9 Hz), 133.7 (m), 131.5 (t, *J* = 10 Hz), 128.6 (s), 128.1 (m), 127.8 (d, *J* = 25 Hz), 127.1 (s). ^{31}P NMR: (CD_2Cl_2, δ): -0.8 (s, BINAP). Anal. Calc for $C_{44}H_{32}Cu_1F_3O_3P_2S_1$: C, 64.71; H, 3.86; N, 5.75. Found: C, 64.78; H, 3.90; N, 5.66.

Synthesis of [(BINAP)Cu(NCMe)][PF$_6$]. A solution of $[Cu(NCMe)_4][PF_6]$ (0.195 g, 0.52 mmol) in 5 mL of THF was added to a THF solution of 35 mL with BINAP ((±)-2,2'-bis(diphenylphosphino)-1,1'-binaphthalene) (0.327 g, 0.53 mmol). The solution was allowed to stir for 3 h, and the solvent was reduced in vacuo to 15 mL. Approximately 20 mL of hexanes was added to precipitate a white solid. The resulting solid was collected by vacuum filtration and dried under reduced pressure (0.417 g, 91% yield). ^{1}H NMR (CD_2Cl_2, δ): 7.80 (4H, m), 7.60 (10H, m), 7.35 (2H, t, *J* = 7 Hz), 7.17 (2H, m), 7.05 (6H, m), 6.78 (2H, t, *J* = 7 Hz), 6.72 (2H, d, *J* = 8 Hz), 6.60 (4H, t *J* = 7.2 Hz), 2.47 (3H, s, C*H*3CN). ^{13}C NMR (CD_2Cl_2, δ): 139.7 (bs, CH3*C*N), 135.3 (t, *J* = 9 Hz), 133.9 (s), 133.6 (t, *J* = 9 Hz), 132.1 (s), 130.5 (s), 130.2 (t, *J* = 5 Hz), 129.8 (s), 128.6 (s), 128.2 (t, *J* = 6 Hz), 127.7 (s), 127.5 (s), 127.3 (s), 3.6 (s, *C*H$_3$CN). ^{31}P NMR (CD_2Cl_2, δ): 2.5 (s, BINAP), -144.2 (septet, $^1J_{PF}$ = 710 Hz, PF_6). Anal. Calc for $C_{46}H_{35}Cu_1F_6N_1P_3$: C, 63.34; H, 4.04; N, 1.61. Found: C, 63.20; H, 4.11; N, 1.70.

Synthesis of 1,2-bis(di-tert-butyl)phosphinoethane (dtbpe). The actual procedure used, based on the original German literature procedure is reported here due to the

sensitivity of this reaction.[53] *Tert*-butyllitium (1.7 M solution in pentane, 100 mL, 0.17 mol) was diluted with dry hexanes (approx. 50 mL) in a 250 mL round bottom schlenk flask in the glovebox. 1,2-Bis(dichlorophosphino)ethane (Strem, 10 g, 0.042 mol) was added to fresh diethyl ether (100 mL) in a 500 mL round bottom schlenk flask. Both solutions were sealed off with valve and septum, removed from the glovebox, and placed under N_2 on the schlenk line. In order to ensure controlled slow addition of the ^{t}BuLi to the reaction flask, a dried >100 mL addition funnel was attached to the larger flask containing the phosphine, and was purged out with N_2 via the flask. Once the addition funnel was cooled and purged, the ^{t}BuLi was transferred to the closed addition funnel via a cannula. The phosphine/ether solution was chilled to -78 °C, and the ^{t}BuLi was added to the solution in a controlled, slow manner over approximately an hour. The solution was reacted at -78 °C for 2 hours, then at 0 °C for 1 hour, and then allowed to warm to room temperature. The solution was then purged into the glove box for workup. To remove the majority of the LiCl byproduct, the solution was filtered through a large-diameter medium frit. The filtrate was then allowed to gravity filter through a well-packed Celite column, built with hexanes, to remove any remaining LiCl. The flask and column were washed with hexanes. The solvent was removed from the filtrate until the product began to precipitate. The solution was then allowed to warm to room temperature and was sealed with a septum and set in a -20 °C glove box freezer overnight. The product crystallized and was isolated by filtration and briefly dried. The filtrate was returned to the freezer and a second crop of product was collected, overall yield (5.78 g, 43% yield). ^{1}H NMR (C_6D_6, δ): 1.77 (4H, d, $^2J_{PP}$ = 3.6 Hz, methylene), 1.16 (4H, d, $^3J_{PP}$ = 10.8 Hz, methylene) (Shown below in Figure 2.24). ^{31}P NMR (C_6D_6, δ): 36.18.

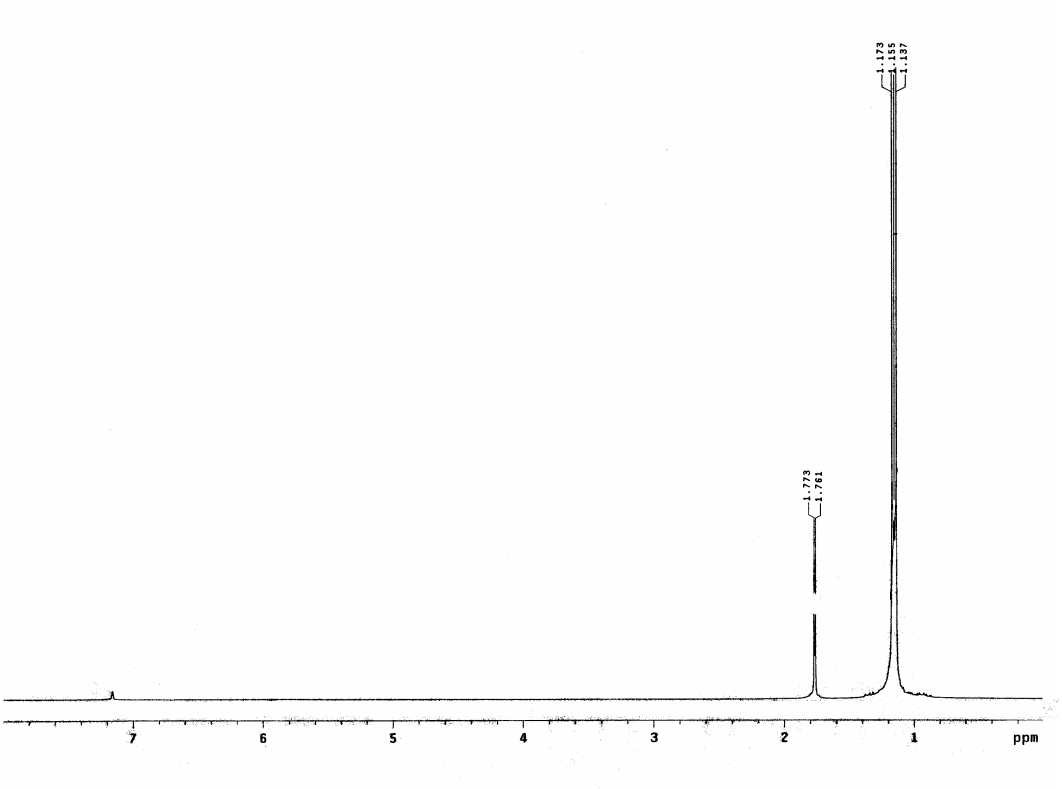

Figure 2.24 ^{1}H NMR spectrum of dtbpe in C_6D_6.**Synthesis of [(dtbpe)Cu(NCMe)][PF$_6$].** The bisphosphine dtbpe (0.213 g, 0.67 mmol) was dissolved in approximately 50 mL of CH_2Cl_2, and $[Cu(NCMe)_4][PF_6]$ (0.249 g, 0.67 mmol) was added to the solution. The solution was stirred at room temperature for 2 h, and the solvent was removed in vacuo. A light yellow solid was isolated (0.362 g, 95% yield). Complex 3 can be further purified by dissolution in methylene chloride followed by precipitation with hexanes. ^{1}H NMR ($CDCl_3$, δ): 2.33 (3H, s, NCC*H*3), 1.88 (4H, s, methylene), 1.27 (36H, vt, *N* = 14 Hz, t-Bu). ^{13}C NMR ($CDCl_3$, δ): 119.2 (s, N*C*Me), 33.8 (vt, *N* = 15 Hz, quat t-Bu), 29.7 (s, methyl), 20.7 (vt, *N* = 25 Hz, methylene), 2.5 (s, NC*C*H3). ^{31}P NMR ($CDCl_3$, δ): 31.8 (bs, dtbpe), -143.7 (septet, $^{1}J_{PF}$ = 710 Hz, PF6). IR (CCl_4): ν_{CN} = 2276 cm^{-1}. CV (CH_2Cl_2, TBAH, 100 mV/s): $E_{1/2}$ =

1.28 V (II/I). Anal.Calc for $C_{20}H_{43}Cu_1F_6N_1P_3$: C, 42.29; H, 7.63; N, 2.47. Found: C, 42.06; H, 7.64; N, 2.23.

Synthesis of [(dtbpe)Cu(NH_2Ph)][PF_6]. Method A. To a stirred THF solution (50 mL) of [(dtbpe)CuNCMe][PF_6] (0.6265 g, 1.1 mmol) was added LiNHPh (0.1085 g, 1.1 mmol). The resulting solution was stirred for 2 h at room temperature; then the solvent was removed in vacuo. The nonvolatiles were dissolved in approximately 10 mL of CH_3CN and applied to a silica column, which was eluted with approximately 50 mL of CH_3CN. The solvent was removed in vacuo, and the resulting white powder was dissolved in CH_2Cl_2. The product was precipitated upon addition of hexanes and filtered to isolate a white powder (0.3824 g, 78% yield). **Method B.** To a stirred THF solution (30 mL) of [(dtbpe)Cu(NCMe)][PF_6] (3) (0.2367 g, 0.42 mmol) was added aniline (38 μL, 0.42 mmol). The resulting solution was stirred for 1 h at room temperature, and the solvent was removed in vacuo. The resulting pale yellow solid (0.228 g, 97% yield) was vacuum-dried overnight. ^{1}H NMR spectroscopy revealed clean formation of the amine complex. Prior to the solid-state X-ray diffraction study, a counterion metathesis reaction to yield [(dtbpe)Cu(NH_2Ph)][BF_4] was performed. Crystals suitable for a solid-state X-ray diffraction study were grown at room temperature by layering a THF solution of [(dtbpe)Cu(NH_2Ph)][PF_6] with cyclohexane. ^{1}H NMR ($CDCl_3$, δ): 7.28 (2H, t, *J* = 7 Hz, *m*-phenyl), 7.14 (2H, d, *J* = 7 Hz, *o*-phenyl), 7.05 (1H, t, *J* = 7 Hz, *p*-phenyl), 5.46 (2H, bs, N*H*$_2$), 1.88 (4H, s, methylene), 1.17 (36H, vt, *N* = 14, *tert*-butyl). ^{13}C NMR ($CDCl_3$, δ): 142.5 (bs, ipso-Ph), 129.8, 123.6 and 119.2 (all s, phenyl *o*, *m*, and *p*), 33.9 (vt, *N* = 12 Hz, quat t-Bu), 30.4 (vt, *N* = 8 Hz, methyl), 20.9 (vt, *N* = 25 Hz, methylene). ^{31}P NMR (CD_2Cl_2,

δ): 29.8 (s, dtbpe), -143.7 (septet, $^{1}J_{PF}$ = 714 Hz, PF_6). IR (CH_2Cl_2): ν_{NH} = 3345, 3295 cm^{-1}. CV (CH_2Cl_2, TBAH, 100 mV/s): $E_{p,a}$ = 1.31 V (II/I). Anal. Calc for $C_{24}H_{47}Cu_1F_6N_1P_3$: C, 46.48; H, 7.64; N, 2.26. Found: C, 46.23; H, 7.50; N, 2.59.

Synthesis of [(dtbpe)Cu(μ-Cl)]$_2$. The white solid dtbpe (bis(di-*tert*-butyl)phosphino ethane; 0.5455 g, 1.71 mmol) was dissolved in approximately 30 mL of CH_2Cl_2. CuCl (0.1672 g, 1.69 mmol) was added to the dtbpe solution and allowed to stir until all of the CuCl dissolved (approximately 2 h). The solvent was then removed under reduced pressure, and the resulting white solid product was isolated (0.6342 g, 90% yield). The complex can be further purified by dissolution in methylene chloride followed by precipitation with hexanes. Crystals suitable for a solid-state X-ray diffraction study were grown at room temperature by layering a solution of [(dtbpe)Cu(μ-Cl)]$_2$ in CH_2Cl_2 with cyclohexane. ^{1}H NMR (CD_2Cl_2, δ): 1.86 (4H, br s, methylene), 1.25 (36H, vt, N = 13 Hz). ^{13}C NMR (CD_2Cl_2, δ): 33.9 (vt, N = 9 Hz, quat t-Bu), 30.4 (vt, N = 9 Hz, methyl), 20.8 (vt, N = 25 Hz, methylene). ^{31}P NMR (CD_2Cl_2, δ): 25.6 (s). CV (CH_2Cl_2, TBAH, 100 mV/s): $E_{1/2}$ = 0.55 V (II/I, quasi-reversible), $E_{p,a}$ = 0.88 V (II/I). Anal. Calc for $C_{36}H_{80}Cl_2Cu_2P_4$: C, 51.79; H, 9.66. Found: C, 51.64; H, 9.74.

Synthesis of (dtbpe)Cu(NHPh). Method A. The white powder [(dtbpe)Cu(μ-Cl)]$_2$ was weighed out (0.257 g, 0.62 mmol) and dissolved in approximately 40 mL of benzene. LiNHPh (0.063 g, 0.64 mmol) was added to the solution and allowed to stir for 1 h. The pale yellow solution was filtered through a fine-porosity frit to remove the LiCl. The filtrate was dried in vacuo, and the product was isolated as a yellow powder (0.2176 g, 75% yield). **Method B.** The copper complex [Cu(NHPh)]$_4$ (0.056 g, 0.36 mmol) was added to a benzene

(30 mL) solution of dtbpe (0.114 g, 0.358 mmol). The solution immediately turned yellow and was allowed to stir at room temperature for 20 min. The volatiles were removed under reduced pressure to yield a yellow powder (0.167 g, 98% yield). ^{1}H and ^{31}P NMR spectra of the isolated yellow solid are consistent with the quantitative formation of (dtbpe)Cu(NHPh) . Crystals suitable for a solid-state X-ray diffraction study were grown at room temperature by layering a THF solution of (dtbpe)Cu(NHPh) with cyclohexane. ^{1}H NMR (C_6D_6, δ): 7.34 (2H, t, J = 7 Hz, *m*-Ph), 7.23 (2H, d, J = 7 Hz, *o*-Ph), 6.67 (1H, t, J = 7 Hz, *p*-Ph), 4.70 (1H, bs, N*H*), 1.37 (4H, bs, methylene), 1.06 (36H, vt, N = 12 Hz, *t*-Bu). ^{13}C NMR (C_6D_6, δ): 162.3 (bs, ipso Ph), 129.6, 117.0, and 110.9 (all s, phenyl *o*, *m*, and *p*), 33.6 (br s, quat t-Bu), 30.5 (vt, N = 10 Hz, methyl), 21.3 (vt, N = 24 Hz, methylene). ^{31}P NMR (C_6D_6, δ): 30.2 (s). IR (C_6H_6): ν_{NH} = 3332 cm^{-1}. CV (THF, TBAH, 100 mV/s): $E_{p,a}$ = 0.10 V (II/I). Satisfactory elemental analysis was not obtained due to the air-sensitive nature of the material.

Reaction of (dtbpe)Cu(NHPh) with Trityl Cation. (dtbpe)Cu(NHPh) (0.080 g, 0.17 mmol) was dissolved in THF (10 mL). A solution of [Ph_3C][OTf] (0.066 g, 0.169 mmol) in THF (5 mL) was added and the pale yellow solution became cloudy and was stirred for several hours. The reaction mixture was filtered, washed with hexanes and the solvent was removed from the filtrate in vacuo. A ^{1}H NMR revealed formation of tritylaniline (Ph_3CNHPh)[57], and a copper product, which is likely (dtbpe)Cu(OTf) (Figure 2.25). A small amount of Ph_3CH is observed, but there is no other evidence for nitrene formation.

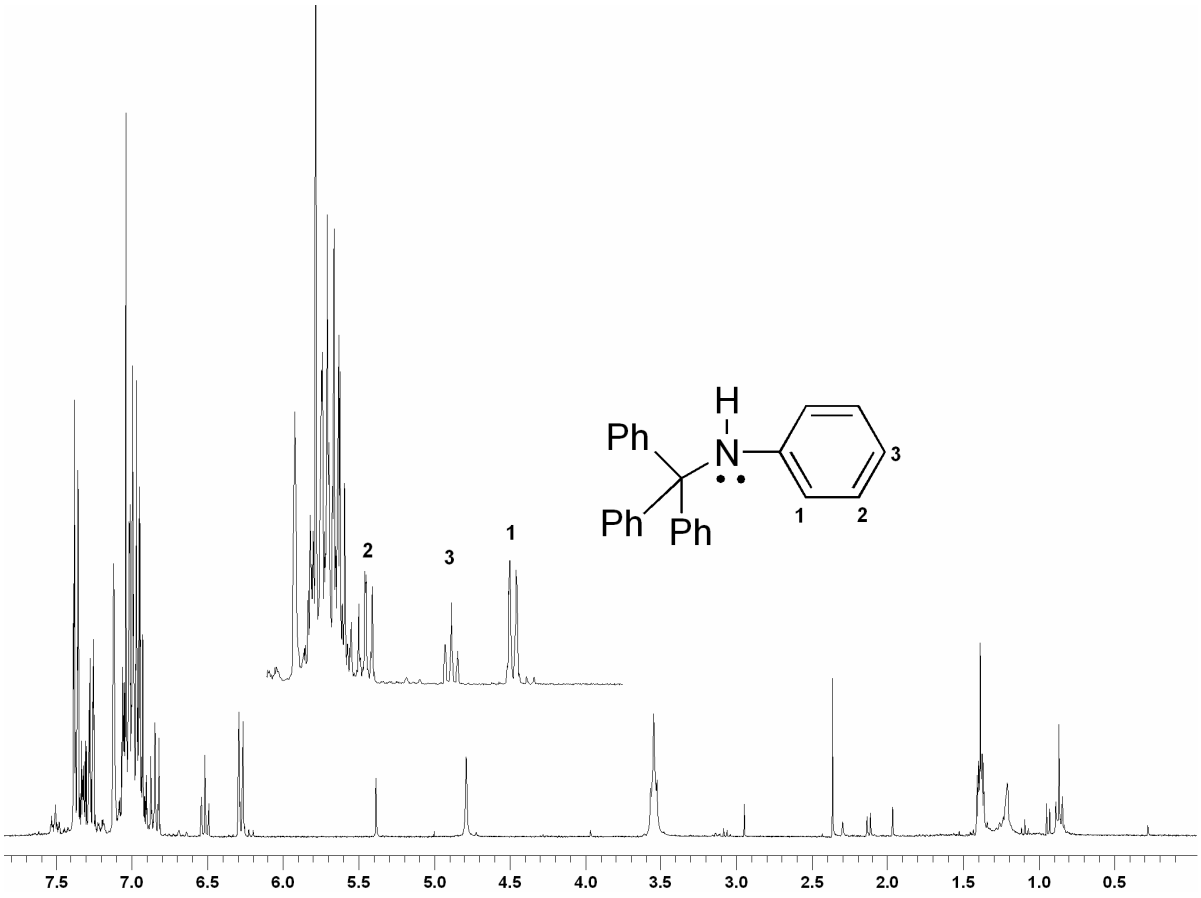

Figure 2.25. Crude ^{1}H NMR spectrum of (dtbpe)Cu(NHPh) and [Ph_3C][OTf] reaction with trityl aniline product indicated in C_6D_6

Kinetics of (dtbpe)Cu(NHPh) and bromoethane. Bromoethane (87 μL, 1.17 mmol) was added to a solution of (dtbpe)Cu(NHPh) (0.046 g, 0.097 mmol) in C_6D_6 (2.4 mL) with hexamethylbenzene (0.0008 g, 0.005 mmol) as an internal standard ([Cu] = 0.04). The solution was immediately divided between 3 screw-cap NMR tubes and frozen in an acetone/dry ice slush bath. Sequentially, the reaction mixtures were each allowed to warm to room temperature and the reactions were followed by ^{1}H NMR at room temperature at even time intervals. The integration of the peaks due to the disappearance of (dtbpe)Cu(NHPh) and the appearance of ethyl aniline versus the internal standard were used to calculate the

rate of the reaction, k_{obs} = 5.5(2) × 10^{-4}. Crystals of a copper byproduct, likely [(dtbpe)Cu(Br)]$_2$ were observed. ^{1}H NMR spectra in $CDCl_3$ were similar to that of [(dtbpe)Cu(Cl)]$_2$; however, this complex was not isolated. Addition of an authentic sample confirmed production of *N*-ethylaniline.

Reaction of (dtbpe)Cu(NHPh) with iodoethane. To a screw cap NMR tube, (dtbpe)Cu(NHPh) was added (10.8 mg (0.023 mmol)) with C_6D_6 (0.8644 g (11.1 mmol)). Iodoethane was added to the solution (18.2 μL (0.228 mmol)) along with ferrocene as an internal standard. The formation of *N*-ethylaniline was observed within 5 minutes by ^{1}H NMR. Crystals of a copper byproduct, likely [(dtbpe)Cu(I)]$_2$ were observed; however, this complex was not isolated.

Reaction of (dtbpe)Cu(NHPh) with 2-chloroethyl benzene. To a screw cap NMR tube, (dtbpe)Cu(NHPh) was added (0.0145 mg (0.031 mmol)) with approximately 0.7 mL C_6D_6. To the solution, 2-chloroethyl benzene was added (4 μL, (0.031 mmol)). An initial NMR was taken, and the solution was heated overnight in an 80°C hot oil bath. An NMR was taken, revealing new resonances: ^{1}H NMR (C_6D_6, δ): 5.60 (d, J = 17.4 Hz), 5.07 (d, J = 10.8 Hz), indicating styrene production.

Reaction of (dtbpe)Cu(NHPh) with styrene. A solution of (dtbpe)Cu(NHPh) (0.0199 g, 0.042 mmol) and approximately 0.70 mL C_6D_6 was added to a screw cap NMR tube. An initial NMR was taken, and styrene was added (9.7 μL, 0.084 mmol). The solution was left at room temperature overnight, and a second NMR was taken showing no new peaks. The solution was then heated in an 80°C hot oil bath for 3 days. A third NMR was taken of the brown solution again showing no new peaks.

Hydroamination catalysis of olefins by (dtbpe)Cu(NHPh) (representative procedure). A 0.04 M solution of (dtbpe)Cu(NHPh) (0.012 g, 0.024 mmol) in C_6D_6 (0.6 mL) was placed in a NMR tube with a known amount of hexamethyldisiloxane (10 μL, 0.0005 mmol) as an internal standard and sealed with a septa. For reactions that required significant heating (>50 °C), a screw-cap NMR tube was used. Twenty equivalents of the amine and the olefin were added by syringe, aniline (45 μL, 0.49 mmol) and acrylonitrile (37 μL, 0.49 mmol). The reaction was monitored at regular intervals by ^{1}H NMR for appearance of the new amine product versus the internal standard. Production of the organic products was confirmed by comparison with reported ^{1}H NMR data.[58-60]

Control Reaction: (dtbpe)Cu(Cl) with acrylonitrile and aniline. (dtbpe)Cu(Cl) (0.0075 g, 0.018 mmol) was dissolved in C_6D_6 (0.7 mL) in a J. Young NMR tube with hexamethylbenzene (0.0022 g, 0.014 mmol) as a standard. The chloride complex was not completely soluble in C_6D_6. Aniline (33 μL, 0.36 mmol) and acrylonitrile (24 μL, 36 mmol) were added by syringe, and the reaction was monitored at regular intervals by ^{1}H NMR for 10 days. No new peaks corresponding to an amine product were observed. There was no decomposition of the copper complex.

Control Reaction: dtbpe with acrylonitrile and aniline. The bisphosphine (dtbpe) (0.011 g, 0.033 mmol) was dissolved in C_6D_6 (0.7 mL) in an NMR tube with hexamethylbenzene (0.0013 g, 0.008 mmol) as the standard and aniline (60 μL, 0.66 mmol). Acrylonitrile (44 μL, 0.67 mmol) was added by syringe, and the reaction was monitored at regular intervals by ^{1}H NMR for 10 days. No new peaks corresponding to an amine product were observed. There was no decomposition of the copper complex.

Reaction of [(dtbpe)Cu(NCMe)][PF_6] with PhINTs. [(dtbpe)Cu(NH_2Ph)][PF_6] (0.248 g, 0.44 mmol) was dissolved in THF (15 mL) in a schlenk flask, and chilled to -78 °C under N_2 on a schlenk line. A slurry of PhINTs (0.183 g, 0.49 mmol) was transferred via large bore cannula into the [Cu] solution. The resulting solution was stirred for 1 hour at -78 °C, and was then warmed to room temperature. The pale yellow solution was brought into a glovebox for workup. The solvent was reduced to 10 mL and hexanes was added to precipitate a white solid, which was collected by vacuum filtration. An X-Ray quality crystal was grown by slow diffusion of cyclohexane into a solution of THF, which revealed reaction of the phosphine ligand and PhINTs.

Synthesis of (dtbpe)Cu(OAc). CuOAc (0.146 g, 1.1 mmol) was added to a colorless solution of dtbpe (0.305 g, 0.96 mmol) in THF (20 mL). The solution immediately turned a dark brown and was stirred for 4 hours at which time the solution was orange slurry. The solution was filtered through Celite to remove the orange solids, and the filtrate was reduced *in vacuo* to approximately 2 mL. Hexanes (10 mL) was added to precipitate a white solid, which was collected by vacuum filtration and dried (0.326 g, 80% yield). X-ray quality crystals were grown by layering a solution of (dtbpe)Cu(OAc) in THF with pentane. ^{1}H NMR ($CDCl_3$, δ): 2.02 (s, 3H, OCOCH_3), 1.77 (vt, *N* = 5.1 Hz, 4H, methylene CH_2), 1.20 (vt, *N* = 12.6 Hz, 36H, C(CH_3)$_3$). ^{13}C NMR ($CDCl_3$, δ): 178.6 (s, O*C*OCH$_3$), 33.4 (vt, *J* = 9 Hz, , *C*(CH$_3$)$_3$), 30.3 (vt, *N* = 9.4 Hz, C(*C*H$_3$)$_3$), 23.2 (s, OCO*C*H$_3$), 20.63 (vt, *N* = 25.8 Hz, methylene CH_2). ^{31}P NMR ($CDCl_3$, δ): 26.4 (s). Anal. Calcd. For $C_{20}H_{43}Cu_1O_2P_2$: C, 54.46: H, 9.83 : O, 7.26. Found: C, 54.39: H, 9.97; O, 7.20.

Synthesis of (dtbpe)Cu(Me). A slurry of complex **5** (0.579 g, 1.3 mmol) in diethyl ether (10 mL) was chilled to -60 °C for 30 minutes. Anhydrous ethanol (0.2 mL, 3.4 mmol) was added to a solution of 2.0 M $AlMe_3$ (1.7 mL, 3.4 mmol) in ether (5 mL), which bubbled vigorously upon mixing. This solution was added dropwise to the solution of **5**, and was stirred at -60 °C for one hour during which time the solution was a homogeneous mixture. The volatiles were removed *in vacuo*. A minimal amount of hexanes (approximately 3 mL) was added resulting in the formation of a precipitate after overnight storage at -20 °C under N_2. The white product was collected by vacuum filtration and dried, and stored under N_2 at -20 °C (0.136 g, 25% yield). ^{1}H NMR (C_6D_6, δ): 1.46 (bs, 4H, methylene C*H*$_2$), 1.09 (vt, *N* = 12.6 Hz, 36H, C(C*H*$_3$)$_3$), 0.35 (bs, 3H, (C*H*$_3$)). ^{13}C NMR (C_6D_6, δ): 34.5 (vt, N = 6 Hz, *C*(CH$_3$)$_3$), 31.3 (vt, N = 10 Hz, C(*C*H$_3$)$_3$), 22.1 (vt, N = 23 Hz, methylene *C*H$_2$), -7.1 (br s, CuC*H*$_3$). ^{31}P NMR (C_6D_6, δ): 33.1 (s). CV (THF, TBAH, 100 mV/s): $E_{p,a}$ = 0.4 V. This complex decomposes over a period of days under inert atmosphere and this instability precludes satisfactory elemental analysis.

Heating of (dtbpe)Cu(Me) in C_6D_6. (dtbpe)Cu(Me) (0.035 g, 0.088 mmol) was dissolved in C_6D_6 (approximately 0.6 mL) and hexamethyldisiloxane (3 μL, 0.014 mmol) was added as an internal standard. The reaction was heated for 18 hours at 80 °C. The formerly pale yellow solution was colorless and the tube had an orange-gold film on it, presumably Cu(0). ^{1}H NMR of the reaction mixture revealed NMR peaks consistent with ethane (0.8 ppm) and free dtbpe, and a ^{31}P NMR was consistent with free dtbpe. An authentic sample of dtbpe was added and an increase in the peaks associated with dtbpe confirmed the product was free ligand.

Heating of (dtbpe)Cu(Me) in C_6D_6 with furan. (dtbpe)Cu(Me) (0.0098 g, 0.025 mmol) was dissolved in C_6D_6 (approximately 0.6 mL) with hexamethyldisiloxane (2 μL, 0.009 mmol) as an internal standard. Approximately 5 equivalents furan (9 μL, 0.12 mmol) was added and the solution was sealed in a J. Young NMR tube and heated for 18 hours at 80 °C. The formerly pale yellow solution was colorless and the tube had an orange-gold film on it, presumably Cu(0). ^{1}H NMR of the reaction mixture revealed NMR peaks consistent with ethane (0.8 ppm) and free dtbpe, and a ^{31}P NMR was consistent with free dtbpe. The furan peaks were unchanged. An authentic sample of dtbpe was added and an increase in the peaks associated with dtbpe confirmed the product was free ligand.

References

1. Tolman, C. A. *Chem. Rev.* **1977,** 77, 313-348.
2. van Leeuwen, P. W. N. M.; Dierkes, P. *J. Chem. Soc., Dalton Trans.* **1999**, 1519-1530.
3. Gusev, D. G.; Madott, M.; Dolgushin, F. M.; Lyssenko, K. A.; Antipin, M. Y. *Organometallics* **2000,** 19, 1734-1739.
4. Moulton, C. J.; Shaw, B. L. *J. Chem. Soc., Dalton Trans.* **1976**, 1020-1024.
5. Jensen, C. M. *Chem. Commun.* **1999**, 2443-2449.
6. Albrecht, M.; Koten, G. v. *Angew. Chem., Int. Ed. Eng.* **2001,** 40, 3750-3781.
7. van der Boom, M. E.; Milstein, D. *Chem. Rev.* **2003,** 103, 1759-1792.
8. Conner, D.; Jayaprakash, K. N.; Cundari, T. R.; Gunnoe, T. B. *Organometallics* **2004,** 23, 2724-2733.
9. Zhang, J. B.; Gunnoe, T. B.; Peterson, J. L. *Inorg. Chem.* **2005,** 44, 2895-2907.
10. Blue, E. D.; Gunnoe, T. B.; Brooks, N. R. *Angew. Chem., Int. Ed. Eng.* **2002,** 41, 2571-2573.
11. Kenneth M. Merz, J.; Hoffmann, R. *Inorg. Chem.* **1988,** 27, 2120-2127.
12. Yam, V. W. W.; Cheng, E. C. C. *Gold Bull.* **2001,** 34, 20-23.
13. Yam, V. W. W.; Lo, K. K. W. *Chem. Soc. Rev.* **1999,** 28, 323-334.
14. Pyykko, P. *Chem. Rev.* **1997,** 97, 597-636.
15. Balzani, V.; Juris, A.; Venturi, M.; Campagna, S.; Serroni, S. *Chem. Rev.* **1996,** 96, 759-833.
16. Sullivan, R. M.; Martin, J. D. *J Am Chem Soc* **1999,** 121, 10092-10097.
17. Yam, V. W.-W.; Cheng, E. C. C. *Angew. Chem.* **2000,** 39, 4240-4242.
18. Che, C. M.; Mao, Z.; Miskowski, V. M.; Tse, M. C.; Chan, C. K.; Cheung, K. K.; Phillips, D. L.; Leung, K. H. *Angew. Chem., Int. Ed. Eng.* **2000,** 39, 4084-4088.
19. Blue, E. D.; Davis, A.; Conner, D.; Gunnoe, T. B.; Boyle, P. D.; White, P. S. *J. Am. Chem. Soc.* **2003,** 125, 9435-9441.
20. Tsuda, T.; Watanabe, K.; Miyata, K.; Yamamoto, H.; Saegusa, T. *Inorg. Chem.* **1981,** 20, 2728-2730.
21. Eriksson, H.; Hakansson, M. *Organometallics* **1997,** 16, 4243-4244.
22. Hope, H.; Power, P. P. *Inorg. Chem.* **1984,** 23, 936-937.
23. Power, P. P. *Prog. Inorg. Chem.* **1991,** 39, 75-112.
24. Chen, H.; Olmstead, M. M.; Shoner, S. C.; Power, P. P. *J. Chem. Soc., Dalton Trans.* **1992**, 451-457.
25. Tsuda, T.; Miwa, M.; Saegusa, T. *J. Org. Chem.* **1979,** 44, 3734-3736.
26. Kitagawa, Y.; Oshima, K.; Yamamoto, H.; Nozaki, H. *Tetrahedron Lett.* **1975**, 1859-1862.
27. Gambarotta, S.; Bracci, M.; Floriani, C.; Chiesivilla, A.; Guastini, C. *J. Chem. Soc., Dalton Trans.* **1987**, 1883-1888.
28. Conner, D.; Jayaprakash, K. N.; Gunnoe, T. B.; Boyle, P. D. *Inorg. Chem.* **2002,** 41, 3042-3049.

29. Pauling, L., *The nature of the chemical bond, and the structure of molecules and crystals : an introduction to modern structural chemistry*. 3 ed.; Cornell University Press: Ithaca, NY, 1960.
30. Conner, D.; Jayaprakash, K. N.; Gunnoe, T. B.; Boyle, P. D. *Organometallics* **2002,** 21, 5265-5271.
31. Allred, A. L. *J. Inorg. Nucl. Chem.* **1961,** 17, 215-221.
32. Seligson, A. L.; Trogler, W. C. *Organometallics* **1993,** 12, 744-751.
33. Nettekoven, U.; Hartwig, J. F. *J. Am. Chem. Soc.* **2002,** 124, 1166-1167.
34. Zhao, P.; Krug, C.; Hartwig, J. F. *J. Am. Chem. Soc.* **2005,** 127, 12066-12073.
35. Kawatsura, M.; Hartwig, J. F. *J. Am. Chem. Soc.* **2000,** 122, 9546-9547.
36. Utsunomiya, M.; Kuwano, R.; Kawatsura, M.; Hartwig, J. F. *J. Am. Chem. Soc.* **2003,** 125, 5608-5609.
37. Clark, H. R.; Clark, R.; Jones, M. M. *Inorg. Chem.* **1971,** 10, 28-33.
38. Kannan, S.; James, A. J.; Sharp, P. R. *Inorg. Chim. Acta* **2003,** 345, 8-14.
39. Reger, D. L.; Huff, M. F.; Lebioda, L. *Acta Crystallogr., Sect. C* **1991,** 47, 1167-1169.
40. Lail, M.; Arrowood, B. N.; Gunnoe, T. B. *J. Am. Chem. Soc.* **2003,** 125, 7506-7507.
41. Lail, M.; Bell, C. M.; Conner, D.; Cundari, T. R.; Gunnoe, T. B.; Petersen, J. L. *Organometallics* **2004,** 23, 5007-5020.
42. Pittard, K. A.; Lee, J. P.; Cundari, T. R.; Gunnoe, T. B.; Petersen, J. L. *Organometallics* **2004,** 23, 5514-5523.
43. Pittard, K. A.; Cundari, T. R.; Gunnoe, T. B.; Day, C. S.; Petersen, J. L. *Organometallics* **2005,** 24, 5015-5024.
44. Goj, L. A.; Lail, M.; Pittard, K. A.; Riley, K. C.; Gunnoe, T. B.; Petersen, J. L. *Chem. Commun.* **2006**, 982-984.
45. Feng, Y.; Lail, M.; Barakat, K. A.; Cundari, T. R.; Gunnoe, T. B.; Petersen, J. L. *J. Am. Chem. Soc.* **2005,** 127, 14174-14175.
46. Feng, Y.; Lail, M.; Foley, N. A.; Gunnoe, T. B.; Barakat, K. A.; Cundari, T. R.; Petersen, J. L. *J. Am. Chem. Soc.*, , in press.
47. Dempsey, D. F.; Girolami, G. S. *Organometallics* **1988,** 7, 1208-1213.
48. Coan, P. S.; Folting, K.; Huffman, J. C.; Caulton, K. G. *Organometallics* **1989,** 8, 2724-2728.
49. Mankad, N. P.; Laitar, D. S.; Sadighi, J. P. *Organometallics* **2004,** 23, 3369-3371.
50. Mankad, N. P.; Gray, T. G.; Laitar, D. S.; Sadighi, J. P. *Organometallics* **2004,** 23, 1191-1193.
51. Goj, L. A.; Blue, E. D.; Munro-Leighton, C.; Gunnoe, T. B.; Petersen, J. L. *Inorg. Chem.* **2005,** 44, 8647-8649.
52. Goj, L. A.; Blue, E. D.; Delp, S. A.; Gunnoe, T. B.; Cundari, T. R.; Petersen, J. L. *manuscript submitted* **2006**.
53. Pörschke, K. R.; Pluta, C.; Proft, B.; Lutz, F.; Krüger, C. *Z. Naturforsch., B: Chem. Sci.* **1993,** 48, 608-626.
54. Kubas, G. J. *Inorg. Synth.* **1979,** 19, 90.
55. Yamada, Y.; Yamamoto, T.; Okawara, M. *Chem. Lett.* **1975**, 361-362.

56. Sodergren, M. J.; Alonso, D. A.; Bedekar, A. V.; Andersson, P. G. *Tetrahedron Lett.* **1997,** 38, 6897-6900.
57. Canle, M.; Clegg, W.; Demirtas, I.; Elsegood, M. R. J.; Maskill, H. *J. Chem. Soc., Perkin. Trans. 2* **2000**, 85-92.
58. Wabnitz, T. C.; Spencer, J. B. *Org. Lett.* **2003,** 5, 2141-2144.
59. Li, K.; Horton, P. N.; Hursthouse, M. B.; Hii, K. K. *J. Organomet. Chem.* **2003,** 665, 250-257.
60. Bartoli, G.; Cimarelli, C.; Palmieri, G. *J. Chem. Soc., Perkin. Trans. 1* **1994**, 537-543.

Chapter 3: Reactivity of β-diketiminate Copper(I) Complexes with Nitrene Sources

3.1 Introduction

Nitrene and oxo complexes of copper have been sought for verification of proposed intermediacy in important catalytic reactions, to investigate the role of oxo species in biological systems, and for fundamental interest in the reactivity of these species. Isolation of both classes of complexes has been elusive, and for the nitrene complex, this is likely due to the high formal oxidation state of the metal center with a dianionic ligand, which often requires copper(III). This high oxidation state of copper is known, but only in a few systems including super- and semi-conductors, systems with porphyrin-type or four-coordinate donating ligands capable of "intramolecular" redox chemistry (e.g., porphyrin ligands can reduce the Cu to yield Cu(II) species) and low-temperature observations of Cu(III) oxo complexes.[1-6] The combination of a high oxidation state metal center and the presence of a reactive oxo or nitrene ligand causes these complexes to be quite rare, and, in fact, no example of a well-defined monomeric copper nitrene complex has been reported.

As discussed above (section 1.3.2), nitrene complexes are proposed intermediates in olefin aziridination catalysis. Our interest in such systems also stems from questions about the nature of the reactivity of these species. The formally dianionic nitrene ligands possess 3 electron pairs and can form formal triple bonds with 1σ and 2π interactions. In a 3-coordinate Cu complex with a monoanionic ancillary ligand and a dianionic nitrene ligand, the formally Cu(III) metal center would be d^8, giving a 14-electron complex without π-bonding, and an 18-electron complex with a full M-nitrene triple bond. Three coordinate

Cu(III) has two orbitals available for π interaction, a dπ and the 4p orbital. Early transition-metal nitrene complexes are typically nucleophilic; however, late transition-metal frontier orbitals are comparatively low in energy and can potentially accept lone pair donation to create an electrophilic nitrene fragment. Evidence for overall electrophilic character of late transition-metal nitrenes is derived from nitrene transfer reactions to Lewis bases such as phosphines or olefins;[7-10] however, direct nucleophilic addition to a nitrene fragment has not been definitively demonstrated and remains conjective. Also, the nucleophilicity of our Cu(I) amido complexes (see Ch. 2) suggests that the Cu 4p orbital does not likely participate substantially in π-bonding, and hence, does not mitigate the nucleophilicity of the amido complex. Thus, the likelihood of a truly electrophilic nitrene remains in question, despite common claims that olefin aziridination requires such reactivity (cf. Fischer carbene chemistry and olefin cycloproponation).

Oxo ligands are isoelectronic to nitrene ligands, and copper oxo species are thought to be present in proteins. Copper species bind and activate oxygen to form Cu oxo complexes that are involved in hydroxylation and oxidation reactions, among others.[6] Two pertinent types of copper-oxygen complexes that have been isolated and characterized include $[Cu(III)(\mu\text{-}O)]_2$ (oxo) and $Cu(II)(\eta^2\text{-}O_2)$ (peroxo) (Figure 3.1). Sterically bulky ancillary ligands can inhibit formation of the μ-oxo complexes.[11] Therefore, formation of peroxo complexes (A in Figure 3.1) is typically favored in systems with extremely bulky ligands, while smaller ligand bite angles tend to favor the bis μ-oxo form (B in Figure 3.1).[6]

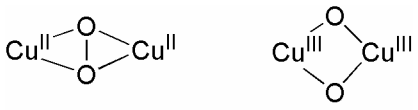

A. B.

Figure 3.1. Copper oxo species: A) Cu(II)(η^2-O_2) and B) [Cu(III)(μ-O)]$_2$.

Using the results of studies of the Cu-oxo systems as a benchmark, the most promising ligands for synthesis of isolable Cu nitrene complexes are systems where the oxo form has been observed. Examples of ligand classes that have been used to isolate structurally characterized [Cu(III)(μ-O)]$_2$ complexes are shown in Figure 3.2.[11-17] Commonly, the instability of [Cu(III)(μ-O)]$_2$ complexes is due to their propensity to abstract a hydrogen atom and form copper(II) hydroxo systems. Examples of these hydroxo complexes that are decomposition products of the μ-oxo and peroxo complexes are quite common.[14, 18-20]

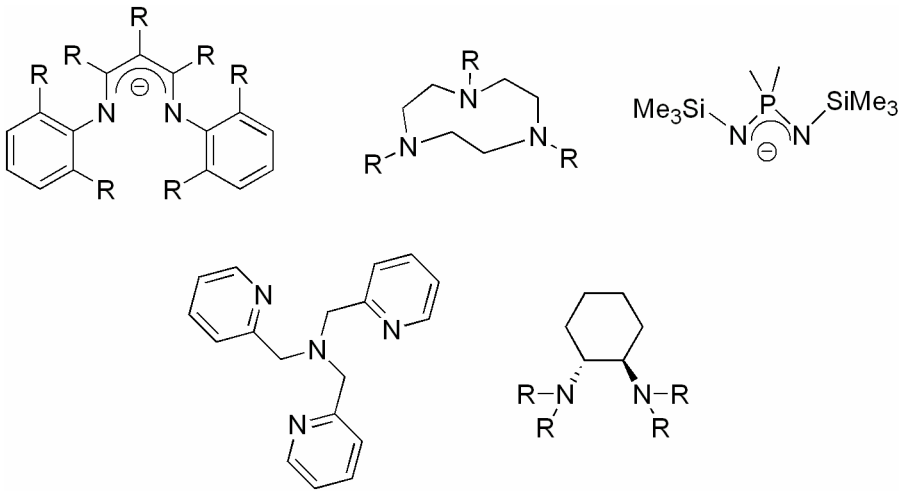

Figure 3.2. Ligand types utilized to isolate Cu(III) oxo complexes.

3.2 System and Ligand Rationale

One class of ligands that has been used successfully with copper to isolate copper(III) μ-oxo complexes is β-diketiminate ligands (NN).[21, 22] (NN) ligands are often called "nacnac" ligands, as the nitrogen-substituted version of acetylacetonate, or "acac." Nacnac ligands are bulky and electron-donating, and the steric and electronic properties are readily tuned by altering the substituents on the aryl rings as well as the carbon backbone. In addition, they lack trivalent phosphorus atoms, which are susceptible to oxidation via nitrene or oxo transfer to form phosphinimines or phosphine oxides, respectively. The two specific ligands we incorporated posses bulky aryl substituents on the nitrogen and methyl groups on the backbone. The substitution on the aryl rings is 2,6-diisopropyl (^{i}PrNN) and 2,6-dimethyl substitution (MeNN) (Figure 3.3). Varying the substitution on the aryl rings allows possible exploration of the steric effects on reactivity. The preparation of these ligands and the corresponding (NN)Cu(NCMe) complexes have been reported.[21, 23] Acetonitrile is a labile ligand and may allow the addition of a nitrene fragment to form copper(III) nitrene complexes.

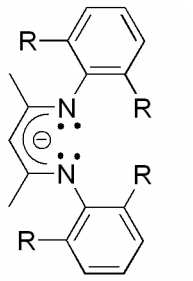

^{i}PrNN: R= isopropyl
MeNN: R= methyl

Figure 3.3. β-diketiminate (NN) ligand.

3.3 Attempted Preparation of Cu Nitrene Complexes

As mentioned above (section 1.3), there are a few late transition-metal nitrene complexes and the most closely related to the proposed Cu(III) nitrene systems is a nickel nitrene complex synthesized by Hillhouse and coworkers.[24] There are currently, to our knowledge, no examples of isolated monomeric copper(III) nitrene complexes (nor published examples of any Cu nitrene). We took two general approaches toward the synthesis of a nitrene complex. The first is overall hydride abstraction from a copper(I) amido complex (pathway A), and the second is nitrene addition to a copper(I) complex with a labile ligand (pathway B) (Scheme 3.1). The two nitrene sources utilized in these studies were *N*-(*p*-tolylsulfonyl)imine phenyliodinane (PhINTs) and azides such as phenyl and tosyl azide.

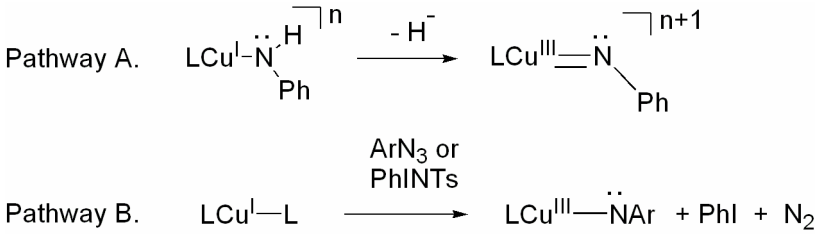

Scheme 3.1. Routes of preparation of a Cu nitrene complex: A) overall hydride abstraction B) reaction with nitrene source.

3.3.1 Abstraction of Hydride from Cu(I) Anilido Complexes

We attempted to generate an amido complex in situ, followed by hydride abstraction. When (MeNN)Cu(NCMe) is reacted with LiNHPh, followed by addition of triphenylcarbenium trifluoromethansulfonate (trityl triflate), [Ph_3C][OTf], a mixture of copper complexes is observed; approximately 30% of the starting complex remains and as

with earlier reactions with trityl cation and amido species, production of trityl amine (Ph_3CNHPh) is observed by ^1H NMR spectroscopy (Scheme 3.2). One of the copper species observed is likely the Cu(I) system with coordinated trityl amine (MeNN)Cu{NHPh(CPh_3)}.

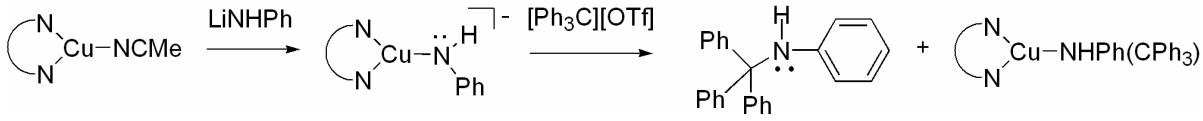

Scheme 3.2. Reaction of (^{i}PrNN)Cu(NCMe) with LiNHPh and $[Ph_3C][OTf]$.

3.3.2 Reaction of (MeNN)Cu(NCMe) or (^{i}PrNN)Cu(NCMe) with PhINTs

When (MeNN)Cu(NCMe) is reacted with PhINTs, the solution turns reddish-brown immediately. The bound acetonitrile peak disappears and new peaks which correspond with free iodobenzene appear in the ^1H NMR spectrum, indicating a reaction with PhINTs to generate "NTs". Two new doublets at 7.94 and 6.79 ppm appear, which are possibly resonances due to the tosyl aryl protons for a (MeNN)Cu(=NTs) complex. These aryl resonances are not due to PhINTs starting material or tosyl amine, a potential decomposition product. In addition, the ligand backbone and methyl peaks shift slightly from 4.79 and 1.66 ppm to 4.83 and 1.55 ppm, respectively (Figure 3.4). This product decomposes to a dark brown material after a few hours at room temperature and was not cleanly isolated nor fully characterized after numerous attempts. Other possibilities for this complex include amido and amine complexes, although none of the broad peaks present in the NMR integrate for 2 protons, discounting the formation of an amine complex, and no counterion is present to support a cationic amido complex. When styrene is added to the potential nitrene, a small amount of (MeNN)Cu(η^2-styrene) complex is observed, but no aziridine is produced

(Scheme 3.3). The styrene complex may form from the putative nitrene product or from unreacted (MeNN)Cu(NCMe) that is present.

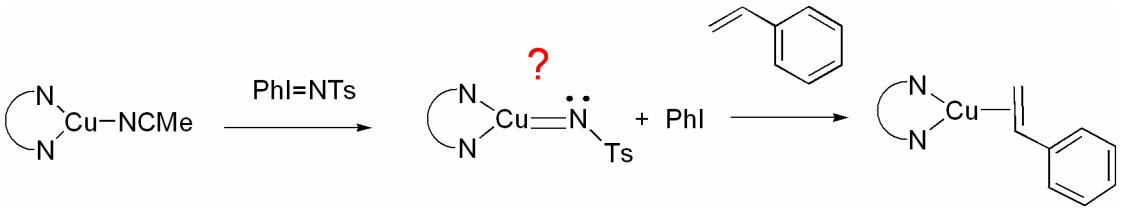

Scheme 3.3. Reaction of potential nitrene with styrene.

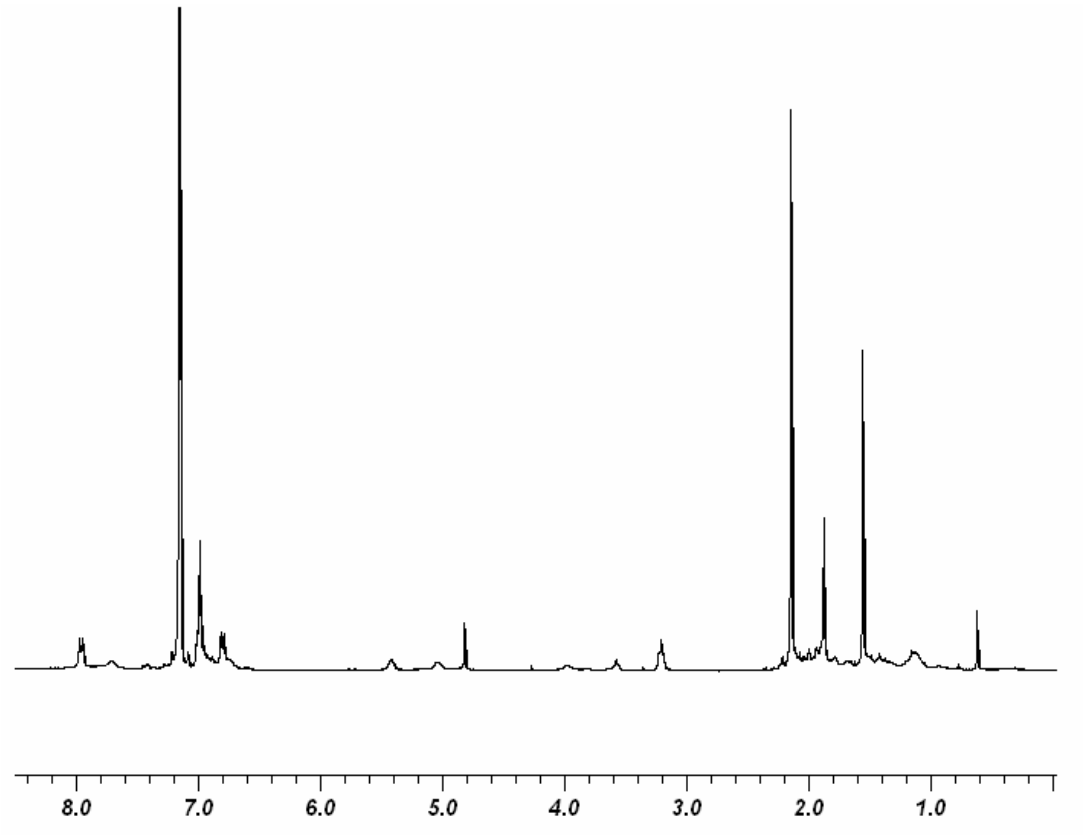

Figure 3.4. ^{1}H NMR spectrum of putative (MeNN)Cu(=NTs) in C_6D_6.

When (^{i}PrNN)Cu(NCMe) is reacted with PhINTs, the solution turns brown, and the ^{1}H NMR spectrum reveals multiple products with some new peaks that are similar to the

product observed for (MeNN)Cu(NCMe); however, the potential (^{i}PrNN)Cu(=NTs) decomposed after a few hours at room temperature and was not cleanly isolated for characterization. When this product is reacted with styrene, no aziridine forms, but a small amount of (^{i}PrNN)Cu(η^2-styrene) is observed. While these reactions may be forming nitrene complexes, the products are not active for olefin aziridination and were not isolable. It is most likely that the complexes produced here are (NN)Cu(NH_2Ts) complexes, because the Ts aryl peaks are downfield of free tosyl amine and the N*H*$_2$ ^{1}H NMR resonances could be too broad to integrate properly.

3.3.3 Reaction of (NN)Cu(NCMe) with PhN_3

Reaction of (MeNN)Cu(NCMe) with phenyl azide (PhN_3) yields a transient dark blue product which quickly decomposes to green at room temperature, followed ultimately by another color change to brown. The green species appear to be paramagnetic complexes, most likely d^9 copper(II), as NMR spectra revealed no resonances due to the MeNN ligand, nor is aniline observed. The brown mixture also contains NMR silent materials, however, aniline is observed in this NMR. A crystal was grown from the crude reaction mixture and an X-ray structure of a Cu(II) dimer [(MeNN)Cu(μ-OH)]$_2$ was solved (Figure 3.5, Table 3.1). The possible pathways for the formation of this complex are discussed below. This hydroxide complex has been previously reported by Warren et al, and this complex was isolated from their attempts to observe a Cu(III) oxo complex using the same metal-ligand system.[20]

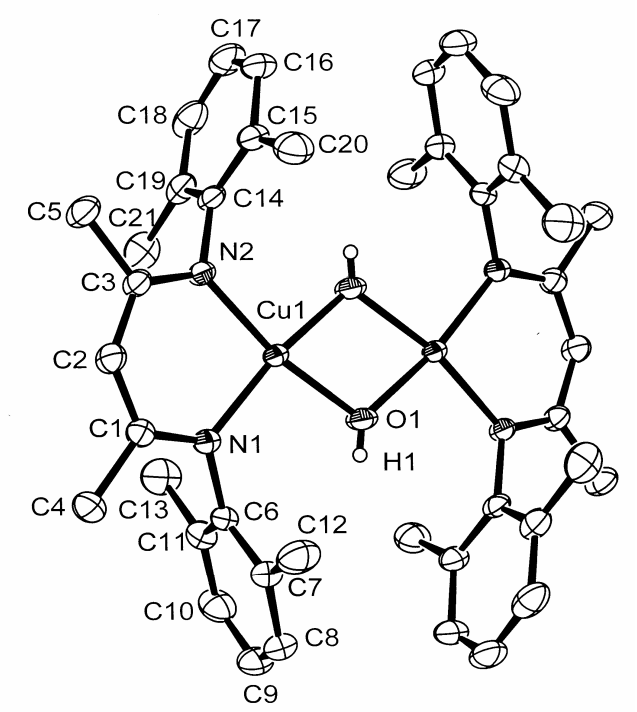

Figure 3.5. ORTEP of $[(MeNN)Cu(\mu\text{-}OH)]_2$ (30% probability). Hydrogen atoms (except for OH) excluded for clarity. Selected Bond Distances (Å): Cu(1)-O(1), 1.908(2); Cu(1)-O(1)', 1.914(2); Cu(1)-N(2), 1.9346(19); Cu(1)-N(1), 1.9444(17); Cu(1)-Cu(1)', 3.0489(5). Selected Bond Angles (º): O(1)-Cu(1)-O(1)', 74.19(10); O(1)-Cu(1), N(2)168.49(9); O(1)'-Cu(1)-N(2), 95.49(8); O(1)-Cu(1)-N(1), 95.93(8); O(1)'-Cu(1)-N(1), 168.93(9); N(2)-Cu(1)-N(1), 94.77(8); Cu(1)-O(1)-Cu(1)', 105.8(1).

Table 3.1. Selected crystallographic data and collection parameters for $[(MeNN)Cu(\mu\text{-}OH)]_2$.

	$[(MeNN)Cu(\mu\text{-}OH)]_2$
empirical formula	C21H26N2OCu
formula wt	385.98
crystal system	monoclinic
space group	C2/c
a, Å	23.577(1)
b, Å	10.6882(6)
c, Å	15.3944(9)
β, º	90.0
V (Å^3)	3872.0(4)
Z	8
D_{calcd}, g cm^{-3}	1.324
crystal size (mm)	0.08 × 0.38 × 0.75
*R*1, w*R*2 {I>2σ(I)}	0.0402, 0.1052
GOF	1.044

When (^{i}PrNN)Cu(NCMe) is reacted with PhN_3 at room temperature, a deep blue color appears immediately from the reaction of the two yellow compounds and gas evolution (N_2) is observed. The blue color persists longer than in the previously described reaction with (MeNN)Cu(NCMe), up to 30 minutes at room temperature, at which time the color of the solution changes to an intense green. Exposure to non-inert atmospheric conditions causes rapid decomposition to a brown complex. Cooling a solution of (^{i}PrNN)Cu(NCMe) and PhN_3 to –78 °C after reaction for 3 minutes at room temperature results in persistence of the blue color for at least 24 hours, after which time it decomposes to the green complex. The combination of (^{i}PrNN)Cu(NCMe) and PhN_3 at –78 °C and –45 °C does not form either the blue or green complexes, but eventually decomposes to the brown mixture. Reactions at –20 °C and 0 °C form green mixtures directly after approximately 5 minutes, without observation of the blue complex. Therefore, the reaction to form the blue complex, possibly a nitrene system, has a relatively low activation barrier, but does require at least ambient temperature to occur. However, the product is thermally unstable and decomposes relatively quickly at room temperature. Multiple attempts were made to isolate and crystallize both the green and blue complexes using numerous solvent systems and various conditions and temperatures, but no crystals were obtained. The green and brown solutions are NMR silent, and thus are presumed to result from paramagnetic Cu(II) complexes. It is likely that the complex decomposes to form the copper(II) species [(^{i}PrNN)Cu(μ-OH)]$_2$, similar to the complex isolated in the reaction of (MeNN)Cu(NCMe) and PhN_3.

Temperature-controlled NMR experiments were performed to attempt in situ observation of a nitrene complex. Addition of PhN_3 to (^{i}PrNN)Cu(NCMe) in the glove box

gave a quick color change to the intense blue color, and the complex was kept at -78 °C until it was transferred to the pre-cooled (–78 °C) NMR probe. The blue color remained, but the complex appeared to be paramagnetic, as indicated by the decrease in the intensity of the NMR peaks of (^{i}PrNN)Cu(NCMe) starting material compared to the solvent peaks. This solution was allowed to warm slowly to room temperature and was monitored by ^{1}H NMR spectrum. Multiple resonances appeared as the solution was warmed, indicating decomposition and the solution was green upon removal from the NMR at room temperature.

The formation of the Cu(II) hydroxide complex as the final decomposition product is likely formed via one of two pathways: A) hydrolysis of the nitrene complex to form an oxo complex and amine, followed by hydrogen atom abstraction; or B) hydrogen atom abstraction, perhaps from solvent, to form an amido complex followed by reactions with H_2O to form the hydroxo complex and free amine (Scheme 3.4).

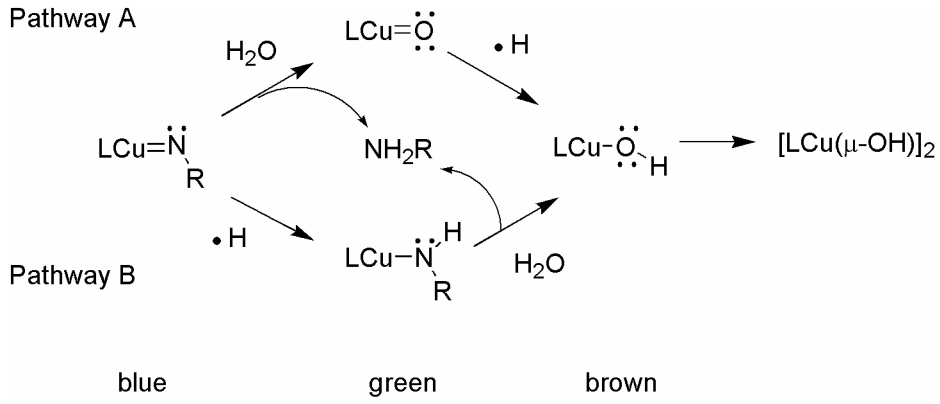

Scheme 3.4. Possible decomposition pathways for a Cu(III) nitrene complex.

The hydrolysis of nitrene complexes to form oxo complexes and organic amine has been shown to occur readily.[9, 10, 25, 26] For example, Bergman et al. have observed hydrolysis

of an iridium nitrene complex to form a μ–oxo complex.[9] Espenson has also studied the kinetics of the oxo/nitrene interchange and has observed a $\Delta S^{\ddagger} < 0$, which points to a four center transition state for the metathesis reaction.[25, 27] The most common decomposition pathway for Cu^{III}(μ-oxo) complexes is hydrogen atom abstraction; for example, the original report of $[(MeNN)Cu(\mu\text{-}OH)]_2$ was in reactions directed toward isolation of oxo complexes.[20] The exact mechanism of this process is not well understood and the source of hydrogen atoms is not often clear, although solvent and glassware are obvious potential sources.

If pathway A is active, then the blue complex formed during the reaction of both β-diketiminate copper(I) acetonitrile complexes with phenyl azides may react with trace amounts of water, to form the green species, an oxo complex, which would then rapidly abstract a hydrogen atom to form the isolated copper(II) hydroxo complex (Scheme 3.5). Pathway B is also possible, as other Cu(III) complexes, in addition to Cu(III) oxo complexes described above have been demonstrated to abstract hydrogen atoms.[28] Experimental evidence favors pathway B, because the green complex is stable at room temperature until it is exposed to ambient conditions, at which time the brown hydroxo species is formed (Scheme 3.6). No examples of room temperature-stable Cu(III) oxo complexes have been isolated. In addition, the green complex is NMR silent, which is consistent with a Cu(II) amido complex, and the byproduct of hydrolysis, aniline, is only observed after formation of the brown species. The blue complex may be a Cu(III) nitrene; however even low temperature NMR experiments did not allow observation of a diamagnetic NMR spectrum for this species, and, thus, we have no <u>direct</u> evidence for the identity of this complex.

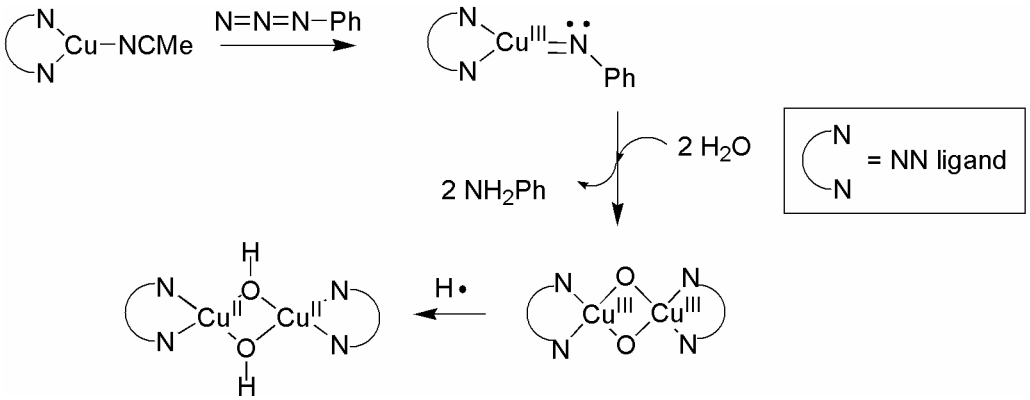

Scheme 3.5. Potential decomposition pathway of Cu(III) nitrene complexes by hydrolysis and hydrogen atom abstraction.

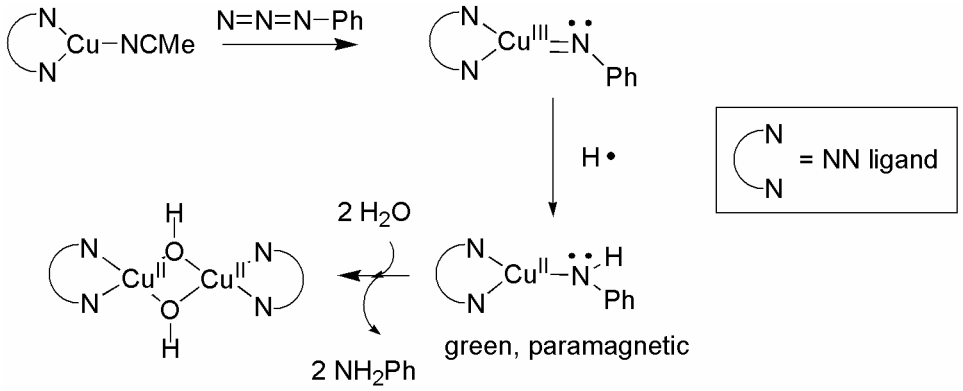

Scheme 3.6. Likely decomposition pathway for Cu(III) nitrene complex by hydrogen atom abstraction and hydrolysis.

3.3.5 Nitrene Trapping Experiments

There are many examples of using a Lewis base to trap nitrene complexes.[7-10] For example, Bergman and coworkers have successfully observed nitrene transfer to phosphines with monomeric and bridging nitrene complexes.[9, 10] Therefore, experiments to trap the proposed nitrene species using the Lewis base trimethylphosphine were attempted. Indeed, reaction of the product of the potential copper nitrene (^{i}PrNN)Cu(NPh) with excess PMe_3

yielded phosphinimine and (^{i}PrNN)Cu(PMe_3). However, these reactions were conducted using impure mixtures, and thus the reactivity of the starting materials was also investigated. It was found that the copper starting material, (^{i}PrNN)Cu(NCMe) readily reacts with PMe_3 to release free acetonitrile and form (^{i}PrNN)Cu(PMe_3) (Scheme 3.7). In addition, Staudinger and Mayer discovered in 1919 that formation of *N*-phenyltriphenyliminophosphorane from

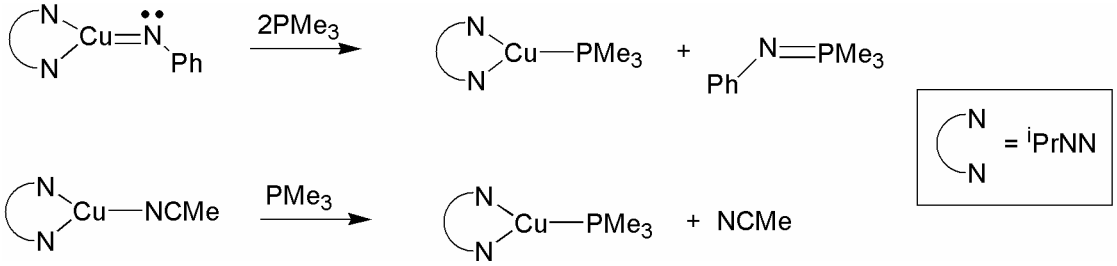

Scheme 3.7. Reactions of the potential nitrene (^{i}PrNN)Cu(=NPh) and (^{i}PrNN)Cu(NCMe) with PMe_3.

triphenylphosphine and phenyl azide is a spontaneous reaction (eq 1).[29] This reaction is general for formation of phosphinimines from aryl azides and phosphines or phosphate, occurs at room temperature and is known as the Staudinger reaction. The phosphinimine formed can subsequently undergo hydrolysis to form amine and phosphine oxide.[30, 31] In addition, the other nitrene source used in our studies, PhINTs, has been reported to form phosphinimines upon reaction with triphenylphosphine in an analogous fashion (eq 2).[32] For this reaction, reflux reaction conditions are reported; however, we found that this reaction occurs rapidly at room temperature. The proposed pathway is decomposition of the I-N ylide to form iodobenzene and a free nitrene intermediate, which can then react with triphenylphosphine to form *N*-sulfonyltriphenylphosphinimine. Reaction with trimethylphosphine is not reported specifically, but we observe analogous reactivity to form *N*-sulfonyltrimethylphosphinimine from reaction of PMe_3 and PhINTs at room temperature.

A new ^{31}P NMR peak at 26.5 ppm in $CDCl_3$ versus a resonance for free PMe_3 of –60.6 ppm are observed for Me_3P=NTs.

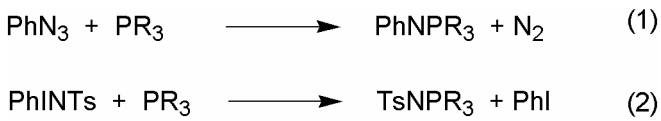

Due to the reactivity of the starting materials with trimethylphosphine, these attempts to trap the nitrene complex do not conclusively support formation of nitrene complexes. Therefore, a Lewis acid was considered as a trapping agent. Combination of BF_3 and PhN_3 does not result in formation of a new adduct. However reaction of the potential nitrene, (^{i}PrNN)Cu(=NPh) or (^{i}PrNN)Cu(NCMe) with BF_3 resulted in multiple new peaks and a complicated product mixture.

3.3.6 Nitrene Synthesis Summary

Although we have evidence for formation of a copper nitrene system, we were not successful in isolating these systems. We postulate that the nitrene does form in the experiments with azides, but is very reactive and decomposes quickly. We did not observe aziridination with the potential nitrenes in the PhINTs or azide systems. An even more strongly donating ancillary ligand set may stabilize the formal Cu(III) oxidation state and enhance stability or, in contrast, an approach utilizing systems containing electron-withdrawing ligand systems to enhance the Cu-nitrene bonding, may increase the likelihood of formation of an isolable nitrene. We have shown from this research that phosphine ligands should be avoided in the synthesis of nitrene complexes, and that decomposition

most likely occurs via hydrogen atom abstraction to form a Cu(II) amido complex, which can decompose further to form a Cu(II) hydroxide complex.

3.4 Catalytic Aziridination Reactions

Because nitrenes are thought to be intermediates in aziridination catalysis, we tested the potential nitrene precursor complexes, (^{i}PrNN)Cu(NCMe) and (MeNN)Cu(NCMe), for catalytic activity. For both complexes, we observed production of *N*-(*p*-tolylsulfonyl)-2-phenyl aziridine at ambient temperature from styrene and PhINTs. The reaction using (MeNN)Cu(NCMe), with 5 mol% catalyst gave 97% yield at ambient temperature (Table 3.2). Using 5 mol% (^{i}PrNN)Cu(NCMe) complex, 57% yield was observed. For reactions with cyclohexene, *N*-(*p*-tolylsulfonyl)-7-azabicyclo[4.1.0]heptane was produced in 79% yield using 5 mol% (MeNN)Cu(NCMe), and in trace quantities with 5 mol% (^{i}PrNN)Cu(NCMe) as catalyst. Reactions with 1-hexene yielded *N*-(*p*-tolylsulfonyl)-2-*n*-butylaziridine in approximately 89% yield with 5 mol% (MeNN)Cu(NCMe) and 13% yield with 5 mol% (^{i}PrNN)Cu(NCMe). The conversions with (MeNN)Cu(NCMe) are similar to those published with other Cu-catalyzed aziridination catalysis; however, the conversions for (^{i}PrNN)Cu(NCMe) are poor in comparison.[33-37]

Table 3.2. Catalytic aziridination of olefins with NNCu(NCMe) complexes.

Catalyst	Substrate	Product	% Conversion
1	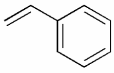	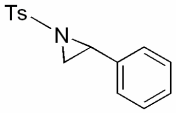	97
1		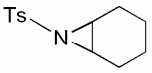	79
1	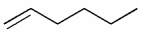	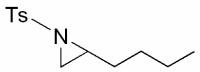	89
2	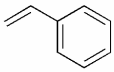	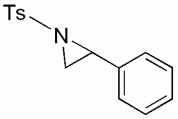	57
2		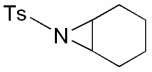	trace
2	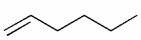	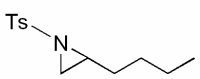	13

(MeNN)Cu(NCMe) (**1**), (^{i}PrNN)Cu(NCMe) (**2**) * All reactions at ambient temperatures, and 5 mol%

Independently, aziridination catalysis was observed by the Warren group with similar complexes, only differing in the labile ligand.[33] Due to their reports, the rates and mechanism of our reaction were not studied in detail. The rapidity and mild conditions of this catalysis may be indicative of the high reactivity of putative Cu(III) nitrene complexes, which underscores the difficulty in isolating these complexes. It is noted that for reactions in which a ^{1}H NMR spectrum was obtained before addition of PhINTs, a new (MeNN)Cu(η^2-styrene) complex was formed, which could be involved in the catalytic cycle (Figure 3.6). Catalysis was also attempted with azides as the nitrene source; however, production of aziridine with these substrates was not observed. The electron-withdrawing tosyl group may play an important role in this catalysis in stabilizing a Cu(II) nitrene intermediate.

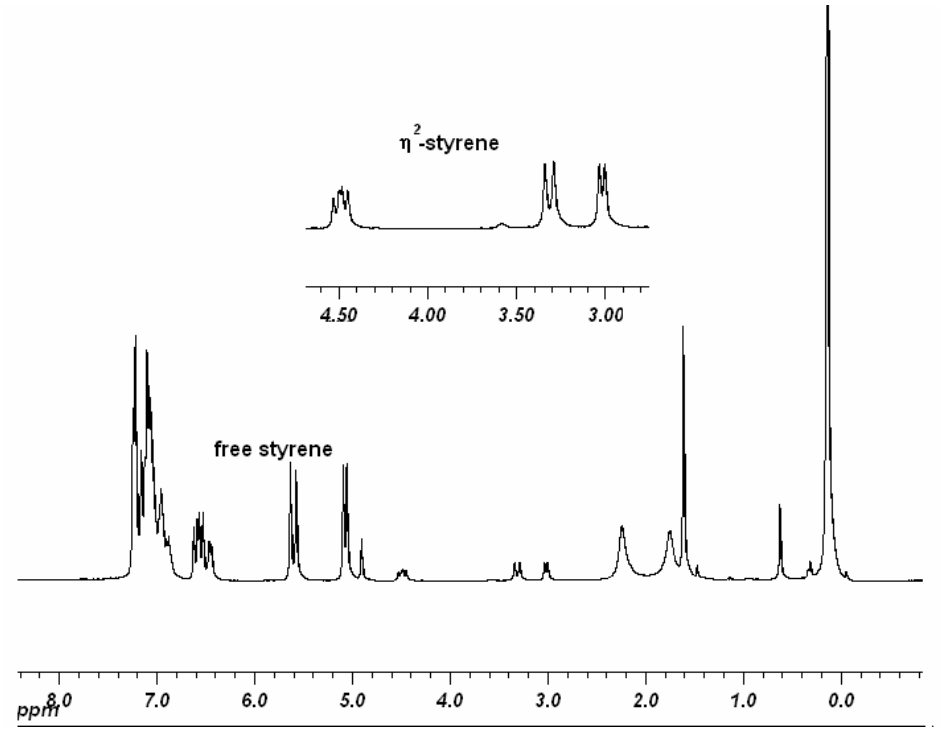

Figure 3.6. ^{1}H NMR spectrum of catalytic aziridination experiment before addition of PhINTs, production of (MeNN)Cu(η^2-styrene) complex in C_6D_6.

3.5 General Experimental Methods.

All reactions and procedures were performed under anaerobic conditions in a nitrogen-filled glovebox or using standard Schlenk techniques. Glovebox purity was maintained by periodic nitrogen purges and monitored by an oxygen analyzer. ^{1}H and ^{13}C NMR spectra were obtained on a Varian Mercury 300 or 400 MHz. All ^{1}H and ^{13}C NMR spectra were referenced against tetramethylsilane using residual proton signals (^{1}H NMR) or the ^{13}C resonances of the deuterated solvent (^{13}C NMR). ^{31}P NMR spectra were obtained on a Varian 300 or 400 MHz spectrometer and referenced against external 85% H_3PO_4. ^{19}F NMR spectra were obtained on a Varian Mercury 300 or 400 MHz and referenced against the external standard C_6F_6 (-163 ppm). Variable-temperature NMR experiments were

performed on a Varian Mercury 300 or 400 MHz spectrometer. IR spectra were obtained on a Mattson Genesis II spectrometer either as thin films on a KBr plate or in solution using a KBr solution cell. Elemental analyses were performed by Atlantic Microlabs, Inc.

Hexanes and CH_2Cl_2 were purified by passage through a column of activated alumina. THF and benzene were dried by distillation over sodium/benzophenone. Pentane was distilled over sodium. Diethyl ether was degassed and stored over 4 Å sieves. C_6D_6 and toluene-d_8 were degassed via three freeze-pump-thaw cycles and stored over 4 Å sieves. Styrene was passed through a silica column and vacuum distilled. Aniline was dried over CaH_2 followed by vacuum distillation.

LiNHPh was generated by reaction of aniline with 1 equivalent of *n*-BuLi in benzene followed by addition of hexanes and vacuum filtration to collect the resulting white precipitate. $[Cu(NCMe)_4][PF_6]$ was prepared according to the published procedure.[38] Synthesis of (^{i}PrNN) and (MeNN) were completed using the synthesis and simplified workup reported by Power, et al.[23] Syntheses of (^{i}PrNN)Cu(NCMe) and (MeNN)Cu(NCMe) were accomplished using the general procedures published by Tolman.[21] PhINTs was synthesized used the modified water-free preparation described by Andersson based on the original procedure.[39, 40] ArN_3 was synthesized using the preparation from Lindsay and Allen[41] and the workup from Zhu and Ma,[42] as described below. $[Ph_3C][OTf]$ was prepared by reaction of $[Ph_3C][Cl]$ with [TMS][OTf] in CH_2Cl_2, followed by precipitation with hexanes. CuCl was purchased from Strem Chemical and used as received. All other reagents were used as purchased from commercial sources.

Synthesis of PhN_3. Phenylhydrazine HCl (9.956 g, 0.069 mol) was placed in a 500 mL 2-neck flask with a stir bar. Water (50 mL), diethyl ether (30 mL), and hydrochloric acid (6 mL) were added to the flask, and the biphasic slurry was chilled to -5°C in an ice/salt bath. Sodium nitrite (5.7 g, 0.083 mol) was dissolved in water (25 mL) and placed in an addition funnel above the chilled, stirring reaction flask. The sodium nitrite solution was added dropwise over about 45 minutes to an hour, so as to not allow the reaction to warm above 5 °C. The reaction solution became an intense yellow/orange color, and was allowed to stir for 30 minutes at 0 °C after the final addition of sodium nitrite. The organic layer was then separated and the water layer was extracted twice with ethyl acetate (25 mL). The organic fractions were combined and washed with brine, and then dried with $MgSO_4$. After filtration the solvent was removed and a reddish-orange oil remained. The residual oil was loaded on a silica gel column, and eluted with petroleum ether/ethyl acetate (10:1) to collect the first fraction of pale yellow solution, leaving the dark red and intense yellow impurities on the column. This solution was purged with nitrogen and brought into the glove box. The solvent was removed, and the yellow oil product was stored over sieves, under N_2 in the freezer. Analytical data for PhN_3: ^{1}H NMR ($CDCl_3$, δ): 7.03 (m, 2H), 7.15 (t, J = 7.5 Hz, 1H), 7.36 (m, 2H); IR (film cm^{-1}) 2101. *p*-Tolyl azide can be prepared in an analogous fashion. Analytical data for *p*-tolyl azide: ^{1}H NMR ($CDCl_3$, δ): 2.35 (s, 3H), 6.93 (d, J = 6.6 Hz, 2H), 7.16 (d, J = 6.6 Hz, 2H); IR (film cm^{-1}) 2106.

Reaction of (MeNN)Cu(NCMe) with LiNHPh and $[Ph_3C][OTf]$. (MeNN)Cu(NCMe) (0.036 g, 0.087 mmol) was dissolved in THF (10 mL) and LiNHPh (0.012 g, 0.118 mmol) was added. The pale yellow solution was stirred for 30 minutes, at

which point the solution was slightly brown. Trityl triflate was added, and the solution immediately turned darker brown. After 2 hours of stirring, the solvent was removed and a crude ^{1}H NMR was taken (Figure 3.7). There was no evidence of the expected triphenylmethane byproduct, but a product that appeared consistent with the amine trityl aniline and some of the amine complex (MeNN)Cu(NHPhCPh$_3$), possessing similar ^{1}H NMR resonances to the independently synthesized (MeNN)Cu(NH$_2$Ph).

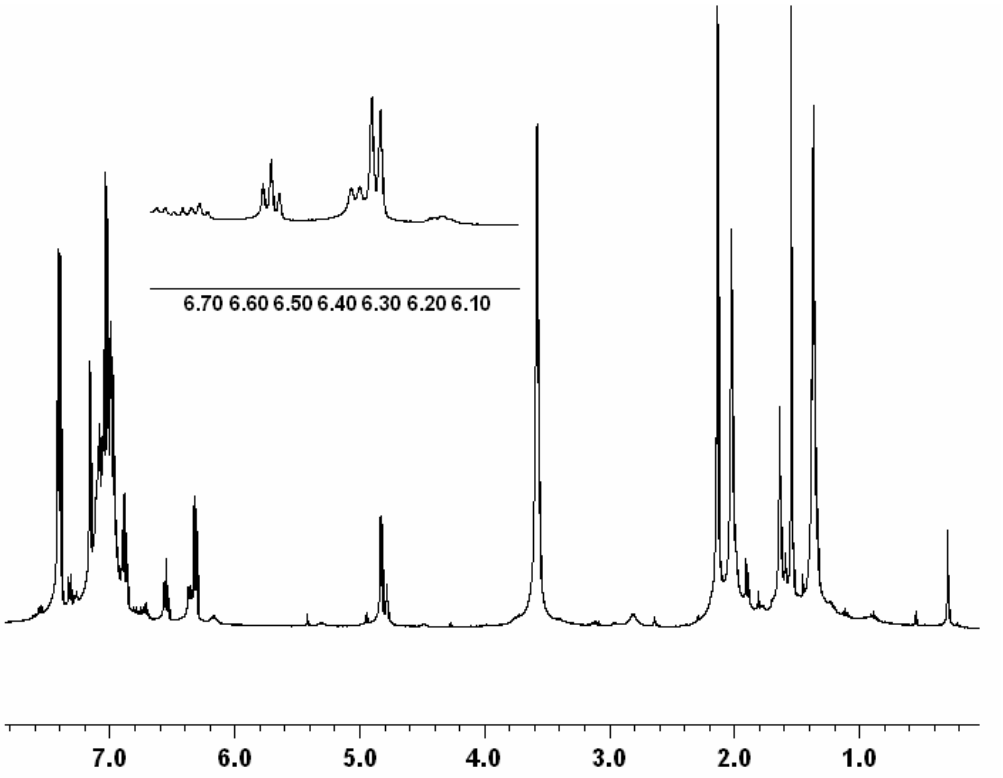

Figure 3.7. Crude ^{1}H NMR spectrum of (MeNN)Cu(NCMe) + LiNHPh + [Ph$_3$C][OTf] reaction in C_6D_6.

Synthesis of (MeNN)Cu(NH$_2$Ph). (MeNN)Cu(NCMe) (0.053 g, 0.130 mmol) was dissolved in THF (10 mL) and aniline (0.015 mL, 0.166 mmol) was added. The solution was initially pale yellow and after stirring for 1 hour, the color was a pale green. The solvent was removed in vacuo, at which time a ^{1}H NMR was obtained in C_6D_6, which corresponded

with an amine complex (Figure 3.8). Full characterization of this complex was not obtained. ^{1}H NMR (C_6D_6, δ): 7.07 – 6.93 (multiplets, ligand aryl *m* and *p*, amine aryl *m*), 6.67 (t, J = 7 Hz, 1H, amine aryl *p*), 6.30 (d, J = 7.5 Hz, 2H, amine aryl *o*), 4.74 (s, 1H, ligand backbone C*H*), 2.70 (bs, 2H, N*H*), 1.99 (s, 12H, ligand aryl CH_3), 1.61 (s, 6H, ligand backbone CH_3), 1.52 (s, free NCMe).

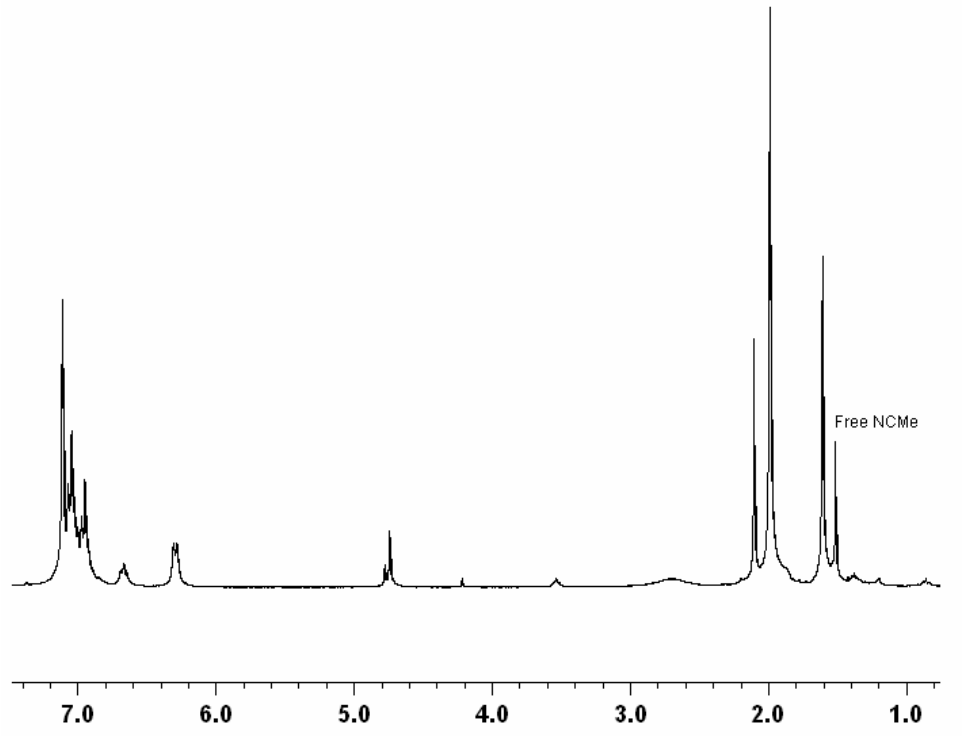

Figure 3.8. ^{1}H NMR spectrum of (MeNN)Cu(NH_2Ph) in C_6D_6.

Reaction of (MeNN)Cu(NCMe) and PhINTs. PhINTs (0.035 g, 0.094 mmol) was added to a stirred solution of (MeNN)Cu(NCMe) (0.038 g, 0.092 mmol) in THF (15 mL). The color of the solution changed from yellow to brownish-red immediately. After 30 minutes of stirring at room temperature, the solution was filtered and a small amount of yellow solid was removed. The solvent was removed in vacuo from the filtrate. ^{1}H NMR of the crude reaction mixture revealed peaks corresponding to iodobenzene (C_6D_6, δ): 7.44 (d, J

= 8.1 Hz) and 6.59 (t, *J* = 8.1 Hz), and a new product (potential nitrene). The crude reaction mixture was purified by dissolution in acetonitrile and filtration to remove a small amount of yellow solid. The red-brown filtrate was dried and an NMR spectra was obtained (shown in section 3.3.1 above). X-ray quality crystals were grown from this reaction mixture at -20 °C from a solution of pentane (5 mL). ^{1}H NMR (C_6D_6, δ): 7.94 (2H, d, *J* = 8 Hz, tosyl aryl), 7.03-6.80 (overlapping multiplets – *p*- and *m*- ligand *N* aryl), 6.79 (2H, d, *J* = 8 Hz, tosyl aryl), 4.83 (1H, s, ligand backbone C*H*), 2.14 (12H, s, *Me*NN), 1.87 (3H, s, tosyl CH_3), 1.55 (6H, s, ligand backbone methyl).

Reaction of Styrene with potential nitrene (MeNN)Cu(=NTs). The potential nitrene formed in the reaction of (MeNN)Cu(NCMe) and PhINTs (0.025 g, 0.046 mmol) was dissolved in C_6D_6. Styrene was added via pipet (approx. 0.1 mL, 0.87 mmol), and the reaction was checked by ^{1}H NMR after 18 hours. The NMR revealed production of a small amount of (MeNN)Cu(η^2-styrene) complex, but no peaks corresponding to the production of *N*-(*p*-tolylsulfonyl)-2-phenyl aziridine were observed.

Reaction of (^{i}PrNN)Cu(NCMe) and PhINTs. PhINTs (0.044 g, 0.117 mmol) was added to a stirred solution of (^{i}PrNN)Cu(NCMe) (0.061 g, 0.117 mmol) in THF (10 mL). The color of the solution changed from yellow to brownish immediately. After 30 minutes of stirring at room temperature, the solvent was removed in vacuo. ^{1}H NMR (C_6D_6, δ) of the crude reaction mixture revealed peaks corresponding to iodobenzene (Figure 3.9): (C_6D_6, δ): 7.44 (d, *J* = 6 Hz), 6.86 (t, *J* = 6 Hz) and 6.59 (t, *J* = 6 Hz), and a new product (potential nitrene): ^{1}H NMR (C_6D_6, δ): 7.94 (2H, d, *J* = 8 Hz, tosyl aryl), 7.03-6.80 (overlapping multiplets – *p*- and *m*- ligand *N* aryl), 6.79 (2H, d, *J* = 8 Hz, tosyl aryl), 4.83

(1H, s, ligand backbone C*H*), 2.14 (12H, s, *Me*NN), 1.87 (3H, s, tosyl CH_3), 1.55 (6H, s, ligand backbone methyl). This complex was not isolable.

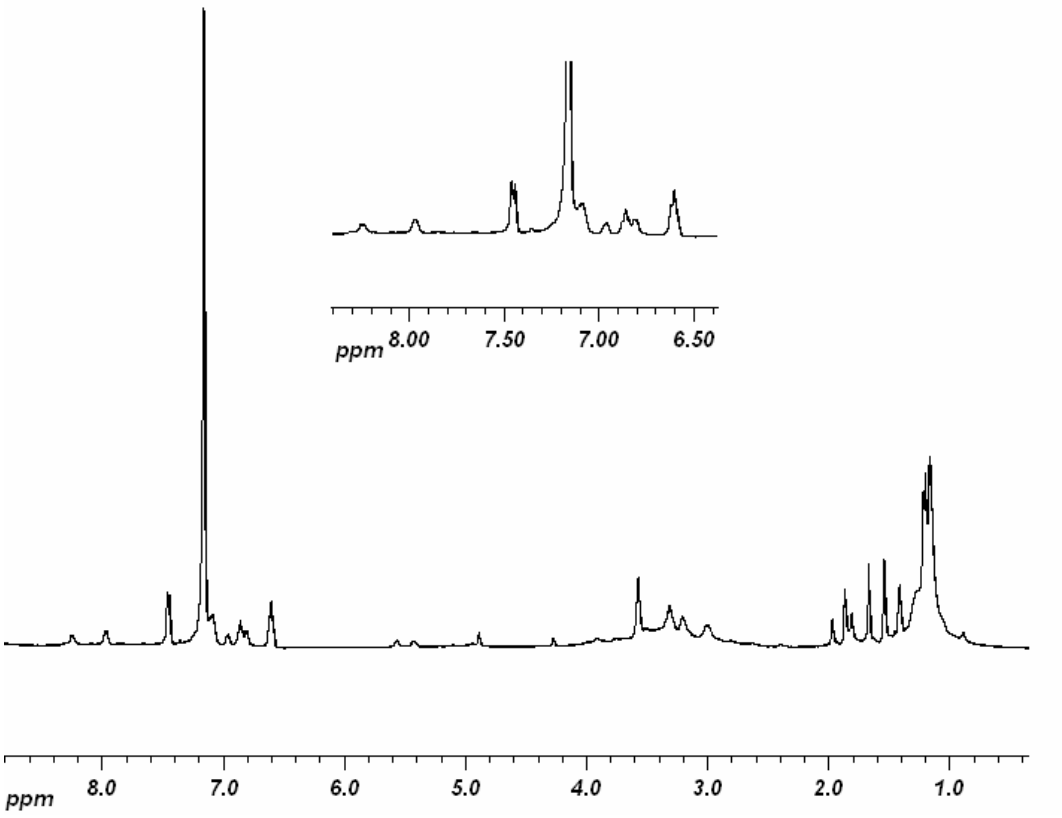

Figure 3.9. ^{1}H NMR spectrum of crude (^{i}PrNN)Cu(=NTs) in C_6D_6.

Reaction of Styrene with potential nitrene (^{i}PrNN)Cu(=NTs). Styrene was added via pipet (approx. 0.1 mL, 0.87 mmol) to an NMR tube containing the crude potential nitrene product formed in the reaction of (^{i}PrNN)Cu(NCMe) and PhINTs in C_6D_6. The reaction was checked by ^{1}H NMR after 24 hours. Peaks corresponding to (^{i}PrNN)Cu(η^2-styrene) were observed; however, no peaks corresponding to the production of *N*-(*p*-tolylsulfonyl)-2-phenyl aziridine were observed.

Reaction of (MeNN)Cu(NCMe) and PhN_3. (MeNN)Cu(NCMe) (0.025 g, 0.062 mmol) was dissolved in THF (20 mL) and PhN_3 (0.007 g, 0.064 mmol) was added via

syringe. The yellow solution turned midnight blue upon addition of the PhN_3. The reaction was stirred for 30 minutes, and the solution was green. ^{1}H NMR of the green crude reaction mixture revealed a paramagnetic complex. Longer sitting or direct exposure to air or water caused further color change to brown.

Reaction of (^{i}PrNN)Cu(NCMe) and PhN_3 at room temperature, persistence at –78 °C. (^{i}PrNN)Cu(NCMe) (0.020 g, 0.038 mmol) was dissolved in approximately 10 mL THF. PhN_3 (0.1 mL, 0.83 mmol) was added. The color of the solution immediately changed from yellow to blue. The solution was placed into a cold well in the glovebox chilled to –78 °C using an acetone/CO_2(s) slush bath. The solution was monitored periodically for color changes. The blue color, representative of the putative nitrene complex persisted for at least 24 hours, at which time the solution color changed to green/black. A ^{1}H NMR spectrum of the paramagnetic green complex is shown below (Figure 3.10). The blue color persists for approximately 30 minutes at room temperature. Upon exposure to air, the solution becomes dark brown and the NMR of this complex contains aniline, but is otherwise paramagnetic (Figure 3.11).

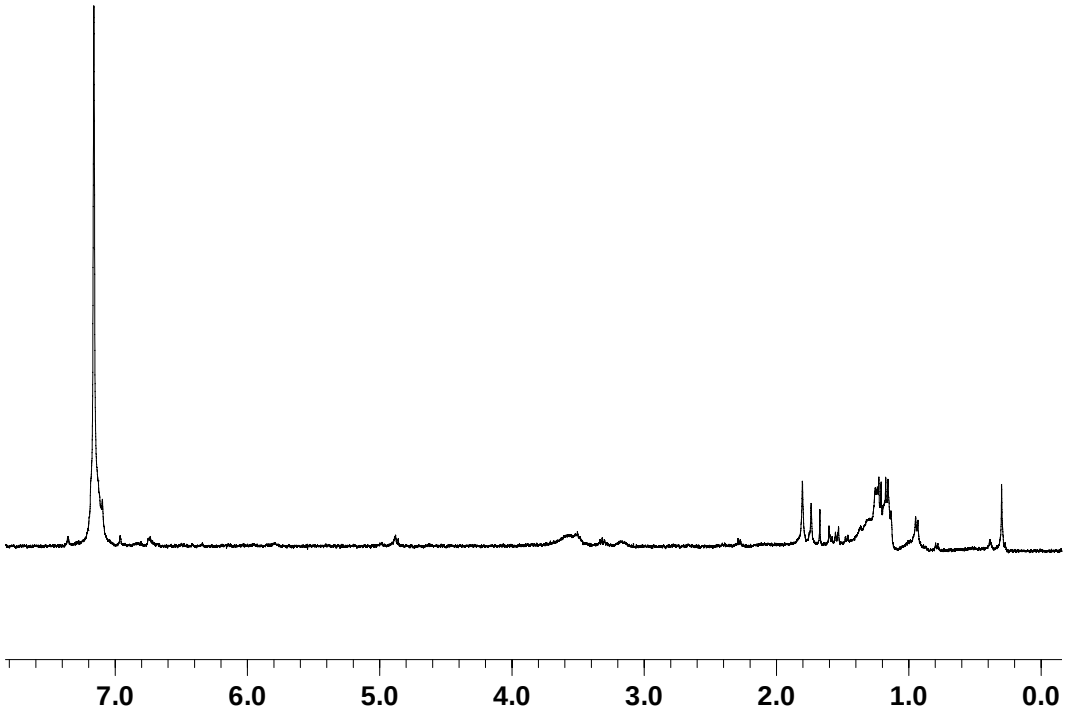

Figure 3.10. ^{1}H NMR spectrum of green paramagnetic complex.

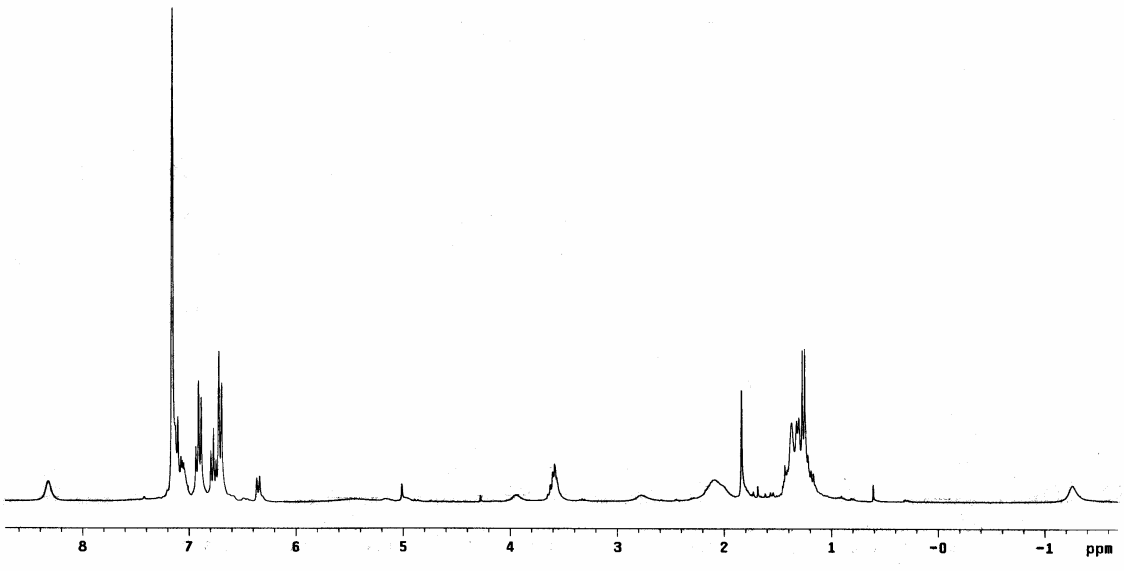

Figure 3.11. ^{1}H NMR spectrum of brown paramagnetic complex containing aniline.

Reaction of (^{i}PrNN)Cu(NCMe) and PhN_3 NMR tube experiments, typical. (^{i}PrNN)Cu(NCMe) (0.023 g, 0.045 mmol) was dissolved in approximately 0.5 mL THF-d_8 in a J. Young NMR tube. An initial ^{1}H NMR was obtained, and the NMR probe was cooled to -78 °C. PhN_3 (3 μL, 0.028 mmol) was added to the NMR tube in the glove box, and the solution immediately changed to an intense blue. The tube was sealed and the solution was kept in an acetone/$CO_{2(s)}$ bath until it was transferred to the NMR. A ^{1}H NMR was taken of the solution at -78 °C, and revealed a paramagnetic complex, as indicated by the significant decrease in the intensity of the NMR resonances due to (^{i}PrNN)Cu(NCMe) as compared to the residual solvent peaks. The solution was warmed to room temperature and monitored periodically by ^{1}H NMR. New resonances appeared, indicating decomposition, and the solution was green upon removal from the NMR.

Reaction of (^{i}PrNN)Cu(NCMe) and PMe_3. (^{i}PrNN)Cu(NCMe) (0.010g, 0.019 mmol) was dissolved in an NMR tube with C_6D_6 (~0.7 mL), and PMe_3 (0.2 mL, 1.9 mmol) was added to the yellow solution. A new copper product, (^{i}PrNN)Cu(PMe_3), was formed as observed by ^{31}P NMR (C_6D_6, δ): -49 (bs). (Free PMe_3: -62 ppm) ^{1}H NMR (C_6D_6, δ): 7.12-7.07 (m, 6H, aryl), 4.98 (s, 1H, backbone C*H*), 3.44 (septet, *J* = 5.5 Hz, 4H, C*H*(CH_3)$_2$), 1.83 (s, 6H, backbone CH_3), 1.26, 1.22 (d, *J* = 5.5 Hz, 12H, CH(CH_3)$_2$), 0.38 (d, *J* = 4.8 Hz, 9H, P(CH_3)$_3$).

Reaction of PhN_3 with PMe_3. PMe_3 (0.1 mL, 0.97 mmol) was added to an NMR tube with C_6D_6 (~0.7 mL), and PhN_3 (0.1 mL, 0.84 mmol) was added. The pale yellow solution changed to true yellow and rapid gas evolution was observed. A new ^{31}P NMR peak for the product PhN=PMe_3 was observed at 3.0 ppm (versus free PMe_3 at -62 ppm).

When this reaction is conducted in $CDCl_3$, the ^{31}P NMR data correspond to the reported data for $PhN{=}PMe_3$ in related trapping experiments.[9]

Reaction of PhINTs with PMe_3. PhINTs (0.024 g, 0.064 mmol) was combined with PMe_3 in an NMR tube with $CDCl_3$ (~0.7 mL) as the solvent. The solution was allowed to sit overnight to react. A ^{31}P NMR spectrum was obtained and a new peak for the product $TsN{=}PMe_3$ was observed at 27 ppm (versus free PMe_3 at -62 ppm).

Reaction of PMe_3 with potential nitrene. (^{i}PrNN)Cu(NCMe) (0.0325g, 0.062 mmol) was combined with PhN_3 (6.6 μL, 0.055 mmol) in an NMR tube with C_6D_6 (~0.7 mL) and hexamethyldisiloxane (2.2 μL, 0.01 mmol) as an internal standard. The solution turned blue immediately, and a ^1H NMR was taken of the solution. The solution turned green before the 2 equivalents of PMe_3 (11.7 μL, 0.11 mmol) were added, which caused the solution to turn more intensely green. New products were formed in this reaction which corresponded to (^{i}PrNN)Cu(PMe_3) (-49 ppm) and $(CH_3)_3P{=}NPh$ (3.2 ppm), as observed by ^{31}P NMR compared to independent syntheses.

Reaction of (^{i}PrNN)Cu(NCMe) and BF_3. (^{i}PrNN)Cu(NCMe) (0.065 g, 0.013 mmol) was dissolved in C_6D_6 (0.7 mL) in an NMR tube. BF_3 (1.6 μL, 0.013 mmol) was added to the yellow solution via syringe. The color immediately became slightly brown-yellow. ^{19}F NMR revealed multiple new peaks.

Reaction of PhN_3 and BF_3. PhN_3 (10 μL, 0.093 mmol) was added to an NMR tube of C_6D_6 (0.7 mL). BF_3 (23.5 μL, 0.18 mmol) was added to the colorless solution via syringe. ^{19}F NMR revealed no new peaks – only that consistent with BF_3 (-148.7 ppm).

Reaction of BF_3 with potential nitrene. (^{i}PrNN)Cu(NCMe) (0.050 g, 0.096 mmol) was dissolved in THF (20 mL). PhN_3 (0.1 mL, 0.89 mmol) was added to the yellow solution and the color changed to a deep blue. BF_3 (0.1 mL, 0.79 mmol) was added to solution, and the color changed to bright green. ^{19}F NMR in C_6D_6 revealed multiple new peaks.

Aziridination catalysis reactions (general procedure). (MeNN)Cu(NCMe) (0.0189 g, 0.046 mmol), styrene (0.0313 g, 0.30 mmol) and PhINTs (0.127 g, 0.34 mmol) were combined in a screw cap NMR tube in C_6D_6 (0.7 mL) with hexamethyldisiloxane as an internal standard (0.015 g, 0.09 mmol). The reaction was followed by ^{1}H NMR until no further production of aziridine was noted. Aziridine production was confirmed by ^{1}H NMR of aziridine products in $CDCl_3$ and comparison to published data.[37] Initial ^{1}H NMR spectra taken of (MeNN)Cu(NCMe) in the presence of styrene before addition of PhINTs indicate production of a new (MeNN)Cu(η^2-styrene) complex with coordinated styrene resonances appearing at (δ, C_6D_6): 4.49 (dd, $^3J_{HH\textit{trans}}$ = 15, $^3J_{HH\textit{cis}}$ = 9 Hz, 1H), 3.31 (d, $^3J_{HH\textit{trans}}$ = 15 Hz, 1H), 3.02 (d, $^3J_{HH\textit{cis}}$ = 9 Hz, 1H).

References

1. Housecroft, C. E.; Sharpe, A. G., Inorganic Chemistry. In 1st ed.; Prentice Hall: New York, 2001; pp 689-690.
2. Fox, J. P.; Ramdhanie, B.; Zareba, A. A.; Czernuszewicz, R. S.; Goldberg, D. P. *Inorg. Chem.* **2004,** 43, 6600-6608.
3. Wasbotten, I. H.; Wondimagegn, T.; Ghosh, A. *J. Am. Chem. Soc.* **2002,** 124, 8104-8116.
4. Victoriano, L. I. *Coord. Chem. Rev.* **2000,** 196, 383-398.
5. Fuping, K.; Shourong, Z.; Huakuan, L.; Keqin, M.; Yunti, C. *Polyhedron* **1997,** 16, 741-747.
6. Lewis, E. A.; Tolman, W. B. *Chem. Rev.* **2004,** 104, 1047-1076.
7. Peréz, P. J.; White, P. S.; Brookhart, M.; Templeton, J. L. *Inorg. Chem.* **1994,** 33, 6050-6056.
8. Sleiman, H. F.; Mercer, S.; McElwee-White, L. *J. Am. Chem. Soc.* **1989,** 111, 8007-8009.
9. Dobbs, D. A.; Bergman, R. G. *Organometallics* **1994,** 13, 4594-4605.
10. Dobbs, D. A.; Bergman, R. G. *J. Am. Chem. Soc.* **1993,** 115, 3836-3837.
11. Aboelella, N. W.; Lewis, E. A.; Reynolds, A. M.; Brennessel, W. W.; Cramer, C. J.; Tolman, W. B. *J. Am. Chem. Soc.* **2002,** 124, 10660-10661.
12. Mizuno, M.; Hayashi, H.; Fujinami, S.; Furutachi, H.; Nagatomo, S.; Otake, S.; Uozumi, K.; Suzuki, M.; Kitagawa, T. *Inorg. Chem.* **2003,** 42, 8534-8544.
13. Mahadevan, V.; Hou, Z.; Cole, A. P.; Root, D. E.; Lal, T. K.; Solomon, E. I.; Stack, T. D. P. *J. Am. Chem. Soc.* **1997,** 119, 11996-11997.
14. Mahapatra, S.; Halfen, J. A.; Wilkinson, E. C.; Pan, G. F.; Wang, X. D.; Young, V. G.; Cramer, C. J.; Que, L.; Tolman, W. B. *J. Am. Chem. Soc.* **1996,** 118, 11555-11574.
15. Cole, A. P.; Mahadevan, V.; Mirica, L. M.; Ottenwaelder, X.; Stack, T. D. P. *Inorg. Chem.* **2005,** 44, 7345-7364.
16. Straub, B. F.; Rominger, F.; Hofmann, P. *Chem. Commun.* **2000**, 1611-1612.
17. Mahapatra, S.; Jr, V. G. Y.; Kaderli, S.; Zuberbühler, A. D.; Tolman, W. B. *Angew. Chem., Int. Ed. Eng.* **1997,** 36, 130-133.
18. Mahapatra, S.; Kaderli, S.; Llobet, A.; Neuhold, Y. M.; Palanche, T.; Halfen, J. A.; Young, V. G.; Kaden, T. A.; Que, L.; Zuberbuhler, A. D.; Tolman, W. B. *Inorg. Chem.* **1997,** 36, 6343-6356.
19. Mahadevan, V.; Henson, M. J.; Solomon, E. I.; Stack, T. D. P. *J. Am. Chem. Soc.* **2000,** 122, 10249-10250.
20. Dai, X. L.; Warren, T. H. *Chem. Commun.* **2001**, 1998-1999.
21. Spencer, D. J. E.; Reynolds, A. M.; Holland, P. L.; Jazdzewski, B. A.; Duboc-Toia, C.; Le Pape, L.; Yokota, S.; Tachi, Y.; Itoh, S.; Tolman, W. B. *Inorg. Chem.* **2002,** 41, 6307-6321.
22. Bourget-Merle, L.; Lappert, M. F.; Severn, J. R. *Chem. Rev.* **2002,** 102, 3031-3066.
23. Stender, M.; Wright, R. J.; Eichler, B. E.; Prust, J.; Olmstead, M. M.; Roesky, H. W.; Power, P. P. *J. Chem. Soc., Dalton Trans.* **2001**, 3465-3469.
24. Mindiola, D. J.; Hillhouse, G. L. *J. Am. Chem. Soc.* **2001,** 123, 4623-4624.

25. Wang, W. D.; Guzei, I. A.; Espenson, J. H. *Inorg. Chem.* **2000,** 39, 4107-4112.
26. Green, M. L. H.; Hogarth, G.; Konidaris, P. C.; Mountford, P. *J. Chem. Soc., Dalton Trans.* **1990**, 3781-3787.
27. Wang, W. D.; Espenson, J. H. *Inorg. Chem.* **2002,** 41, 1782-1787.
28. Lockwood, M. A.; Blubaugh, T. J.; Collier, A. M.; Lovell, S.; Mayer, J. M. *Angew. Chem., Int. Ed. Eng.* **1999,** 38, 225-227.
29. Staudinger, H.; Meyer, J. *Helv. Chim. Acta* **1919,** 2, 635-646.
30. Scriven, E. F. V.; Turnbull, K. *Chem. Rev.* **1988,** 88, 297-368.
31. Gololobov, Y. G.; Kasukhin, L. F. *Tetrahedron* **1992,** 48, 1353-1406.
32. Ou, W.; Wang, Z. G.; Chen, Z. C. *Synth. Commun.* **1999,** 29, 2301-2309.
33. Amisial, L. D.; Dai, X.; Kinney, R. A.; Krishnaswamy, A.; Warren, T. H. *Inorg. Chem.* **2004,** 43, 6537-6539.
34. Hamilton, C. W.; Laitar, D. S.; Sadighi, J. P. *Chem. Commun.* **2004**, 1628-1629.
35. Gillespie, K. M.; Crust, E. J.; Deeth, R. J.; Scott, P. *Chem. Commun.* **2001**, 785-786.
36. Llewellyn, D. B.; Adamson, D.; Arndtsen, B. A. *Org. Lett.* **2000,** 2, 4165-4168.
37. Evans, D. A.; Bilodeau, M. T.; Faul, M. M. *J. Am. Chem. Soc.* **1994,** 116, 2742-2753.
38. Kubas, G. J. *Inorg. Synth.* **1979,** 19, 90.
39. Yamada, Y.; Yamamoto, T.; Okawara, M. *Chem. Lett.* **1975**, 361-362.
40. Sodergren, M. J.; Alonso, D. A.; Bedekar, A. V.; Andersson, P. G. *Tetrahedron Lett.* **1997,** 38, 6897-6900.
41. Lindsay, R. O.; Allen, C. F. H. *Org. Synth.* **1942,** 22, 96.
42. Zhu, W.; Ma, D. *Chem. Commun.* **2004**, 888-889.

Chapter 4: *N*-Heterocyclic Carbene Copper Complexes

4.1 Ligand Rationale

The imdazolyl ligands, commonly called *N*-heterocyclic carbenes (NHC) have enjoyed significant interest in the past several years. These ligands were first synthesized and isolated by Arduengo and have been shown to form stable transition-metal complexes.[1, 2] Their ability to act as strong σ-donors has been compared to phosphine ligands.[3-5] We had early success with a phosphine ligand in the synthesis of a monomeric Cu(I) amido complex and we believed that NHC would provide suitable ligands for similar complexes and would provide for steric and electronic variability. Buchwald, Sadighi and coworkers have reported copper(I) complexes using the IPr (IPr = 1,3-bis(2,6-diisopropylphenyl)imidazol-2-ylidene) ligand (Figure 4.1), including (IPr)CuCl and (IPr)Cu(Me).[6, 7] We utilized these complexes with the bulky and donating IPr ligand as precursors for the synthesis of monomeric copper(I) NHC-ligated amido complexes.

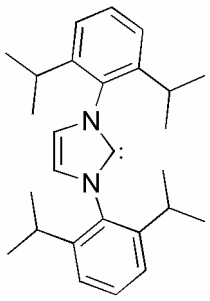

Figure 4.1. The *N*-heterocyclic carbene (NHC) ligand IPr (IPr = 1,3-bis(2,6-diisopropylphenyl)imidazol-2-ylidene).

4.2 Synthesis and Properties of (IPr)Cu(NHPh)

4.2.1 Synthesis and Structure of (IPr)Cu(NHPh)

The synthesis of (IPr)Cu(NHPh) can be accomplished in a number of ways. The previously reported species $[CuNHPh]_4$ can be reacted with the free IPr ligand to form the desired (IPr)Cu(NHPh) complex; however, this is not the most convenient method due to the extreme instability of both $[CuNHPh]_4$ and its precursor, $[Cu(Mes)]_n$ (Mes = mesityl). Analogous to the synthesis of (dtbpe)Cu(NHPh), reaction of (IPr)CuCl with LiNHPh forms the desired amido complex in 58% isolated yield (Scheme 4.1). The byproduct, LiCl, can be removed by filtration to isolate the off-white solid powder after precipitation with hexanes. In addition, work in our group by Dr. Laurel Goj has revealed that the alkyl complexes (IPr)Cu(Me) and (IPr)Cu(Et) can be reacted with aniline to give methane or ethane, respectively, and (IPr)Cu(NHPh) in 70% isolated yield.[8] This reaction does not appear to proceed via a Cu-R bond homolysis as it is not affected by the addition of radical traps. The reaction is proposed to proceed by coordination and activation of aniline, followed by proton transfer to the alkyl ligand to produce methane or ethane and (IPr)Cu(NHPh). To our knowledge, the formally 14-electron complex (IPr)Cu(NHPh) is the second example of a structurally characterized monomeric Cu(I) amido system, the first being (dtbpe)Cu(NHPh).[9]

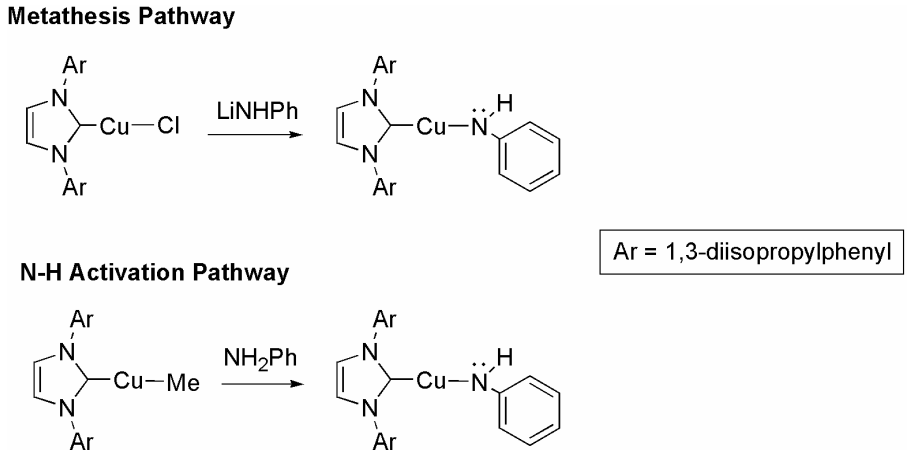

Scheme 4.1. Synthesis of (IPr)Cu(NHPh).

Cyclic voltammetry of this complex reveals an irreversible (scan rate = 100 mV/s) Cu(II/I) oxidation at 0.22 V versus $[Cp_2Co][PF_6]$ (Cp = cyclopentadienyl), and no evidence of a Cu(I/0) reduction at potentials to -2.0 V. This relatively high Cu(II/I) oxidation potential compared to (dtbpe)Cu(NHPh) ($E_{p,a}$ = 0.10 V) indicates decreased electron density for the metal center in the complex, but could be a ligand-based oxidation. This complex was characterized by multinuclear NMR (^{1}H NMR - Figure 4.2), and has an N-H resonance of 3.23 ppm, and easily observable *p*- and *o*-anilido peaks. The N-H stretch is observed at 3366 cm^{-1} in the IR spectrum.

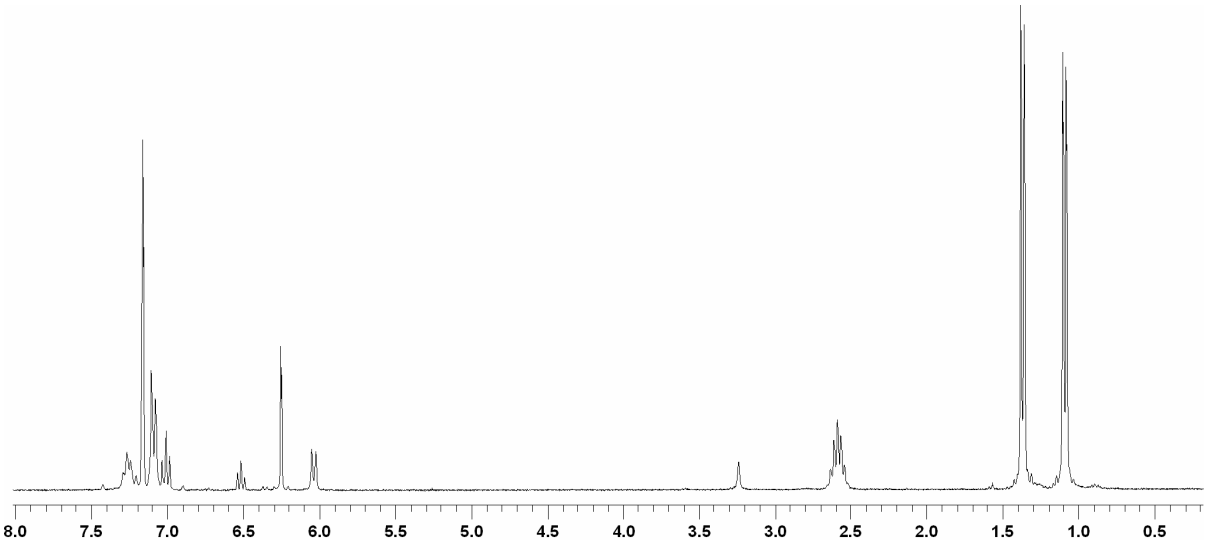

Figure 4.2. ^{1}H NMR spectrum of (IPr)Cu(NHPh) in C_6D_6.

Layering a toluene solution of (IPr)Cu(NHPh) with pentane yielded X-ray quality crystals of the IPr amido complex (Figure 4.3, Table 4.1). The structure reveals an amido nitrogen which is relatively sterically unhindered, although the ligand is quite bulky about the copper (Figure 4.4). The two-coordinate structure of (IPr)Cu(NHPh) possesses an almost linear $C_{carbene}$-Cu-N bond angle of 174.8(1)°. The N-$C_{carbene}$-C_{ipso}-C torsion angle is very small at 0.47°, and thus the carbene plane and the amido phenyl ring are coplanar. The structures of (IPr)Cu(NHPh) and (dtbpe)Cu(NHPh) posses similar Cu-N bond distances; that of the IPr complex is 1.841(2) Å, slightly shorter than the analogous bond distance in (dtbpe)Cu(NHPh) of 1.890(6) Å, and both are consistent with the anticipated length of a Cu-N single bond (see section 2.3.1).[8] This may indicate a slightly weaker Cu-N bond for the dtbpe complex. The N_{amido}-C_{ipso} bond distance is virtually identical for the two complexes with values of 1.351(4) Å for (IPr)Cu(NHPh) and 1.354(9) Å for (dtbpe)Cu(NHPh). This may indicate similarity in the strength of the N-C bond in the two complexes. The N-C bond

lengths in aniline for two symmetry independent molecules are 1.40 Å and 1.39 Å, for a difference of approximately 0.04 Å between aniline and the Cu(I) amido complexes.[10]

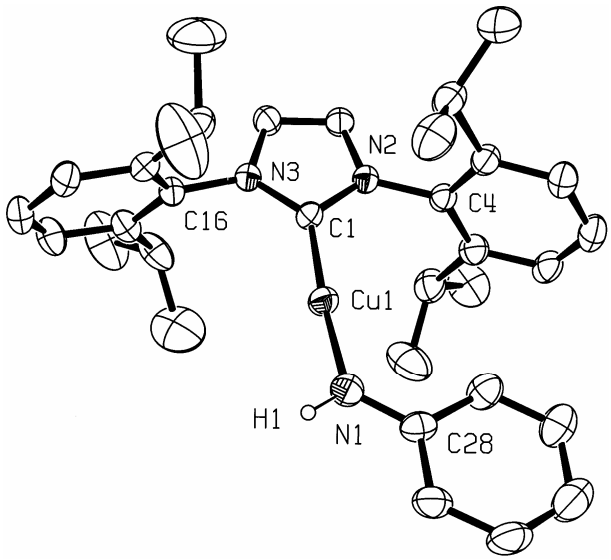

Figure 4.3. ORTEP of (IPr)Cu(NHPh) (30% probability). Selected Bond Distances (Å): N3-C1 1.353(3), N2-C1 1.359(3), Cu1-C1 1.875(3), Cu1-N1 1.841(2), N1-C28 1.351(4). Selected Bond Angles (º): N2-C1-Cu1 124.0(2), C1-Cu1-N1 174.8(1), Cu1-N1-C28 127.4(2).

Table 4.1. Selected crystallographic data and collection parameters for (IPr)Cu(NHPh).

	(IPr)Cu(NHPh)
empirical formula	$C_{33}H_{42}N_3Cu$
formula wt	544.24
crystal system	orthorhombic
space group	$P2_12_12_1$
a, Å	11.915(2)
b, Å	12.453(2)
c, Å	20.742(4)
β, º	90.0
V (Å^3)	3077.7(10)
Z	4
D_{calcd}, g cm^{-3}	1.175
crystal size (mm)	0.28 × 0.34 × 0.50
*R*1, w*R*2 {I>2σ(I)}	0.0422, 0.1011
GOF	1.023

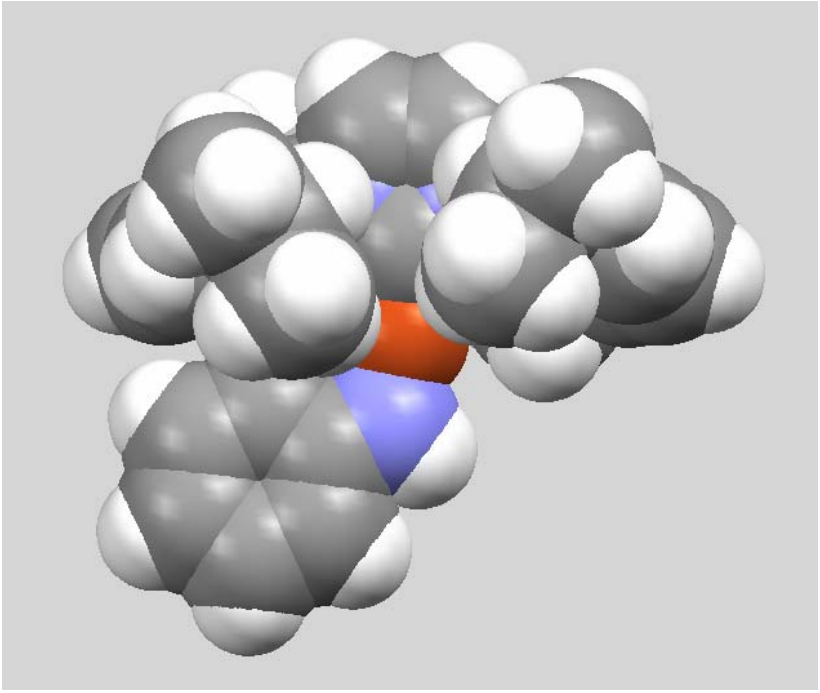

Figure 4.4. Space-filling model from the structure of (IPr)Cu(NHPh) (Red = Cu, blue = N, grey = C, white = H).

4.2.2 Variable Temperature NMR of (IPr)Cu(NHPh)

The ability of the phenyl π* system to accept electron density from the amido lone pair stabilizes late transition-metal aryl amido complexes and is the major reason for their relative abundance when compared with parent and alkyl amido complexes. Resonance structures that show this stabilization are depicted in Figure 4.5. A few groups have observed hindered bond rotation about N_{amido}-C_{ipso} bonds of aryl amido.[11-14] There is also

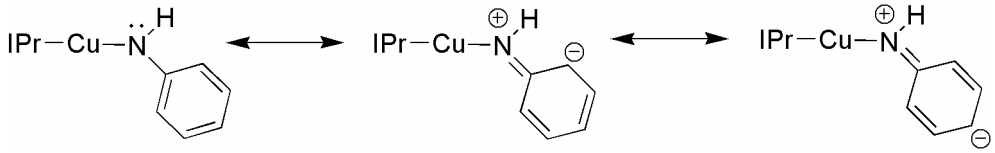

Figure 4.5. Resonance structures for delocalization of amido lone pair.

potential for donation of the amido lone pair to the metal center, which would cause hindered bond rotation about the M-N_{amido} bond (Scheme 4.2). Variable temperature ^{1}H NMR spectroscopy from 22 °C to -80 °C was used to study (IPr)Cu(NHPh) in toluene-d_8. Decoalescence of the amido phenyl ortho peak was observed at -40 °C and two new ortho peaks appear, forming broad peaks at

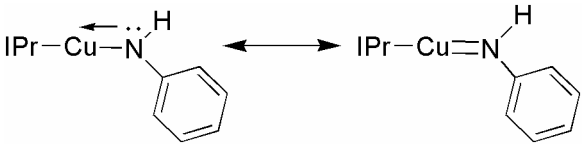

Scheme 4.2. Potential donation of anilido nitrogen to metal center and hindered Cu-N bond rotation.

-80 °C (Figure 4.6). The para and meta amido phenyl peaks and the IPr backbone peaks shift, but decoalescence is not observed for these peaks. The observed changes in the NMR are consistent with hindered bond rotation about the N_{amido}-C_{ipso} bond only, and hindered bond rotation about the Cu-N_{amido} bond is not observed at the accessible temperatures, indicating that the barrier to rotation is low. The rate of N-C bond rotation at the coalescence temperature (-40 °C) is $k_{coal} = 6.39 \times 10^2$ s^{-1}, which corresponds to $\Delta G^{\ddagger} = 10.5$ kcal/mol for the hindered bond rotation about the N_{amido}-C_{ipso} bond. In addition, the rates of bond rotation and free energies of activation for the hindered bond rotation were calculated for other temperatures in the fast exchange regime using line broadening, and the rates are observed to increase and $\Delta G^{\ddagger}$ to decrease as the temperature increases (Table 4.2). An Eyring plot of this data reveals $\Delta H^{\ddagger} =$ 7.28 kcal/mol and $\Delta S^{\ddagger} = -14.3$ eu (Figure 4.7), which is consistent with a single transition state and two ground states.

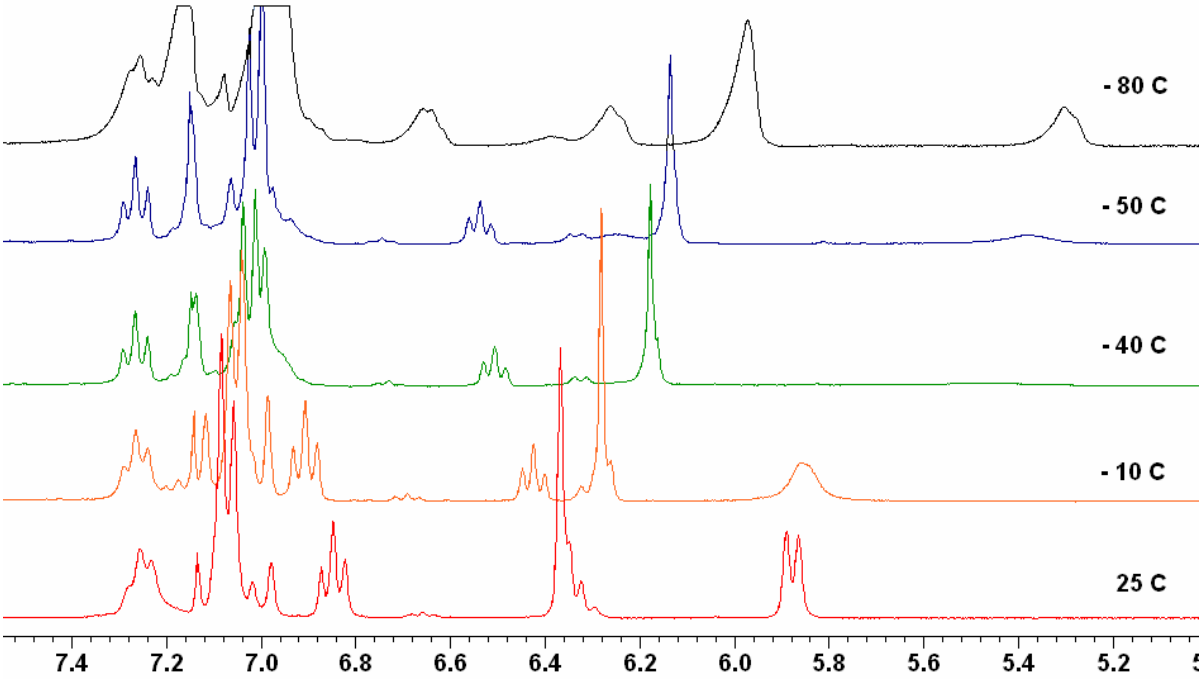

Figure 4.6. Variable temperature 1H NMR spectra of (IPr)Cu(NHPh) in the downfield region.

Table 4.2. Variable temperature rates of N_{amido}-C_{ipso} bond rotation and calculated Gibbs free energies of activation for (IPr)Cu(NHPh).

Temperature (°C)	k_T (s^{-1})	$\Delta G^{\ddagger}$ (kcal/mol)
0	8.67×10^3	11.0
-10	2.89×10^3	11.2
-20	1.55×10^3	11.0
-40	6.39×10^2	10.5

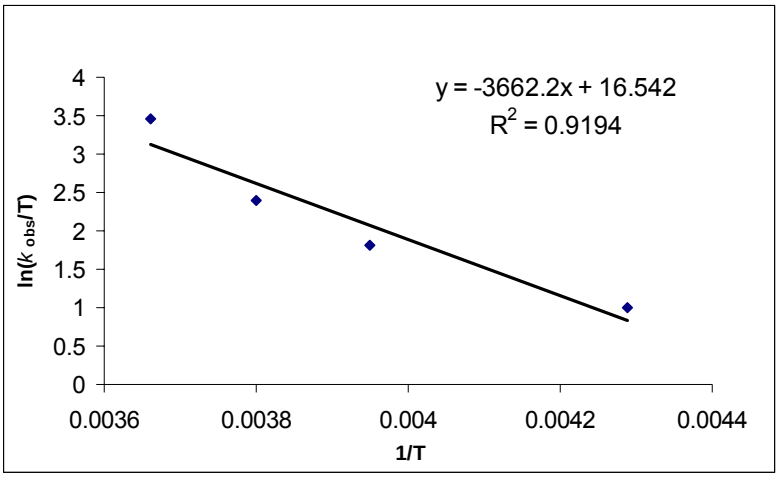

Figure 4.7. Eyring plot for N_{amido}-C_{ipso} bond rotation.

4.3 Reactivity of Cu(I) Anilido Complexes.

(IPr)Cu(NHPh) is stable compared to (dtbpe)Cu(NHPh). The phosphine-ligated complex is only stable for approximately a week in inert atmosphere at room temperature, for longer periods at –20 °C, and decomposes in C_6D_6 at slightly elevated temperatures (> 60 °C). The NHC-ligated complex is stable for at least a month at room temperature in the glovebox. In addition, (IPr)Cu(NHPh) has been heated in C_6D_6 with 5 mol% C_6H_6 in a J-young NMR tube to 80 °C for four days without evidence of decomposition. This increased stability is an advantage because of the potential for more thorough study of reactivity. Reactions with strong acids, such as HCl, quickly form (IPr)CuCl and aniline. (IPr)Cu(NHPh) reacts with H_2O to form aniline and an uncharacterized copper complex (possibly a Cu-OH system).

4.3.1 Reactivity of Anilido Complexes with Bromoethane.

We have reported that the anilido complexes $TpRu(PMe_3)_2NHPh$ and (dtbpe)Cu(NHPh) undergo apparent S_N2 reactions with bromoethane to produce the corresponding M-Br complexes and ethylaniline.[9] (IMes)Cu(NHPh) and (SIPr)CuNHPh have been synthesized by Sam Delp and Dr. Laurel Goj, respectively, via metathesis reactions between (NHC)Cu(Cl) and LiNHPh and by N-H activation of aniline by the (NHC)Cu(Me) complexes.[15] These (NHC)Cu(NHPh) (NHC = IPr, SIPr or IMes) complexes also undergo S_N2 reactions with bromoethane. In order to compare the impact of ligand variation on nucleophilic anilido reactivity, kinetic studies were undertaken with (IPr)Cu(NHPh), (SIPr)Cu(NHPh) and (IMes)Cu(NHPh). The rate of the reactions of these complexes with bromoethane to produce the (NHC)CuBr complex and ethylaniline under pseudo-first order conditions were measured by ^{1}H NMR spectroscopy (Scheme 4.3, Figure 4.8). The identity of (IPr)Cu(Br) was confirmed by elemental analysis, and production of EtNHPh was confirmed by ^{1}H NMR spectroscopy. The rates and half-lives of these reactions and those of previously reported complexes are summarized in Table 4.3.

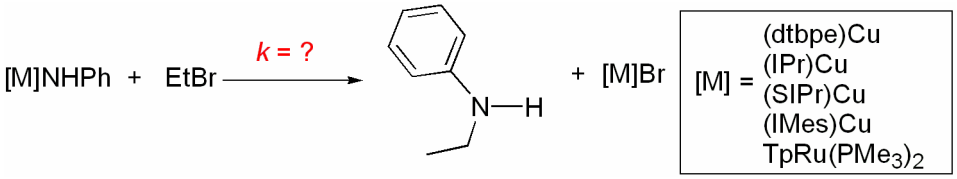

Scheme 4.3. Nucleophilic substitution reaction of amido complexes with bromoethane.

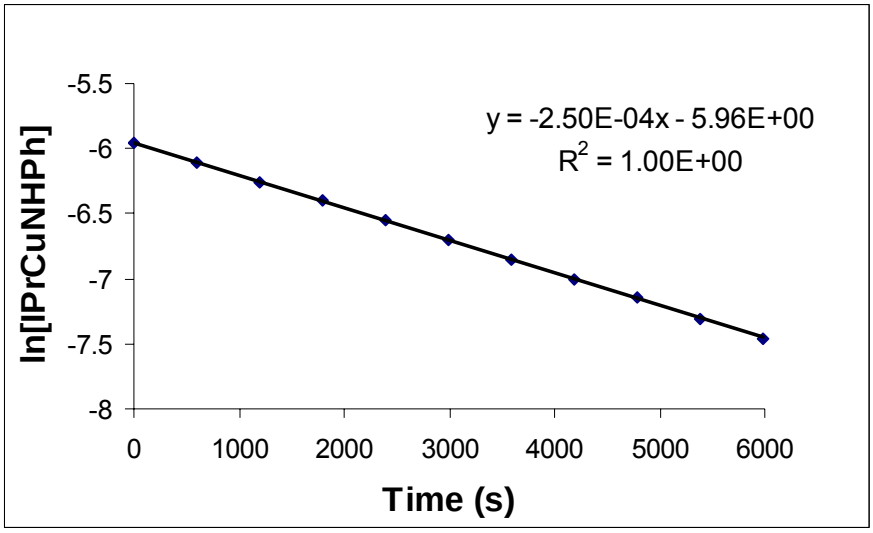

Figure 4.8. Representative plot of ln[(IPr)Cu(NHPh)] versus time for the formation of ethyl aniline with 12 eq of bromoethane in C_6D_6 (representative plots for the kinetics of reaction (SIPr)Cu(NHPh) and (IMes)Cu(NHPh) with bromoethane can be found in the experimental section).

Table 4.3. Kinetic data for the reaction of bromoethane with (IPr)Cu(NHPh), (SIPr)Cu(NHPh), (IMes)Cu(NHPh), (dtbpe)Cu(NHPh) and $TpRu(PMe_3)_2(NHPh)$ with bromoethane (RT = room temperature).

Amido Complex	Temp (°C)	k_{obs} (s^{-1})	$t_{1/2}$	$\Delta G^{\ddagger}$ (kcal/mol)
(dtbpe)Cu(NHPh)[a]	RT	$5.5(2) \times 10^{-4}$	21.0(6) min	21.7
(IMes)Cu(NHPh)	RT	$3.3(3) \times 10^{-4}$	35(3) min	22.0
(IPr)Cu(NHPh)	RT	$2.4(2) \times 10^{-4}$	49(4) min	22.2
(SIPr)Cu(NHPh)	RT	$1.1(1) \times 10^{-4}$	109(8) min	22.6
$TpRu(PMe_3)_2(NHPh)$[a]	80	$8.6(3) \times 10^{-6}$	22 hr	29.0

[a]reported in Chapter 2

The copper(I) anilido complexes undergo significantly more rapid reaction with bromoethane than the TpRu anilido complex. For the (NHC)Cu(NHPh) complexes, the reactivity decreases in the order IMes > IPr > SIPr (Scheme 4.4). Combined experimental and computational studies conducted on (NHC)Cp*RuCl systems by Nolan et al. reveal that the coordination ability of the NHC complexes is strongly affected by the steric profile of the

ligands.[16] For example, they find that the experimental BDE of the IMes complex is 4.5 kcal/mol higher than the IPr complex and the difference in the reaction rate between (IMes)Cu(NHPh) and (IPr)Cu(NHPh) is possibly due to a reduced donating ability for IPr versus IMes, which would result in a more electron rich copper system and a more nucleophilic anilido nitrogen. Alternatively, the reduced steric bulk of the IMes ligand could result in an increased rate of reaction for the bimolecular reaction. Although the saturated backbone of the SIPr ligand should result in a more donating ligand, we observe that (SIPr)Cu(NHPh) is less reactive than (IPr)Cu(NHPh)**.**

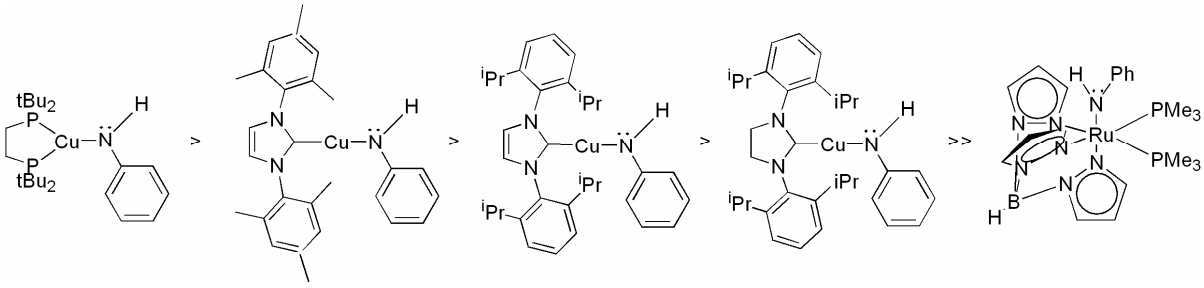

Scheme 4.4. Order of nucleophilic reactivity for the series of amido complexes.

The three-coordinate phosphine-ligated copper(I) anilido complex (dtbpe)Cu(NHPh) reacts most rapidly with bromoethane. We postulated that the increased electron density of the 3-coordinate (dtbpe)Cu(NHPh) system might accelerate the nucleophilic reactivity compared with the two-coordinate (NHC)Cu(NHPh) systems. To test the possibility, we attempted to coordinate a Lewis base to (IPr)Cu(NHPh) and probe the impact on the rate of reaction with bromoethane. However, PMe_3 does not coordinate strongly enough to the (NHC)Cu(NHPh) system. Furthermore, the reaction of (IPr)Cu(NHPh) and bromoethane in the presence of PMe_3 does not produce ethylaniline, but rather yields an a uncharacterized copper complex. It is possible that PMe_3 acts as a nucleophile to attack bromoethane to give

[$EtPMe_3$][Br] or other products. The combination of (IPr)Cu(NHPh) and ^{t}BuNC reveals new resonances (^{1}H NMR spectroscopy) for the alkyl fragments of the NHC ligand. In addition, shifts in the resonances due to anilido ligand are observed and the ^{t}BuNC peak shifts downfield from 0.94 ppm for free isonitrile to 0.90 ppm. These observations are consistent with an equilibrium between (IPr)Cu(NHPh) and (IPr)Cu(NHPh)(CN^{t}Bu) (Scheme 4.5).

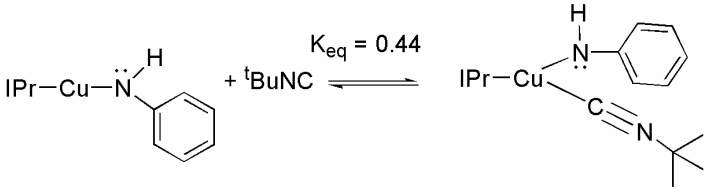

Scheme 4.5. Equilibrium between (IPr)Cu(NHPh) and ^{t}BuNC with (IPr)Cu(NHPh)(CN^{t}Bu).

The equilibrium is K_{eq} = 0.44 at room temperature, and is surprisingly independent of temperature and between 25 °C and -75 °C. It is likely that the steric bulk of the IPr ligand inhibits coordination of the isonitrile. Even though the 3-coordinate complex (IPr)Cu(NHPh)(CN^{t}Bu) is not isolable, the rate of the reaction with bromoethane was determined to discern if the coordination of the isonitrile influences the transformation. The kinetic studies of (IPr)Cu(NHPh) and bromoethane in the presence of 2 equivalents of ^{t}BuNC (relative to [Cu]) reveal a k_{obs} = 2.36(9)x10^{-4} s^{-1}, which is within the standard deviation of the rate observed for (IPr)Cu(NHPh) and bromoethane in the absence of ^{t}BuNC. Therefore, weak binding of ^{t}BuNC does not appear to enhance the nucleophilic reactivity of (IPr)Cu(NHPh).

Cundari et al. have performed computational studies of the copper anilido complexes at the B3LYP/6-31G(d) level of theory.[15] The molecular electronic and structural parameters calculated are shown below (Table 4.4). The calculated structural parameters compare

favorably with the crystal structures that have been solved for (dtbpe)Cu(NHPh), (IPr)Cu(NHPh) and (SIPr)Cu(NHPh).[15] These data show that the NHC complexes are quite similar to each other and distinct from the dtbpe complex. As mentioned above, the Cu-N bond of the dtbpe complex is longer (0.05 Å) than those of the NHC complexes, and potentially implies a weaker Cu-N bond for the dtbpe complex. Consistent with this conclusion, the calculated homolytic Cu-N bond dissociation energies for the anilido complexes are: BDE(Cu-N kcal/mol): (IPr): 87.3; (IMes): 88.3; (SIPr): 86.7; (dtbpe) 81.8. The weaker Cu-N bond of (dtbpe)Cu(NHPh) may explain the enhanced reactivity observed with bromoethane.

Table 4.4. Calculated Molecular and Electronic Structural Properties of Cu(I)-Amido complexes[a]

	Cu-N[b]	Cu···Hα[b]	Cu-N-C_{ipso}	ε_{HOKSO} [c]	ε_{LUKSO} c	qN[d]	qCu[d]
Ligand	Å	Å	°	EV	EV	a.u.	a.u.
IPr	1.822	2.509	126.8	-3.62	-0.55	-0.82	0.25
IMes	1.815	2.519	124.8	-3.61	-0.60	-0.84	0.25
SIPr	1.818	2.522	123.2	-3.68	-0.45	-0.83	0.25
dtbpe	1.872	2.485	135.4	-3.64	-0.14	-0.80	0.05

[a]Properties calculated at optimized geometries for full ligand models at the B3LYP/6-31G(d) level of theory. [b]Distance (Å) from copper to proton attached to amido nitrogen. [c]Energies (eV) of the highest occupied and lowest unoccupied Kohn-Sham orbitals, HOKSO and LUKSO, respectively. [d]Mulliken atomic charges at amido nitrogen and copper.

The calculated atomic charges do not carry a high degree of certainty, so only trends based on the relative values will be noted. All of the anilido complexes possess negative charge at the anilido nitrogen, which is consistent with the nucleophilic reactivity observed for these systems; however, that of the dtbpe complex is slightly less negative than the NHC

complexes. The calculated LUMO and HOMO for (dtbpe)Cu(NHPh) and (IMes)Cu(NHPh) are shown below (Figure 4.9). For (dtbpe)Cu(NHPh), the LUMO is indeed primarily a Cu-based 4p orbital, but for (IMes)Cu(NHPh) the LUMO is NHC ligand-based. As expected from the strong nucleophilicity of the nitrogen, the HOMO for both complexes is largely non-bonding in nature with minimal Cu character and corresponds to the primary lone pair on the amido nitrogen. Significant anilido aryl π* character is demonstrated in the HOMO for both complexes, consistent with experimental observations that indicate some delocalization of the amido nitrogen electron density into the phenyl π* system. In addition, computations indicate rotation of the Cu-N bond by 90° is only +1 kcal/mol higher in enthalpy than the ground state orientation, which suggests a low barrier for torsion. This is consistent with the lack of observation of Cu-N bond rotation by variable temperature NMR and virtually no amido lone pair to Cu-p orbital π interaction.

Based on these combined experimental and computational studies, the (NHC)Cu(NHPh) complexes and (dtbpe)Cu(NHPh) are more nucleophilic than a corresponding Ru(II) anilido species, $TpRu(PMe_3)_2(NHPh)$.[17] From these results and the fact that Cu(I) is less electronegative than Ru(II) (1.9 vs. 2.2),[18] we propose that the bonding in these copper amido complexes is polar covalent and that they possess a nucleophilic nitrogen, with non-existent or minor donation of the nitrogen lone pair to the Cu p orbital. This conclusion is consistent with the Cu-N bond length, computational studies, the fact that no Cu-N bond rotational barrier is observed and the highly nucleophilic reactivity of the Cu(I) complexes with bromoethane.

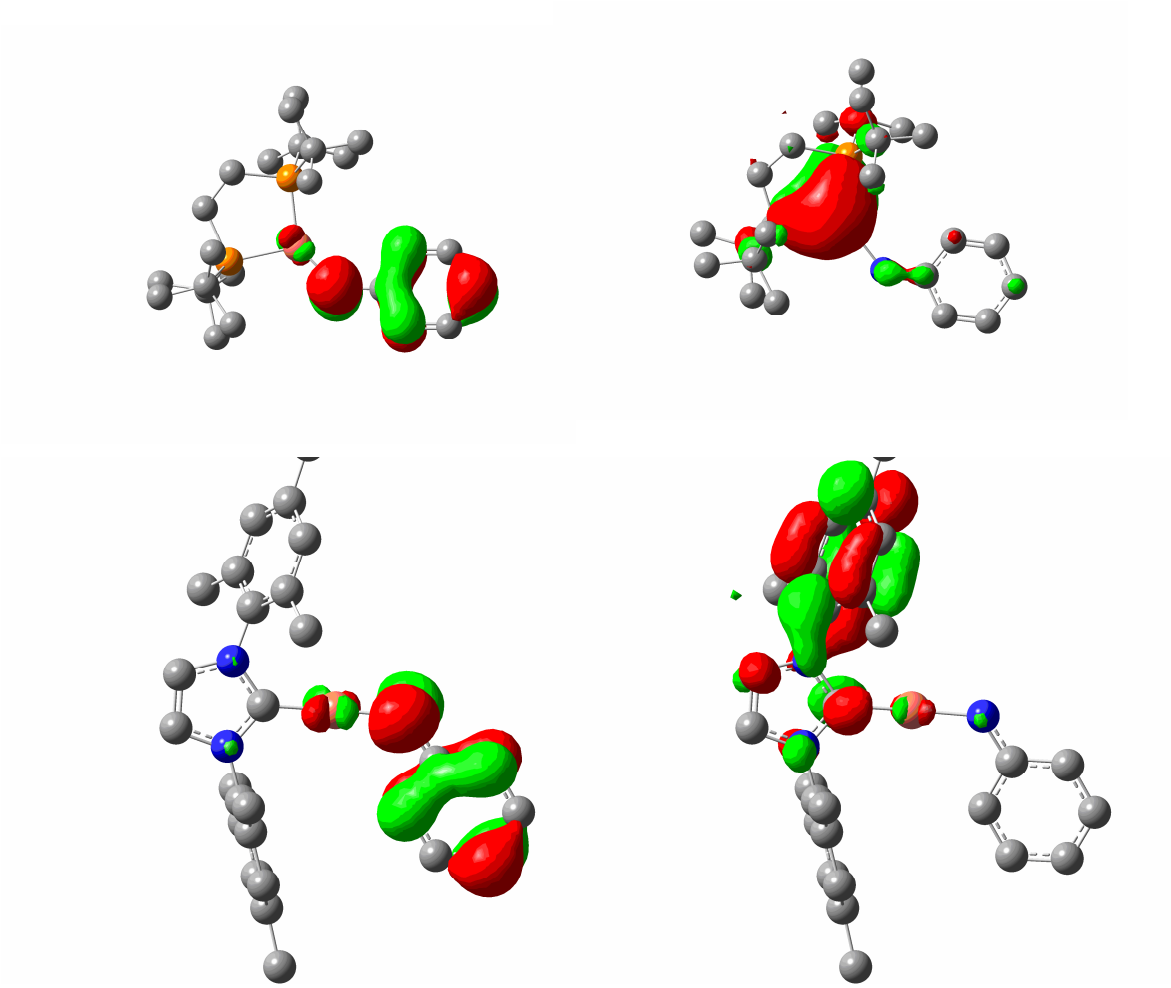

Figure 4.9. Highest occupied (left) and lowest unoccupied (right) Kohn-Sham orbitals for (dtbpe)Cu-anilido (top pair) and (IMes)Cu-anilido (bottom pair). Orbitals for other N-heterocyclic carbene copper(I) complexes are similar.

4.3.2 Experimental and Computational Study of the Thermodynamics of (IPr)Cu(NHPh) and Benzene or Dihydrogen.

(IPr)Cu(NHPh) was heated in either C_6H_6 or C_6D_6 to 80 °C for 24 hours, and no reaction occurred, nor was decomposition observed. Conversely, (IPr)Cu(Ph) reacts with aniline in *benzene* at room temperature to form (IPr)Cu(NHPh) and benzene (Scheme 4.6).

The phenyl complex is completely consumed after 24 hours. If it is assumed that the presence of 5% (IPr)Cu(NHPh) could be detected by ^{1}H NMR spectroscopy, it is likely that $K_{eq} \geq 1000$ for the conversion of (IPr)Cu(Ph) and aniline to (IPr)Cu(NHPh) and benzene. (IPr)Cu(NHPh)/benzene are strongly favored in this system, whereas the phenyl complex and aniline are favored in the Ir system studied by Hartwig et al ($K_{eq} = 105$).[19]

When (IPr)Cu(NHPh) was placed under 60 psi of H_2 in benzene at ambient temperature, no reaction occurred after 18 hours. The amido complex persists, and neither aniline or the previously reported $[(IPr)Cu(\mu\text{-}H)]_2$ are observed. In order to determine whether kinetics or thermodynamics is responsible for the lack of reactivity, $[(IPr)Cu(\mu\text{-}H)]_2$ was synthesized according to the procedure reported by Sadighi et al.[20] The reaction of $[(IPr)Cu(\mu\text{-}H)]_2$ with aniline rapidly produces gas (presumably H_2) and (IPr)Cu(NHPh) at room temperature (Scheme 4.6). Appearance of the amido and H_2 and disappearance of the hydride were confirmed by ^{1}H NMR.

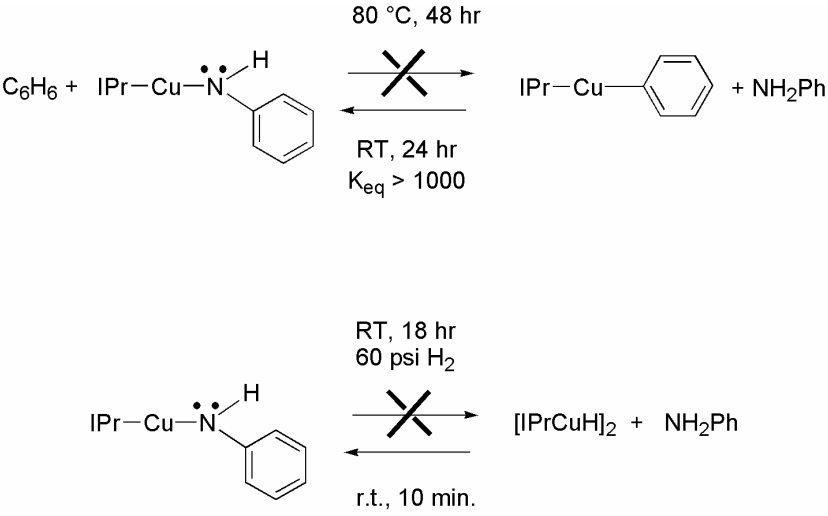

Scheme 4.6. Reactions of (IPr)Cu(NHPh) with benzene and dihydrogen.

Therefore, the amido complex appears to be thermodynamically favored over (IPr)Cu(Ph)/NH_2Ph or $[(IPr)Cu(\mu\text{-}H)]_2/NH_2Ph$, respectively. These experimental observations are consistent with computational studies for the equilibrium between (IPr)Cu(NHPh)/H_2 and $[(IPr)Cu(\mu\text{-}H)]_2$ and NH_2Ph. For the reaction of (IPr)Cu(NHPh) and H_2, calculations by Cundari et al. reveal ΔH = +7 kcal/mol and a ΔG of approximately +17 kcal/mol. This result is opposite to that observed with a number of late transition-metal amido complexes,[21] but similar to the reactivity observed with some early transition-metal complexes in which the amido was favored over hydride.[22]

4.3.3 Catalytic Hydroamination.

In addition to the catalysis observed with (dtbpe)Cu(NHPh) for the hydroamination of electron-withdrawing olefins, catalysis can be performed using the (NHC)Cu(NHPh) complexes. This catalysis and a mechanistic study have been reported for (IPr)Cu(NHPh).[23] The reactivity of these catalysts is comparable to the phosphine amido. In general, the phosphine amido (dtbpe)Cu(NHPh) is less stable, and yields using (dtbpe)Cu(NHPh) as catalyst are slightly lower for some of the olefins with reactive functional groups (Table 4.5). However, there were a few examples that were more successful using (dtbpe)Cu(NHPh) as catalyst component with (IPr)Cu(NHPh). One example is methylacrylate, where catalysis with 5 mol% (dtbpe)Cu(NHPh) gives 92% conversion after 18 hours at room temperature, which is significantly improved compared with the 55% conversion achieved using (IPr)Cu(NHPh).

Table 4.5. Comparison of hydroamination catalysis by (dtbpe)Cu(NHPh) and (IPr)Cu(NHPh).

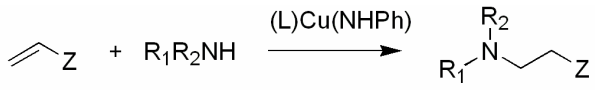

				(dtbpe)Cu(NHPh)		(IPr)Cu(NHPh)*	
Olefin	Nucleophile	Product	Temp (°C)	Time (hr)	% conv.	Time (hr)	% conv.
	$PhNH_2$	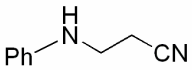	RT	3	> 95	12	> 95
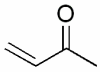	$PhNH_2$	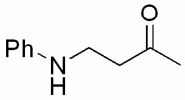	RT	5 mins	92	5 mins	100
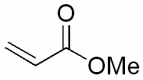	$PhNH_2$	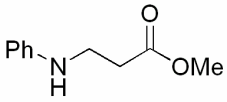	RT	4	99	19	55
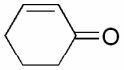	$PhNH_2$	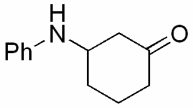	RT	3	66	16	80
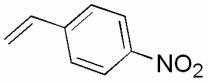	$PhNH_2$	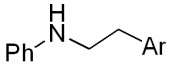	50	8	29	72	72
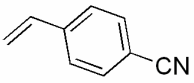	$PhNH_2$	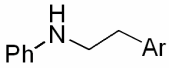	50	18	6	35	0
	$^tBuNH2$	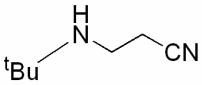	RT	11 days	58	22	57
	Et_2NH	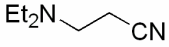	RT	12	95	9	>95
	$(PhCH_2)_2NH$	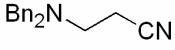	RT	7 days	86	90	60

* Reactions performed by Colleen Munro-Leighton

The mechanism of this reaction has been studied by Colleen Munro-Leighton and is proposed to occur via nucleophilic attack by the amido nitrogen on the free/uncoordinated electrophilic carbon of the olefin to form a zwitterionic intermediate. Subsequent proton migration forms the alkyl aryl amido complex (IPr)Cu($NPhCH_2CH_2CN$) (Scheme 4.7).[23] (IPr)Cu($NHCH_2CH_2CN$) has been observed by ^1H NMR spectroscopy in the catalytic cycle

and has been independently synthesized and found to be active for catalysis of hydroamination. This alkyl arylamido complex can then coordinate amine to initiate proton transfer, reform the catalyst and produce free amine. Because the alkyl aryl amido complex can be observed and is active for catalysis, the mechanism of this reaction is most likely pathway 1 in Scheme 4.7.[23] In addition, β-hydride elimination to form imine products is not observed, whereas imines are commonly observed in reactions that proceed via an olefin insertion into the M-N bond such as pathway 2. [24, 25] Further study of this catalysis and extension to enantioselective hydroamination reactions continues in our group.

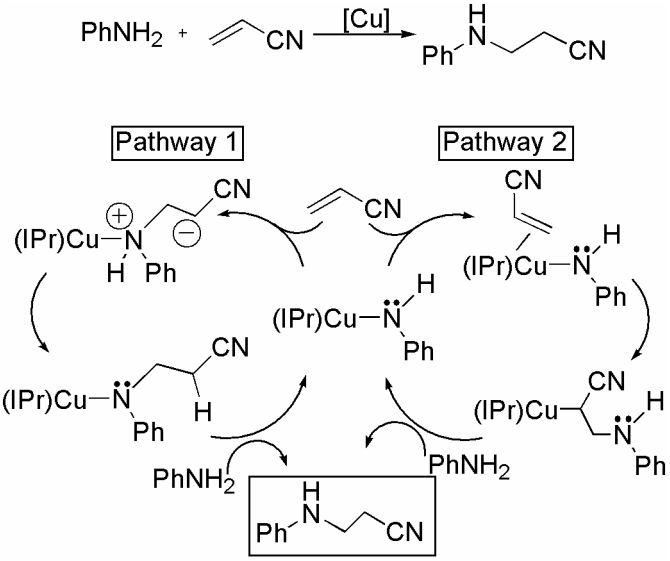

Scheme 4.7. Proposed mechanisms of catalytic hydroamination by (IPr)Cu(NHPh).

4.3.4 Aryl Amination Reactions.

The development of Pd-catalyzed aryl amination began with the discovery of the stoichiometric reaction and over time developed into a catalytic system for a limited number of substrates. Detailed mechanistic studies and tuning of the catalyst system has allowed the

use of an increasingly diverse set of substrates, and recently has even been extended to aryl ethers (Scheme 4.8).[26-28] As discussed in Chapter 1, Buchwald and coworkers have reported catalytic aryl amination by Cu(I) salts and various neutral ligands, proposing a Cu(I) amido

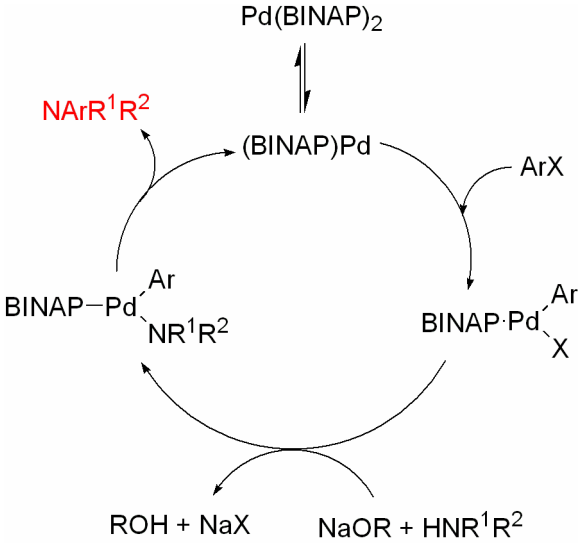

Scheme 4.8. Mechanism of aryl amination catalyzed by (BINAP)Pd(0).

complex as an intermediate. Copper has distinct cost advantage over Pd; however, there are as of yet no detailed mechanistic studies of this catalysis. The primary reason for this was the lack of well-characterized, isolable copper amido complexes. We are interested to explore the application of our Cu(I) amido complexes towards: 1) stoichiometric reactions with aryl halides to produce amines, 2) catalytic production of aryl amines and 3) the mechanism of this reaction. It is unlikely that the copper-catalyzed aryl amination reaction is directly analogous to the palladium-catalyzed reaction, because this would involve the unlikely oxidative addition of aryl halide to Cu(I) to form a Cu(III) aryl halide complex. Therefore, delineation of the role of the Cu(I) amido complex in this catalysis may allow greater understanding of the mechanism of this reaction and improvement of the catalysis.

The stoichiometric reaction of (IPr)Cu(NHPh) with phenyliodide in C_6D_6 heated to 120 °C for 18 hours lead to formation of diphenylamine in 45% yield, as verified by addition of an authentic sample (Scheme 4.9). All the (IPr)Cu(NHPh) reacts, and small colorless crystals form in the reaction tube that are most likely due to the formation of (IPr)Cu(I). The ^{1}H NMR spectrum of these crystals in $CDCl_3$ is consistent with the production of (IPr)Cu(I), which was independently synthesized by reaction of IPr with CuI (eq 1). Control reactions of aniline and phenyliodide in the absence of Cu catalyst at 130 °C for 48 hours do not produce amine. In addition, a control reaction containing 5 mol% free IPr ligand at 130 °C does not produce diphenylamine after 48 hours.

IPr + CuI ⟶ (IPr)Cu(I) (1)

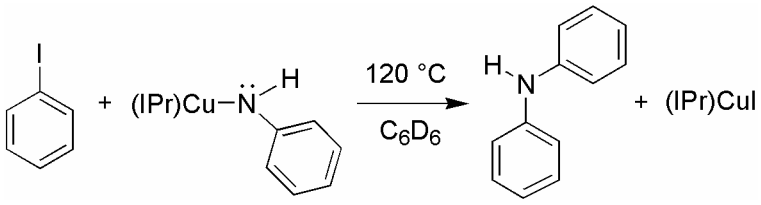

Scheme 4.9. Stoichiometric aryl amination reaction.

Catalytic production of diphenylamine in 50% conversion from phenyl iodide, aniline and K_2CO_3 was observed in the presence of 5 mol% (IPr)Cu(NHPh) in CD_3OD at 120 °C (Scheme 4.10). Also, reaction of 5 mol% (IPr)Cu(NHPh) with phenyl triflate, aniline and K_2CO_3 at 60 °C after 24 hrs in CD_3OD results in 51% conversion. Analogous catalytic trials with phenylbromide and phenylchloride did not produce diphenylamine even after heating to 200 °C. Further investigation of these reactions reveals that (IPr)Cu(NHPh) in the presence

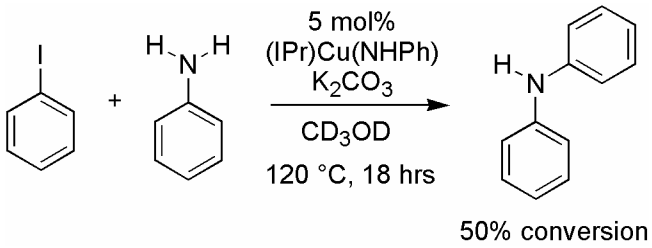

Scheme 4.10. Catalytic aryl amination of phenyl iodide in CD_3OD.

of CD_3OD decomposes to (IPr)Cu(OCD_3) and HNDPh immediately as observed by ^1H NMR spectrum (Scheme 4.11). The production of (IPr)Cu(OCD_3) has been confirmed by reaction of (IPr)Cu(Me) and CD_3OD to produce CH_3D and (IPr)Cu(OCD_3). This complex was not isolated, but it can be concluded that very little amido complex is present in the catalytic

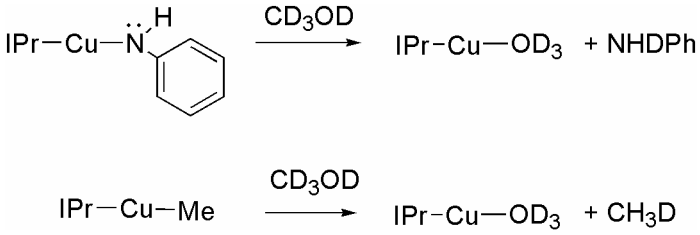

Scheme 4.11. Reaction of (IPr)Cu(NHPh) and (IPr)Cu(Me) with methanol.

reactions described above. Therefore, other solvents were investigated to enhance the catalysis. The limiting factor for the reaction appeared to be the solubility of the base used to deprotonate the amido, and catalytic reaction trials in less polar solvents such as C_6D_6 and toluene-d_8 using Cs_2CO_3, K_2CO_3 or KO^{t}Bu gave no production of diphenylamine. DMSO-d_6 was next tried to enhance the solubility of the base salts used. Initial trials indicated reaction of aniline, phenyl iodide and K_2CO_3 at 130 °C in DMSO-d_6 with 5 mol% (IPr)Cu(NHPh) gave 17% conversion to diphenylamine after 17.5 hrs. Use of Cs_2CO_3 in DMSO-d_6 did not enhance the conversion to diphenylamine. Further refinement of these conditions and kinetic

and mechanistic studies of this catalysis are being conducted by Dr. Laurel Goj, and these studies have revealed that (IPr)Cu(I) is the likely resting state of the catalyst, and is active for catalysis. In addition, the catalytic reaction is 1st order in [Cu] and zero order in [NH_2Ph], which are consistent with a rate determining step of activation of the aryl iodide.[29]

4.4 Attempts at Nitrene Synthesis.

Due to the relatively poor coordinating ability of triflate, (IPr)CuOTf was identified as a potential precursor for a Cu(III) nitrene complex. (IPr)Cu(OTf) is synthesized by metathesis of (IPr)Cu(Cl) with AgOTf and has been fully characterized by multinuclear NMR spectroscopy and a solid-state X-ray crystal structure analysis (Figure 4.10, Figure 4.11, Table 4.6) This reaction occurs readily at room temperature in THF. The triflate complex was reacted with a number of nitrene sources, including phenyl and *p*-tolyl azide,

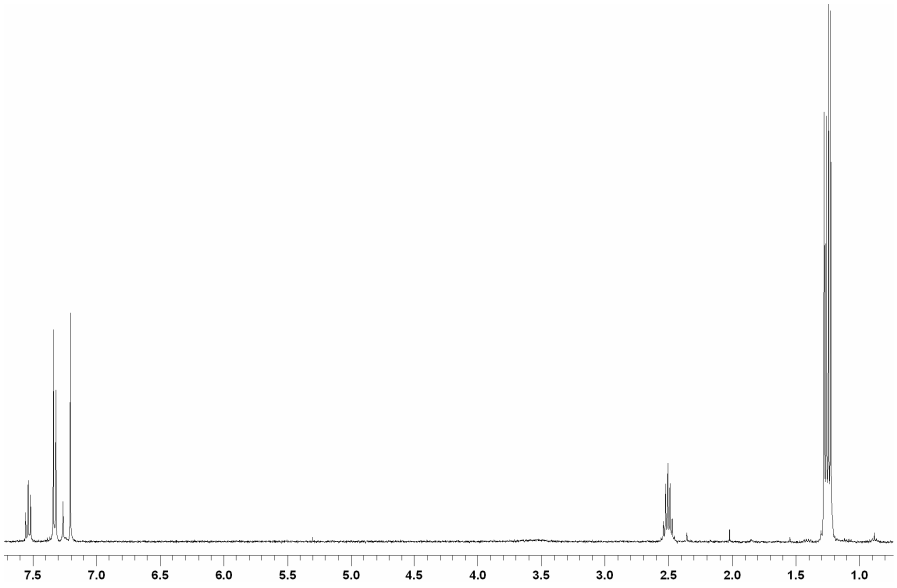

Figure 4.10. ^{1}H NMR spectrum of (IPr)Cu(OTf) in $CDCl_3$.

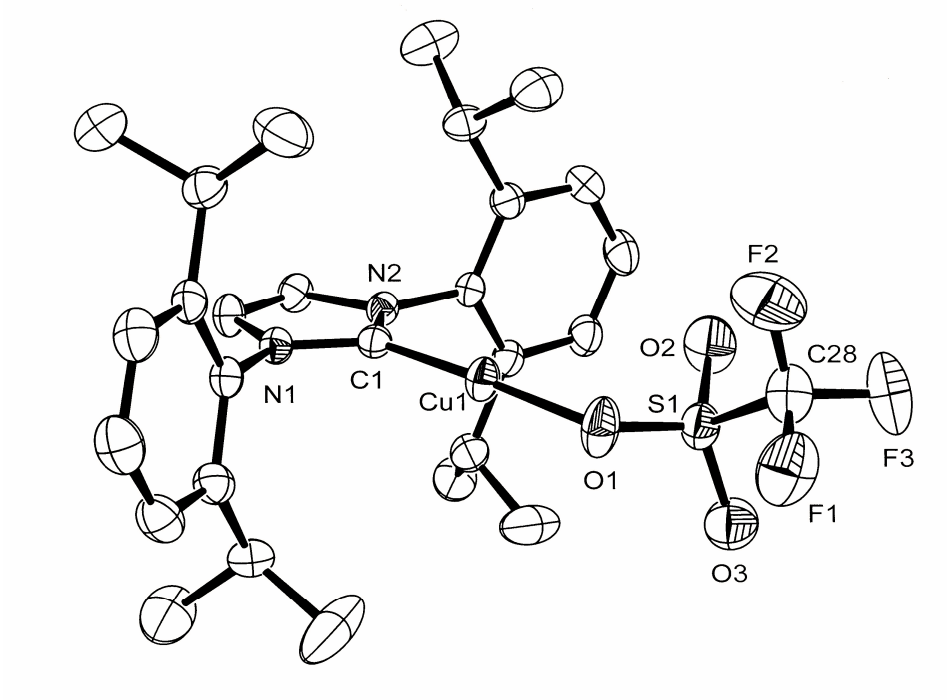

Figure 4.11. Partially labeled ORTEP of (IPr)Cu(OTf) at 30% probability (hydrogen atoms omitted). Selected bond distances (Å): Cu1-O1 1.875(2), Cu1-C1 1.863(3), O1-S1 1.469(3), O2-S1 1.423(3), O3-S1 1.405(3), C1-N1 1.353(4), C1-N2 1.346(4). Selected bond angles (º): C1-Cu1-O1 175.6(1), Cu1-O1-S1 121.9(1), O1-S1-C28 100.2(2), O1-S1-O3 112.6(2), O1-S1-O2 113.8(2).

Table 4.6. Selected crystallographic data and collection parameters for (IPr)Cu(OTf).

	(IPr)Cu(OTf)
empirical formula	$C_{28}H_{36}CuF_3N_2O_3S$
formula wt	601.19
crystal system	orthorhombic
space group	$P2_12_12_1$
a, Å	10.5522(5)
b, Å	14.2330(7)
c, Å	20.4481(10)
β, º	90.0
V (Å^3)	3071.1(3)
Z	4
D_{calcd}, g cm^{-3}	1.300
crystal size (mm)	0.25× 0.38× 0.40
*R*1, w*R*2 {I>2σ(I)}	0.0453, 0.1050
GOF	1.009

as well as PhINTs. No apparent reaction occurs with the azides, and reaction with PhINTs produces a green solution, most likely a copper(II) hydroxide complex, and tosyl amine. Strategies towards net abstraction of hydride from the amido complex included reactions with two equivalents of AgOTf and base, AgOTf and benzoquinone (for single electron oxidation, followed by hydrogen atom abstraction), or $[Ph_3C][BF_4]$, but all resulted in decomposition of the amido complex and formation of the corresponding amine.

4.5 Reaction of (NHC)Cu(I) Complexes with Strong Acids

NHC ligands are relatively unreactive, and have proven to be robust anchors for catalysis;[30] however, they have been shown to undergo reactivity in some cases.[31] For example, reductive elimination, C-H activation of the nitrogen substituents and displacement by other ligands have all been observed. In addition, partial hydrogenation of the imidazolium ring and dihydroxylation of the NHC backbone by OsO_4 have been observed.

The reaction of (IPr)Cu(OTF) with HOTf forms a new species with a downfield resonance in the ^{1}H NMR spectrum at 8.87 ppm in $CDCl_3$, which is consistent with the formation of an imidazolium moiety; however, the resonances in the ^{1}H NMR spectrum are distinct from [IPrH][Cl] (10.1 ppm). Thus, we presumed that the protonated IPr remained coordinated to Cu. A single crystal was grown and revealed the identity as $[(IPrH)Cu(OTf)(\mu\text{-}OTf)]_2$, which possesses a binuclear copper system bridged by two triflate ligands and an imidazolium η^2 ligand coordinated through the arene ring (Figure 4.12, Table 4.7, Scheme 4.12). For each copper center in the complex, there are two triflate ligands (one terminal and one bridging).

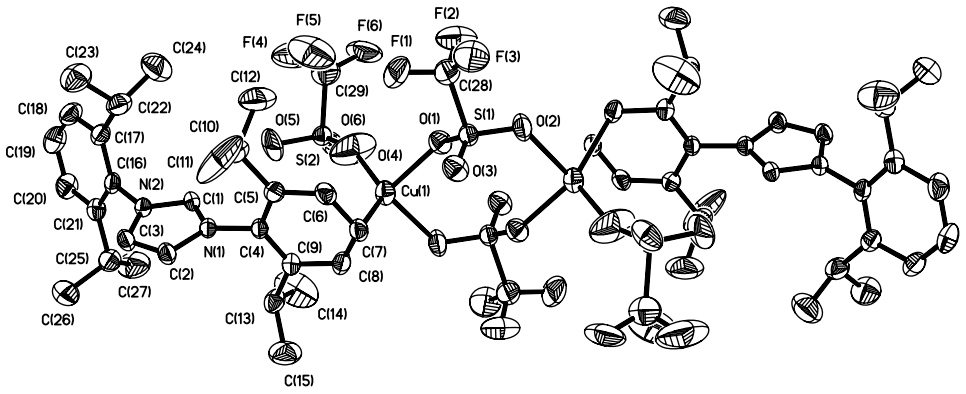

Figure 4.12. Perspective view of the molecular structure of the $[(IPrH)Cu(\eta^1\text{-}OTf)(\mu\text{-}OTf)]_2$ dimer with the atom numbering scheme. Thermal ellipsoids are scaled to 30% probability. Selected bond distances (Å): Cu(1)-O(4), 1.933(5); Cu(1)-O(1), 2.126(2); Cu(1)-O(2), 2.205(2); Cu(1)-C(7), 2.094(2); Cu(1)-C(8), 2.354(2) C(4)-C(9), 1.378(3); C(4)-C(5), 1.401(3); C(5)-C(6), 1.396(3); C(6)-C(7), 1.378(3); C(7)-C(8), 1.380(3); C(8)-C(9), 1.412(3). Selected bond angles (°): O(4)-Cu(1)-O(1), 97.3(1); C(7)-Cu(1)-O(1), 104.8(1); O(4)-Cu(1)-C(7), 130.5(1); O(4)-Cu(1)-C(8), 118.8(1); C(7)-Cu(1)-C(8), 35.5(1); O(1)-Cu(1)-C(8), 138.0(1).

Table 4.7. Selected crystallographic data and collection parameters for $[(IPrH)Cu(\eta^1\text{-}OTf)(\mu\text{-}OTf)]_2$.

	$[(IPrH)Cu(\eta^1\text{-}OTf)(\mu\text{-}OTf)]_2\text{-}CH_2Cl_2$
empirical formula	$C_{30}H_{39}Cl_2CuF_6N_2O_6S_2$
formula wt	836.19
crystal system	Triclinic
space group	$P\bar{1}$
a, Å	10.3339(7)
b, Å	10.8422(7)
c, Å	18.1032(11)
β, °	92.768(1)
V (Å^3)	1944.3(2)
Z	2
D_{calcd}, g cm^{-3}	1.428
crystal size (mm)	0.20 × 0.22 × 0.32
*R*1, w*R*2 {I>2σ(I)}	0.0650, 0.1617
GOF	0.990

The imidazolium ligand is coordinated η^2 through the C3-C4 bond of one of the arene rings. The distances between Cu and the C7 and C8 carbons are 2.09 and 2.35 Å, respectively. There are a number of Cu(I)-η^2 arene complexes, and the Cu(I)-C_{aryl} bond distances vary from 2.072 Å to 2.455 Å, averaging around 2.17 Å and typically the bond distances are not uniform.[32-40] This crystal structure has significant disorder, largely due to the presence of the triflate ligands, but establishes the η^2-coordination of the copper to the aryl ring.

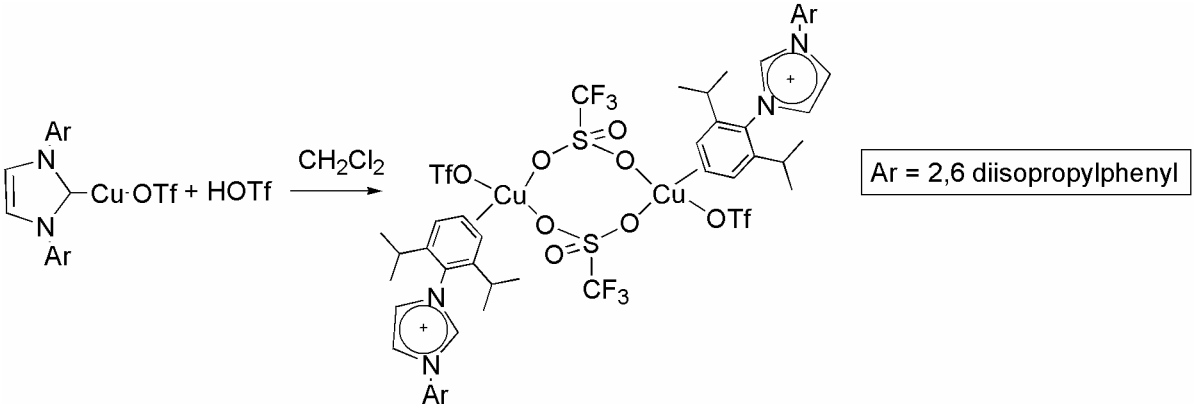

Scheme 4.12. Synthesis of $[(IPrH)Cu(OTf)(\mu\text{-}OTf)]_2$.

4.6 Summary

We have isolated and characterized a number of new copper(I) halide complexes and the first two monomeric examples of copper(I) amido complexes, (dtbpe)Cu(NHPh) and (IPr)Cu(NHPh). These synthetic strategies have been utilized by others in our group to synthesize two additional monomeric amido complexes, (IMes)Cu(NHPh) and (SIPr)Cu(NHPh). These Cu(I) anilido complexes have been shown to be more nucleophilic than a related Ru(II) anilido complex in reactivity studies with bromoethane, and reveal

increasing nucleophilicity in the order (SIPr)Cu(NHPh) < (IPr)Cu(NHPh) < (IMes)Cu(NHPh) < (dtbpe)Cu(NHPh). Given that our Ru(II) amido complexes and related systems reported by Bergman and coworkers are amongst the most highly reactive transition-metal amido complexes, *the enhanced reactivity of the Cu systems compared to Ru suggests that the Cu complexes might be exploited for a variety of metal-mediated processes.* (IPr)Cu(NHPh) is thermodynamically favored over (IPr)Cu(Ph)/NH_2Ph or $[(IPr)Cu(\mu\text{-}H)]_2$/$NH_2Ph$, respectively. Computational studies are consistent with the observed reactivity and indicate strong Cu-N bonds with a nucleophilic amido nitrogen. (dtbpe)Cu(NHPh) and (IPr)Cu(NHPh) are active for hydroamination catalysis of electron-withdrawing olefins, and (IPr)Cu(NHPh) is observed to undergo stoichiometric and catalytic aryl amination with PhI and PhOTf. The mechanism and analysis of the scope of these reactions will continue to be investigated. Reactions towards synthesis of a Cu(III) nitrene complex with LCu(I) (L = dtbpe, NN, or IPr) complexes have largely resulted in decomposition to amine products and Cu(II) species. However, reactions with (NN)Cu(NCMe) complexes and phenyl azide did result in formation of a non-isolable transient species which may be either a Cu(III) nitrene or a Cu(II) species. Reaction of (IPr)Cu(OTf) with strong acid yields a protonated carbene ligand indicated by an downfield peak which binds η^2 through the imidazolium phenyl ring of the amido complex. The synthesis and reactivity studies described herein have provided a foundation for continued fundamental studies of copper(I) non-dative species and mechanistic and applied C-X (X = N, O, or S) bond-forming catalytic investigations.

4.7 General Experimental Methods.

All reactions and procedures were performed under anaerobic conditions in a nitrogen-filled glovebox or using standard Schlenk techniques. Glovebox purity was maintained by periodic nitrogen purges and monitored by an oxygen analyzer. ^{1}H and ^{13}C NMR spectra were obtained on a Varian Mercury 300 or 400 MHz. All ^{1}H and ^{13}C NMR spectra were referenced against tetramethylsilane using residual proton signals (^{1}H NMR) or the ^{13}C resonances of the deuterated solvent (^{13}C NMR). ^{19}F NMR spectra were obtained on a Varian Mercury 300 or 400 MHz and referenced against the external standard C_6F_6 (-163 ppm). Variable-temperature NMR experiments were performed on a Varian Mercury 300 or 400 MHz spectrometer. IR spectra were obtained on a Mattson Genesis II spectrometer either as thin films on a KBr plate or in solution using a KBr solution cell. Electrochemical experiments were performed under a nitrogen atmosphere using a BAS Epsilon Potentiostat. Cyclic voltammograms were recorded in a standard three-electrode cell from -2.00 V to +2.00 V with a glassy carbon working electrode and tetrabutylammonium hexafluorophosphate as electrolyte. Tetrabutylammonium hexafluorophosphate was dried under dynamic vacuum at 140 °C for 48 h prior to use. All potentials are reported versus NHE (normal hydrogen electrode) using cobaltocenium hexafluorophosphate as an internal standard. Elemental analyses were performed by Atlantic Microlabs, Inc.

Hexanes and CH_2Cl_2 were purified by passage through a column of activated alumina. Toluene, THF and benzene were dried by distillation over sodium/benzophenone. Pentane was distilled over sodium. C_6D_6, $CDCl_3$, toluene-d_8 and CD_3OD were degassed via three freeze-pump-thaw cycles and stored over 4 Å sieves. Aniline was dried over CaH_2

followed by vacuum distillation. Bromoethane and the phenyl halides were degassed and stored over 4Å molecular sieves. LiNHPh was generated by reaction of aniline with 1 equivalent of *n*-BuLi in benzene followed by addition of hexanes and vacuum filtration to collect the resulting white precipitate. IPr,[41, 42] (IPr)CuCl,[6] $[(IPr)Cu(\mu\text{-}H)]_2$,[20] (IPr)Cu(Me),[7] $[Cu(NCMe)_4][PF_6]$,[43] (IPr)Cu(Ph), (SIPr)Cu(NHPh) and (IMes)Cu(NHPh),[15] were prepared according to published procedures. PhINTs was prepared according to the published procedure, using the water-free preparation reported by Andersson et al.[44, 45] ArN_3 was synthesized using the preparation from Lindsay and Allen[46] and the workup from Zhu and Ma,[47] as described in Chapter 3. $[Cu(NHPh)]_4$ was prepared according to a previously reported procedure,[48] and the precursor mesitylcopper was prepared according to a separate procedure.[49] CuCl was purchased from Strem Chemical and used as received. All other reagents were used as purchased from commercial sources.

(IPr)Cu(NHPh). Method A. The copper complex (IPr)CuCl (0.186 g, 0.38 mmol) was added to a THF solution (15 mL) of LiNHPh (0.038 g, 0.38 mmol), which turned yellow immediately, and was allowed to stir for 1 hour at room temperature. The solvent was removed *in vacuo*. The off-white solid was dissolved in benzene and filtered through Celite. The eluent was concentrated to 5 mL, and a solid was precipitated upon addition of 10 mL of hexanes. The off-white solid was isolated by filtration and dried (0.103 g, 50 % yield). **Method B.** Complex (IPr)Cu(Me) was (0.479 g, 1.03 mmol) dissolved in approximately 10 mL of benzene. Aniline (0.3 mL, 3.3 mmol) was added to the solution and heated in a pressure tube to 60 ºC for 24 hours. The volatiles were removed under reduced pressure and the resulting off-white solid was isolated by filtration from a slurry in THF and

hexanes (0.393g, 70 % yield). Crystals suitable for a solid-state X-ray diffraction study were grown at room temperature by layering a toluene solution of (IPr)Cu(NHPh) with pentane. Variable temperature ^{1}H NMR studies were conducted in toluene-d_8. ^{1}H NMR (C_6D_6, δ): 7.28 (t, J = 8 Hz, 2 H, *para*-Ph), 7.10 (d, J = 8 Hz, 4H, *ortho*-Ph), 7.01 (t, J = 8 Hz, 1H, *meta*-NPh), 6.52 (t, J = 7 Hz, 1H, *para*-NPh), 6.25 (s, 2H, NC*H*), 6.03 (d, J = 8 Hz, 2H, *ortho*-NPh), 3.23 (bs, 1H, NH), 2.59 (sept, J = 7 Hz, 4H, C*H*$(CH_3)_2$), 1.37 (d, J = 7 Hz, 12H, CH(C*H*$_3)_2$), 1.09 (d, J = 7 Hz, 12H, CH(C*H*$_3)_2$). ^{13}C NMR (C_6D_6, δ): 182.2 (s, N*C*Cu) 161.3, 129.4, 116.5, 110.7 (NPh), 146.5, 135.5, 131.0, 124.8, (IPr phenyl), 122.7 (N*C*H), 29.6 (s, *C*H$(CH_3)_2$), 25.5 (s, CH(*C*H$_3)_2$), 24.3 (s, CH(*C*H$_3)_2$). IR (C_6H_6): ν_{NH} = 3366 cm^{-1}. CV (THF, TBAH, 100 mV/s): $E_{p,a}$ = 0.22 V (II/I).

Reactivity of copper(I) anilido complexes with bromoethane. All of the following kinetic studies were conducted with [Cu] = 0.04 M**.**

Kinetics of (IPr)Cu(NHPh) and bromoethane. Bromoethane (73 μL, 0.99 mmol) was added to a solution of (IPr)Cu(NHPh) (0.045 g, 0.082 mmol) in C_6D_6 (2.0 mL) with hexamethylbenzene (0.0031 g, 0.019 mmol) as an internal standard. The solution was immediately divided between 3 screw-cap NMR tubes and frozen in an acetone/dry ice slush bath. Sequentially, the reaction mixtures were each allowed to warm to room temperature and the reactions were followed by ^{1}H NMR at room temperature at even time intervals. The integration of the peaks due to the disappearance of (IPr)Cu(NHPh) and the appearance of ethyl aniline versus the internal standard were used to calculate the rate of the reaction, k_{obs} = 2.4(2) × 10^{-4}. The formation of *N*-ethylaniline was confirmed by addition of pure *N*-ethylaniline to the final reaction products. Insoluble crystals formed in the NMR tube during

reaction and these were analyzed to confirm the byproduct IPrCuBr, Anal. Calc for $C_{27}H_{36}Br_1Cu_1N_2$: C, 60.95; H, 6.82; N, 5.27. Found: C, 61.10; H, 6.93; N, 5.29.

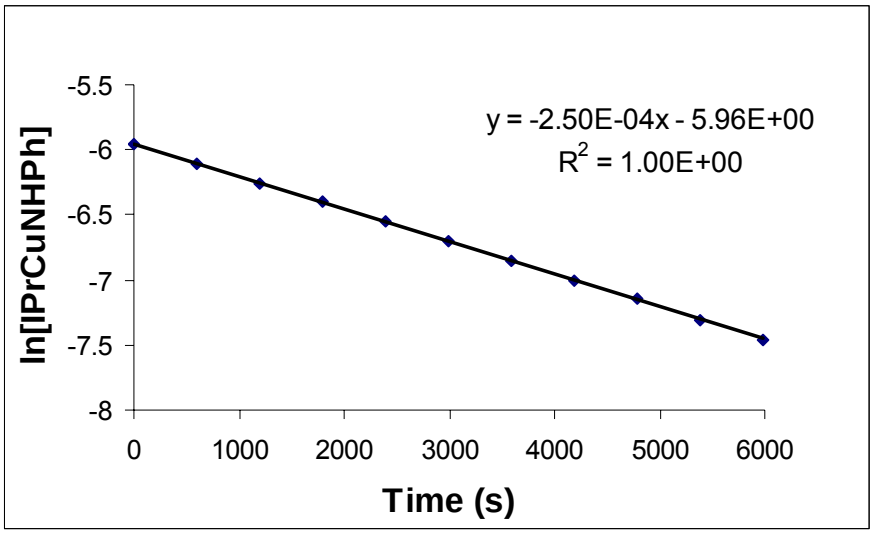

Figure 4.13. Representative plot of ln[(IPr)Cu(NHPh)] versus time for the formation of ethyl aniline with 12 eq of bromoethane in C_6D_6.

Kinetics of (SIPr)Cu(NHPh) and bromoethane. Bromoethane (65 μL, 0.88 mmol) was added to a solution of (SIPr)Cu(NHPh) (0.041 g, 0.075 mmol) in C_6D_6 (1.9 mL) with hexamethylbenzene (0.015 g, 0.071 mmol) as an internal standard. The solution was immediately divided between 3 screw-cap NMR tubes and frozen in an acetone/dry ice slush bath. Sequentially, the reaction mixtures were each allowed to warm to room temperature and the reactions were followed by ^{1}H NMR at room temperature at even time intervals. The integration of the peaks due to the disappearance of (SIPr)Cu(NHPh) and the appearance of ethyl aniline versus the internal standard were used to calculate the rate of the reaction, k_{obs} = $1.1(1) \times 10^{-4}$.

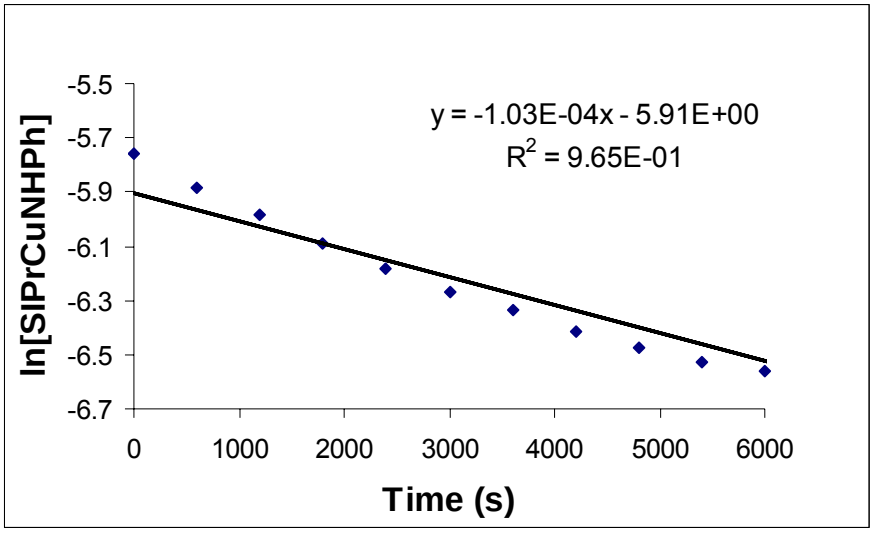

Figure 4.14. Representative plot of ln[(SIPr)Cu(NHPh)] versus time for the formation of ethyl aniline with 12 eq. of bromoethane in C_6D_6.

Kinetics of (IMes)Cu(NHPh) and bromoethane. Bromoethane (87 μL, 1.17 mmol) was added to a solution of (IMes)Cu(NHPh) (0.045 g, 0.098 mmol) in C_6D_6 (2.4 mL) with hexamethyldisiloxane (20 μL, 0.094 mmol) as an internal standard. The solution was immediately divided between 3 screw-cap NMR tubes and frozen in an acetone/dry ice slush bath. Sequentially, the reaction mixtures were each allowed to warm to room temperature and the reactions were followed by ^{1}H NMR at room temperature at even time intervals. The integration of the peaks due to the disappearance of (IMes)Cu(NHPh) and the appearance of ethyl aniline versus the internal standard were used to calculate the rate of the reaction, k_{obs} = $3.3(3) \times 10^{-4}$.

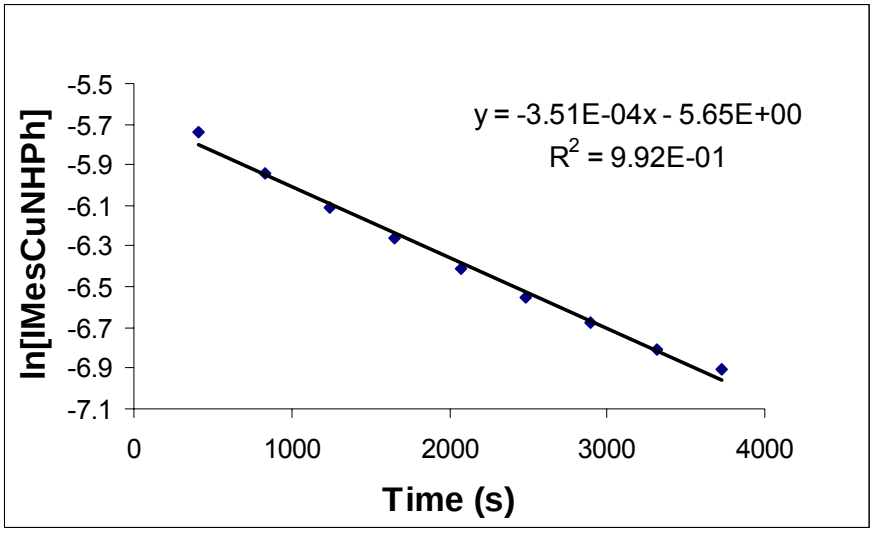

Figure 4.15. Representative plot of ln[(IMes)Cu(NHPh)] versus time for the formation of ethyl aniline with 12 eq. of bromoethane in C_6D_6.

Reaction of (IPr)Cu(NHPh) with *tert*-butylisocyanide. (IPr)Cu(NHPh) (9.4 mg, 0.017 mmol) was dissolved in toluene-d_8 (0.7 mL) in a J. Young NMR tube with hexamethyldisiloxane (2 μL, 0.009 mmol) as an internal standard and 2 equivalents of *tert*-butylisocyanide (4 μL, 0.035 mmol). A ^{1}H NMR spectrum was taken at room temperature. Distinct new resonances appear for the alkyl peaks of the NHC ligand (Figure 4.16). The downfield methyl peak for the 2-coordinate complex has a chemical shift of 1.34 ppm, and the new peak of the 3-coordinate complex appears at 1.44 ppm. The solution was allowed to equilibrate and K_{eq} = 0.44 at room temperature using the integration of the methyl peaks. Variable temperature NMR of the solution between 25 °C and -75 °C demonstrated that the equilibrium is surprisingly independent of temperature, and does not favor the 3-coordinate complex at lower temperatures.

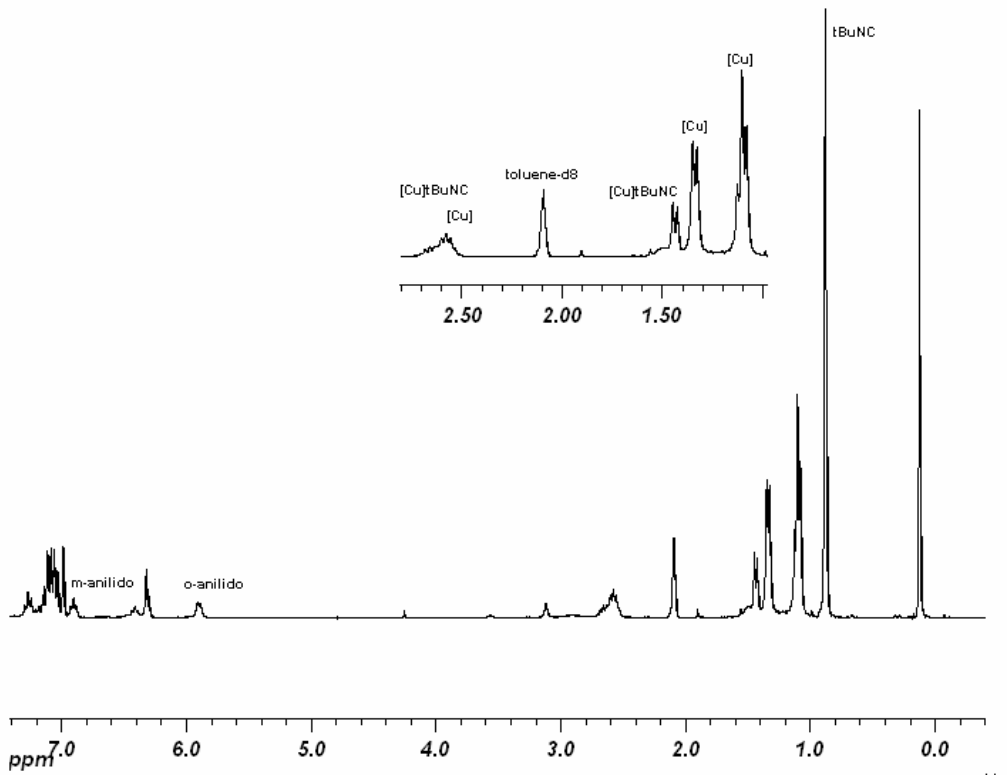

Figure 4.16. ^{1}H NMR spectrum of equilibrium of (IPr)Cu(NHPh) and ^{t}BuNC.

Kinetics of (IPr)Cu(NHPh) and bromoethane with (^{t}BuNC). (IPr)Cu(NHPh) (16.1 mg, 0.030 mmol) was dissolved in C_6D_6 (0.73 mL) in a J. Young NMR tube with hexamethyldisiloxane (6.2 μL, 0.030 mmol) as an internal standard and 2 equivalents of *tert*-butylisocyanide (6.7 μL, 0.059 mmol). Bromoethane (12 equivalents, 26.3 μL, 0.35 mmol) was added by syringe, and immediately the reaction was frozen in an acetone/$CO_{2(s)}$ slush bath. The reaction was then allowed to warm to room temperature just before the reaction was monitored at regular intervals by ^{1}H NMR. The integrals of the formation of ethyl aniline and disappearance of the amido complex were recorded versus the internal standard to calculate $k_{obs} = 2.36(9)\text{x}10^{-4}$ s^{-1}, corresponding to a $t_{1/2} = 49.1$ min.

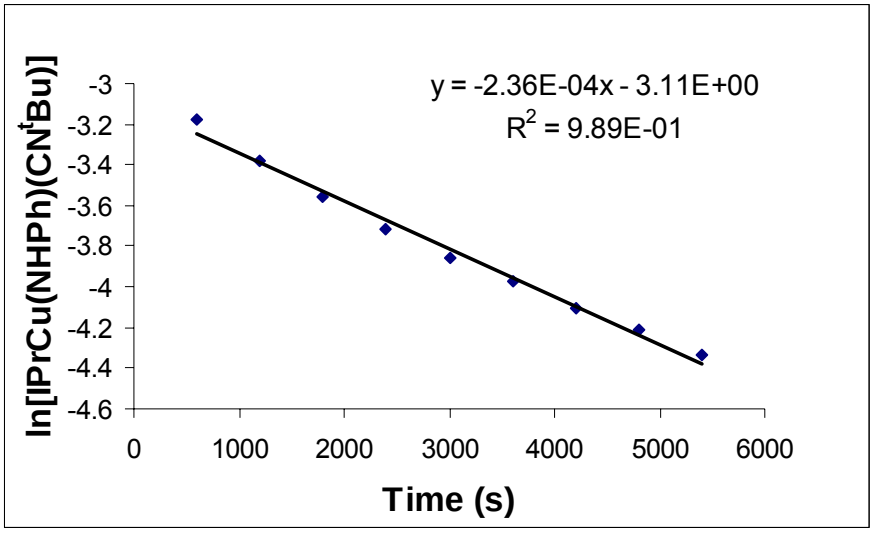

Figure 4.17. Representative plot of ln[(IMes)Cu(NHPh)] versus time for the formation of ethyl aniline with 12 eq. of bromoethane in C_6D_6.

Reaction of (IPr)Cu(NHPh) and benzene. A solution of (IPr)Cu(NHPh) (0.0123 g, 0.022 mmol), C_6H_6 (6 μL, 0.067 mmol) and hexamethylbenzene (0.0002 g, 0.017 mmol) in C_6D_6 (0.7 mL) was sealed in a J. Young NMR tube and heated to 80 °C for 24 hours. The reaction was monitored by ^{1}H NMR periodically, and after 48 hours, the NMR remained the same with no reaction and no decomposition of (IPr)Cu(NHPh).

Reaction of (IPr)Cu(Ph) and aniline. A solution of (IPr)Cu(Ph) (0.0165 g, 0.031 mmol) was dissolved in C_6D_6 (0.774 g, 9.19 mmol) with hexamethyldisiloxane (5 μL, 0.024 mmol) as an internal standard and added to a J. Young NMR tube. Aniline (3.1 μL, 0.034 mmol) was added to the tube, which was then sealed. The solution was monitored by ^{1}H NMR, and complete reaction to form (IPr)Cu(NHPh) and disappearance of (IPr)Cu(Ph) occurred within 24 hours. Calculated based on >90 % conversion, $K_{eq} > 1000$.

Reaction of (IPr)Cu(NHPh) and H_2. (IPr)Cu(NHPh) (0.043 g, 0.079 mmol) was dissolved in benzene (15 mL) in a glass high-pressure tube. The tube was pressurized with H_2 to 60 psi for 18 hours. The solution turned slightly brown. Solvent was removed from the solution in vacuo and a ^{1}H NMR (C_6D_6) was taken of the residue. The resonances were consistent with the starting material and a small amount of decomposition and no resonances due to $[(IPr)Cu(\mu\text{-}H)]_2$ were observed.

Reaction of $[(IPr)Cu(H)]_2$ and aniline. The bright yellow solid $[(IPr)Cu(\mu\text{-}H)]_2$ (approximately 0.01g, 0.022 mmol) was dissolved in C_6D_6 and added to a J. Young NMR tube. Aniline (~ 0.1 mL) was added to the tube, which was then sealed. Gas evolution was observed and the solution was colorless after 10 minutes. Complete reaction to form (IPr)Cu(NHPh) and H_2 (4.47 ppm) and disappearance of $[(IPr)Cu(\mu\text{-}H)]_2$ within 10 minutes was confirmed by ^{1}H NMR by comparison with data for (IPr)Cu(NHPh) and observations of H_2 in C_6D_6.

Reaction of (IPr)Cu(NHPh) with PhI. (IPr)Cu(NHPh) (0.0136 g, 0.025 mmol) was dissolved in C_6D_6 (0.7 mL) in a J. Young NMR tube along with hexamethylbenzene (0.0018 g, 0.011 mmol) as a standard. Phenyl iodide (5.6 μL, 0.05 mmol) was added, and the reaction was heated to 120 °C for 24 hours. New peaks corresponding to diphenylamine (45% yield by ^{1}H NMR integration) and the product was confirmed by ^{1}H NMR after addition of an authentic sample of diphenylamine. Crystals formed in the NMR tube, and these were confirmed by ^{1}H NMR in $CDCl_3$ to be (IPr)CuI, which was independently synthesized.

Control Reaction: NH_2Ph + PhI. NH_2Ph (10 μL, 0.11 mmol) and phenyl iodide (12.3 μL, 0.11 mmol) were combined in C_6D_6 (0.7 mL) in a J. Young NMR tube along with hexamethylbenzene (0.0022 g, 0.014 mmol) as a standard. The reaction was heated to 130 °C for 4 days. The reaction was monitored periodically by ^1H NMR and no new peaks corresponding to diphenylamine appeared.

Control Reaction: NH_2Ph + PhI with IPr. IPr (0.0180 g, 0.046 mmol), NH_2Ph (4.2 μL, 0.046 mmol) and phenyl iodide (5.2 μL, 0.046 mmol) were combined in C_6D_6 (0.7 mL) in a J. Young NMR tube along with hexamethylbenzene (0.0038 g, 0.023 mmol) as a standard. The reaction was heated to 120 °C for 2 days. The reaction was monitored periodically by ^1H NMR and no new peaks corresponding to diphenylamine appeared.

Synthesis of (IPr)Cu(I). IPr (0.193 g, 0.50 mmol) and CuI (0.095 g, 0.50 mmol) were combined in THF and allowed to stir for 18 hours. The solution was filtered, and solvent was removed *in vacuo* from the filtrate. The white residue was dissolved in CH_2Cl_2 and filtered. The solution was reduced to approximately 5 mL, and a white solid was precipitated with hexanes. The white powder was collected by vacuum filtration (133 mg, 46% yield). X-Ray quality crystals were grown by slow diffusion of pentane into a saturated CH2Cl2 solution. NMR spectra were very similar to IPrCuCl. ^1H NMR ($CDCl_3$, δ): 7.51 (2H, t, J = 8 Hz, p-phenyl), 7.31 (4H, d, J = 8 Hz, m-phenyl), 7.15 (2H, s, backbone CH), 2.59 (4H, septet, J = 7 Hz, iPr C*H*), 1.33, 1.26 (24H, d, J = 7 Hz, iPr CC*H*$_3$). X-Ray quality crystals were grown by slow diffusion of pentane into a saturated CH_2Cl_2 solution. ^{13}C NMR ($CDCl_3$, δ): 183.3 (s, N*C*Cu), 145.7, 134.3, 130.7, 124.3 (s, IPr phenyl), 123.1 (s, N*C*H),

29.1 (s, *C*H(CH_3)$_2$), 25.1, 24.2 (s, CH(*C*H_3)$_2$). Anal Calc for $C_{27}H_{36}Cu_1I_1N_2$: C, 56.01; H, 6.28; N, 4.84; Found: C, 55.67; H, 6.25; N, 4.76.

Representative procedure for catalytic aryl amination: Reaction of PhI with aniline and 5 mol% (IPr)Cu(NHPh). (IPr)Cu(NHPh) (0.0040 g, 0.0074 mmol) was dissolved in DMSO-d_6 (0.7 mL) in a J. Young NMR tube along with hexamethyldisiloxane (2 μL, 0.0094 mmol) as a standard, aniline (13.4 μL, 0.147 mmol) and phenyliodide (16.5 μL, 0.147 mmol). K_2CO_3 was added (0.0203 g, 0.147 mmol) and the tube was sealed and heated to 120 °C for 18 hours. The reaction was monitored by ^{1}H NMR to observe production of diphenylamine, and the yield was calculated by integration.

Catalytic Control Reaction: PhI with aniline and K_2CO_3. Aniline (12.4 μL, 0.136 mmol), phenyliodide (15.2 μL, 0.136 mmol) and K_2CO_3 (0.0376 g, 0.27 mmol) were combined in CD_3OD (0.7 mL) in a J. Young NMR. The tube was sealed and heated to 120 °C for 48 hours. The reaction was periodically monitored by ^{1}H NMR, and no new peaks corresponding to diphenylamine appeared.

Reaction of (IPr)Cu(NHPh) with CD_3OD. (IPr)Cu(NHPh) was dissolved in CD_3OD and a ^{1}H NMR was obtained. New peaks consistent with formation of NHDPh in CD_3OD were observed (7.08 (2H, t, *J* = 7.8 Hz, *m*-aryl), overlapping peaks: 6.70 (2H, d, *J* = 7.5 Hz, *o*-aryl) and 6.67 (1H, t, *J* = 7.5 Hz, *p*-aryl).), and a copper complex, most likely (IPr)Cu(OD_3) [(7.59 (2H, s, IPr backbone), 7.53 (1H, d, *J* = 5.7 Hz, IPr *p*-phenyl), 7.39 (2H, d, *J* = 5.7 Hz, IPr *m*-phenyl), 2.62 (4H, septet, *J* = 5 Hz, C*H*(CH_3)$_2$), 1.32, 1.26 (24H, d, *J* = 5.4 Hz, CH(C*H*$_3$)$_2$)].

Reaction of (IPr)Cu(Me) with methanol. (IPr)Cu(Me) was dissolved in CD_3OD and a ^1H NMR was obtained. Gas evolution was observed, and formation of ethane was observed by NMR (0.8 ppm), and peaks identical to those observed in the reaction of (IPr)Cu(NHPh) with CD_3OD (listed above) were observed. In addition, (IPr)Cu(Me) (0.0064 g, 0.014 mmol) was dissolved in C_6D_6 in an NMR tube and 2.6 equivalents of CH_3OH (1.5 μl, 0.037 mmol) were added. The tube was sealed with a septum and only partial reaction occurred at room temperature, so the reaction was heated to 60 °C for 18 hours. A complex similar to that observed above, but shifted due to the solvent was observed, with a OCH_3 peak at δ = 0.18 (Figure 4.18); however, integration of the OCH_3 peak is incorrect perhaps due to exchange with the excess methanol in solution. ^1H NMR (C_6D_6, δ): 7.23-7.18 (m, IPr *p*-phenyl), 7.06 (2H, d, *J* = 7.8 Hz, IPr *m*-phenyl), 6.28 (2H, s, IPr backbone), 2.57 (4H, septet, *J* = 6.9 Hz, C*H*$(CH_3)_2$), 1.40, 1.09 (24H, d, *J* = 6.9 Hz, CH(C*H*$_3)_2$), 0.18 (s, OC*H*$_3$).

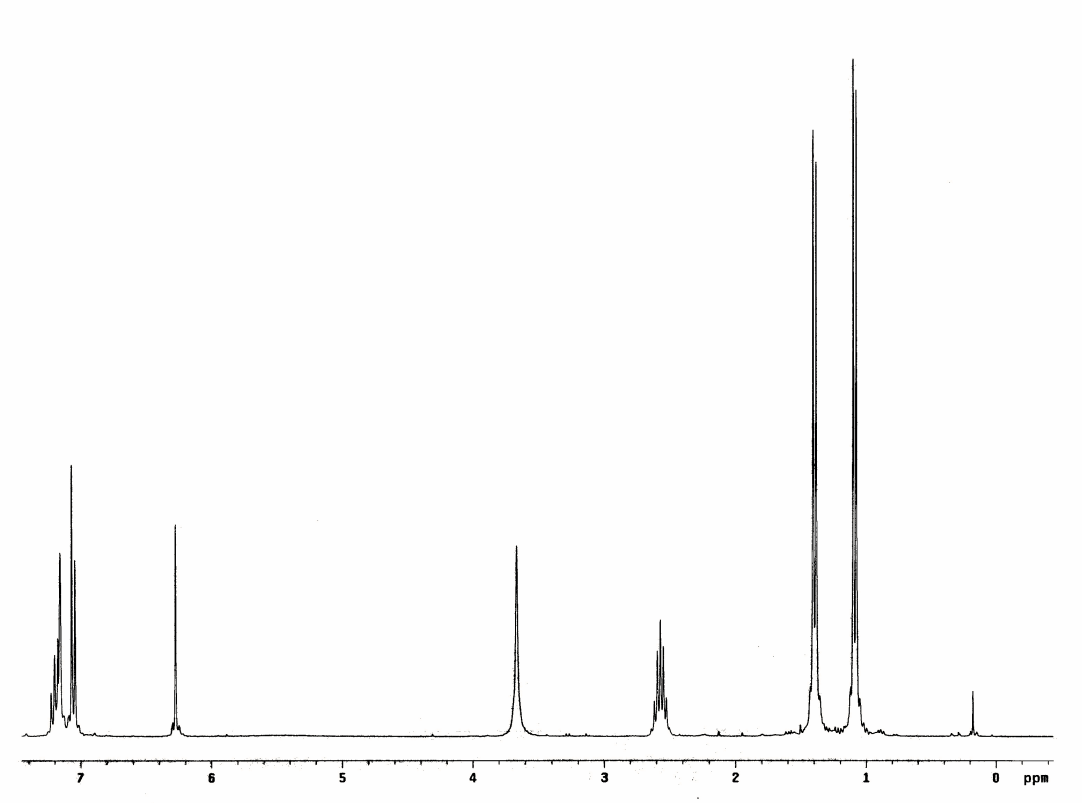

Figure 4.18. ^{1}H NMR spectrum of (IPr)Cu(OMe) in C_6D_6.

Synthesis of (IPr)Cu(OTf). (IPr)CuCl (0.251 g, 0.52 mmol) was combined with AgOTf (0.133 g, 0.52 mmol) in approximately 25 mL THF. The solution turned brown after 5 minutes of stirring. After stirring for 30 minutes, AgCl was removed by filtration through Celite, and the filtrate was reduced to approximately 5 mL *in vacuo*. Hexanes (10 mL) were used to precipitate the product, and the white powder (0.234 g, 77% yield) was collected via filtration and dried. X-ray quality crystals of this complex were grown from a solution of CH_2Cl_2 layered with pentane. ^{1}H NMR ($CDCl_3$, δ): 7.53 (t, *J* = 8 Hz, 2H, *p*-phenyl), 7.33 (d, *J* = 8 Hz, 4H, *m*-phenyl), 7.21 (s, 2H, NC*H*), 2.54 (sept, *J* = 7 Hz, 4H, C*H*(CH_3)$_2$), 1.26, 1.30 (d, *J* = 7 Hz, 24H, CH(C*H*$_3$)$_2$). ^{13}C NMR (C_6D_6, δ): 177.9 (s, N*C*Cu), 145.5, 134.0,

131.0, 124.5 (s, IPr phenyl), 123.9 (s, NCH), 29.1 (s, *C*H(CH_3)$_2$), 24.9 (s, CH(*C*H_3)$_2$), 24.3 (s, CH(*C*H_3)$_2$). ^{19}F NMR ($CDCl_3$, δ): -76.0 (s). Anal Calc for $C_{28}H_{20}Cu_1F_3N_2O_3S_1$: C, 55.94; H, 6.04; N, 4.66; Found: C, 55.47; H, 6.00; N, 4.62.

[(IPrH)Cu(OTf)(μ-OTf)]$_2$. (IPr)CuOTf (0.111 g, 0.19 mmol) was dissolved in CH_2Cl_2 (20 mL) in a pressure tube. HOTf (33 μL, 0.37 mmol) was added, the pressure tube was sealed and the reaction mixture was heated to 60 °C for 2 hours. At the end of heating, there was a slightly pink precipitate at the bottom of the tube. The solution was filtered and to remove the pink solids and the filtrate was dried *in vacuo*. The off-white solid was dissolved in approximately 5 mL THF, and a white precipitate formed after addition of hexanes (10 mL), which was collected by filtration and dried (0.095 g, 68 % yield). X-Ray quality crystals were grown from a solution of [(IPrH)Cu(OTf)(μ-OTf)]$_2$ in CH_2Cl_2 layered with pentane. ^{1}H NMR ($CDCl_3$, δ): 8.96 (bs, 2H, N(C*H*)N), 7.75 (s, 4H, backbone protons), 7.63 (t, $^3J_{HH}$ = 8 Hz, 4H, *para* aryl), 7.40 (d, $^3J_{HH}$ = 8 Hz, 8H, *meta* aryl), 2.41 (septet, $^3J_{HH}$ = 7 Hz, 8H, ^{i}Pr methine), 1.31 (d, $^3J_{HH}$ = 7 Hz, 24H, ^{i}Pr methyl), 1.24, (d, $^3J_{HH}$ = 7 Hz, 24H, ^{i}Pr methyl). ^{13}C NMR ($CDCl_3$, δ): 145.1 (N*C*HN), 137.8, 132.2, 129.7, 126.4 (aryl), 124.9 (N*C*H*C*HN), 29.5 (*C*H(CH_3)$_2$), 24.7, 24.1 (CH(*C*H_3)$_2$). ^{19}F NMR ($CDCl_3$, δ): -75.0.

References

1. Arduengo, A. J.; Harlow, R. L.; Kline, M. *J. Am. Chem. Soc.* **1991,** 113, 361-363.
2. Arduengo, A. J.; Krafczyk, R.; Schmutzler, R.; Craig, H. A.; Goerlich, J. R.; Marshall, W. J.; Unverzagt, M. *Tetrahedron* **1999,** 55, 14523-14534.
3. Huang, J.; Schanz, H. J.; Stevens, E. D.; Nolan, S. P. *Organometallics* **1999,** 18, 2370-2375.
4. Lee, M. T.; Hu, C. H. *Organometallics* **2004,** 23, 976-983.
5. Ofele, K.; Herrmann, W. A.; Mihalios, D.; Elison, M.; Herdtweck, E.; Scherer, W.; Mink, J. *J. Organomet. Chem.* **1993,** 459, 177-184.
6. Jurkauskas, V.; Sadighi, J. P.; Buchwald, S. L. *Org. Lett.* **2003,** 5, 2417-2420.
7. Mankad, N. P.; Gray, T. G.; Laitar, D. S.; Sadighi, J. P. *Organometallics* **2004,** 23, 1191-1193.
8. Goj, L. A.; Blue, E. D.; Munro-Leighton, C.; Gunnoe, T. B.; Petersen, J. L. *Inorg. Chem.* **2005,** 44, 8647-8649.
9. Blue, E. D.; Davis, A.; Conner, D.; Gunnoe, T. B.; Boyle, P. D.; White, P. S. *J. Am. Chem. Soc.* **2003,** 125, 9435-9441.
10. Fukuyo, M.; Hirotsu, K.; Higuchi, T. *Acta Crystallogr., Sect. B* **1982,** 38, 640-643.
11. Powell, K. R.; Peréz, P. J.; Luan, L.; Feng, S. G.; White, P. S.; Brookhart, M.; Templeton, J. L. *Organometallics* **1994,** 13, 1851-1864.
12. Albeniz, A. C.; Calle, V.; Espinet, P.; Gomez, S. *Inorg. Chem.* **2001,** 40, 4211-4216.
13. Jayaprakash, K. N.; Gunnoe, T. B.; Boyle, P. D. *Inorg. Chem.* **2001,** 40, 6481-6486.
14. Conner, D.; Jayaprakash, K. N.; Gunnoe, T. B.; Boyle, P. D. *Inorg. Chem.* **2002,** 41, 3042-3049.
15. Goj, L. A.; Blue, E. D.; Delp, S. A.; Gunnoe, T. B.; Petersen, J. L.; Cundari, T. R. *manuscript in preparation* **2006**.
16. Hillier, A. C.; Sommer, W. J.; Yong, B. S.; Petersen, J. L.; Cavallo, L.; Nolan, S. P. *Organometallics* **2003,** 22, 4322-4326.
17. Conner, D.; Jayaprakash, K. N.; Gunnoe, T. B.; Boyle, P. D. *Organometallics* **2002,** 21, 5265-5271.
18. Allred, A. L. *J. Inorg. Nucl. Chem.* **1961,** 17, 215-221.
19. Kanzelberger, M.; Zhang, X. W.; Emge, T. J.; Goldman, A. S.; Zhao, J.; Incarvito, C.; Hartwig, J. F. *J. Am. Chem. Soc.* **2003,** 125, 13644-13645.
20. Mankad, N. P.; Laitar, D. S.; Sadighi, J. P. *Organometallics* **2004,** 23, 3369-3371.
21. Fryzuk, M. D.; Montgomery, C. D. *Coord. Chem. Rev.* **1989,** 95, 1-40.
22. Hillhouse, G. L.; Bercaw, J. E. *J. Am. Chem. Soc.* **1984,** 106, 5472-5478.
23. Munro-Leighton, C.; Blue, E. D.; Gunnoe, T. B. *J. Am. Chem. Soc.* **2006,** 128, 1446-1447.
24. Hartwig, J. F. *Pure Appl. Chem.* **2004,** 76, 507-516.
25. Zhao, P.; Krug, C.; Hartwig, J. F. *J. Am. Chem. Soc.* **2005,** 127, 12066-12073.
26. Hartwig, J. F. *Angew. Chem., Int. Ed. Eng.* **1998,** 37, 2046-2067.
27. Hartwig, J. F. *Acc. Chem. Res.* **1998,** 31, 852-860.
28. Shekhar, S.; Ryberg, P.; Hartwig, J. F.; Mathew, J. S.; Blackmond, D. G.; Strieter, E. R.; Buchwald, S. L. *J. Am. Chem. Soc.* **2006,** 128, 3584-3591.

29. Goj, L. A.; Blue, E. D.; Gunnoe, T. B.; Cundari, T. R.; Petersen, J. L. *manuscript submitted* **2006**.
30. Herrmann, W. A. *Angew. Chem., Int. Ed. Eng.* **2002,** 41, 1290-1309.
31. Crudden, C. M.; Allen, D. P. *Coord. Chem. Rev.* **2004,** 248, 2247-2273.
32. Laitar, D. S.; Mathison, C. J. N.; Davis, W. M.; Sadighi, J. P. *Inorg. Chem.* **2003,** 42, 7354-7356.
33. Sundararaman, A.; Lalancette, R. A.; Zakharov, L. N.; Rheingold, A. L.; Jakle, F. *Organometallics* **2003,** 22, 3526-3532.
34. Amisial, L. D.; Dai, X.; Kinney, R. A.; Krishnaswamy, A.; Warren, T. H. *Inorg. Chem.* **2004,** 43, 6537-6539.
35. Dattelbaum, A. M.; Martin, J. D. *Polyhedron* **2006,** 25, 349-359.
36. Hamilton, C. W.; Laitar, D. S.; Sadighi, J. P. *Chem. Commun.* **2004**, 1628-1629.
37. Lee, S. Y.; Na, S. J.; Kwon, H. Y.; Lee, B. Y.; Kang, S. O. *Organometallics* **2004,** 23, 5382-5385.
38. Turner, R. W.; Amma, E. L. *J. Am. Chem. Soc.* **1966,** 88, 1877-1882.
39. Hubig, S. M.; Lindeman, S. V.; Kochi, J. K. *Coord. Chem. Rev.* **2000,** 200-202, 831-873.
40. H.Schmidbaur; W.Bublak; B.Huber; G.Reber; G.Muller. *Angew. Chem., Int. Ed. Eng.* **1986,** 25.
41. Jafarpour, L.; Stevens, E. D.; Nolan, S. P. *J. Organomet. Chem.* **2000,** 606, 49-54.
42. Böhm, V. P. W.; Weskamp, T.; Gstöttmayr, C. W. K.; Herrmann, W. A. *Angew. Chem., Int. Ed. Eng.* **2000,** 39, 1602-1604.
43. Kubas, G. J. *Inorg. Synth.* **1979,** 19, 90.
44. Yamada, Y.; Yamamoto, T.; Okawara, M. *Chem. Lett.* **1975**, 361-362.
45. Sodergren, M. J.; Alonso, D. A.; Bedekar, A. V.; Andersson, P. G. *Tetrahedron Lett.* **1997,** 38, 6897-6900.
46. Lindsay, R. O.; Allen, C. F. H. *Org. Synth.* **1942,** 22, 96.
47. Zhu, W.; Ma, D. *Chem. Commun.* **2004**, 888-889.
48. Tsuda, T.; Watanabe, K.; Miyata, K.; Yamamoto, H.; Saegusa, T. *Inorg. Chem.* **1981,** 20, 2728-2730.
49. Eriksson, H.; Hakansson, M. *Organometallics* **1997,** 16, 4243-4244.